Calibration of Mechanistic-Empirical (ME) Design Methods and Development of Statistical Performance Models for Optimized Life-Cycle Asset Management of Jointed Concrete Pavements in California

By

Ashkan SABOORI

DISSERTATION

Submitted in partial satisfaction of the requirements for the degree of

DOCTOR OF PHILOSOPHY

in

Civil and Environmental Engineering

in the

OFFICE OF GRADUATE STUDIES

of the

UNIVERSITY OF CALIFORNIA

DAVIS

Approved:

Professor John Harvey, Chair

Professor Mark Rashid

Professor Jeffery Roesler

Committee in Charge
2024

ABSTRACT

The primary goal of this dissertation is to develop frameworks, quantitative models, and databases to support data-driven, informed, and integrated decision-making for managing the vast transportation infrastructure in California. This research focuses on optimizing maintenance and rehabilitation (M&R) strategies for jointed plain concrete pavements (JPCP) to ensure cost-effectiveness and minimal disruption to traffic flow. The study aims to address the need for improved performance models for slab and lane replacement procedures, considering the unique environmental and traffic conditions in California.

The dissertation comprises several key components:

- Development of Performance Models: This research develops empirical-mechanistic models to predict the performance of slab and lane replacement treatments on JPCP. These models are intended to enhance the decision-making framework within Caltrans' pavement management system (PMS), optimizing M&R strategies based on life-cycle costs and environmental impacts. The performance models utilize extensive pavement condition data collected through Caltrans' automated pavement condition survey (APCS), which includes high-definition images and laser measurements of performance indices such as surface roughness, transverse and longitudinal cracking, corner cracking, and faulting.
- Calibration of ME Design Models: The study involves the calibration of the mechanistic-empirical pavement design guide (MEPDG) models to California's specific conditions. Previous attempts at local calibration by other state highway agencies have been limited in scope and data availability. This research leverages a much larger dataset from Caltrans' PMS database, covering diverse climate regions and pavement conditions across the state. The calibration process aims to improve the accuracy of performance prediction for transverse cracking model.
- Incorporating Longitudinal Cracking in Design: Longitudinal cracking, a prevalent issue in California's dry climate, has not traditionally been considered in pavement design models developed for more humid climates. This study identifies the underlying causes of longitudinal cracking, including differential shrinkage, slab geometry, and traffic loading, and proposes design recommendations to mitigate this distress. Through finite element simulations and analysis of PMS data, the study develops a comprehensive understanding of the factors contributing to longitudinal cracking.

- Framework for Optimized Pavement Management: The dissertation proposes a robust framework for managing the state's highway network, ensuring cost-effective and durable pavement designs that accommodate California's unique environmental and traffic conditions. By developing performance models for slab and lane replacement, the research enhances the ability to predict pavement performance and optimize maintenance and rehabilitation strategies. The findings provide practical solutions for extending the service life of rigid pavements and minimizing disruptions to traffic flow.
- Statewide Data Collection and Analysis: The study collects statewide median values for JPCP design variables from historical test data of JPCP projects across California. This data serves as a benchmark for assessing pavement performance and is crucial for calibrating the MEPDG models using an extensive dataset from the Caltrans PMS database. The calibration approach developed in this study considers within-project, between-project, and between-contractor variability, thereby improving the reliability of performance predictions.

The research addresses critical gaps in the knowledge and practice of pavement engineering, particularly in the context of California's diverse climate regions. By providing a comprehensive analysis of the factors influencing slab and lane replacement performance, developing accurate performance prediction models, and proposing new design guidelines for longitudinal cracking, this dissertation contributes significantly to the field of pavement management. The outcomes of this research offer a robust framework for efficient asset management, ensuring that maintenance and rehabilitation activities are performed in a timely, cost-effective manner, thereby extending the service life of California's highway network and reducing traffic disruptions.

ACKNOWLEDGEMENT

This research was primarily funded by the California Department of Transportation, Division of Research and Innovation. It was also partly supported by a PhD grant from the U.S. Department of Transportation, awarded by the National Center of Sustainable Transportation (NCST) at the UC Davis Institute of Transportation Studies.

I want to express my deep gratitude to my advisor, Professor John Harvey, for his continued support and insight throughout my PhD years. Without his guidance, this work would not have been possible. I am also grateful to my dissertation committee members, Professor Mark Rashid and Professor Jeffrey Roesler, for their support and guidance on my dissertation. Additionally, I would like to thank Dr. Jeremy Lea and Dr. Angel Mateos for their guidance and supervision throughout all phases of this research. My heartfelt thanks go to all the UCPRC members who have helped and supported my research pursuits.

I am incredibly grateful to my parents, Mehdi and Farzaneh, for their unwavering support and sacrifices. Their continuous love and encouragement have been vital in completing this work. I am also deeply indebted to my brother, Anoosh, for being such an amazing mentor and support during all stages of my life. I would also like to extend my gratitude to my sister-in-law, Aida, whose support during difficult times and her presence, especially during my time at Davis, was a blessing.

Most importantly, I would like to thank my brother Arash, my role model in life. Without him, I would not be where I am today. His continuous and unconditional support throughout my life has shaped who I am and made this achievement possible. I am profoundly grateful for everything he has done for me, and I truly appreciate his support from the bottom of my heart.

TABLE OF CONTENTS

LIST OF FIGURES

LIST OF TABLES

ACRONYMS

AADTT	Average Annual Daily Truck Traffic
AASHTO	American Association of State Highway and Transportation Officials
AB	Aggregate base
APCS	Automated Pavement Condition Survey
ASR	Alkali-silica reaction
ATPB	Asphalt-treated permeable base
BCV	Between-contractor variability
BPV	Between-project variability
BVS	Blind Verification Sections
CDF	Cumulative distribution function
CLMM	Cumulative link mixed model
CTB	Cement-treated base
CTE	Coefficient of thermal expansion
EICM	Enhanced Integrated Climate Model
FHWA	Federal Highway Administration
FLX	Untied flexible (shoulder type)
GPR	Ground-penetrating radar
HDM	*Highway Design Manual*
HMA	Hot mix asphalt
IRI	International Roughness Index
JPCP	Jointed plain concrete pavements
LCB	Lean concrete base
LTE	Load transfer efficiency
LTPP	Long-Term Pavement Performance
ME design	Mechanistic-Empirical Design
MEPDG	*Mechanistic-Empirical Pavement Design Guide*
MR	Modulus of Rupture
NAP	Not applicable (no shoulder)
PMS	Pavement management system
PCC	Portland cement concrete
PCS	Pavement condition survey

PPRC	Partnered Pavement Research Center
RIG	tied concrete (shoulder type)
SHS	State highway system
UCPRC	University of California Pavement Research Center
WIM	Weigh-in-motion
WPV	Within-project variability
WRF	Widened concrete (shoulder type)

CHAPTER 1. Introduction

The extensive California state highway network comprises over 50,000 lane-miles of pavement, accommodating approximately 35 million vehicles annually. Among these roadways, approximately 37,000 lane-miles are “flexible” pavements, meaning that they are surfaced with asphalt concrete, while the remaining 13,000 lane-miles consist of “rigid” pavements surfaced with hydraulic cement concrete, typically portland cement concrete (PCC). A portion of the flexible pavement inventory is composed of rigid pavements that have been overlayed with asphalt concrete. Rigid pavements, often chosen for high-traffic routes, boast comparatively less maintenance and rehabilitation (M&R) throughout their operational lifespan, thereby minimizing traffic disruptions caused by maintenance activities.

Fundamental to the cost-effective design and management of pavement is the ability to determine the performance of alternative pavement structures. In 2005, the California Department of Transportation (Caltrans) changed its design approach from reliance on past observed field performance for design (empirical design) to the use of mechanistic-empirical (ME) design in which mechanistic models are used to calculate critical responses (stresses, deformations and strains) in the pavement under traffic and environmental loading, and the calculated responses are then empirically correlated with structural and functional distresses (Kannekanti & Harvey, 2007). ME design allows new materials and structural designs to be introduced into practice after calculation of the critical responses and initial determination of performance estimated using existing empirical correlations, as opposed to the empirical approach which requires waiting a significant amount of time (typically decades) to wait for field performance data to become available.

A substantial portion of California's rigid pavements has exceeded their originally intended design life of 20 years and is now approaching the end of their functional service life. This situation underscores the pressing necessity for the identification of sections requiring M&R or complete reconstruction using field calibrated ME design models. Beginning around 2000, Caltrans also increased the required design life for new rigid pavements from 20 to 40 years. An updated empirical calibration of performance models considering the 40 year designs built between 2000 and 2020 was needed. A part of the new 40 year designs of the early 2000s was the use of widened truck lanes intended to reduce transverse cracking distress. However, a large gap in design practice was a total lack of consideration of longitudinal cracking in rigid pavement design, a distress for which a mechanistic model was first identified by the University of California Pavement Research Center (UCPRC) for Caltrans in the late 1990s, and which is potentially made worse using widened lanes.

In addition, in the early 2020s, Caltrans changed the definition of design life from a pavement condition requiring major rehabilitation to a condition requiring minor rehabilitation for both rigid and flexible pavement, a change that was included in the latest version of the Caltrans flexible pavement design method (Wu et al, 2021). At the same time, a new framework was needed for design reliability, meaning the consideration of the probabilistic nature of pavement performance, considering both variability of materials, conditions, and contractor quality between different projects, and within project variability of site conditions and construction quality of each project's contractor (Lea and Harvey, 2015; Wu et al., 2022). The work started in the late 1990s (Lea and Harvey, 2002) by the UCPRC on developing Caltrans performance data collected since the late 1970s for use in modeling, significantly improved and accelerated by Caltrans' rebooting of its pavement management system (PMS) in the early 2010s, provided an opportunity to address these needs (Wu et al., 2021; Fu et al., 2013). The investment by Caltrans in the quality and quantity of the Caltrans PMS data combined with the new approach for considering reliability provide the means for the first-ever calibration of ME design models in the world using comprehensive network-level data (thousands to tens of thousands of lane-km of data) rather than the conventional approach of using tens to hundreds of short test sections (typically less than 200 lane-km of data) (Khazanovich et al., 2004; Sachs et al., 2015; Mu et al., 2018).

To address the reconstruction and rehabilitation of jointed plain concrete pavements in California more effectively, it is imperative to enhance the design of these roadways and develop performance models for common preventive maintenance and major rehabilitation procedures, such as slab replacement and lane replacement. This study centers on the creation of performance models for slab and lane replacement procedures, enabling the prediction of jointed plain concrete pavement performance over time during its service life. Furthermore, it facilitates the estimation of the appropriate timing for maintenance or major rehabilitation. Additionally, there is a need for a mechanistic-empirical design specific to jointed plain concrete pavements calibrated for the unique conditions, materials, and design approaches of California.

Chapter 3 provides a comprehensive analysis of the factors influencing slab replacement projects. Following a thorough examination of these factors, efforts will be made to formulate a performance model for the slab replacement procedure. This model will find application in the pavement management system, contributing to the improved management of jointed plain concrete pavements in California and facilitating decision-making regarding maintenance processes for the pavement network.

In Chapter 4, a sensitivity analysis of Pavement ME, a well-established nationally calibrated mechanistic-empirical approach to pavement design, is presented. This chapter delves deeply into Pavement ME,

exploring the key design variables specific to Jointed Plain Concrete Pavements (JPCP). These identified variables subsequently inform the calibration of the transverse cracking model within Pavement ME, a vital objective that sets the stage for the subsequent chapters.

Chapter 5 initiates with the development of a performance model for the lane replacement process in jointed plain concrete pavements. This model serves as a tool for calibrating the Pavement ME transverse cracking model, the central focus of this chapter. Calibration was performed using extensive pavement condition survey data derived from California's highway network. An innovative approach to transverse cracking model calibration is presented, utilizing survey data and the design variables from the University of California Pavement Research Center database.

Chapter 6 embarks on an exhaustive analysis of longitudinal cracking failures in California. This involves an extensive factorial of finite element simulations to determine the conditions under which jointed plain concrete pavements are more likely to exhibit longitudinal cracking prior to transverse cracking—a critical addition to the conventional design criteria for JPCP that only considers transverse cracking, considering that rigid pavement slabs are typically not considered "failed" and in need of replacement until they have both a transverse and a longitudinal crack (called "3rd stage cracking" by Caltrans). Based on these findings, design criteria for mitigating longitudinal cracking, which is more prevalent in the California dry climate context than transverse cracking, is proposed.

CHAPTER 2. Background, Problem Statement, and Research Objectives

2.1. Introduction

Rigid pavements are constructed from Portland Cement Concrete (PCC) and are most typically used on roadways with heavy traffic because they require less maintenance and rehabilitation (M&R) during their service lives compared to flexible pavements, which results in less disruption of traffic flow for M&R activities.

There are three types of concrete pavements: continuously reinforced concrete pavement (CRCP), precast concrete pavement (PCP), and jointed plain concrete pavement (JPCP). JPCP is the most common type of rigid pavement constructed in California, much of which is undoweled (no load transfer devices at the joints), and dates back to the original expansion of the National Highway System (NHS) in the 1970s and 1980s. Plain concrete means that there is no reinforcing steel in the slabs. A significant portion of the rigid pavement in California has been in service for many years and those sections are near to the end of their functional service life and long past their original design life of 20 years. Therefore, there is an urgent need for identification of sections in need of M&R or reconstruction. Furthermore, prioritization of the projects and their appropriate treatment should be done based on benefit per cost of each alternative, while considering the budget limitations of the agency.

Preventive maintenance can be the most cost-effective means of protecting the State's infrastructure investment. Based on a report by Caltrans in 2015, the average cost for state highway operation and protection program (SHOPP) roadway rehabilitation project to treat one lane-mile of minor concrete pavement rehabilitation was $364,000 and the average cost of pavement maintenance was $98,000 per lane-mile, therefore, pavement maintenance results in a cost ratio of about 4:1 (Caltrans, 2015b). If the ratio of design lives between rehabilitation and preventive maintenance is less than the cost ratio then preventive maintenance is more cost-effective. The efficient design of new pavements and implementing preventive treatments at optimal intervals can result in lower life cycle cost. The long-term performance of a rigid pavement depends on proper pavement design, the construction quality, and appropriately timed maintenance and repairs. Premature failures of rigid pavements are often the result of one or a combination of these issues: inadequate design, poor construction quality, and failure to carry out on-time maintenance treatments.

Caltrans spent more than $4 billion on pavement projects on over 16,000 lane miles between 2010 and 2014 (Caltrans 2015a). The tremendous costs of pavement network management in the state of California clearly show the importance of an effective and efficient pavement management system (PMS). Such system requires reliable and updated performance data collected from the network. Caltrans has invested in the Automated Pavement Condition Survey (APCS) which captures high-definition images of the pavement surface for determining cracking index through post-image processing. APCS vehicles are also equipped with laser sensors to measure surface roughness, reported as international roughness index (IRI), on every lane-mile of the state's network. The collected data are used to measure and monitor the main performance indices across the network and develop models that can predict the future values of such performance indices. These predictive models, called performance prediction models, are used to determine when performance indices reach trigger values for M&R based on the agency's decision tree, prioritize projects, identify likely most cost-efficient treatments, and conduct budget allocation among sections in need of M&R. This approach allows Caltrans to efficiently control further damage and extend the life of the existing pavement by replacing the parts that have shown early failure. Good performance models are needed to optimize the decision trees for minimum life cycle cost.

Two common types of procedures specific to rigid pavements are "slab replacement", which is maintenance or minor rehabilitation depending on the percentage of slabs replaced, and "lane replacement", which is partial reconstruction/major rehabilitation. Slab replacement extends the life of the existing pavement by replacing the parts that have shown early failure. Lane replacement is a complete reconstruction of a lane when the lane is so deteriorated that it is considered to be at the end of its service life and not cost-efficient to replace the failed slabs one by one.

Lane replacement is used to replace entire lanes and can be applied to selected lanes on multilane highways when other lanes have significant remaining service life. Slab Replacement is a preservation strategy used to replace individual failed slabs with rapid strength concrete (RSC) when much of the remaining pavement segment is still in good condition. Rapid strength concrete will not normally be used for lane replacement projects due to its high cost. However, it will be utilized in situations where minimizing closure duration is critical. In the PMS decision tree, if third-stage cracking in JPCP exceeds 3%, it triggers slab replacement maintenance. However, if the cracking surpasses 10%, it necessitates lane replacement reconstruction.

Cracking in concrete slabs can be categorized into three main types: (1) transverse cracking, (2) longitudinal cracking, (3) and corner cracking as shown in Figure 2.1. Transverse cracks appear

perpendicular to the pavement centerline and extend across the entire slab from one longitudinal edge to the other. Longitudinal cracks appear parallel to the pavement centerline and extend along the entire slab from one transverse joint to the other. Corner cracks occur in one quadrant of a slab and have one endpoint on a longitudinal joint and the other on a transverse joint. Other types of cracking are also possible, such as diagonal cracks or "deformed" transverse or longitudinal cracks, but these are uncommon and are caused by localized issues, such as subsidence.

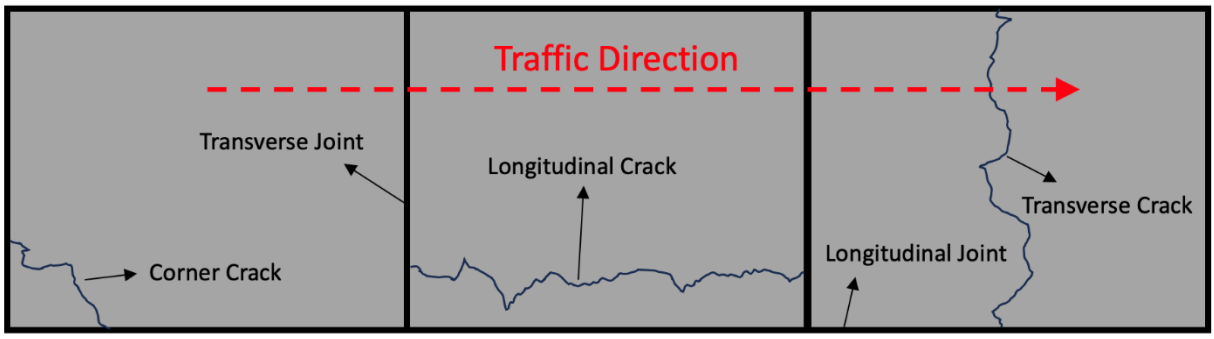

Figure 2.1: Corner, longitudinal, and transverse cracks in JPCP

Caltrans has traditionally categorized the cracking in JPCP in terms of its severity into two main groups: (1) first- stage cracking and (3) third-stage cracking as shown in Figure 2.2. In the official Caltrans definition, first-stage cracking is a crack that breaks the concrete slab into two pieces; this crack can be a transverse, longitudinal, or diagonal crack. Third- stage cracking is defined as a set of two or more intersecting longitudinal or transverse cracks that divide the concrete slab into two or more pieces. However, despite these written definitions, Caltrans raters have long used the simpler definitions that a slab has first-stage cracking if it is divided into two pieces and it has third-stage cracking if it is divided into three or more pieces. Corner cracking is not considered in either of these two definitions, and it is defined and measured separately.

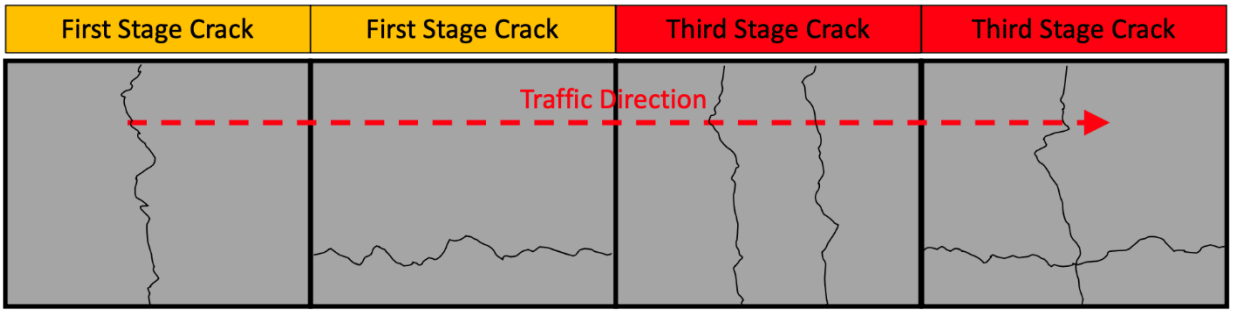

Figure 2.2: First and third stage cracking in JPCP

A goal of this research is to develop performance models for slab replacement and lane replacement in concrete pavement to be used in a decision-making framework, for optimized management of rigid pavements considering life-cycle costs and environmental impacts. Empirical-mechanistic models will be developed that can be used at the network level for budget allocation and project prioritization, and the same information will be used to validate and calibrate mechanistic-empirical models for use at the project level for design.

Mechanistic-empirical (ME) models are empirical but with the variables and potentially the structure of the model based on understanding of pavement damage and distress mechanisms. Historically, pavements in California were designed by empirical performance models developed by collecting long-term performance data of in-service pavements and engineering judgment (Harvey et al., 2000). That practice changed significantly in 2005 when Caltrans adopted ME pavement design (Kannekanti & Harvey, 2007). The mechanistic models of an ME design are used to predict pavement response (deflection, stress, and strain) due to external loads (traffic, climate, and aging). Mechanistic models are developed based on mechanistic analysis of the pavement structures considering the magnitude and the frequency of the loads applied to them. The empirical part relates the pavement response (damage) to pavement distresses observed in the field, hence the mechanistic-empirical name.

Major distresses considered in the ME design of rigid pavements are the percent of PCC slabs with transverse cracking, international roughness index, and faulting. To optimize the design by the ME approach, the empirical distress models that incorporate the results of the calculated mechanistic responses, that are location-specific, should be calibrated with field data. As part of this research, the PMS data containing a significant amount of performance data for rigid pavements across California were used to update the empirical calibration of the ME models previously done with much less extensive data by (Kannekanti & Harvey, 2007). In addition, the prediction of initial transverse cracking in current ME methods will need to be extended to prediction of multiple cracks in the slab, referred to as "3rd stage cracking" which is the Caltrans PMS criterion for both slab replacement and lane replacement.

As mentioned, ME design only considers the transverse cracking, roughness index, and faulting as major performance indices. Longitudinal cracking is not a common distress in most states in the more humid areas of the United States east of the Rocky Mountains. However, condition surveys of pavements in California have shown that longitudinal cracking occurs as frequently as transverse cracking (Harvey et al., 2000). The abundance of longitudinal cracking in California is due to differential shrinkage between the top and the bottom of the slab caused by dry climate and sometimes also use of widened slabs. Studies

have shown that many factors can cause an upward curling of the slab, which suggests that transverse joint loading and drying shrinkage stresses deserve greater consideration since they may lead to longitudinal cracking in concrete pavement (Hiller et al., 2002; Chen et al., 2007; and Ceylan et al., 2013). Therefore, mechanistic-empirical models used for the design of rigid pavements in California should be able to address longitudinal cracking as well. One of the objectives of this study is to incorporate longitudinal cracking as a design criterion for JPCP in California by recommending different design considerations.

In the following sections, a brief background and summary of the literature survey are presented to identify past efforts in these areas and the current state of the knowledge and discuss the challenges and shortcomings of each study. Major gaps in knowledge are then summarized in the next section based on the findings of the literature survey. Research objectives are then presented followed by a summary of expected contributions to the knowledge.

2.2. Slab Replacement and Lane Replacement Performance Prediction Models

Pavement deteriorates due to combined effects of traffic loads and climate conditions. Cracking is a typical distress in jointed plain concrete pavements which is the result of fatigue damage of concrete slabs under repeated application of traffic loads. Faulting is another common distress that happens in JPCP that results in an increase in roughness (measured as IRI), and higher fuel consumption in vehicles (Zaabar & Chatti, 2015). Faulting is the difference in elevation across a transverse joint usually associated with undoweled JPCP. A dowel is a smooth, round steel bar used to provide a mechanical connection between slabs without restricting horizontal joint movement. As is shown in Figure 2.3, dowels are placed across transverse joints of a concrete pavement to transfer loads and ensure proper alignment between adjacent slabs. This helps to reduce joint faulting, improve load transfer efficiency, and extend the pavement's service life. They are crucial for preventing differential deflection and maintaining the structural integrity of the pavement.

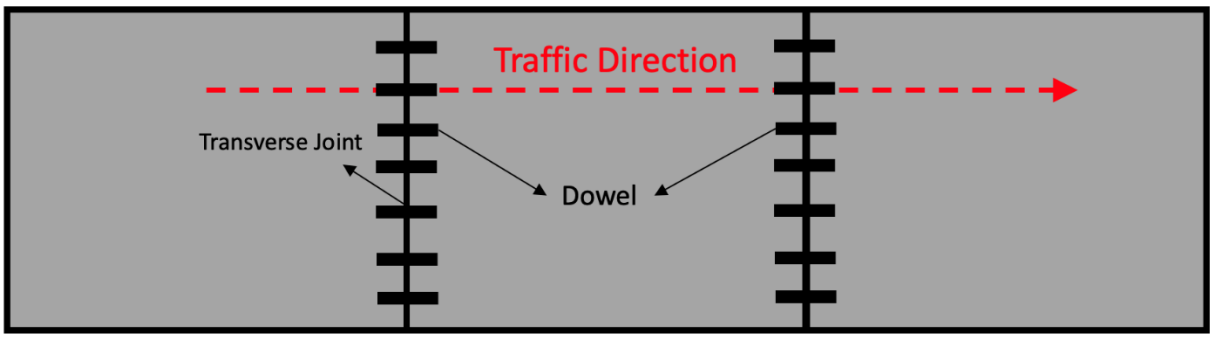

Figure 2.3: Dowel placement in JPCP

Depending on the type and the severity of the distress in the pavement, various types of M&R for JPCP exist. If the goal is to eliminate the faulting distress in the pavement, diamond grinding the surface of the concrete pavement is a viable option to provide a smooth surface for a better ride quality. On the other hand, if the distress that needs to be fixed is cracking, the options are slab replacement, lane replacement, and crack, seat and hot mix asphalt (HMA) overlay (CSOL). CSOL is a pavement rehabilitation strategy that consists of cracking existing JPCP slabs into segments from 3 to 5 ft. long and overlaying with an asphalt pavement layer. Among these, CSOL involves flexible pavement and is not the focus of this research which is focused on rigid pavements. However, slab replacement and lane replacement are the most common treatment procedures done on JPCP and their performance will be studied in this research.

Slab replacement is a maintenance and preservation strategy that involves replacing individual cracked slabs, using rapid strength concrete to minimize the traffic closure time, when much of the remaining pavement segment is still in good condition. Grinding these pavements to remove faulting and other ride issues is also done when needed. Conversely, lane replacement is a reconstruction procedure implemented when a significant portion of the lane is approaching failure, rendering maintenance treatments ineffective. This process involves replacing the deteriorated concrete slabs on a slab-by-slab basis. Although this method is more costly and results in extended traffic closures, it is necessary to restore the structural integrity and functionality of the pavement.

A pavement management system is a set of tools and methods that assist decision makers in determining cost-effective strategies for maintaining, upgrading, and operating a network of pavements. PMS can be used to determine the most appropriate time to rehabilitate pavement, the most cost-effective method, and the money it will cost to maintain a roadway system at a desirable condition level.

Caltrans has been collecting pavement condition data from the California highway network on a regular basis since 1978. For JPCPs, these data include surface roughness index (since 1995), percent of the surfaces that are cracked in the transverse and longitudinal directions (3rd stage cracking), percent of slabs with corner cracking, and faulting (Saboori et al., 2018). Since 2011, Caltrans has invested in the automated pavement condition survey (APCS) which uses high-definition images and lasers to measure performance indices in every lane on the highway network. The result is an enriched performance database along with traffic, climate, and pavement structure data that are used in the California pavement management system called PaveM. These data can be used to predict the future performance of the pavements, assuming that generally the designs and practices are similar. PaveM targets future repairs that provide the best value for the least amount of money. PaveM makes decisions based on a project optimization tool that uses pavement condition, pavement type, climate, and project history to propose the right repair treatment at the right time.

Performance models are essential for PaveM to flag pavements with a future expected need for maintenance or rehabilitation treatment and choose appropriate repairs in a timely fashion that provide the best value for the cost. Performance models are a set of statistically developed tools to predict the future condition of the pavement based on the historical performance data along with traffic, climate, and other sources of relevant data available.

Performance models for different types of treatment for flexible pavements have been previously developed by University of California Pavement Research Center (UCPRC) researchers and incorporated into PaveM (Tseng, 2012). However, there are no performance models available for slab and lane replacement procedures done on concrete pavement in California's pavement management system.

This research aims to develop new performance models for cracking in slab and lane replacement procedures to be incorporated in PaveM to optimize and facilitate the subsequent treatments for rigid pavements. More details on the data collection and development processes for these models are discussed in later chapters. These models will be of use in other places with similar climates and use of rapid strength concrete for slab replacement, and similar climates for lane reconstruction.

2.3. Mechanistic-Empirical Pavement Design Guide (MEPDG) Calibration

Historically pavements were designed using the American Association of State Highway and Transportation Officials (AASHTO) empirical method that is based a road test performed in 1958 to 1960

(AASHTO, 1993). This approach was purely empirical and did not consider different climate regions and material types. In 1998, the AASHTO Joint Task Force on Pavements (JTFP) initiated a National Cooperative Highway Research Program (NCHRP) project to develop a mechanistic-empirical based design approach for new pavement structures and their rehabilitation. The result of this project was the MEPDG in 2004 (Olidis et al., 2004). The MEPDG was an innovative tool to analyze and design pavement structures by using mechanical principles to calculate the stress, strain, and deflections developed due to traffic loads and environmental conditions and relate them to pavement performance (damage and subsequent distresses) through empirical models. Figure 2.4 shows the schematic representation of the MEPDG methodology to predict pavement distresses:

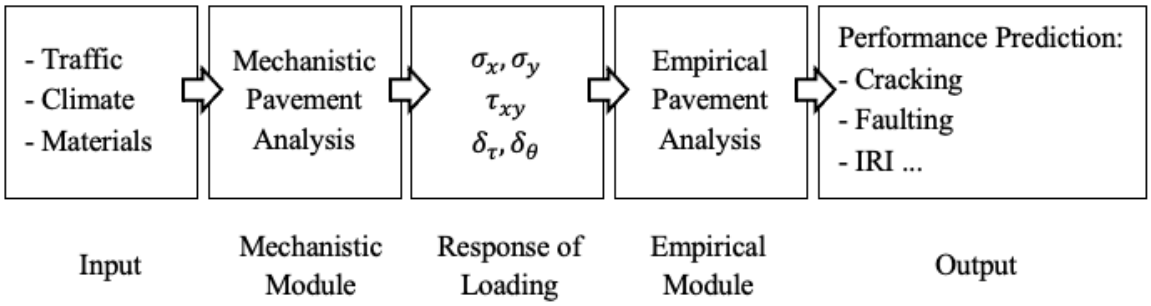

Figure 2.4: Schematic representation of steps in MEPDG analysis (Zhong, 2017)

For JPCP, the distresses predicted by MEPDG are the percent of slabs with transverse cracking, IRI, and faulting. MEPDG first calculates the pavement responses such as stress, strain, and deflection at critical locations utilizing the mechanistic approach and relates those responses to damage using Miner's Law (Miner, 1945) in the case of fatigue damage.

Miner's Law, also known as the Palmgren-Miner linear damage rule, is a method used in fatigue analysis to predict the cumulative damage and failure of a material under varying stress cycles. According to Miner's Law, the total damage in a material subjected to cyclic loading is the sum of the individual damage fractions accumulated during each stress cycle. The law is mathematically expressed as:

$$\sum \frac{n_i}{N_i} = C$$

where:

- n_i is the number of cycles at a specific stress level i
- N_i is the total number of cycles to failure at that specific stress level i
- C is a constant, typically assumed to be 1 for failure prediction

In this equation, the term $\frac{n_i}{N_i}$ represents the fraction of the material's life consumed by the cycles at stress level i. Miner's Law states that failure occurs when the sum of these fractions equals or exceeds the constant C. The value of N_i, the number of cycles to failure at a specific stress level, is determined empirically and is a function of the stress amplitude σ_i and the material's strength properties. It is often represented by an empirical equation derived from fatigue testing data, such as the S-N curve (stress-life curve), which plots the relationship between stress amplitude and the number of cycles to failure. By using Miner's Law, engineers can estimate the remaining life of a material or structure subjected to various stress levels by summing up the damage fractions from each stress cycle. This approach helps in predicting when a material will fail under cyclic loading conditions, aiding in the design and maintenance of structures to prevent unexpected failures.

MEDPG predicts distresses occurring in pavement by empirical models calibrated using performance data obtained from various test sections. Initially, in developing MEPDG, the JPCP transverse cracking model was calibrated based on performance of only 196 field sections with 516 field cracking observations located in 24 states obtained from the Long-Term Pavement Performance (LTPP) and Federal Highway Administration (FHWA) studies (Yu et al., 1998). These data for initial calibration were collected from across the US. However, due to its uneven distribution among different states in the United States, it did not necessarily reflect the conditions such as climate and material properties that exist in each state in the US. Since MEPDG was globally calibrated with these data, NCHRP recommended that every local agency needs to locally calibrate the MEPDG to adjust the model predictions to the conditions specific to each region. Figure 2.5 shows the distribution of pavement sections used to calibrate the MEPDG globally.

According to NCHRP, states and regions that notice a significant difference between the model predictions with the performance data, should consider the local calibration. The local calibration is performed to eliminate this difference through minimizing the bias and standard error between observed pavement distress values obtained from PMS data and pavement performance predictions calculated by MEPDG.

The conventional approach to calibrating an ME method, which has been used since calibration of the Shell Method and Asphalt Institute Method in the 1970s and early 1980s, through calibration of the MEPDG consists of the following steps (Wu et al., 2021):

- Identify short sections of pavement.
    - Preferably most of the pavements have some failure on them, otherwise the time to failure would be uncertain because it hasn't occurred yet.
    - The sections need to have a construction time history.
- Collect the materials properties on the test sections.
- Back-calculate the traffic and materials properties to the time of construction.
- Simulate the performance using measured materials properties using Miner's Law, which has the following issues:
    - The response engine calculating critical stresses, strains, and deformations is unverified.
    - The damage evolution and predicted state of damage on the section is also unverifiable because use of Miner's Law forces the shape of the damage evolution curve.
    - Only the end state of distress is used for calibration.
- Find calibration coefficients for the calculated damage-to-distress transfer function to minimize the errors between observed and measured distress.
- Use the variability around the minimized error transfer function for reliability.

The conventional approach has several limitations:

- It requires expensive and time-consuming sampling and testing of materials properties for each section, resulting in a small number of sections being available for calibration.
- It ignores the fact that a design-bid-build (low-bid) designer does not know the performance-related properties of the materials the contractor will bring to the job; this results in a blurred understanding of the sources of variability and their consideration in the design reliability approach.

A few State Highway Agencies (SHA) in the US have calibrated MEPDG with their data which resulted in better performance predictions compared to nationally calibrated MEPDG. Arizona, Minnesota, Colorado, Florida, Indiana, Missouri, Iowa, Ohio, and Oregon are the states that have attempted to calibrate MEPDG for JPCP.

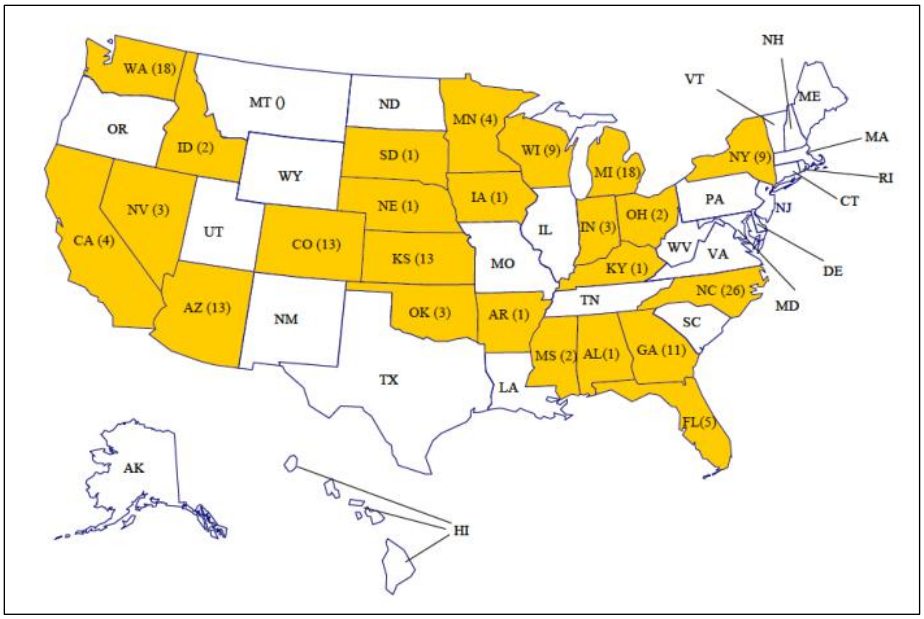

Figure 2.5: Geographical distribution of the new JPCPs used for initial national MEPDG calibration (NCHRP, 2004)

Minnesota (Velasquez et al., 2009) performed a calibration for rigid pavements and concluded that no adjustment was needed for the faulting model however they needed to recalibrate the transverse cracking model. Iowa (Ceylan et al., 2013) chose a very limited set of 35 JPCP sections and found that the nationally calibrated faulting model significantly underestimates the faulting in the state, whereas the transverse cracking and IRI models overestimate the values observed in the JPCP sections, although making statistical inference based on such a small number of sections is debatable. They recalibrated transverse cracking, faulting, and IRI models and reached models with lower bias and standard errors. Arizona (Darter et al., 2014) performed a sensitivity analysis on MEPDG based on the standard pavement design practices available in their state to find the variables with the most influence on the model predictions. The sensitivity analysis guided them to invest in collecting input data for the most important variables and use the default or average values for less critical input variables for which they did not have sufficient data. They recalibrated transverse cracking, faulting, and IRI models with PMS data.

The MEPDG models for JPCP with their coefficients that should be calibrated are shown in Table 2.1. Table 2.2 shows the locally calibrated MEPDG coefficients for rigid pavement performance models developed by the SHAs in the states of Arizona, Colorado, and Florida. The results show that significantly different coefficients are possible in different states compared to the coefficients that are nationally calibrated.

Table 2.1: Distress transfer functions in MEPDG (NCHRP, 2004)

Performance Model	Transfer Function	Coefficients
Transverse Cracking	$CRK = \frac{100}{1 + \boldsymbol{C_4}(DI_F)^{\boldsymbol{C_5}}}$	C_1, C_2 C_4, C_5
Faulting	$FAULTMAX_0 = \boldsymbol{C_{12}} * \delta_{curling} * \left[log(1 + \boldsymbol{C_5} * 5.0^{EROD}) * log\left(\frac{P_{200} * WetDays}{P_s}\right)\right]^{\boldsymbol{C_6}}$ $FAULTMAX_i = FAULTMAX_0 + \mathbf{C_7} * \sum_{j=1}^{m} DE_j * log(1 + \boldsymbol{C_5} * 5.0^{EROD})^{\boldsymbol{C_6}}$ $\Delta Fault_i = \boldsymbol{C_{34}} * (FAULTMAX_{i-1} - FAULT_{i-1})^2 * DE_i$ $Fault_m = \sum_{i=1}^{m} \Delta Fault_i$ $C_{12} = C_1 + C_2 * FR^{0.25}$ $C_{34} = C_3 + C_4 * FR^{0.25}$	C_1, C_2, C_3 C_4, C_5 C_6, C_7
Roughness Index (IRI)	$IRI = IRI_I + \boldsymbol{C_1}CRK + \boldsymbol{C_2}SPALL + \boldsymbol{C_3}TFAULT + \boldsymbol{C_4}SF$	C_1, C_2 C_3, C_4

Table 2.2: Calibrated MEPDG coefficients for Arizona, Colorado, and Florida (Zhong, 2017)

Coefficients	Model	MEPDG	Arizona	Colorado	Florida
C1	Cracking	2.000E+00	2.000E+00	2.000E+00	2.839E+00
C2		1.220E+00	1.220E+00	1.220E+00	9.647E-01
C4		1.000E+00	1.900E-01	6.000E-01	5.460E-01
C5		-1.990E+00	-2.067E+00	-2.050E+00	-5.946E-01
C1	Faulting	1.018E+00	3.550E-02	5.104E-01	4.047E+00
C2		9.166E-01	1.147E-01	8.380E-03	9.166E-01
C3		2.848E-03	4.360E-03	1.470E-03	2.848E-03
C4		8.837E-04	1.100E-07	8.345E-03	8.837E-04
C5		2.500E+02	2.000E+04	5.999E+03	2.500E+02
C6		4.000E-01	2.309E+00	8.404E-01	7.900E-02
C7		1.833E+00	1.890E-01	5.929E+00	1.833E+00
C8		4.000E+02	4.000E+02	4.000E+02	4.000E+02
C1	IRI	8.203E-01	6.000E-01	8.203E-01	8.203E-01
C2		4.417E-01	3.480E+00	4.417E-01	4.417E-01
C3		1.493E+00	1.220E+00	1.493E+00	2.256E+00
C4		2.524E+01	4.520E+01	4.520E+01	2.524E+01

In 2005, Caltrans decided to adopt ME design procedures for designing pavements in California. To calibrate the models, researchers at UCPRC sampled 52 concrete pavements and 43 crack, seat, and overlay sections, covering all the state's major climate regions, and collected all the inputs needed to run MEPDG (Kannekanti et al., 2006). California has more pavement climate regions than any other state

using national definitions for climate region. No other state has the range of wet to dry and hot to cold conditions, and variability of subgrade conditions found in the state. However, they had limitations in their study listed as follows:

- Data recorded in the Caltrans PMS database, transverse, IRI, and faulting were very limited for local calibration.
- The definition for transverse cracking was not consistent with the one defined in MEDPG guide. Therefore, researchers needed to adjust the measurements with an approximate solution.
- Poor quality of IRI data in the Caltrans PMS database.
- Difficulty in obtaining project-specific information such as construction year, pavement structure, and material properties.
- The calibration dataset did not cover all the different pavement sections commonly designed and constructed in California including design features such as tied concrete shoulders, widened truck lanes, different base types, and doweled transverse joints.

After running MEPDG on selected pavement sections, researchers at UCPRC concluded that concrete stiffness and friction/bonding/creep between the PCC and base layer had a significant impact on the cracking model predictions. They found that MEDPG models generally gave better predictions, even with default model parameters, using estimated stiffness from compressive strength, and 136 months to loss of full friction provided the best calibration for transverse cracking, although with massive variability resulting in a poor correlation with observed performance. However, in addition to the large variability, they stated that the cracking model might under-predict the cracking in coastal climate regions and thus needs further investigation. They recommended that the nationally calibrated coefficients for cracking model remain unchanged and 136 months to loss of friction between concrete and base should be used to get better results. They reported that the faulting model predictions were reasonable for the predominant undoweled pavements, and the model parameters did not need recalibration. They were not able to recalibrate the IRI model due to the poor quality of IRI data in the Caltrans PMS at the time of study.

Since 2005, Caltrans has considerably increased investment in data collection from the state highway network and has done a better QA/QC on data collection and cleaning and as a result, a much more reliable dataset is now available in the PMS database. Data such as pavement structure, base type, shoulder type, slab length, construction year that were scarce in the previous study are now abundantly available, almost for every project over the past 30 years. However, some project-specific data such as material properties for concrete and lower layers still are not available.

Having an extensive pavement condition database with much better-quality data and changes that have been made in MEPDG since its first release, urged Caltrans to decide to recalibrate the updated MEPDG for their design needs. As part of this research, efforts were made to recalibrate the MEPDG with the available data for California.

The proposed calibration approach developed in this study to calibrate PavementME aims to improve calibration and the reliability approach used in ME design by doing the following:

- Use all the good quality distress performance data and as-built data in the Caltrans PMS databases collected since 1978and quality checked over the last 10 years; this provides orders of magnitude more performance data for calibration, with the data organized by project.
- Use median properties to match median performance, and use the variability of observed median performance to determine between-project variability, after using PavementME account for the effects of climate, pavement cross section, and traffic.
- Back-calculate within-project variability by matching the shape of observed performance time history.

2.4. Longitudinal Cracking Design Criteria for JPCP in California

In jointed plain concrete pavements, longitudinal cracks form parallel to the direction of traffic whereas, transverse cracks appear in the perpendicular direction. Historically, longitudinal cracking has not been considered in pavement design due to a lack of understanding of the mechanical processes involved in drying shrinkage, which is a significant factor in the occurrence of such cracking. Additionally, longitudinal cracking is uncommon in humid climates, which is where design methods like MEPDG were initially developed.

A few studies in states with dry climates in the US have shown that longitudinal cracking in JPCP is as common as transverse cracking and it should be addressed in the design process. Based on pavement condition surveys in California, Harvey et al. (2000) stated that longitudinal cracking is as frequent as transverse cracking in California. They have observed that longitudinal cracking occurs mostly on the wheel path and in slabs with high faulting and can run the entire slab length and happens in consecutive slabs.

Chen and Won (2007) conducted field investigations on identifying the underlying causes of longitudinal cracking in concrete pavement in Texas. They found that late and shallow saw cutting of longitudinal saw cut joints, inadequate base support under the concrete slab, and having high CTE aggregates in the concrete mixtures were the main reasons for longitudinal cracking in Texas, however, they did not consider the drying shrinkage and the environmental impacts in their study. Using finite-element analysis, Hiller and Roesler (2002) compared the critical tensile stress near the transverse joint (critical for longitudinal cracking) to those at the mid-slab edge (critical for transverse cracking) for California-type JPCP and concluded that residual negative gradients due to built-in temperature curling and differential drying shrinkage together with traffic loading can cause either longitudinal, transverse, or corner fatigue cracks depending on the slab geometry and shoulder type. Another study by Ruiz et al. (2008) measured the significant curled-up shape of concrete slabs through profile analysis and concluded that the main mechanism of longitudinal cracking was the action of heavy traffic loads on curled slabs. Xiao and Wu (2018) performed field investigation and numerical simulations for concrete pavement in Louisiana and concluded that in addition to construction problems, slabs widened to 15 ft. and tied concrete shoulders would increase the likelihood of longitudinal cracking. They also developed an empirical model that predicts the length of longitudinal cracking by considering traffic, age of service, slab geometry (length, width, shoulder type, and slab thickness), subgrade resilient modulus, and base stiffness as predictors, however, their empirical model does not utilize damage as an input variable and therefore is not compatible with MEPDG damage prediction results.

All these studies showed that longitudinal cracking commonly occurs in dry climates, but they have not developed a mechanistic-empirical model that can also be used in MEDPG as an analysis tool and a design criterion. To develop guidelines for design of JPC pavements considering longitudinal cracking, one should notice that the critical load and stress locations for longitudinal cracking are different than those for transverse cracking that necessitates a new analysis if longitudinal cracking is to be considered. This new analysis needs to consider different load positions and compute stresses at different locations.

Lederle (2014) initiated a study to incorporate a longitudinal cracking prediction model in the MEPDG, one that was not included in the original MEPDG, based on mechanistic-empirical pavement design. A model compatible with the MEPDG framework for predicting and analyzing incremental damages from longitudinal cracking was developed, and stresses exerted from axle loading and environmental loading at critical locations related to longitudinal cracking were computed. In this approach, as usual, the concrete pavement is designed for transverse cracking, IRI, and faulting and once all these design criteria were met, it will be checked for longitudinal cracking potential. The longitudinal damage model determines the

level of longitudinal damage at various locations along the transverse joint. The highest level of damage at any node along the transverse joint is considered as the level of longitudinal damage. The damage ratio will be computed as the ratio of longitudinal damage to transverse damage. If the damage ratio is less than 1, then transverse fatigue damage will control, though this does not guarantee that the design is acceptable, and that longitudinal cracking will not occur. A damage ratio greater than 1 indicates that longitudinal cracking will be the dominate failure mode but does not automatically disqualify the pavement design. To minimize the amount of longitudinal cracking which will occur, the longitudinal cracking fatigue damage must be below the acceptable threshold that has not been set in the study.

While the damage ratio is a useful tool in the design process, it should not be treated as the only criteria for determining if longitudinal cracking is a problem in a specific pavement design. A damage ratio less than 1 indicates that transverse cracking will be the predominate failure type but does not indicate that longitudinal cracking will not occur. Indeed, if both transverse and longitudinal fatigue cracking damage are high, both distresses could be seen. Likewise, a damage ratio greater than 1 does not guarantee that longitudinal cracking will be a problem. If both transverse and longitudinal fatigue cracking damage are very low, it is entirely possible that the damage ratio could be greater than one while neither fatigue damage is high enough to result in significant cracking. Therefore, the damage ratio should merely be used as a quick comparison tool to determine the predominate failure mode, but fatigue damage levels should also be examined.

In this study, various design parameters are assessed and analyzed for their impact, including slab length, slab thickness, shoulder type, load transfer efficiency (LTE), base type, and coefficient of thermal expansion (CTE), on stress distribution at critical locations, particularly focusing on longitudinal cracking. To achieve this, finite element software (ISLAB2000) was used to simulate the traffic and environmental loads on JPCP and calculate the induced tensile stresses at critical locations for both transverse and longitudinal cracks. The findings from our investigation will be utilized to propose new design guidelines for JPCPs under diverse climate regions in California and different load conditions.

2.5. Problem statement and gaps in the knowledge

Based on the previous discussion presented in this chapter, the current gaps in the knowledge are:

- Efficient asset management requires life cycle thinking, the ability to predict how the section will perform in the future and estimate when future maintenance and repairs are required. As discussed earlier, maintaining road transportation infrastructure is extremely expensive, and PMS

are used to predict future maintenance and rehabilitation treatments and their costs. Currently, the performance models are overly simplistic, considering only pavement age as a variable to predict performance, which is inadequate. Reliable performance models are essential for an efficient PMS.

- MEPDG models need to be calibrated for the region in which pavement design is being conducted. This calibration should be done using historical field data specific to the region. Previously, a few other state agencies have conducted such calibrations, however, those efforts included data from a very limited number of pavement segments (less than 50). Such calibration has not been done in California and as mentioned earlier, models calibrated for other regions are not necessarily applicable to sections in California and the very limited scope and number of sections that were included in studies by other states make such models even less applicable for California.
- The MEPDG models have never been calibrated using extensive PMS data before. The conventional calibration approach has several limitations:
    - It requires expensive and time-consuming sampling and testing of materials properties for each section, resulting in a small number of sections being available for calibration.
    - It ignores the fact that a design-bid-build (low-bid) designer does not know the performance-related properties of the materials the contractor will bring to the job; this results in a blurred understanding of the sources of variability and their consideration in the design reliability approach.
- While jointed plain concrete pavements are conventionally designed to address transverse cracking, faulting, and IRI, the MEDPG does not consider longitudinal cracking, although it is common in the dry western states. Longitudinal cracking is a significant issue in California, necessitating the inclusion of design guidelines to mitigate this specific distress in JPCP structures.

2.6. Research Objectives

The objectives of this study are as follows:

- **Investigate Parameters Affecting Slab Replacement Treatments:** Examine the factors influencing the performance of slab replacement treatments on JPCP. Develop cracking performance models that can be integrated into the pavement management system (PMS) as a decision-making tool for selecting appropriate future treatments.

- **Analyze Lane Replacement Reconstruction Procedures:** Study the parameters affecting the performance of lane replacement reconstruction. Recommend suitable design practices and develop performance models for cracking in lane replacements. These models should accurately predict the future performance of concrete pavements and be usable within the California PMS.
- **Collect Statewide Median Design Values:** Collect statewide median values for JPCP design variables from historical test data of JPCP projects across California. This data will serve as a benchmark for assessing pavement performance.
- **Calibrate MEPDG Models Using Extensive Data:** Utilize Pavement ME software to run approximately 10,000 scenarios from the PMS database to calibrate the MEDPG transverse cracking model. This extensive calibration will enhance the accuracy of performance predictions.
- Use all the good quality distress performance data and as-built data in the Caltrans PMS databases collected since 1978and quality checked over the last 10 years; this provides orders of magnitude more performance data for calibration, with the data organized by project.
- Use median properties to match median performance, and use the variability of observed median performance to determine between-project variability, after using PavementME account for the effects of climate, pavement cross section, and traffic.
- Back-calculate within-project variability by matching the shape of observed performance time history.
- **Develop New MEPDG Calibration for Variability:** Develop a new MEPDG calibration procedure that considers within-project, between-project, and between-contractor variability observed in PMS data. This calibration will improve the reliability of performance predictions by accounting for diverse conditions and practices.
- **Calibrate Transverse Cracking Model:** Calibrate the MEPDG transverse cracking model for JPCP based on comprehensive California PMS data using a novel statistical approach. This calibration will provide more accurate predictions of transverse cracking occurrences.
- **Conduct Finite Element Simulations and Compare with PMS Data:** Perform hundreds of finite element simulations using ISLAB2000 and compare the results with findings from PMS data analysis. Investigate the causes of longitudinal cracking in California, considering factors such as material properties, environmental conditions, and design and construction practices. Propose design recommendations for JPCP to mitigate longitudinal cracking effectively.

CHAPTER 3. Slab Replacement Cracking Performance Model

3.1. Introduction

Most of the JPCP roads in California are now well past their initial design life and have thus been subject to considerable maintenance actions over the last twenty years. However, besides complete replacement, or overlaying the concrete with asphalt, there are few maintenance options for JPCP, especially for busy roads where closure options are limited. The California Department of Transportation (Caltrans) has thus had a standard practice of replacing badly cracked slabs, using rapid strength concrete, and grinding these pavements to remove faulting and other ride issues when needed (Caltrans, 2004). This whole procedure is categorized as the 'slab replacement' treatment in Caltrans records.

The practice of slab replacement involves the removal of the old cracked slab, cleaning of the base material and joints, and then casting of a new slab in place. This is mostly performed in an overnight closure. The new slabs are then ground during a second closure to match the profile of the surrounding pavement. In some cases, the base material is also removed, and a full-depth slab is cast, or the base is replaced with asphalt. Dowels and tie bars might also be installed, although this is uncommon, because the time to drill the holes or perform retrofit is a limitation. Because the slabs must be opened to traffic within hours of construction, it is a requirement that some type of rapid set cement be used.

As with other maintenance treatments, the stated design life for these replaced slabs is ten years. Because these slabs use rapid set concrete, and lack some of the features typically associated with good slab design (such as possibly a smooth base to allow expansion and contraction), there has always been some question about the field performance of these replaced slabs. To complicate the issue, while the replaced slabs are very noticeable on construction, they often age to a color similar to the surrounding slabs, and there are often slab replacements in a section from more than one slab replacement project over time, resulting in various replaced slabs of different ages. This, along with some anecdotal evidence of early-age cracking of these slabs, has resulted in Caltrans engineers not having a good sense of how well these replaced slabs are performing, despite some initial studies.

Concurrent with these concerns about the performance of replaced slabs, Caltrans has adopted Pavement Management System, known as PaveM since 2011. This is used to optimize and facilitate the maintenance and rehabilitation of the existing state highways in a timely and cost-efficient manner. As part of this process Caltrans has been updating and improving their data collection procedures, by moving

from manual data collection to automated data collection at highway speed. Along with providing per slab cracking data, these surveys also provide high quality right-of-way and downwards images of the pavement, enabling desktop surveys of all lanes.

Caltrans has been collecting pavement condition data from the California highway network on a regular basis since 1978. For JPC pavements these data include surface roughness (from 1995), percent of the surfaces that are cracked in the transverse and longitudinal direction, percent of slabs with corner cracking, and joint and crack condition. For the purposes of management, Caltrans has used two criteria for the condition of slabs, known as first and third stage cracking. The official Caltrans definitions are that a slab is first stage cracked if it has non-intersecting transverse, longitudinal, or diagonal cracks, and third stage cracked if it has two or more intersecting cracks (longitudinal and transverse) that divide the slab into three or more pieces (Caltrans, 2004). However, despite these being the written definitions, Caltrans condition raters have long used the simpler criteria that a slab is first stage cracked if it is divided to two pieces and third stage cracked if it is divided into more than two pieces.

It should also be noted that there is a different between the terms ‘slab replacement’ and ‘replaced slabs’ and their associated collected data (first and third stage cracking). ‘Slab replacement’ is defined as a stretch of a road that slab replacement treatment has been performed and the first and third stage cracking are calculated as the ratio of cracked slabs, whether new or old slabs, to the total number of slabs in that portion of the road. On the other hand, the term ‘replaced slabs’ is defined only for the actual slabs that have been replaced and first and third stage cracking are calculated as the ratio of cracked replaced slabs to the total number of replaced slabs. In this report, the second definition, replaced slabs, will be used unless otherwise stated.

PaveM, being a fully featured PMS, requires performance models to predict the future condition of treatments, one of which is slab replacement. Updating these performance models is thus an ongoing task as new data from condition surveys become available.

The data available for the Caltrans network also include traffic and climate information. Collecting these data is the initial step for developing performance prediction models. Reliable performance models will identify sections that need M&R and prioritize them based on life cycle costs or environmental life cycle impacts.

The goals of this study were to establish if early age cracking existed, and if the replaced slabs met their design life. In the process, if any factors contributing to early age cracking, such as different cement types, could be established, then these would be investigated. This chapter details the findings of this research, including the development of a statistical model for the performance of these replaced slabs. However, other than the impact of thickness, traffic, and doweled/undoweled condition on the life of these replaced slabs, other factors such as climate region, material [calcium alumino silicate (CSA) or type III cement], base type, and slab length could not be established, mostly due the lack of availability of construction data from these projects. At the end, a brief engineering analysis will be performed on the proposed performance model outcomes and necessary recommendations on design and construction practices will be given.

3.2. Methodology

Figure 3.1 shows the overall flow chart of the methodology.

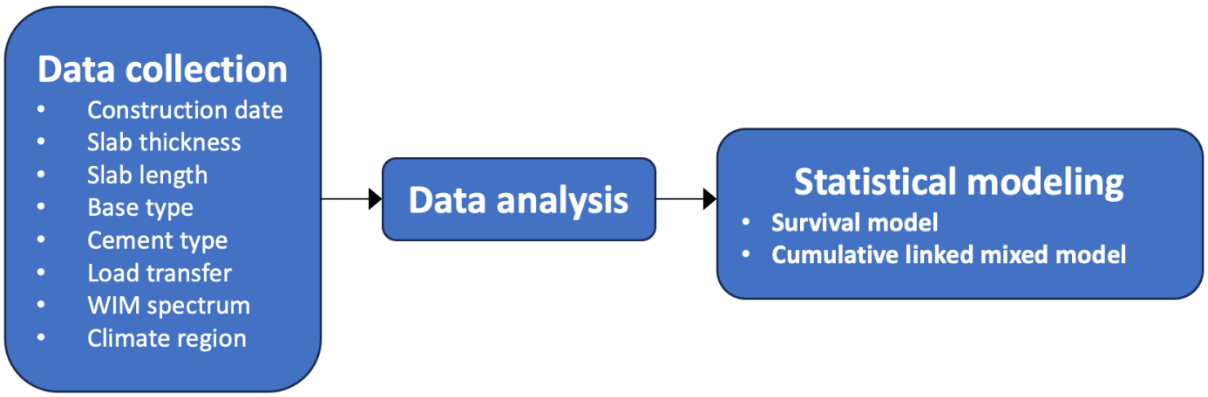

Figure 3.1: Methodology flow chart

To evaluate the performance of replaced slabs, those slabs must first be identified, but Caltrans does not normally record the exact location of replaced slabs in their construction documentation – only the areas where slabs are to be replaced (in fact, in many projects the exact slabs to be replaced are only identified in the construction closure). Even identifying a location for a data collection closure can be difficult because one might find more or less replaced slabs than expected once one is able to actually inspect the slabs. As a result there are few available datasets for this type of modelling work. In addition, there are local differences in materials, specifications, construction practices and environment, which mean that there is significant variability between pavement performance in different regions, so performance prediction models need to be calibrated based on regional data.

Luckily, a previous study in California was conducted by Fugro (Miller, 2014) on the field performance evaluation of slabs replaced with rapid strength concrete. The report for the Fugro project summarizes the results of falling-weight deflectometer (FWD) testing, manual distress surveys, and laboratory testing of core samples. The data from this previous study were made available for the current study, but were of limited scope. In addition to Fugro data, another source of data were the images from the Caltrans Automated Pavement Condition Survey (APCS), that allows one to perform a 'virtual drive' on the state highway network.

The Caltrans APCS highway speed data collection with high-definition cameras, lasers and other sensors to capture pavement condition information. The survey was first conducted in 2011 on the full state network, and then in 2012 on around half of the network. Additional surveys have been performed in 2015 and 2016, but the images and detailed data were not available. Figure 3.2 shows an example of the images available from this survey. To collect data for developing performance models only the 2011 APCS data were used. As a concrete slab ages, it would be more difficult to distinguish the newly replaced slabs from the older existing ones on images, therefore, only the last five years of slab replacement projects done before the 2011 APCS were considered in this study. There were 39 slab replacement projects with available APCS data between 2005 and 2010, constructed in four different climate regions including Inland Valley, Low Mountain, South Coast, and Central Coast. Using additional slab replacement projects from the construction history data in the PMS, it was possible to find these locations within the APCS data and manually extract slab cracking information. The data set assembled includes the project location and construction dates, slab thickness, total number of slabs replaced, number of slabs cracked, traffic information, climate region, and doweled/undoweled condition.

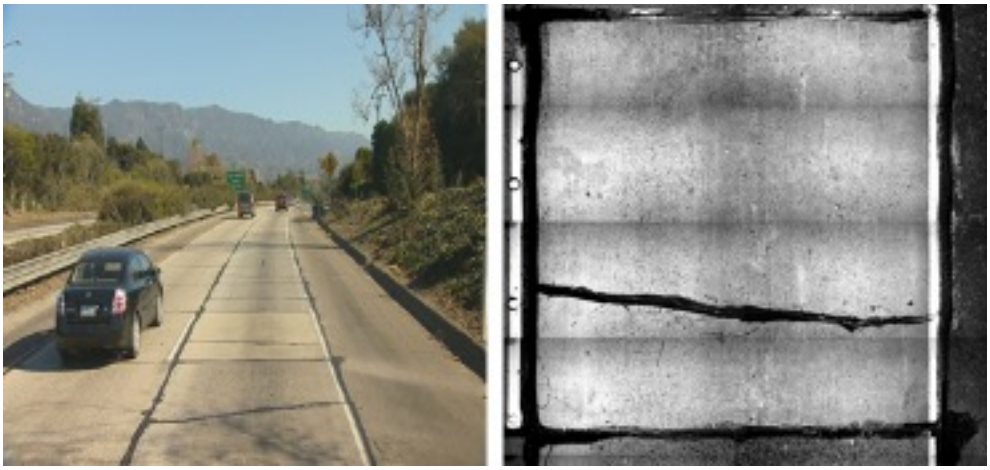

Figure 3.2: Right of Way (ROW) and downwards images of a replaced slab, with a single transverse crack that has been sealed.

Furthermore, some of the projects studied as part of the Fugro survey were evaluated again in this study using the 2011 APCS to provide an additional data point. The Fugro cracking data were adjusted to use the Caltrans working definitions for 1st and 3rd stage cracking.

For the combined set of projects thickness information was extracted from as-built documents and from a 2010 state-wide Ground Penetrating Radar (GPR) study. Construction dates were also extracted from the construction history. The location was used to determine the climate zone based on the Caltrans climate zones for Mechanistic-Empirical design (the same climate zones are also used in the PMS) (Ongel et al., 2004). Traffic data were calculated using estimation of load spectra based on the University of California Pavement Research Center analysis of weigh-in-motion (WIM) data collected by Caltrans (Lu et al., 2008). This procedure has recently been updated, and simplified, and the new process has not yet been published. One of the simplifications is that the previous WIM "groups" have been reduced to five load spectra, with Spectrum 1 having predominantly unloaded axles and Spectrum 5 having predominantly fully loaded axles. Figure A.22 in the appendix illustrates the axle type distribution for different WIM spectrums. The traffic estimation process provides the appropriate Spectrum for each location, along with Average Annual Daily Traffic and Truck Traffic (AADT and AADTT), the annual Equivalent Single Axle Loads (ESALs, using a Caltrans standard power of 4.2), and the ESALs for each lane.

In the Fugro study, load transfer was found to have a significant impact on the performance of the replaced slabs and was used as an approximation for whether the replaced slabs were doweled or undoweled. In this study, doweled/undoweled condition was collected form as-built documents for each slab replacement project, however, for some projects, this information was not available.

Figures 3.2-3.7 show a summary of data collected for this study. There were 4,399 concrete slabs replaced in all slab replacement projects. Figure 3.3 shows the slab count distribution with respect to slab age categorized based on slab condition. This graph shows that most of the slabs are in the initial years of their service life and 737 slabs (about 17% of total replaced slabs) have cracked by the age of four years which shows that early age cracking is a major issue among the slab replacement projects done in California that could be attributed to inefficient design or poor-quality construction practices. There are various design factors that might affect the cracking in slabs such as slab thickness, slab length, mix design (cement type), dowel condition, and base type that some of them will be investigated in the following sections.

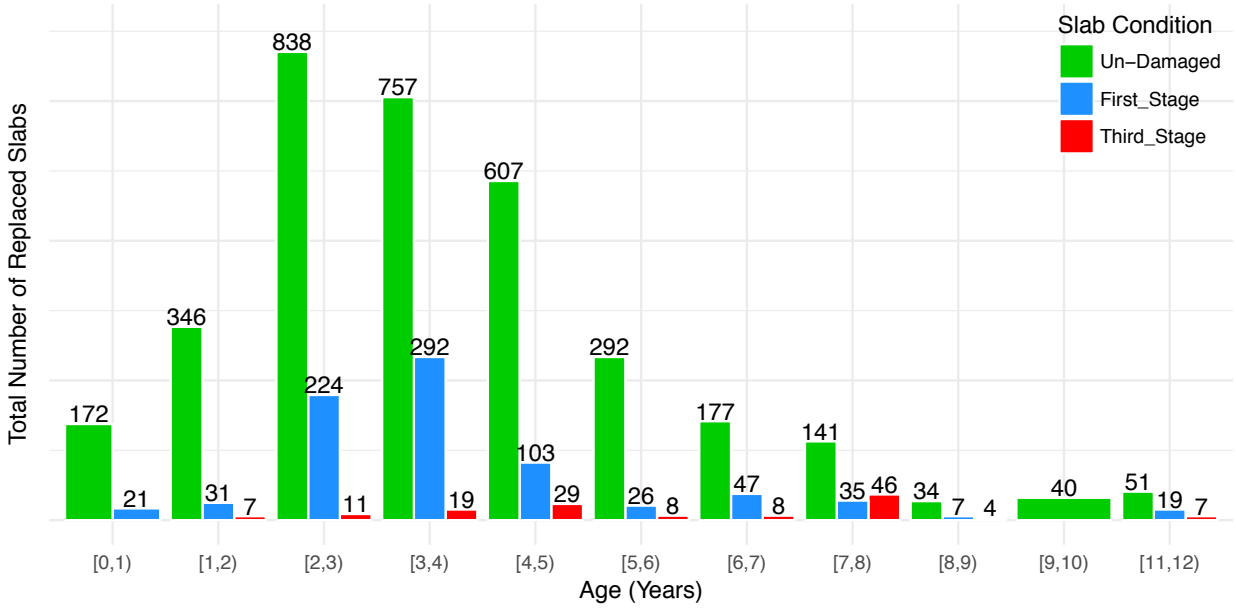

Figure 3.3: Age distribution among replaced slabs

Figure 3.4 is the slab count distribution among different thicknesses categorized based on slab condition. About 35% of slabs with 0.6-0.7 ft., 21% of slabs with 0.7-0.8 ft., 22% of slabs with 0.8-0.9 ft., 12 % of slabs with 0.9-1.0 ft., 8.8% of slabs with 1.0-1.1 ft. and none of the slabs with 1.1 ft. and higher thicknesses have cracked showing that thicker slabs perform much better than thinner ones.

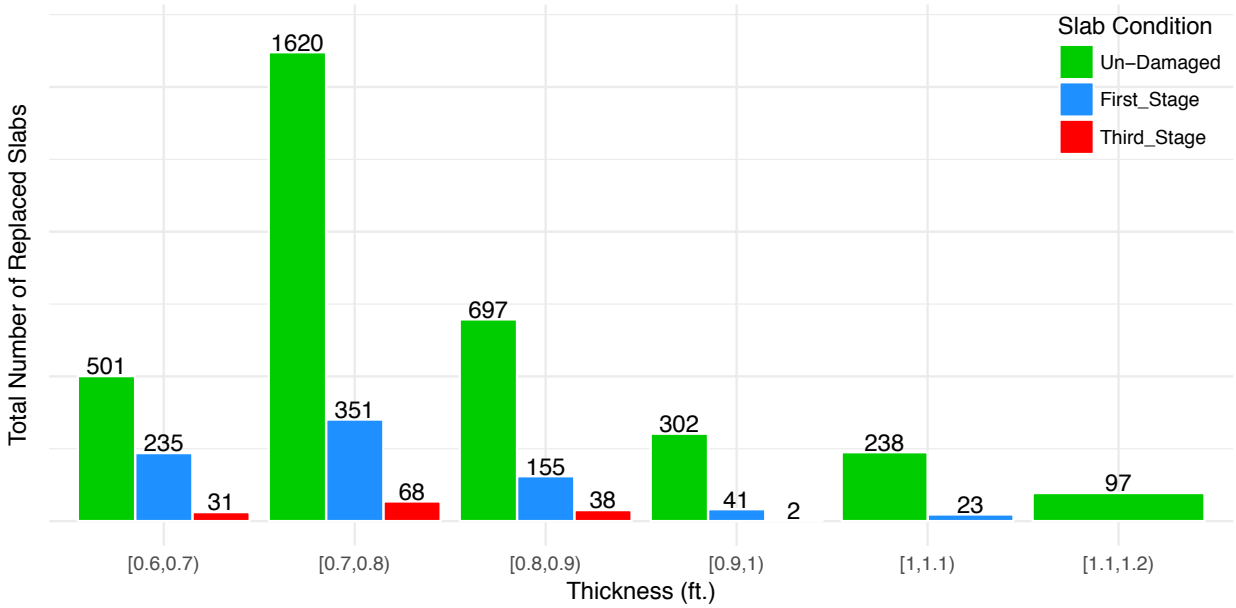

Figure 3.4: Thickness distribution among replaced slabs

Bar plots in Figure 3.5 indicate that most of the replaced slabs were constructed with no dowels and it can be seen that doweled projects performed better than undoweled ones and depicted much less cracking.

This confirms the results published by Fugro that constructing replaced slabs with dowel bars significantly reduces the cracking and increases the ride quality.

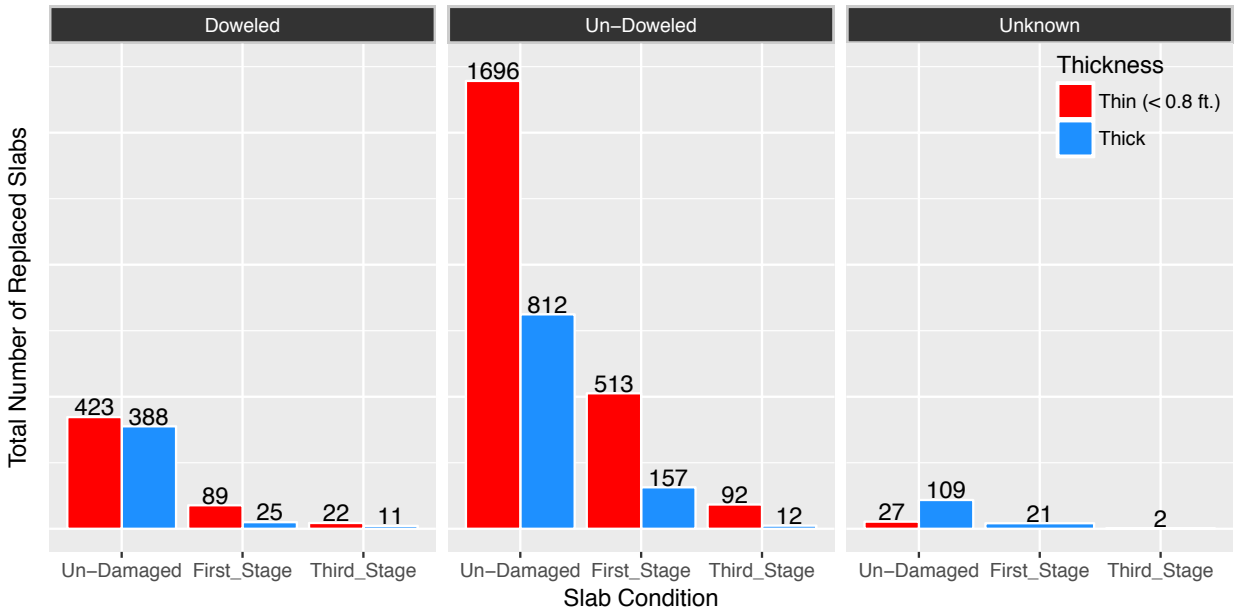

Figure 3.5: Doweled/UnDoweled condition distribution among replaced slabs

Figure 3.6 shows that most of the replaced slabs are under WIM spectrum 2 and 3 which correspond to light to heavy traffic loads.

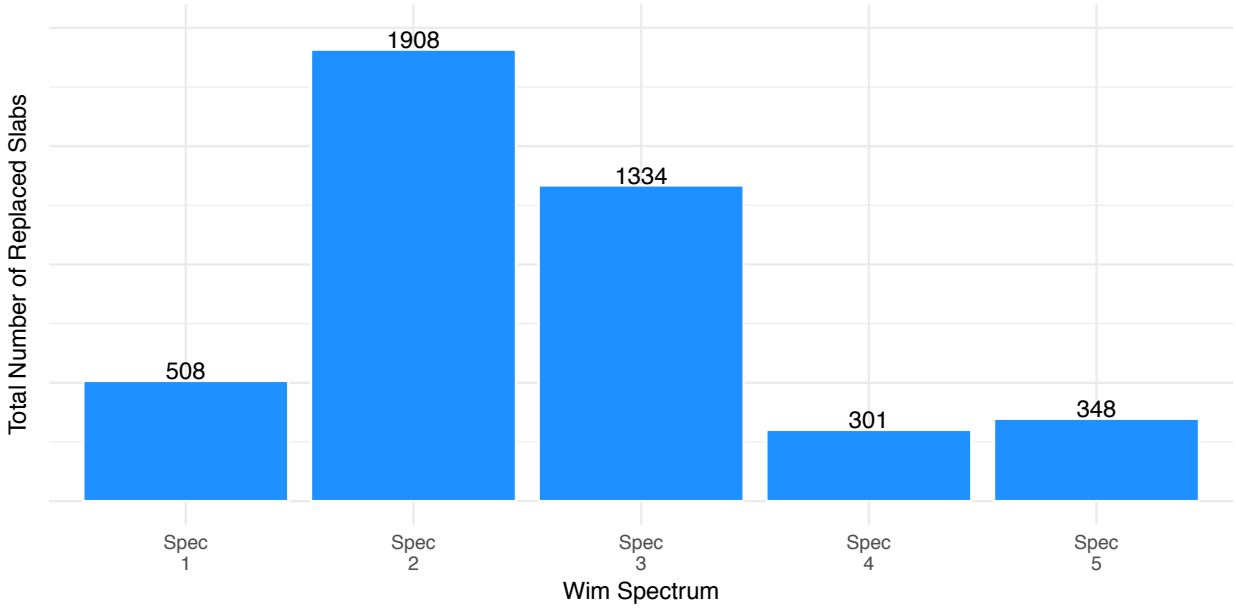

Figure 3.6: Wim spectrum distribution among replaced slabs

Based on Figure 3.7, there were many missing values for cement type, since Caltrans did not document the mix design and material type for slab replacement projects, it was not possible to collect this data for the additional projects added in this study. However, to check the impact of cement type on the performance of replaced slabs and compare the results with the conclusion drawn by Fugro stating that replaced slabs constructed with type III cement performed better than the ones made by CSA, this parameter will be included in the statistical modeling in the next section.

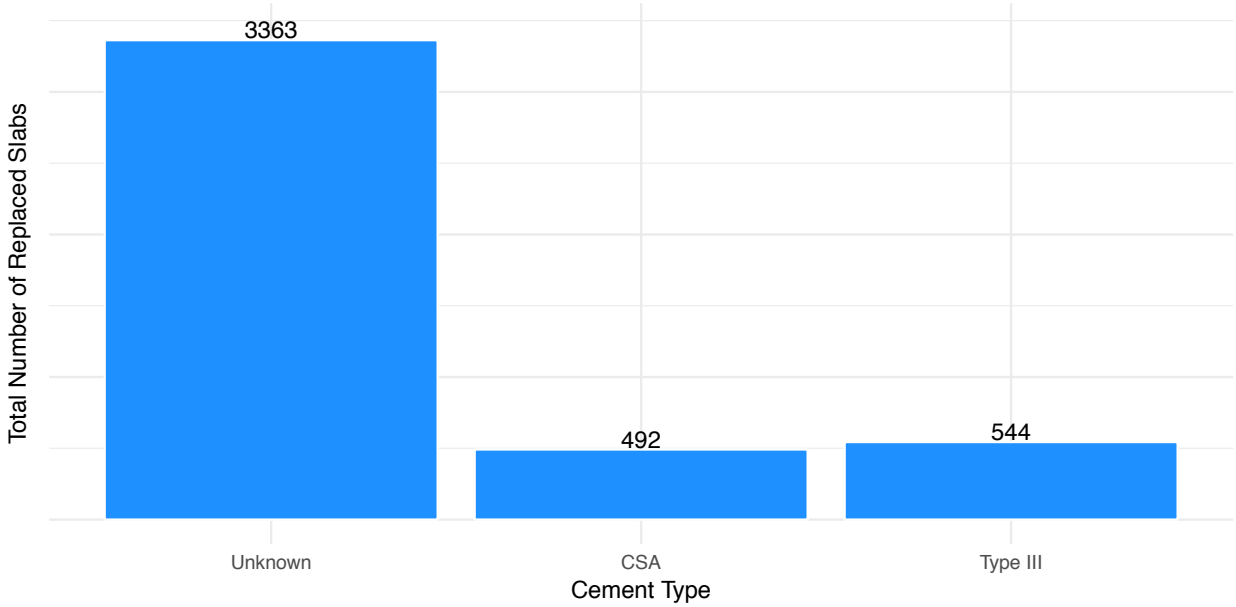

Figure 3.7: Cement type distribution among replaced slabs

Since this parameter has a limited number of data points, an analysis is performed to make sure that cement type variable is not biased towards any other variables that will be included in the model including age, thickness, dowel condition, WIM spectrum. The results of this analysis are shown in Figures 3.8-3.12. It is clear that cement type distribution for both CSA and type III follows the same pattern among all the variables except for climate region.

While climate should have a significant effect on the performance of concrete pavements and, therefore, it should be included in the model, Figure 3.8 shows that the majority of the concrete pavement are within the rural areas in California, which share a moderate climate with low rainfall and no snow. As a result, the pavements in these zones perform similarly, and there was not sufficient data for each climate region in the collected dataset to establish any climate influences. This factor can be included in future models as more data are collected.

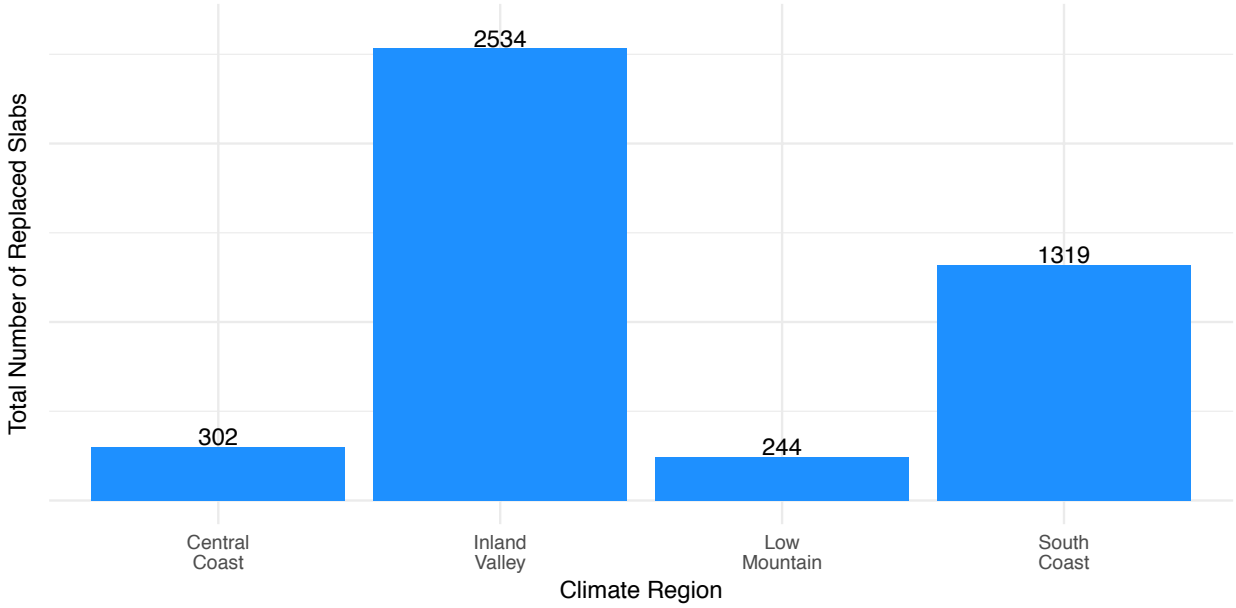

Figure 3.8: Climate region distribution among replaced slabs

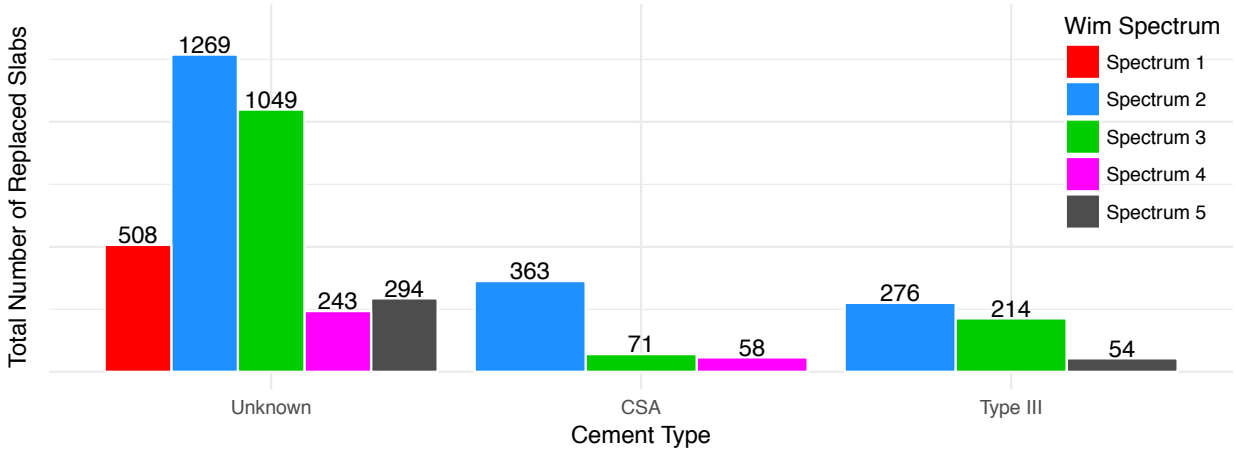

Figure 3.9: Wim spectrum distribution among different cement types

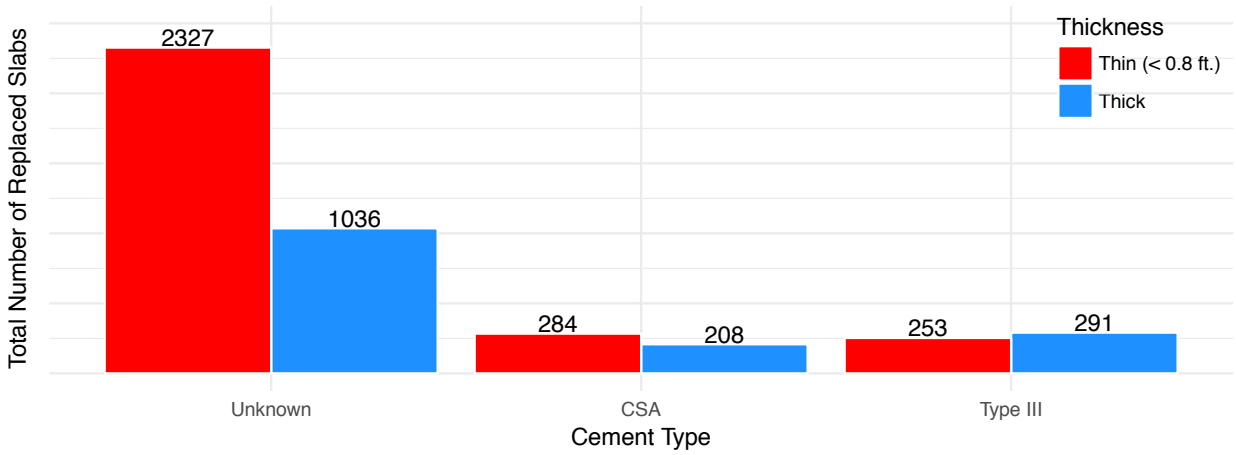

Figure 3.10: Thickness distribution among different cement types

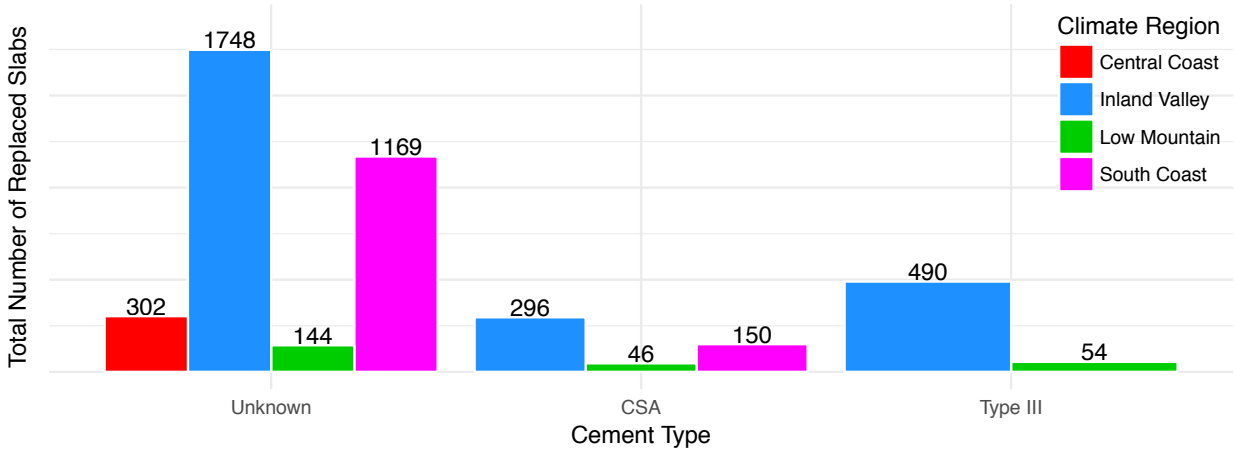

Figure 3.11: Climate region distribution among different cement types

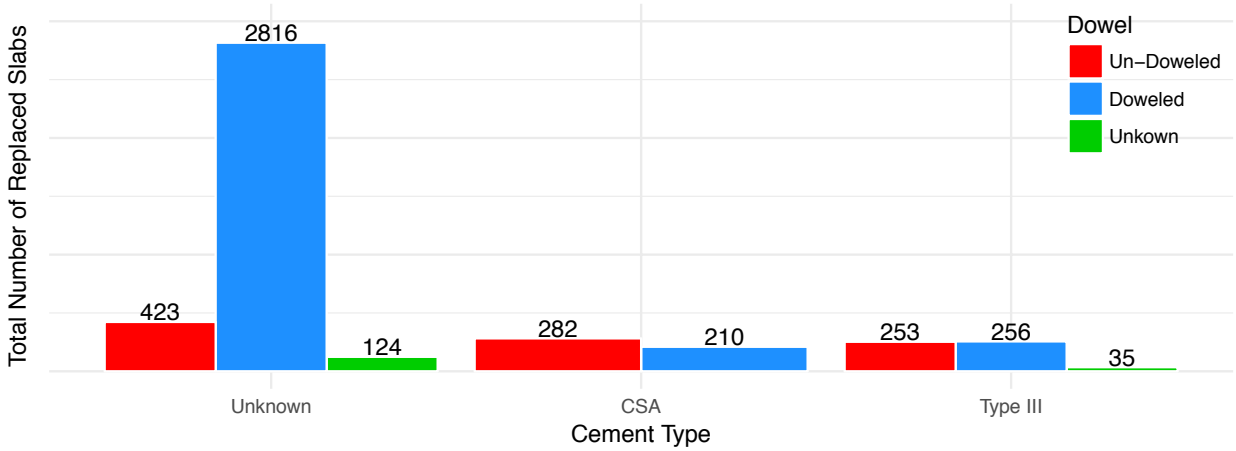

Figure 3.12: Doweled/UnDoweled condition among different cement types

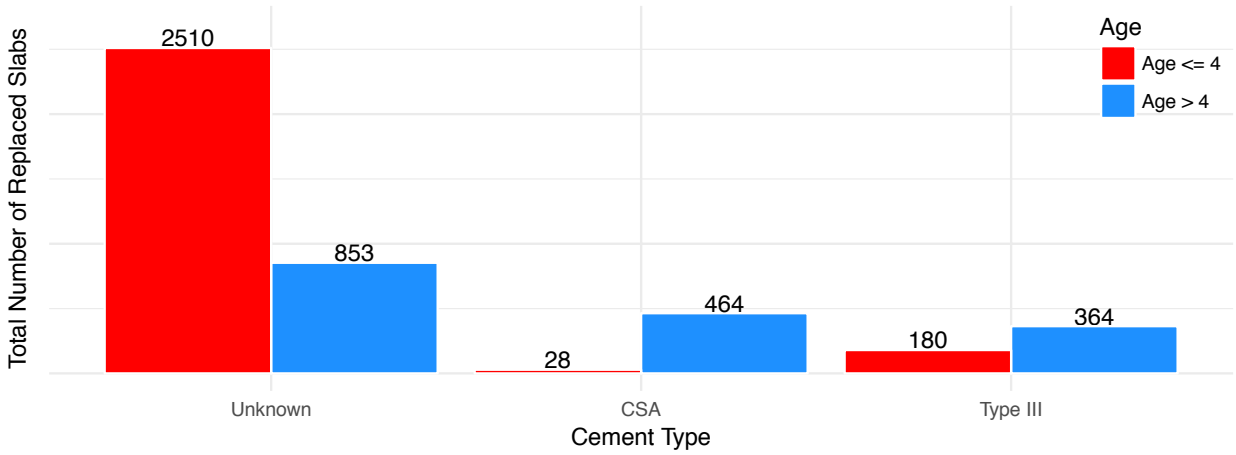

Figure 3.13: Age distribution among different cement types

Figure 3.14 illustrates the percent of cracked slabs against age. The size and color of points represent thickness and annual ESALs in the lane, respectively. The graph shows an increasing trend in percentage of cracked slabs as age increases. Slabs with greater thickness performed better and have lower percentages of cracking compared to thinner slabs. Thinner slabs start to crack at younger ages and a greater portion of them are cracked by an age of seven. It is generally expected that roads with higher ESALs deteriorate faster and more cracking happens during their service life. However, this trend cannot easily be observed from this graph.

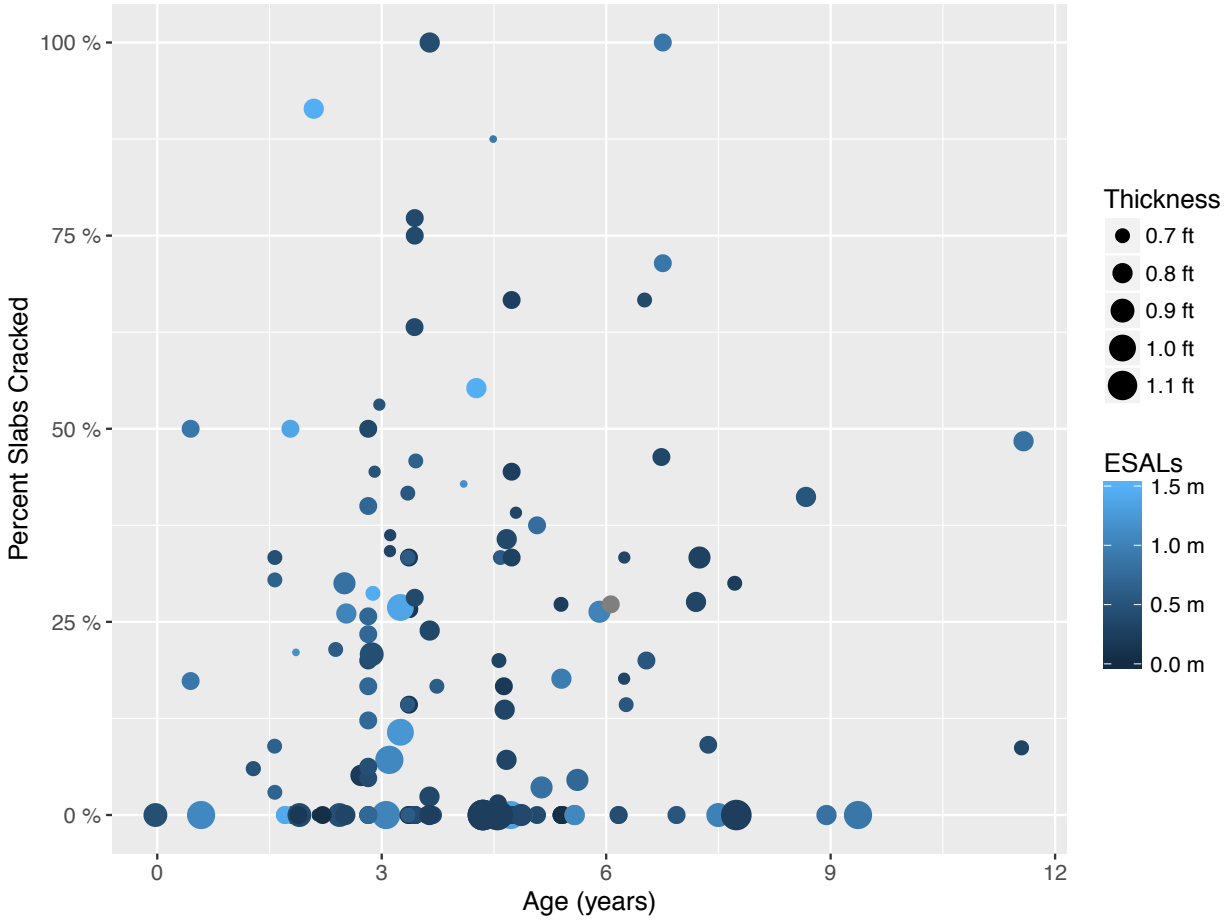

Figure 3.14: First stage cracking percentage (replaced slabs) versus age

3.3. Statistical Modeling and Analysis

3.3.1. Survival Model

To form an initial understanding of the time to failure for replaced slabs a survival analysis was performed using the R software (R Core Team, 2013). The survival probability is the probability that a slab survives from the time of construction to a specific time in the future (*t*, age of slab). The Kaplan-Meier (KM) (Kaplan, 1958) method, which is a non-parametric method, was used to estimate the survival probability of replaced slabs. The survival probability at time t_i is estimated as follows:

$$S(t_i) = S(t_{i-1})(1 - \frac{d_i}{n_i}) \quad (3.1)$$

where: $S(t_i)$ = probability of un-damaged slab at t_i

$S(t_{i-1})$ = probability of un-damaged slab at t_{i-1}

n_i = number of un-damaged slabs before t_i

d_i = number of cracked slabs at t_i

$S(t_i)$ is the survival probability function, which is a step function, and its value changes at each event (when a slab is cracked). In order to fit a KM survival probability to the dataset under study, the `survival` package (Therneau, 2015) was used and to summarize and visualize the results the `survminer` package (Kassambara, 2017) was used.

The Kaplan-Meier method measures the fraction of objects which continue to survive after a specified amount of time after some event. In this study, the object would be the replaced slab and the survival time is measured from the construction time until cracking appears on surface. The slab thickness has been categorized into two categories, thick slabs with a thickness of 0.8 ft. and greater and thin slabs with a thickness less than 0.8 ft.. Figure 3.15 shows the Kaplan-Meier curves for these two categories.

Although thick and thin slabs perform almost equally well in the first three years of service, thicker slabs perform much better in the long term. There is a significant drop in survival probability of thinner slabs in year seven and more than 50 percent of thinner slabs are cracked by year 12. For the thicker slabs, however, only about 8 percent are cracked by this age. Therefore, it can be concluded that making slabs thicker can significantly extend their service life.

Although the KM model returns the survival probability of replaced slabs in the future, it is still a non-parametric method that does not account for all influencing factors (age, thickness, and WIM-spectrum) at the same time. Moreover, while this type of analysis is common in performance modelling literature in pavements, importantly, it is not valid for this type of data. Specifically, the KM analysis assumes that the age is the actual time to failure, not the time until the failure was observed. In pavements, it is very seldom to have the exact time of failure. A survival analysis can be constructed with better assumptions (assuming that the slab cracked at some time between age zero and the observation time), using the interval package. However, once this is done, the survival analysis is not as informative. Therefore, an alternative modeling approach was used in this study, which will be discussed in detail in the following sections. This simpler model is presented to provide a comparison with the more advanced and appropriate models described below.

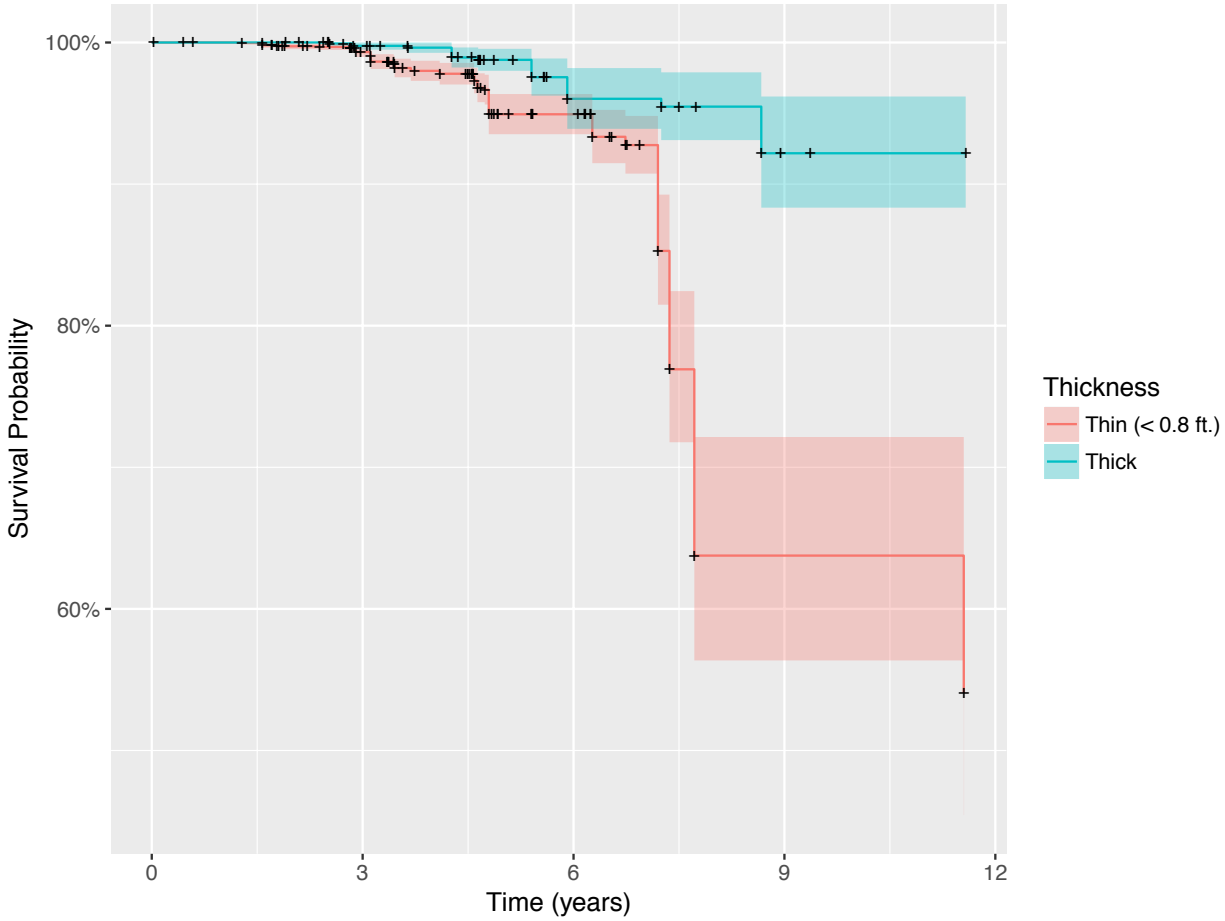

Figure 3.15: Kaplan-Meier survival curve

3.3.2. Cumulative Linked Mixed Model

Slab replacement data can be considered as a short time series panel dataset, where the panels are the individual slabs within locations within projects. The variable of interest is the cracking state, which is a categorical (or ordinal) variable, with three states: un-damaged, first stage cracked and third stage cracked. This variable obviously is not a continuous, normally distributed variable. A generalized linear model (GLM) is thus required, and in this case an ordered logit model (or ordered logistic regression), seems appropriate. In addition, because the data are nested panel data a mixed effects model, which allows each panel to have different regression parameters to account for unexplained variability in each panel is required. This type of model is known as a Cumulative Link Mixed Model (CLMM), which is a specialized form of a generalized linear mixed model accounting for ordinal data, and the generalized form is:

$$\mathbf{g}\big(\mathrm{p}(\mathbf{y} < j)\big) = \boldsymbol{\eta} = \theta_j + \mathbf{X}\boldsymbol{\beta} + \mathbf{Z}\boldsymbol{\gamma} + \boldsymbol{\epsilon} \tag{3.2}$$

where:
$\mathbf{y}$ = vector of outcomes
$g(\cdot)$ = link function
$\boldsymbol{\eta}$ = latent predictor $\sim N(\mathbf{0}, \mathbf{I})$
θ_j = the threshold for level j
$\mathbf{X}$ = matrix of predictor variables
$\boldsymbol{\beta}$ = Vector of fixed effect regression parameters
$\mathbf{Z}$ = matrix of design variables (panel variables)
$\boldsymbol{\gamma}$ = vector of random effects $\sim N(\mathbf{0}, \mathbf{I}\boldsymbol{\xi})$
$\boldsymbol{\epsilon}$ = vector of random errors

In this case the link function is the logistic function, which is the log of the odds that an event occurs, and the probability distribution of the outcomes is treated as a binomial distribution at each transition. Other link functions (particularly the complementary log log function) might be appropriate but did not give improved statistical power in this case. Because the outcomes have a known distribution the error of the latent variable must be scaled to have a unit normal distribution. Notice that the only variable that changes with each threshold is θ_j, so that the transitions from one level to the next are not independent. The major advantage of this structure is that the lower cracking states can inform the growth of third stage cracking, even if a significant number of replaced slabs have not reached this state.

To fit the CLMM, the data were first structured so that each slab was a single sample, with the project level variables repeated for each slab. Equivalently, the data can be treated as a percentage of slabs within each project that are in each of the three categories, and the fit weighted by the number of slabs. These two approaches are equivalent and produce identical results.

Several different predictor variables were tried in the fitting process. Based on the survival model and visual inspection of the data it is clear that age and thickness are important. Since the model is structured as a continuous latent variable, the age must be constrained to being non-negative (forcing zero probability of cracking when age is zero). A log10 transform of age (in years) was used, consistent with many other pavement models. Because Caltrans pavement designs are expressed in US feet, the thickness variable was not changed to millimeters. Most projects only have one observation time, therefore, there is not sufficient data to model panel effects below the project level.

As discussed in relation to Figure 3.5, there did not seem to be an observable trend with ESALs. In fact most models fitted with cumulative ESALs rather than age showed that the rate of damage with ESALs

was lower than that with just age. The reason for this is that, as is well known, is that slabs are more sensitive to damage from heavily loaded axles rather than the AASHTO or Caltrans calculation of ESAL captures. For JPCP an "ESAL" with an exponent of 6-8 should likely be used rather than the 4.2 used in the Caltrans calculation of ESAL. However, because of limitations with the traffic estimation process it was not possible to alter the ESAL exponent. Rather the traffic was categorized into "heavy" traffic, meaning those with WIM axle load spectrums 3, 4 or 5, and light traffic for specturms 1 and 2.

Based on the Fugro study (Miller, 2014), cement type and whether the slabs were doweled have a significant impact on the replaced slabs performance. Therefore, these two variables were included in the model as categorical variables. Cement type had three categories as unknown, CSA, and type III and dowel condition has two categories as doweled and undoweled. As stated earlier, there were many missing values for cement type in the data (categorized as unknown) and attempting to include the cement type in the model without including the records where it is unknown will result in dropping considerable number of observations. However, to investigate the effect of cement type on the replaced slab performance and confirm the conclusion made by Fugro, a model was developed incorporating cement type as a predictor along with other variables including age, thickness, WIM spectrum, and dowel condition. This model will only be used for the sake of comparison between the effects of two cement types on pavement performance based on the coefficients calculated and no other inferences would be made since it was found out that these parameters are statistically insignificant to the model prediction. Therefore, another model will be developed by dropping the cement type from the predictors and will be used to predict the probability of slabs being in any of three conditions (un-damaged, first stage, and third stage).

The following is the formula developed for the cumulative link mix model:

$$\text{logit}\big(p(Y_i < j)\big) = \theta_j - \beta_1 \log(age_i) - \beta_2 th_i - \beta_3 heavy_i - \beta_4 doweled_i - \beta_5 CSA_i - \beta_6 TypeIII_i - u(project_i) \quad (3.3)$$

This model estimates the probability of the i^{th} observation falling in jth category or below where i is index for observations (slabs) and j index is for response categories which in this model is un-damaged, first stage, and third stage cracking. The explanatory variables are age, thickness, and indicator variables for heavily loaded axles, dowel condition, and cement type. θ_j is the threshold coefficient or cut-point. β_1, β_2, β_3, β_4, β_5, and β_6 are model coefficients. Project effects were considered to be random with normal

distribution $u(project_i) \sim N(o, \sigma^2)$. The `clmm2` function in the ordinal package (Christensen, 2015) in `R` was used to fit the model. Because of the low levels of cracking in the data (which is expected, since the majority of the ages are less than ten years, and the expected life is ten years), the procedure would often encounter difficulties. The data were augmented with an additional data point for each slab which indicated that it would have cracked after some long period of time (100 years), forcing the model to also show 100% cracking after this time.

Table 3.1 shows the results of the model fit. As mentioned earlier, in this model, coefficients for CSA and type III cement type are of interest. The p-value for both cement types is high indicating their insignificance to the model prediction. The negative sign in the model coefficients implies the improvement in replaced slab performance by keeping other variables constant. The model coefficients for both CSA and type III are negative which indicate that having these two types in the concrete mix will result in better performance compared to unknown category for cement type. Unknown category can have any distribution of cement type (CSA and type III) and therefore no significant conclusion can be drawn, however, since all the data on cement type were collected by Fugro study and no data were provided by UCPRC, therefore it can be inferred that Fugro project selection could have some bias and tended to choose projects with better performance. This is not surprising since the Fugro study selected projects at least five years old, so many early age cracking projects were excluded. The comparison between coefficients for CSA and type III cement shows that type III cement has more negative coefficient indicating that type III cement is more beneficial to replaced slab performance which is matches the results published by Fugro. This may be related to the generally lower drying shrinkage behavior of CSA compared with type III cement (Mateos et al., 2018).

Table 3.1: Coefficients for the fitted model_1

Random Effect				
	Variance	Standard Deviation		
	4.652731	2.157019		
Location Coefficients				
	Estimate	Standard Error	z value	Pr(>|z|)
log10(Age)	5.9572	0.3615	16.4809	< 2.22E-16
	-4.6556	1.1011	-4.228	2.36E-05
wimCategory_heavy	2.4909	0.5565	4.4759	7.61E-06
	-1.4669	0.2844	-5.1585	2.49E-07
CementType_CSA	-0.2291	0.239	-0.9584	3.38E-01
	-0.7661	0.2405	-3.1851	1.45E-03
Threshold Coefficients				

	Estimate	Standard Error	z value
Un-Damaged->First_Stage	2.513	1.0008	2.5109
First_Stage->Third_Stage	4.9274	1.0055	4.9002
log-likelihood	-2207.897		
AIC	4433.794		

To develop a model that can be used to predict the probability of slabs being in any of three conditions, a new model was developed by dropping the cement type factor from the previous model as it was shown their insignificant impact on the model prediction. Table 3.2 shows the results of the model fit. The coefficient for thickness is negative indicating that thicker slabs decrease the chance of cracking the slab. The coefficient for age is positive implying that older replaced slabs are more prone to first and third stage cracking than younger ones (as expected). The coefficient for the indicator variable 'heavy' is also positive, indicating that slabs on routes with more loaded axles in the spectrum cracked more quickly. This supports the hypothesis that the slabs need a higher exponent for ESALs. The coefficient for replaced slabs with dowels is negative that shows better performance and longer service life for doweled slabs. This confirms the results from Fugro study claiming that slabs with doweled connection have better performance compared to undoweled ones, even though mechanically dowels are considered to not have much effect on tensile stresses causing transverse cracking, although they are the main method of controlling joint faulting. Joint faulting causes dynamic loading on the slab, which is not considered in static analyses typically used for design, and may also influence thermal and drying shrinkage that cause slab deformations causing longitudinal cracking.

Figure 3.16 shows the model prediction against the actual data. The left, middle, and right plots show the probability of a replaced slab to be undamaged, first stage cracked, and third stage cracked, respectively. The model captures the general trend of the data and predicts the performance of replaced slabs well. The model predicts a high probability of undamaged condition for slabs in the first five to six years of construction and a drastic decrease in that probability afterwards. In Figure 3.16, the size of the points represents the slab thickness. The model predicts a high probability of undamaged condition for thicker slabs in the first twelve years of service life and correspondingly a very low probability of first stage and third stage cracked condition even until year 10. The model did not predict any probability more than 50% for third-stage cracking for the first 12 years of service life and this is expected since there were not many replaced slabs reported having third-stage cracks in the dataset.

Table 3.2: Coefficients for fitted model_2

Random Effect	

	Var	Std.Dev		
		1.979664		
Location Coefficients				
		0.2526	21.929	< 2.22E-16
		1.0415	-5.1891	2.11E-07
		0.502	4.7377	2.16E-06
		0.2739	-5.1237	3.00E-07
Threshold Coefficients				
		0.9064	1.9298	
		0.9122	4.568	
log-likelihood	-2213.273			
AIC	4440.547			

Although the model captures the essential trend of the field data, some influencing factors such as slab length, climate region, base type, and cement type were not considered in the model. These factors could be included in future performance modeling efforts as more data become available.

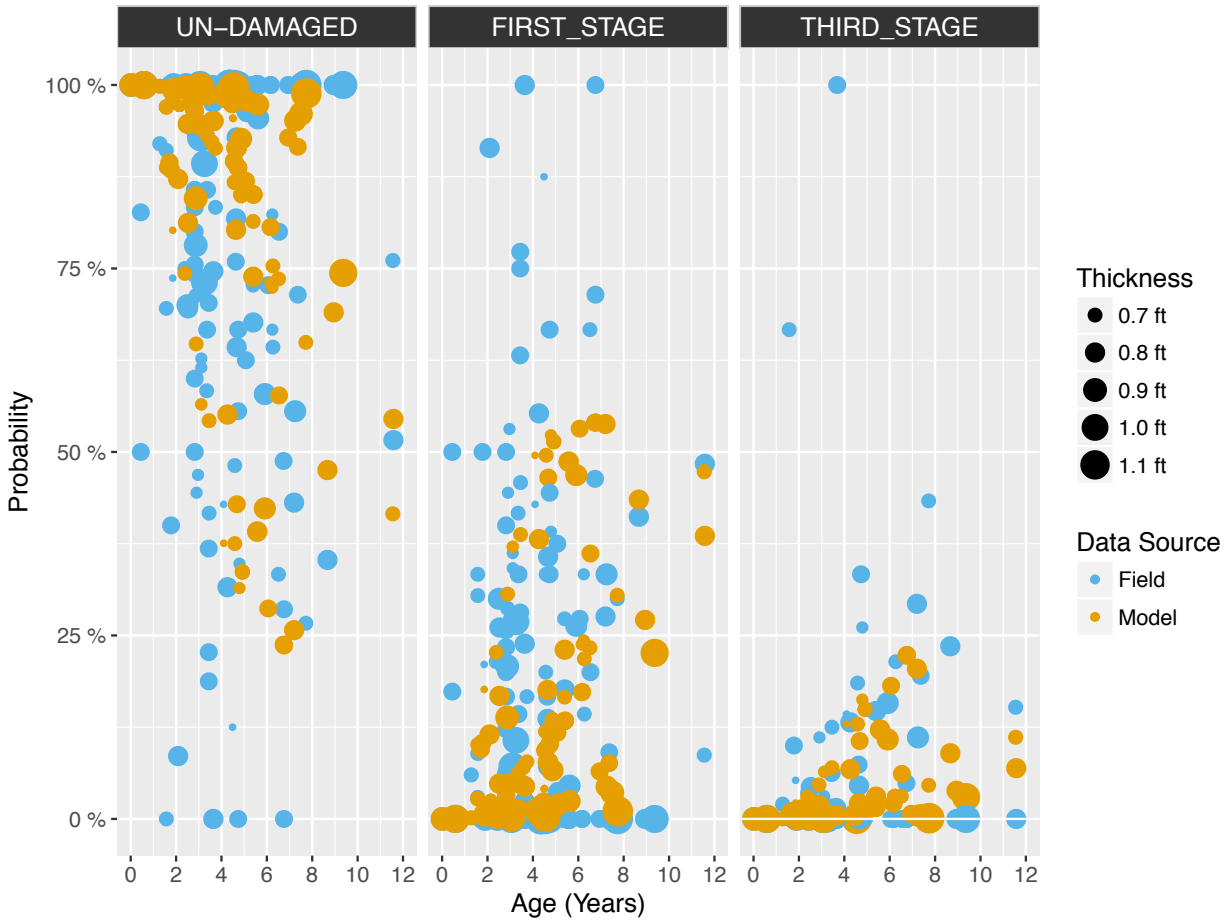

Figure 3.16: Cumulative link mixed model prediction against field data

Figure 3.17 illustrates the sensitivity of replaced slab performance to thickness, age, and dowel condition based on model predictions. The model was used to predict the slabs condition for five different thicknesses (0.6, 0.7, 0.8, 0.9, and 1.0 ft.) and at three different ages (4, 8, and 12 years), with two dowel conditions (doweled and undoweled) with heavy true (i.e. one of the three heavy spectra).

The model predicts higher probability of undamaged state for slabs with higher thickness at earlier ages. Model predictions show that the rate of change in probability due to thickness change depends on the age of slabs and dowel condition. For a 12-year-old undoweled slabs, an increase in the thickness from 0.6 ft. to 1 ft. will cause a 20% increase in undamaged probability, whereas, for a 4-year-old slab, this amount is much higher, about 48% probability. For a doweled slab, these numbers are 43% and 28%, respectively. Therefore, making slabs thicker and doweled will significantly impact the performance of replaced slabs, in particular, this impact will be felt for longer. It can also be observed that thicker slabs are less prone to third-stage cracking in both short and long terms. For an undoweled slab, there is a 23% probability that a slab with 1.0 ft. thickness has third-stage cracking at age 12, while on the other hand, a slab with 0.6 ft.

thickness is much more probable (72%) to have third stage cracking in 12 years. For a doweled slab, these numbers become 7% and 39%, respectively, which are much less than undoweled slabs. Therefore, constructing slabs thicker and doweled will decrease the chance of third stage cracking, the failure criteria defined by Caltrans, significantly.

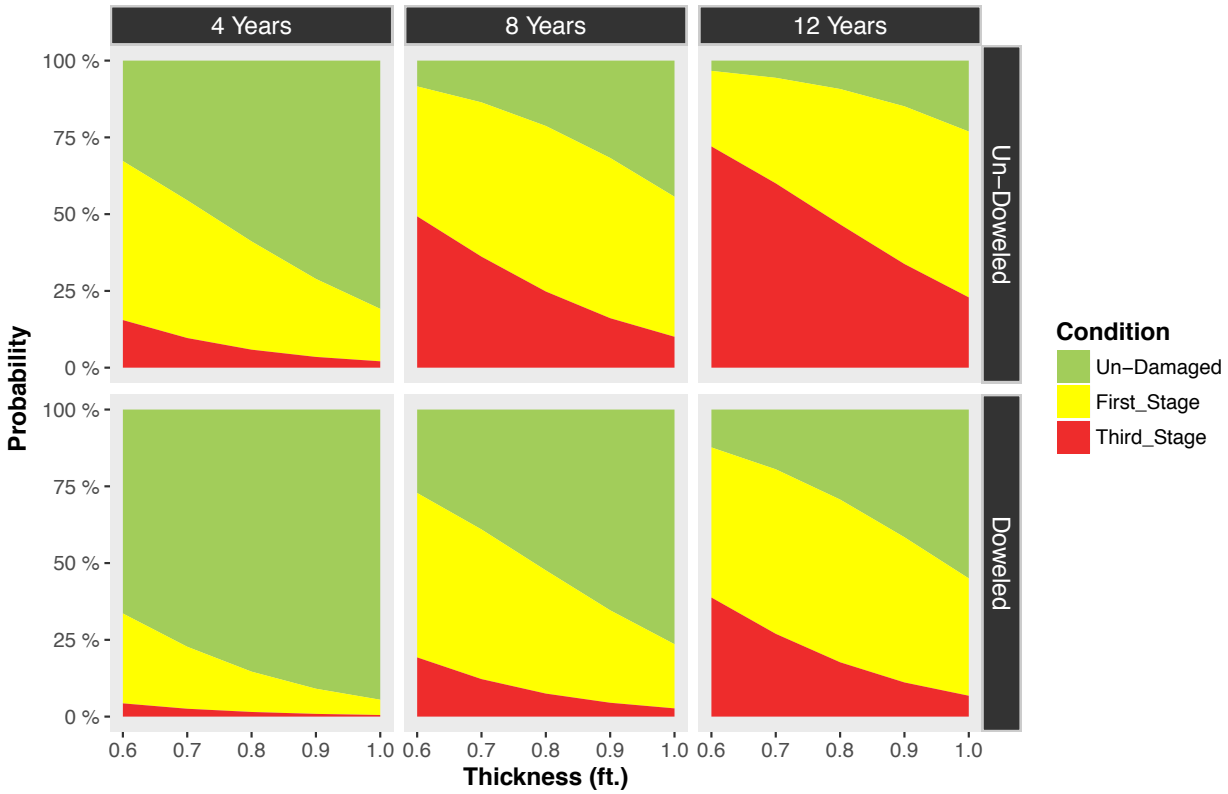

Figure 3.17: Slab performance sensitivity with thickness changes

Another informative output from the model, besides the coefficients, is the between project variability. This has a standard deviation of 1.98, which is large compared to the coefficients for age and thickness. One way of interpreting this number is that projects one standard deviation better or worse than the average project have the same effect as building slabs about 0.37 ft. thinner or thicker. Alternatively, if the average project has a life of ten years, then the worse project would have a life of about 4.4 years, but the better project would have a life of 22.8 years. At a confidence interval of two standard deviations, this difference is even more pronounced, as seen on Figure 3.18. These differences are purely random in this model, although they might be explained with additional variables.

Based on this analysis it is clear that there is significant variability in the performance of replaced slabs, some of which can be explained by thickness, dowel condition, and traffic, but much of which is due to between project variation. On average the replaced slabs have a life close to the ten-year design life.

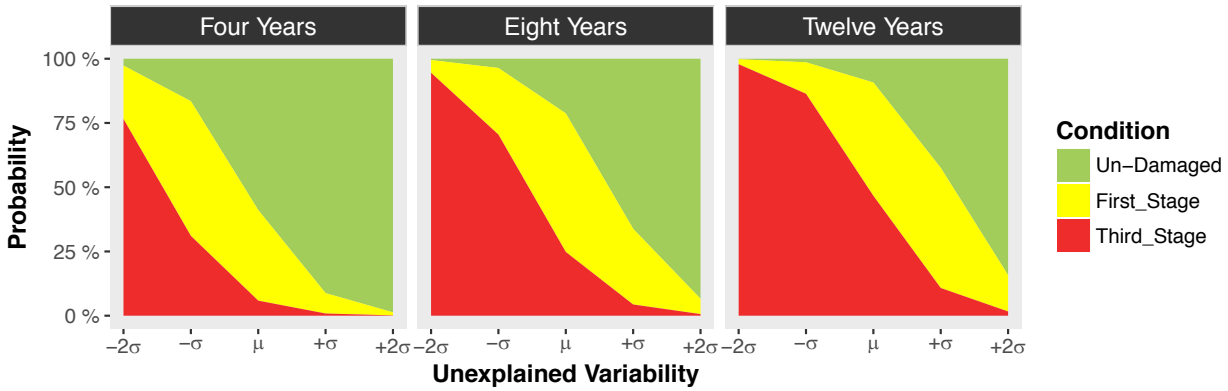

Figure 3.18: Slab performance sensitivity with unexplained variability between projects

3.4. Conclusions and Recommendations

Replacement of cracked slabs in jointed concrete pavements is a standard maintenance practice for Caltrans. Typically, badly cracked slabs are removed and replaced with a rapid set concrete mix, during an overnight closure. In some cases, the base material is also removed and a 'full depth' replacement slab is cast. After construction, the individual slabs are typically ground to match the profile of the surrounding pavement, if the entire road is not scheduled for grinding. There is little existing information on the performance of this type of maintenance, because the collection of the data is difficult. Within a few years, the replaced slabs are hard to distinguish from the original slabs, and often multiple slabs replacements will occur. However, with the availability of downwards images from the Caltrans automated pavement condition survey, along with digitization of historical construction records for the pavement management system it has become possible to develop a dataset to study this practice, and to make observations about performance.

In this study, a performance prediction model was proposed for the replaced slabs within slab replacement treatments done in California. Due to the categorical nature of slab condition variable which can be either un-damaged, first stage cracked, or third stage cracked, a cumulative link mixed regression model was proposed. Slab age, thickness, dowel condition, and WIM spectrum were determined as significant explanatory variables that should be included in the model. There may be additional variables that have significant effects, such as slab length, base type, cement type, and climate region, but due to lack of sufficient data, they were assessed in this study.

Early-age and premature cracking was found to be a major issue in California such that about 17% of total replaced slabs have cracked by the age of 4. The statistical analysis showed that slab thickness and dowel

condition have a significant effect on the cracking pattern. With only a small increase in slab thickness and including the dowel bar in slab construction, the survival rate will increase considerably. Concrete slabs with thickness greater than or equal to 0.8 ft. can have service lives of 12 or more years, while the majority of slabs, which had thickness in the range of 0.6 to 0.8 ft. did not perform as well and more than 50 percent of the slabs cracked before 7 years. Also, constructing slabs with a thickness of 1ft. and with dowel bar will decrease the possibility of cracking in 12 years down to 45%. This number can get as high as 97% in the case of undoweled slab with a thickness of 0.6 ft. As expected, slabs carrying heavier axles (greater WIM spectrum number) deteriorated at a faster pace and had shorter service life.

Given that the stated design life for slab replacement treatments is typically 10 years, the slab replacement treatments using the existing slab thickness are underperforming their design lives. It is thus recommended that Caltrans consider using thicker or full-depth slab replacement with dowel bars more frequently.

To capture the effects of slab length and possibly other design factors such as base type and mix design (cement type) would require a for focused data collection effort, possibly collecting GPS locations for replaced slabs so that they could be tracked into future using the APCS data. Since newly replaced slabs often have a very different color to the original slabs, it may also be possible to develop an algorithm for automatically identifying and tagging these slabs within the APCS data. Other research areas could be the use of additional reinforcement within the slabs (such as wire mesh or fibers), construction practices for handling the in-situ base material once the old slab has been removed (such as partial removal and replacement, improved cleaning methods, possible leveling courses with or without bond breakers) and other ideas.

CHAPTER 4. Pavement ME Sensitivity Analysis (Version 2.5.3)

4.1. Introduction

4.1.1. Previous Calibration and Design Catalog Development

The American Association of State Highway and Transportation Officials (AASHTO) 2002 Mechanistic-Empirical Pavement Design Guide (MEPDG) was calibrated using Long-Term Pavement Performance (LTPP) sections throughout the United States, including some from California (NCHRP, 2003). However, the MEPDG recommends that nationally calibrated models be validated using local data and, if necessary, recalibrated. This makes sense for California because nearly all of the state's climate zones are drier and warmer than the climates of most of the sections in the national calibration set. It also makes sense because much of the national dataset pertains to concrete with limestone aggregates, while the aggregates used in California's concrete are primarily of igneous origin, and these igneous aggregates often have greater coefficients of thermal expansion (CTE) than limestone aggregates. The dry climate and igneous aggregates would tend, respectively, to increase the drying shrinkage gradients and the effects of thermal gradients, increasing the tensile stresses that cause cracking. Further, California has neither the prolonged freezing nor thawing prevalent in the national calibration, which characterize the climatic conditions of a significant portion of the country.

Therefore, to use the MEPDG for pavement design in California, it became necessary to validate the models in the MEPDG based on the performance of the state's pavements, and to recalibrate the models if needed. In addition, the reliability approach used in the software program Pavement ME, which implements the MEPDG models, is based on the national calibration and does not explicitly address the typical localized variability of important variables. Therefore, once the models have been calibrated to account for local conditions, updated design tools based on the calibrated software must be developed. The first step in this process is to perform a sensitivity analysis to check the reasonableness of the models' predictions, to identify potential software issues, and to help identify and understand the inputs that significantly affect the models' outputs.

In 2006, the University of California Pavement Research Center (UCPRC) performed a research study that included an initial sensitivity analysis of jointed plain concrete pavement (JPCP) distress prediction models in the MEPDG (Kannekanti et al., 2006). That study identified the most important variables affecting predicted performance, and studied a design variable that was found to be the most important one for predicting the performance of JPCP pavements in California (Kannekanti et al., 2007)—the time

to loss of bonding between the concrete and the base. After that study, the software was used to produce a preliminary design catalog for the Caltrans Highway Design Manual (HDM); Caltrans further adjusted that catalog to produce the one in the current HDM. The assumptions and results for that preliminary design catalog are documented in Reference (Kannekanti et al., 2006).

As noted, Pavement ME, the current software program developed from the MEPDG models, uses those models to predict IRI, faulting, and transverse cracking. (Note: In this study the design guide is referred to as MEPDG and the software is referred to as Pavement ME.)

The Caltrans pavement management system (PMS) bases its management of JPCP on third-stage cracking, as opposed to first-stage cracking or transverse cracking. First-stage cracking is defined as cracking state where the first crack divides a slab into two pieces. A first-stage crack can be a transverse crack, the only type of cracking modeled by Pavement ME, or a longitudinal crack, which also occurs on Caltrans JPCP (Harvey et al., 2000). Third-stage cracking is defined as a state of cracking that divides a slab into three or more pieces. In California, a transverse crack is one of the crack types that commonly creates a third-stage crack when it combines with a longitudinal crack—although, less frequently, third-stage cracking is also created by two transverse cracks, or two longitudinal cracks.

4.1.2. Earlier Pavement ME Calibration

The traditional approach taken for validating and calibrating mechanistic-empirical (ME) design methods is to collect all input data—including performance, as-built, and detailed materials data—for tens of sections within a state, and to then compare the predicted and measured performance of those sections. For the national calibration of Pavement ME, data were collected on several hundred Long-Term Pavement Performance (LTPP) sections across the US.

The California-focused calibration of an early version of Pavement ME (Kannekanti and Harvey., 2007) followed the traditional approach, and included just 52 JPCP and 43 crack, seat, and overlay (CSOL) sections. At the time they were cored, the sections' first-stage transverse and longitudinal cracking and third-stage cracking were measured, and deflection testing was performed on areas of the sections that had not been overlaid with asphalt. To develop better transverse cracking histories of all the sections, and to learn whether the measured third-stage cracks had begun as a first-stage transverse or a longitudinal crack, it was necessary to produce an estimated transverse cracking history for each section, starting at the time of its construction. But because there were insufficient data and because the section did not come from enough areas of the state to be truly representative of conditions everywhere, it was not possible to

develop a model for predicting whether a third-stage crack had originated as a transverse crack or a longitudinal one. To account for these specifics, a range of potential transverse cracking histories was produced for each section; in these histories, the maximum of the range assumed that all third-stage cracks began as transverse cracks while the minimum of the range assumed that all third-stage cracks began as longitudinal cracks. Although this provided a means for dealing with the lack of data, it also added uncertainty to the calibration performed.

Soon after that calibration, Caltrans requested development of a transfer function that could predict third-stage cracking from transverse cracking predictions; this function was developed and used in the creation of the preliminary design tables that served as the basis for the design tables included in the 2007 HDM. (No documentation of the transfer function's development has been published.) The calibration of Pavement ME that follows this sensitivity study will be to transverse cracking, but it will use a model that is better at separating the first-stage cracking histories in the PMS performance data into estimates of transverse and longitudinal cracking. This is now possible using the much larger and better database that is now available.

4.1.3. Overview of Current Calibration and Design Development

In 2011, Caltrans developed a capacity for Automated Pavement Condition Survey (APCS) data collection from the state highway network, and as a result a much larger and more reliable pavement condition database is now available in the pavement management system (PMS). The result of a considerable effort on the part of Caltrans, that updated database now includes as-built data such as pavement structure, base type, shoulder type, slab length, and construction year. Items that were mostly unavailable for the previous study can now be accessed for almost every project built since 1990, and many built prior to that year. These data provide the capability to validate and calibrate Pavement ME using thousands of performance data observations and to use the explanatory data in the as-built database. Further, in addition to the new data in the PMS, there is also more detailed data collected for Caltrans by the UCPRC on more than 100 projects sampled in the early 2000s and 2010s. These are data for variables not in the PMS as-built database, such as the properties of concrete materials and the stiffnesses of underlying layers.

In the years since the preceding study, Pavement ME has also continued to evolve, with Federal Highway Administration (FHWA) releasing several new versions since 2006 that include improvements to both the models and the implementation of the software.

With the combined updates and improvements to Pavement ME and the increased amount and the higher quality data now in the Caltrans PMS, Caltrans and the UCPRC have taken the opportunity provided to perform a new JPCP cracking prediction model sensitivity analysis and a California-specific calibration whose results can be used to produce updated design tools. This current study undertook those tasks, using the latest version of Pavement ME: version v.2.5.3. And importantly, this study has taken a new approach for the calibration process, whose results will be checked further using the data for the more than 100 sections in the state that have complete sets of detailed data.

This new calibration process approach recognizes that in California's design-bid-build (low-bid) contracting environment, a designer does not actually know the detailed materials properties that will be used when the design is later built. Therefore, the calibration will use statewide median values of the detailed materials properties to calibrate the models using the large performance database, while also calculating the variability of performance caused by differences between the contractors' as-built materials and the statewide median values. The calibration will use the details from the PMS regarding layer types, thicknesses, slab dimensions, shoulder types, dates of construction, and performance data, along with detailed climate and traffic data, to find the coefficients in Pavement ME that on average produce the best match between predicted and observed performance. The distribution of differences between the predicted and the observed performance also provide information needed for introducing reliability into the future design tools.

This study will calibrate Pavement ME to the transverse cracking estimates that result from adding the transverse cracking estimated from first-stage cracking to third-stage cracking. To achieve this result, the study will develop a new model that yields the probability that a first-stage crack is longitudinal or transverse. This effort will use the 2011/2012 APCS data, which accurately separated transverse and longitudinal cracking on all of the JPC pavements across the state, thereby providing sufficient data to produce the model. This model will then be used to predict the rate of transverse and longitudinal cracking development independently for all of the JPCP performance data in the PMS database, including consideration of explanatory variables such as shoulder type, climate region, thickness, and slab dimensions, among others.

The model will also be able to relate the development of transverse cracking to the subsequent development of third-stage cracking. Data about this relationship can be used to set transverse cracking failure levels for the development of design tools, and to relate predicted transverse cracking from Pavement ME to the third-stage cracking used in the PMS.

The calibration of the Pavement ME empirical model transverse cracking coefficients C_4 and C_5 will be made using the predicted portion of transverse cracking from the observed first-stage cracking. The model will also be able to identify situations where longitudinal cracking is expected, and associated design guidance will be developed to help designers limit the possibility of early failure from this cracking mode. Pavement ME was not developed to predict longitudinal cracking because this type of cracking seldom occurs outside of the dry climate regions that are predominant in California and in some other Western states.

As a first step in the validation and calibration process, a sensitivity analysis was performed on the Pavement ME models for JPCP. This step is the subject of this chapter. As noted previously, the sensitivity analysis was performed to check the reasonableness of the models' predictions, to identify potential software issues, and to help identify and understand the inputs that significant affect the models' outputs. The sensitivity analysis included the development of detailed materials properties distributions, followed by an evaluation of the sensitivity of Pavement ME performance predictions to both the variables known to the designer and the distributions of the unknown detailed materials variables.

It should be noted that the ranges of variables considered in this study were selected based on the historical data available in the PMS database for design variables (known to the designer, e.g., portland cement concrete [PCC] slab thickness, PCC slab length, base type, shoulder type, etc.) and the UCPRC material database for non-design variables (not known to the designer, e.g., PCC compressive strength, PCC coefficient of thermal expansion [CTE], PCC shortwave absorptivity, etc.). Therefore, the range selected for each variable reflects past construction practices in California while testing the sensitivity of the models' performance with the variables' changes.

The variables and their ranges used in the sensitivity analysis factorial are different from those that will be used for either calibration or design catalog development. In the calibration process, the range selected for each variable will include all the values ever used for JPCP construction in California, based on the PMS database. The design catalog development will both include selected values from the calibration and additional values intended to reflect future ranges for the design variables in California. The Pavement ME calibration and design catalog development will be explained in detail in the next report produced by this project.

The sensitivity analysis included the models for transverse cracking, mean transverse joint faulting, and smoothness index (International Roughness Index [IRI]).

The results presented in this chapter demonstrate the sensitivity of the results of the Pavement ME design software to the various inputs based on an assessment of the distributions of design variables. In addition, the work presented was also used to identify potential issues with the Pavement ME software and to provide a practical assessment of how best to use Pavement ME for design.

Section 4.2 describes the data available in California pavement management system. In Section 4.3, Pavement ME performance prediction models for transverse cracking, mean transverse joint faulting, and smoothness index are summarized. In Section 4.4, the sensitivity analysis results are presented. Section 4.5 presents the sensitivity analysis study's conclusions. The appendix provides information about the distributions of the detailed materials data available for calibration obtained from various earlier UCPRC projects, including the range, mean, and standard deviations for each variable, and a short description of weigh-in-motion (WIM) groups in California.

4.2. Pavement Management System Data

Pavement management is the process of using available financial resources as efficiently as possible to ensure the highest overall functional performance of a road network, both spatially and with time, while maintaining the structural condition of the pavements to protect the initial investment in construction. To perform pavement management, it is necessary to capture the current functional and structural condition of the network and predict the future condition for different management scenarios. Historically, a team of Caltrans pavement raters conducted a manual pavement condition survey at various locations along the state highway system (SHS) once a year. The pavement raters visually inspected the outside highway lanes for both directions of travel using systematic sampling techniques. Pavement condition assessments were extrapolated for each section of the entire SHS based on those sample locations within each section.

The boundaries of pavement management sections across the network changed annually, as did the locations where surveys occurred. This made building performance histories difficult for the 2006 Pavement ME calibration because the same location was not sampled each year. The changing of section boundaries from year to year also meant that a given pavement's location could be included in a different pavement section in any given year. Typically, jointed plain concrete pavements (JPCPs) sections were approximately one mile long.

Between 2011 and 2012, Caltrans began testing and transitioning to the Automated Pavement Condition Survey (APCS). The APCS can efficiently collect, evaluate, and analyze pavement conditions for all lanes on the SHS. It utilizes vehicles equipped with an array of on-board high-definition cameras, laser sensors, Global Positioning System trackers, and other measurement devices that quickly collect pavement data at highway speeds. The information collected includes geographical locations of the highways, downward-looking pavement surface images, forward right-of-way images, and pavement surface profiles. The data are collected in segments referred to as elements, which are 26.4-foot sections. This is true for both asphalt pavement and continually reinforced concrete pavement (CRCP). The same is done on every concrete slab for a JPC pavement. These data are then aggregated to calculate a weighted average of the pavement condition for each 0.1-mile segment.

Because evaluating condition, especially functional condition, can be subjective, agencies have generally settled on trying to identify and quantify specific distresses. A distress is a measurable phenomenon on the surface of a pavement, such as observable cracking, changes in ride quality (smoothness/roughness), or rutting. Distress is the result of internal deterioration within the pavement, such as bottom-up fatigue cracking or plastic deformation of materials. Deterioration, in turn is the result of internal damage within the materials, which is not observable. This might include particle movement, breaking of bonds, or other atomic/microscopic changes.

These damage processes also take place at different rates at different locations in the pavement because of variability in the materials and construction of the pavement. As a result, distress is observed to accumulate at different rates along the road surface, even within a section that is nominally uniform with regard to construction, traffic, and climate.

This chapter outlines the pavement structural, climate, and traffic variables along with distress measures available in California's pavement management system (called PaveM) database. It also briefly discusses in qualitative terms the effects of different variables on the performance of the JPCP over the service life observed in the data. These same data were used to develop empirical performance models for the Caltrans PMS, which were in turn used to calibrate Pavement ME.

A statistical performance model is developed using data obtained through pavement condition surveys. The model predicts the future performance (condition) of the pavement—in this study, the model predicted performance in terms of cracking as a percent of slabs cracked. As explanatory variables, the model used pavement structural variables such as slab thickness, PCC slab length, base type, shoulder

type, and load transfer efficiency (doweled/undoweled), and nonstructural variables such as climate and traffic loads. This chapter is not intended to cover the development of performance models; however, the results of the performance models for first- and third-stage JPCP cracking developed for the PMS were used to investigate the effects of different variables on the performance of JPCP. Detailed descriptions of the PaveM performance models will be provided in the next chapter.

4.2.1. JPCP Structural Distress Measures in Caltrans PMS Data

4.2.1.1. Concrete Slab Cracking

Cracking is a typical type of distress that occurs in jointed plain concrete due to traffic loading and environmental conditions. Each traffic loading pass applies damage-inducing stress and strain in the concrete slabs, with the minor damage from each load accumulating over thousands to hundreds of millions of load passes until it eventually results in failure in the form of fatigue cracking. Environmental conditions such as the curling caused by differential temperatures in the slab and the warping caused by differential shrinkage also create stress in the concrete that contributes to the damage in the concrete slab.

Cracking in concrete slabs can be categorized into three main types: transverse cracking, longitudinal cracking, and corner cracking. The typical type of cracking in concrete slabs in California is transverse cracking. Transverse cracks appear perpendicular to the pavement centerline and extend across the entire slab from one longitudinal edge to the other. Longitudinal cracks appear parallel to the pavement centerline and extend along the entire slab from one transverse joint to the other. Corner cracks occur in one quadrant of a slab, and have one endpoint on a longitudinal joint and the other on a transverse joint.

Typically, a combination of repeated loads combined with thermal and shrinkage stresses causes transverse cracking in concrete slabs. The initiation and progression of transverse cracking generally occur in two patterns: bottom-up cracking and top-down cracking. In the case of bottom-up cracking, when truck axles are near the longitudinal edge of the slab, midway between the transverse joints, a critical tensile stress occurs at the bottom of the slab with its maximum vector in the longitudinal direction. The presence of high positive vertical temperature gradient (the top of the slab is warmer than the bottom of the slab) through the slab thickness causes additional tensile stress at the bottom of the concrete slab that contributes to bottom-up cracking.

In contrast, heavy trucks with shorter axle spacings load the opposite ends of a slab simultaneously. The result is that higher tensile stresses occur at the top of the slab than the bottom, and consequently

transverse fatigue cracking begins at the top of the slab. Top-down transverse cracking is accelerated by high negative temperature gradients (the top of the slab is cooler than the bottom of the slab) that cause tensile stress at the top of the slab.

Longitudinal cracking in California is primarily caused by high differential drying shrinkage that causes high tensile stresses at the top of the slab, which combined with truck axle loading near the edge of the slab results in top-down cracking. Corner cracking is also caused by a top-down mechanism, where load repetitions at the corner of the slab combined with poor joint and shoulder load transfer, loss of support in the base, and curling and warping stresses cause cracks at the corner of the slab. The lack of support and poor load transfer may be due to the pumping of underlayer material or a loss of load transfer between adjacent concrete slabs, such as an undoweled concrete pavement that does not have tied concrete shoulders.

Caltrans has also categorized the cracking in JPCP in terms of its severity into two main groups: first-stage cracking and third-stage cracking. In Caltrans's official definition, a first-stage crack is a crack that breaks the concrete slab into two pieces; this crack can be a transverse, longitudinal, or diagonal crack. A third-stage crack is a set of two or more intersecting cracks, longitudinal or transverse, that divide the concrete slab into two or more pieces. However, despite these specific definitions, Caltrans raters have long used simpler definitions: a slab has first-stage cracking if it is divided into two pieces, and it has third-stage cracking if it is divided into three or more pieces. It should be noted that corner cracking is not considered in these two categories, and is defined and measured separately.

Caltrans measures cracking as the percent of cracked slabs in a pavement section. Caltrans historically has collected first- and third-stage cracking data only, without defining whether the first-stage cracking is transverse or longitudinal. However, as part of the APCS data collection in 2011 to 2012 and in 2018, Caltrans also collected transverse and longitudinal cracking as individual measures. Therefore, the amount of transverse and longitudinal cracking data in the database comes only from these years, and the amount of data with transverse and longitudinal cracks defined is much smaller than the amount of first- and third-stage cracking data.

4.2.1.2. Transverse Joint Faulting

Faulting is the difference in elevation across a transverse joint between two adjacent concrete slabs or across a transverse crack. It is primarily caused by poor load transfer and is therefore usually an issue with undoweled JPCP.

The main mechanism that causes faulting is movement of fine material, from under the leave concrete slab to under the approach slab, caused by large differences in deflection between the loaded slab and the unloaded slab. These differences in deflection reverse as a wheel travels across a joint, creating a pumping action. Dowel bars significantly decrease relative deflections across transverse joints under load, thus reducing faulting development and further deterioration of joints and corner cracks.

Caltrans measures faulting as the percent of transverse joints in a pavement section with faults greater than a threshold value.

4.2.1.3. International Roughness Index (IRI)

Pavement roughness is generally defined as an expression of pavement-surface irregularities that adversely affect ride quality for vehicles and for users. Roughness is an important pavement characteristic because it affects not only ride quality but also vehicle maintenance costs and fuel consumption. In PaveM, roughness data are quantified using the International Roughness Index (IRI). IRI is used to define a characteristic of the longitudinal profile of a traveled wheel track and constitutes a standardized roughness measurement. In PaveM, IRI is measured in units of inches/mile.

4.2.2. Pavement Structural As-built, Traffic, and Climate Data in the PMS

Caltrans records new JPCP projects as "Lane Replacement" in the PMS database.

The Caltrans condition survey database contains about 260,000 observations of first- and third-stage cracking performance data collected from 30,000 JPCP sections, totaling about 4,300 lane-miles built on 302 lane replacement projects completed between 1947 and 2017. The database's performance data were obtained from manual pavement condition surveys (PCS) conducted from 1978 to 2013 and from the automated pavement condition surveys conducted from 2011 to 2012 and in 2018. Each observation in the condition survey data corresponds to the performance condition of a pavement section in the highway network at the time the survey was done.

These data were divided into approximately uniform subsections as part of the performance modeling effort, with section boundaries kept constant through time and defined as having the same pavement structure from the last construction project, the same traffic loading, and the same climate condition. Figure 4.1 shows the variability in the resulting lengths of these sections in the dataset.

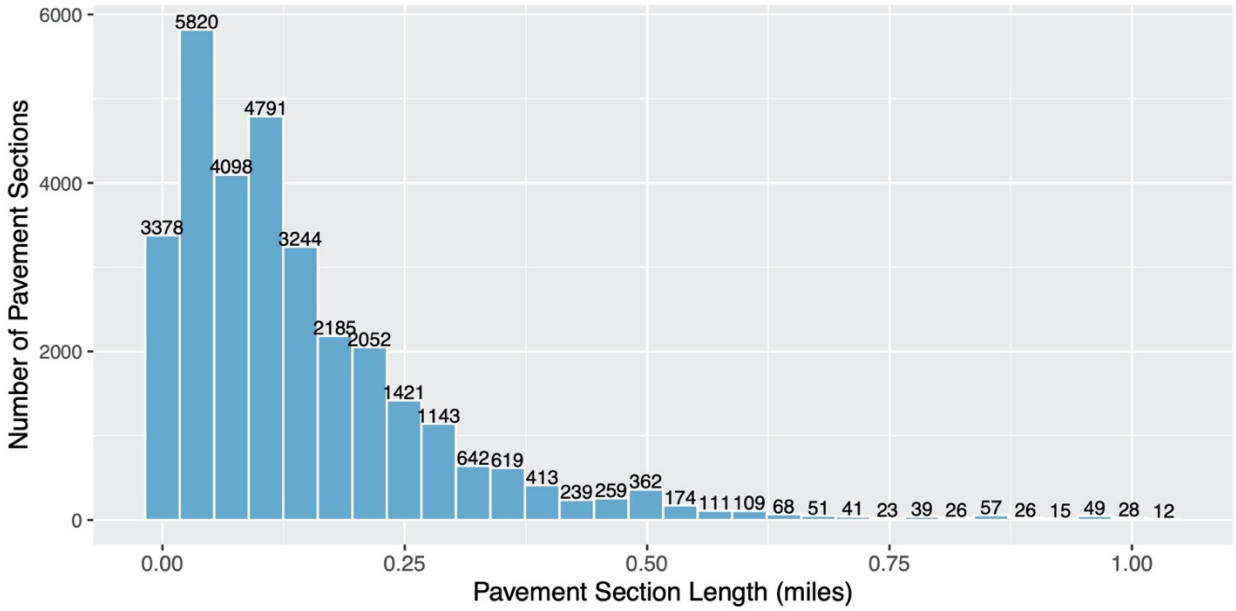

Figure 4.1: Pavement section length distribution

Figure 4.2 shows the JPCP construction year distribution. Construction years in the figure range between 1947 and 2017. Condition survey data were first collected in 1978, thus the oldest JPCP performance histories began in that year.

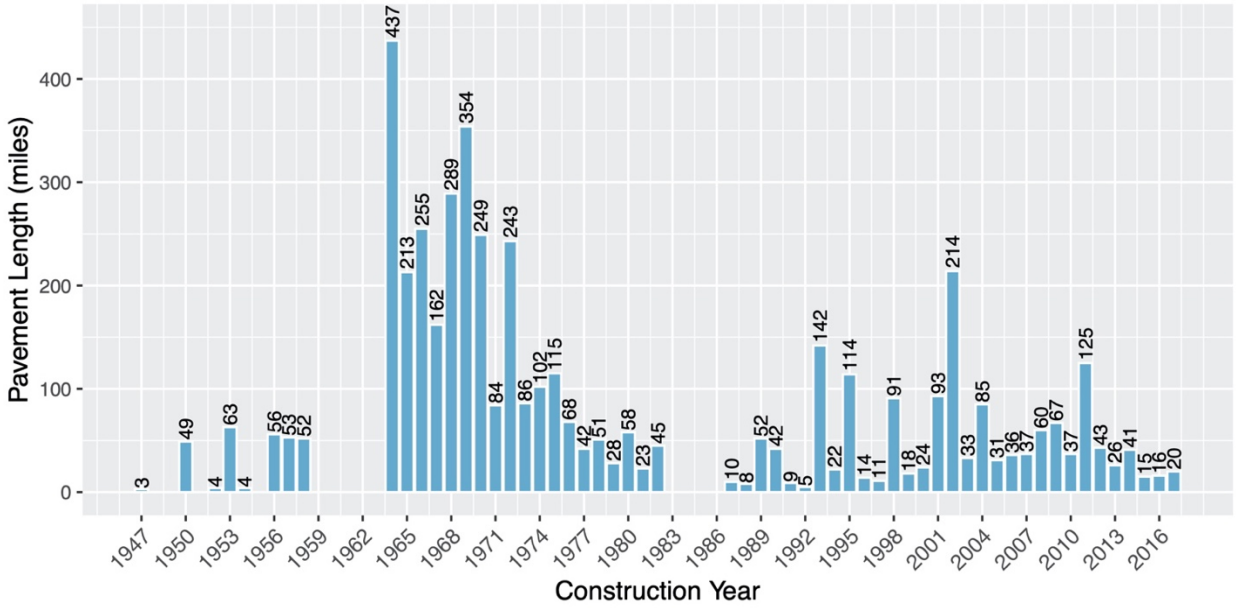

Figure 4.2: JPCP project construction year distribution

Figure 4.3 shows the pavement age distribution for condition survey observations. Each pavement section's age was determined by calculating the difference between its construction date and the date of

the pavement condition survey. Most of the pavement condition observations were taken on pavements that are less than 40 years old in the condition survey dataset.

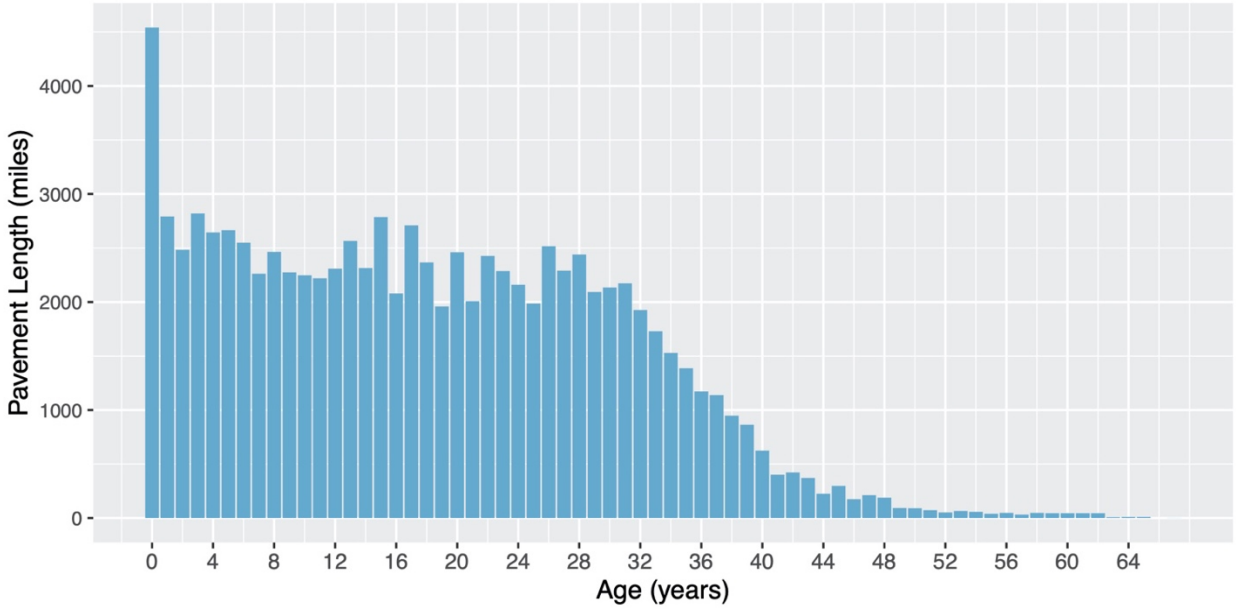

Figure 4.3: Pavement age distribution

The as-built database includes information on PCC slab thickness, PCC slab length, base type, and shoulder type. The as-built database does not record whether JPCP projects are doweled, and no other sources were found to obtain that information. Projects with completion dates after about the year 2000 are highly likely to be doweled JPCP because in 1998 Caltrans standard plans mandated the use of dowels in JPCP projects; consequently, this study made the assumption that they are doweled. In Section 4.2.2.1 through Section 4.2.2.7 of this chapter, the distribution of each of the as-built variables and a qualitative evaluation of their effects on the measured cracking performance of JPCP are discussed.

This large pavement performance database will be used to calibrate the Pavement ME performance models in the next step of this research. Prior to that step, however, a sensitivity analysis study was performed to check the reasonableness of the models in Pavement ME as well as their sensitivity to different input variables, which is the subject of the rest of this chapter. The values chosen for each input variable in this study are based on the historical distributions of the design variables (variables controlled by the designer) shown in this chapter, along with the distributions of the variables not controlled by the designer, shown in the Appendix. It should be noted that the values chosen for the sensitivity analysis are not necessarily those that will be used for Pavement ME calibration, and they will definitely not be the values used for developing catalogs for future designs.

4.2.2.1. PCC Slab Thickness

Figure 4.4 shows the distribution of PCC slab thickness in the PMS database. The PCC slab thickness was categorized into bins with a 0.1-ft. interval. It can be seen that the majority of PCC slabs were constructed with thicknesses between 0.6 to 0.9 ft.

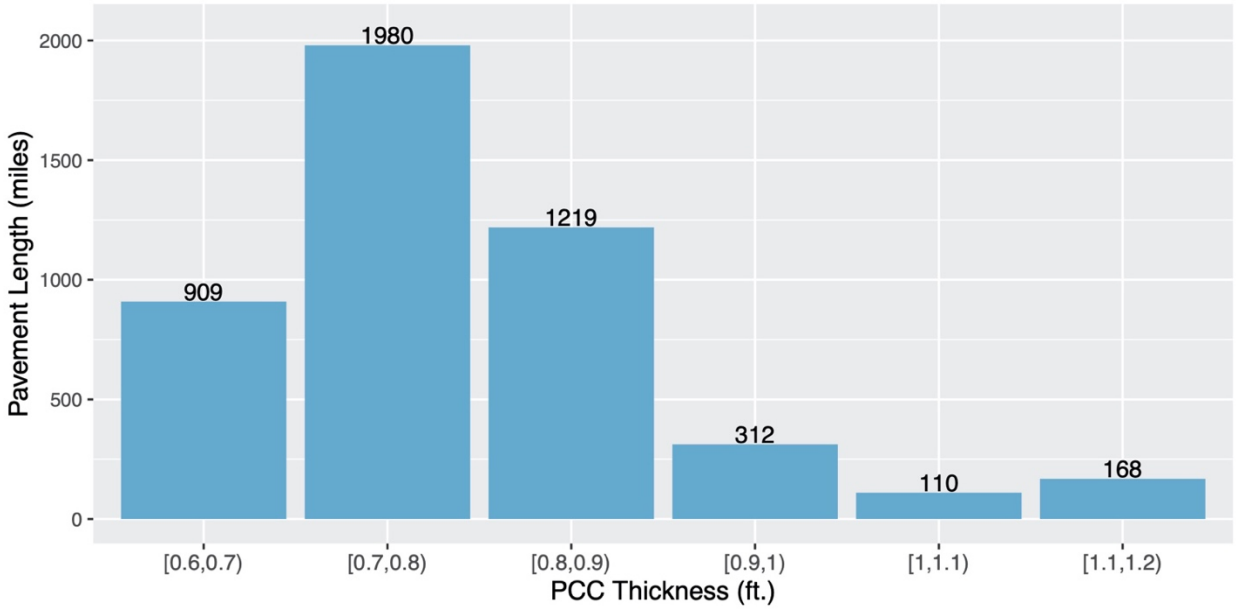

Figure 4.4: PCC slab thickness distribution

Figure 4.5 shows the cracking performance of the JPCP with different thicknesses over the years. The Y-axis represents the first-stage cracking percentage, the X-axis represents the age of the pavement, and each panel corresponds to a PCC slab thickness. The black points in each plot are the observations of cracking in each thickness range, with the size of each point representing the amount of data in lane-miles, with all data in the complete dataset shown with gray-shaded points for reference. It can be seen from Figure 4.5 that thicker slabs perform better, with less first-stage cracking than thinner ones, despite the fact that truck traffic is not controlled in the plot. This indicates that despite the intention of previous Caltrans design methods to account for traffic in a manner that results in similar functional lives, the result has been that locations with thinner slabs fail faster than those with thicker slabs. It is uncertain how much of the difference is due to under- or overestimation of truck traffic, or of the design method not doing a good job of accounting for traffic. There may also be interactions with other variables, such as slab length, base type, and shoulder type that are causing differences in performance because of unequal distributions of those variables' factor levels within each thickness category.

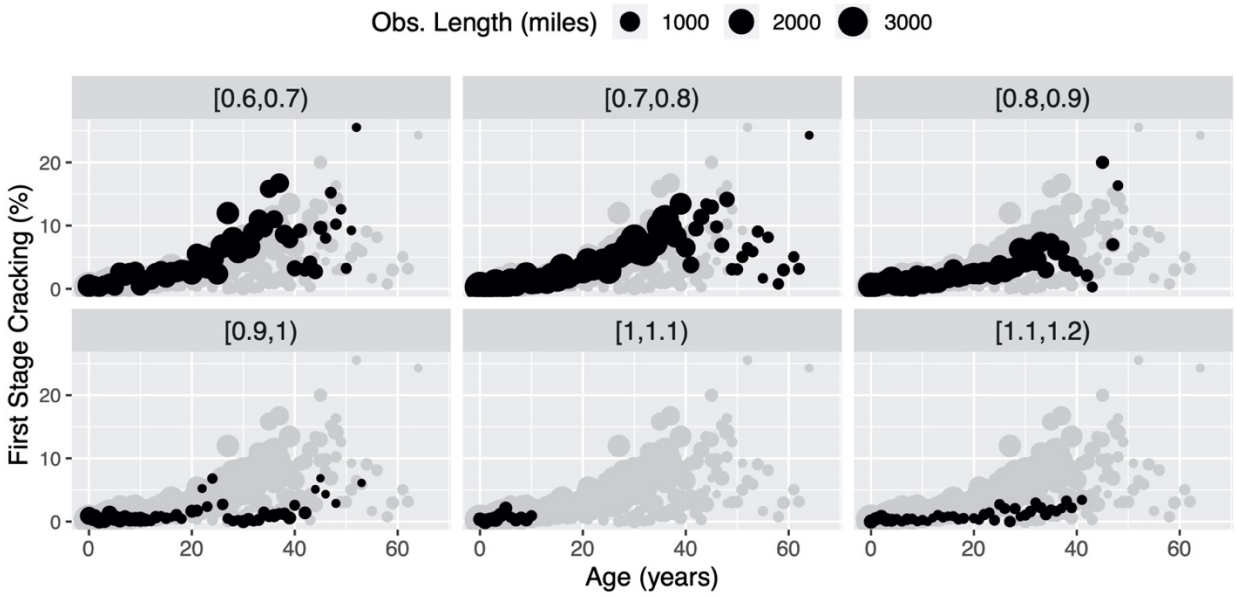

Figure 4.5: JPCP first-stage cracking for different PCC slab thicknesses

4.2.2.2. PCC Slab Length

Figure 4.6 shows the slab length patterns for JPCP constructed in California. Three slab length patterns—12,13,14,15 ft.; 12,13,18,19 ft.; and 15 ft.—are the common patterns that have been constructed in different time intervals over the years in California. Figure 4.7 shows the history of slab length pattern construction over the years. Each panel in the figure corresponds to a 10-year interval of construction years. Before about 1990, the 12,13,18,19 ft. slab length pattern was more common, whereas after 1990 the 12,13,14,15 ft. slab length pattern became the dominant length pattern. The slab length patterns were categorized into two groups for the calibration, with 12,13,14,15 ft. being the short pattern, and 12,13,18,19 ft. being the long pattern.

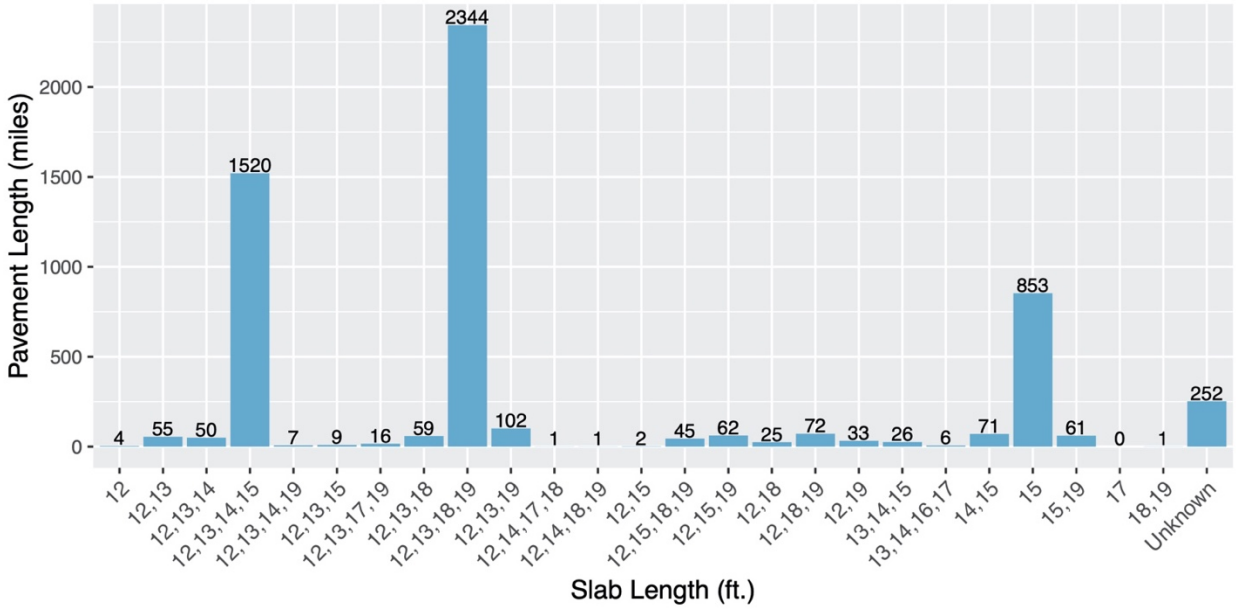

Figure 4.6: PCC slab length distribution

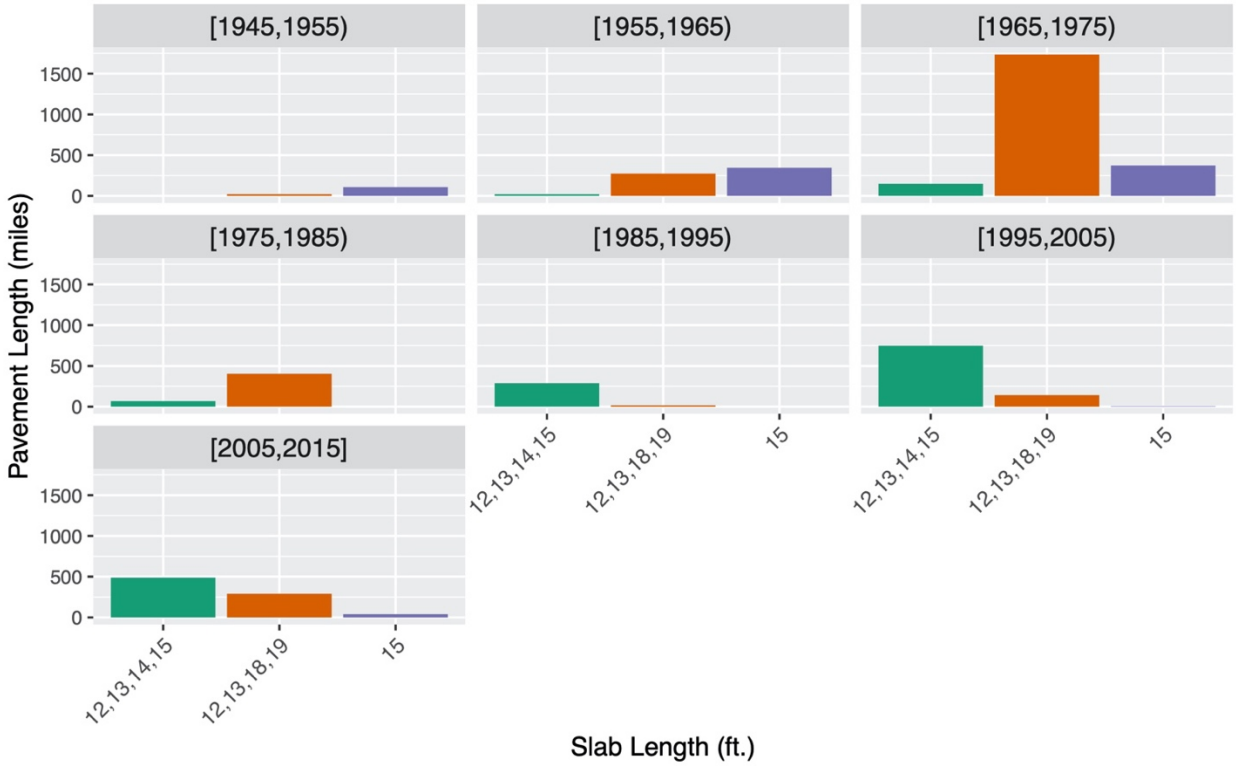

Figure 4.7: PCC slab length pattern history distribution

Figure 4.8 shows that the longer slab pattern had a higher rate of first-stage cracking over the years. However, the difference in performance between different slab length patterns is not as significant as was expected.

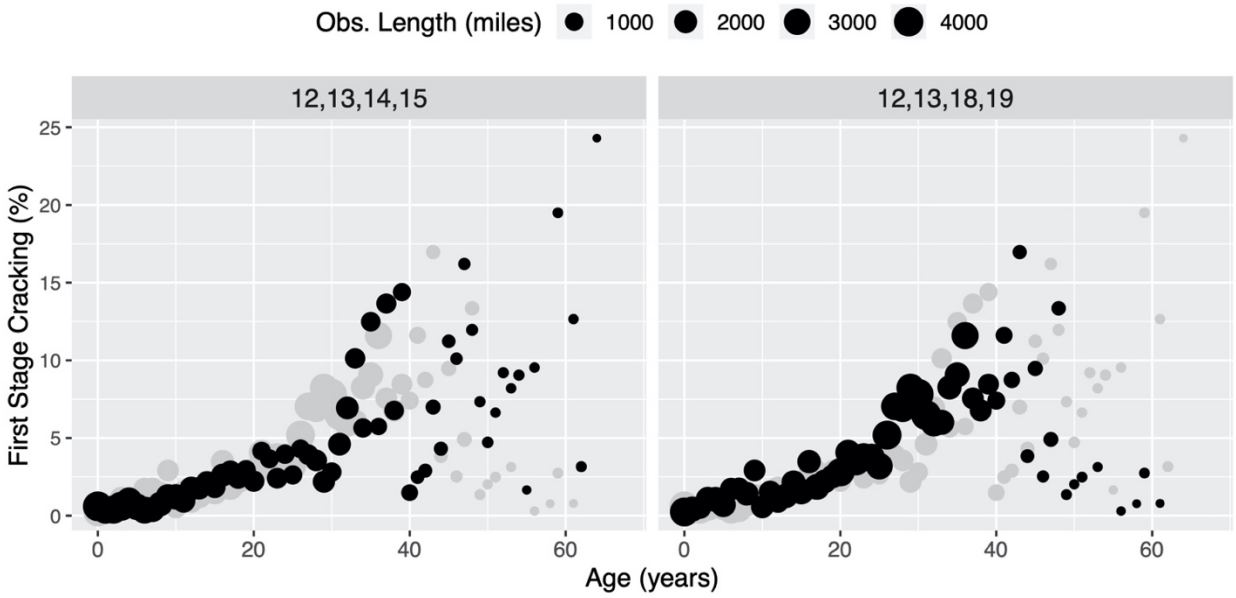

Figure 4.8: JPCP first-stage cracking for different PCC slab length patterns

4.2.2.3. Base Type

Five different base types are in the Caltrans pavement management system performance database: aggregate base (AB), asphalt-treated permeable base (ATPB), cement-treated base (CTB), asphalt base (HMA), and lean concrete base (LCB). Based on Figure 4.9, it can be seen that the majority of JPCP was constructed with CTB, and that ATPB was used the least.

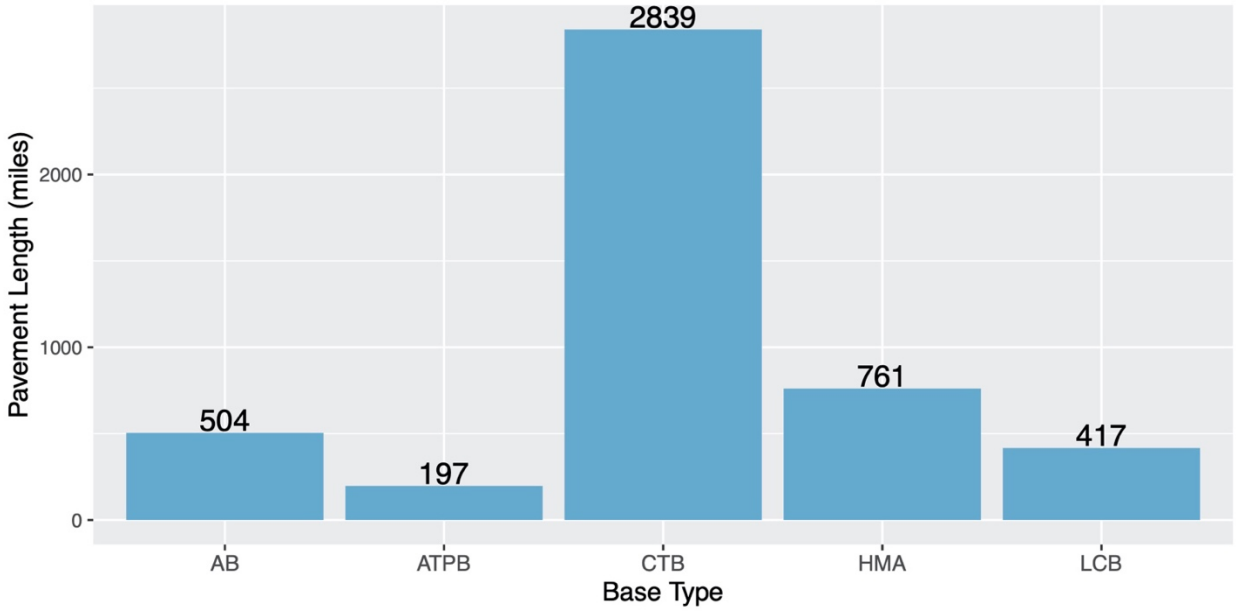

Figure 4.9: Base type distribution

From a first glance at Figure 4.10, one can infer that CTB has the worst performance among the other base types. However, this is not necessarily a correct conclusion, since Figure 4.10 considers only one variable (base type) affecting the performance of the JPCP and does not account for other variables such as PCC slab thickness, PCC slab length, shoulder type, traffic, and climate.

To consider all the variables and their simultaneous interactions on the cracking performance of JPCP, a statistical model based on the performance data was developed. In making its predictions, this model considers the variables PCC slab thickness, PCC slab length pattern, base type, shoulder type, climate, and Average Annual Daily Truck Traffic (AADTT). Predictions from this statistical model are shown in a number of figures that follow, but details of the model will be provided in the next chapter.

Figure 4.11 shows the effects of base type on the performance of the JPCP while keeping the other variables constant and using the predictions of the statistical performance model. The results are for 0.9-ft. PCC slab thickness, flexible shoulder type, 7,000 AADTT, and the Inland Valley climate region. Each panel in the figure corresponds to a different base type and slab length pattern. The green shaded area represents the probability of the pavement being undamaged; the yellow area represents the probability of first-stage cracking, and the red represents the probability of third-stage cracking versus years in service. It can be seen that LCB and ATPB show poorer performance than the rest of the base types, and that AB and CTB show better performance.

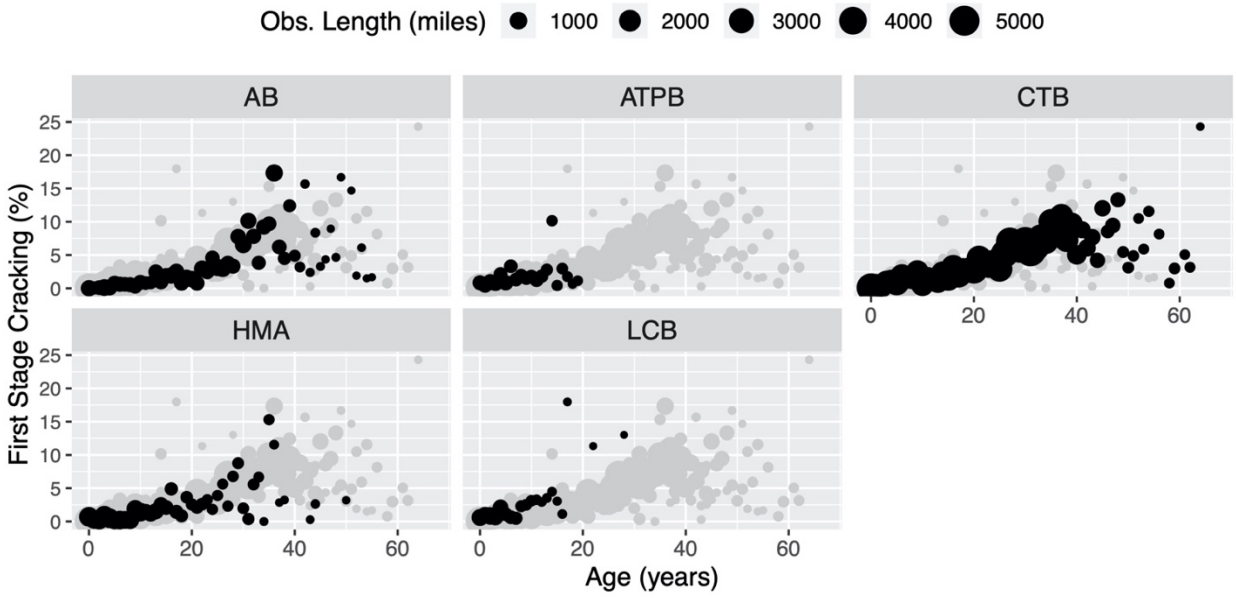

Figure 4.10: JPCP first-stage cracking for different base types

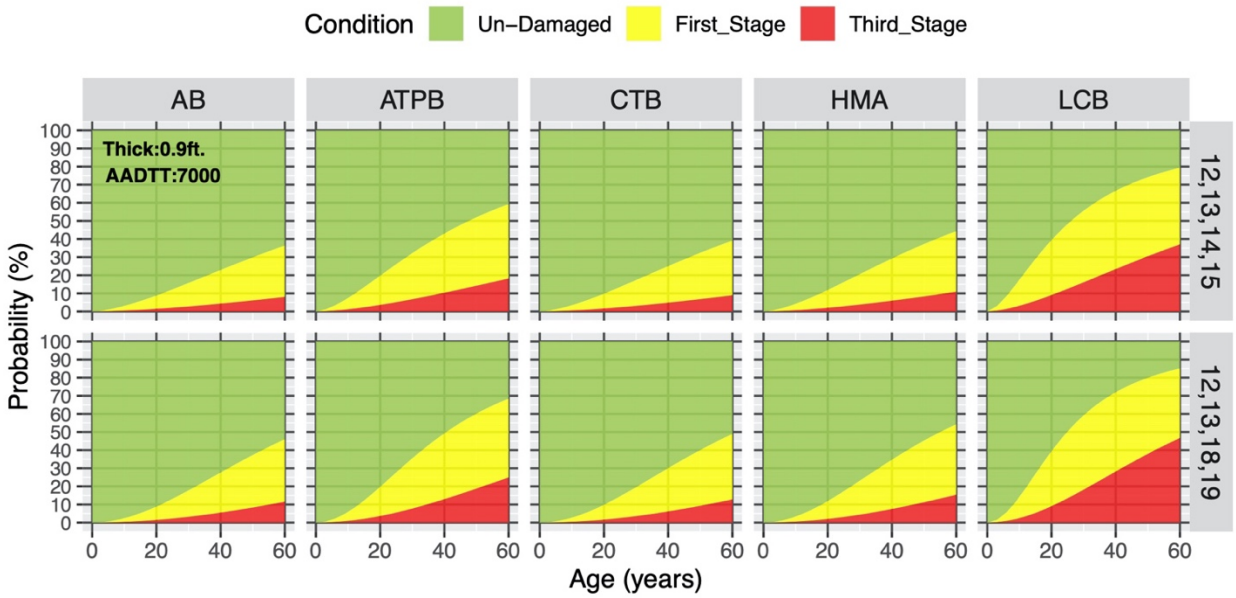

Figure 4.11: Performance model predictions for different base types

4.2.2.4. Shoulder Type

Four different shoulder types are defined in the database: not applicable (NAP) for interior lanes without a shoulder, untied flexible (FLX) shoulder, tied concrete (RIG) shoulder, and widened (WRF) lane. It should be noted that the WRF lane type represented in the database is a 2-ft.–wide shoulder. Figure 4.12 shows the distribution of each of these shoulder types in the database. WRF has the fewest constructed lane-miles of all the shoulder types in the database.

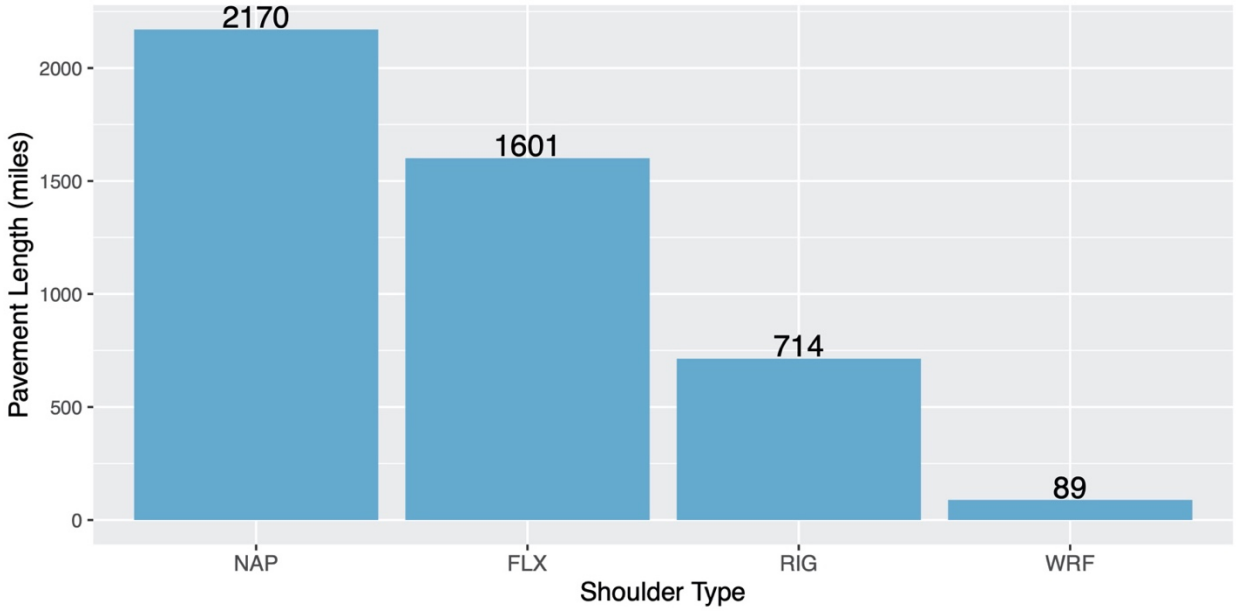

Figure 4.12: Shoulder type distribution

(Note: NAP: not applicable for interior lanes without a shoulder; FLX: untied flexible shoulder; RIG: tied concrete shoulder: WRF: widened lane.)

Looking at Figure 4.13, one might conclude that the flexible shoulder type (FLX) has the poorest performance of all the shoulder types. This is not necessarily a correct conclusion as other pavement structural, traffic, and climate variables were not accounted for in this plot. Figure 4.14 shows the results of the statistical performance model for shoulder type performance while holding all other variables constant. It can be seen that widened lane (WRF) had the most first- and third-stage cracking, followed by the untied flexible (FLX) shoulder type. The tied concrete shoulder (RIG) type had the best performance among all the shoulder types.

To investigate the reason for the poor performance of the widened lanes (WRF), the per-slab performance data from the 2011 – 2012 APCS data were studied. Figure 4.15 shows the amount of cracking for JPCP, with the WRF shoulder type categorized into panels with different base types and PCC slab thicknesses. The panels show the model results for the percentage of slabs with no cracking in green, first-stage cracking in yellow, and third- stage cracking in red versus years in service, with different panels for combinations of shoulder type and PCC slab length. It can be seen by looking at the middle two bottom panels that WRF mitigates the transverse cracking problem for longer slabs. However, it can also be seen that shorter slabs, those less than 16 ft., with widened slabs show increased longitudinal cracking. This susceptibility to longitudinal cracking for shorter slabs explains the poor performance of the WRF shoulder type. Again, it should be noted that the propensity for longitudinal cracking of the widened lanes in the database is for 2-ft. extra-wide lanes. It is expected that better longitudinal cracking performance may be obtained with a 1-ft widened lane; however, it is suggested that the reduction in risk of longitudinal cracking be further investigated through modeling.

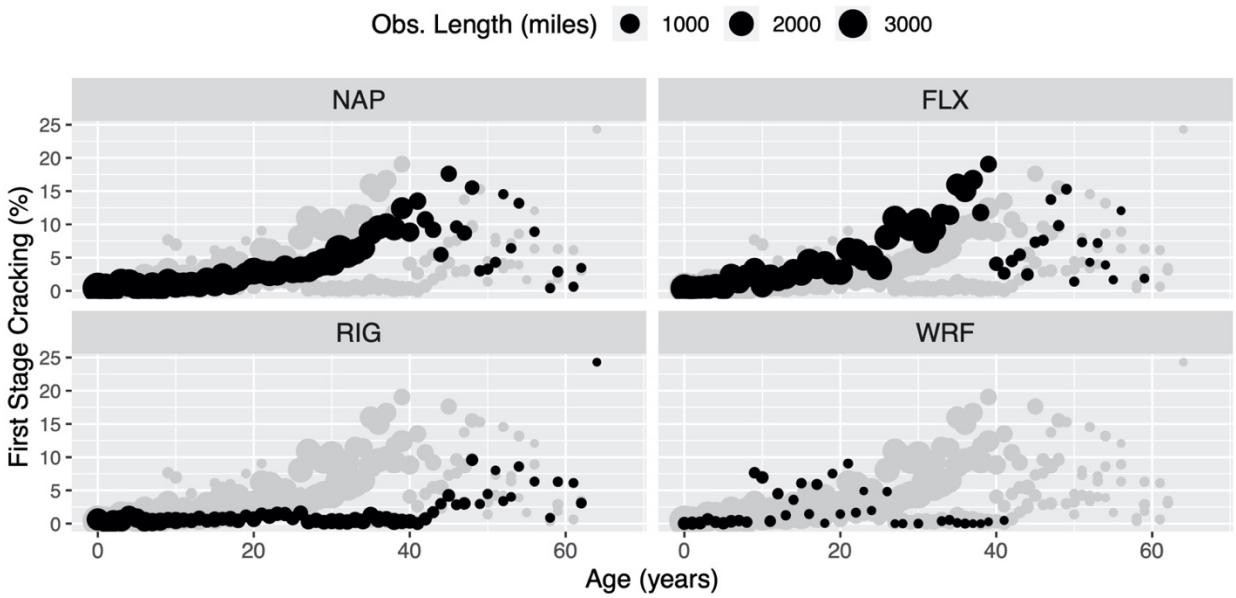

Figure 4.13: JPCP first-stage cracking for different shoulder types

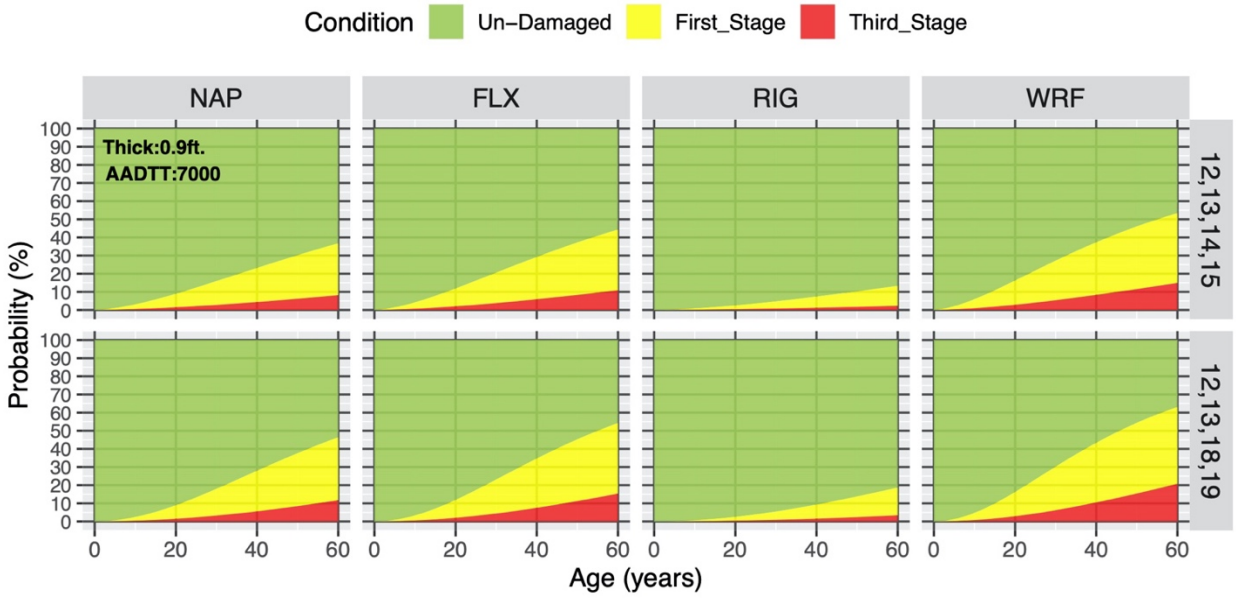

Figure 4.14: Performance model predictions for different shoulder types

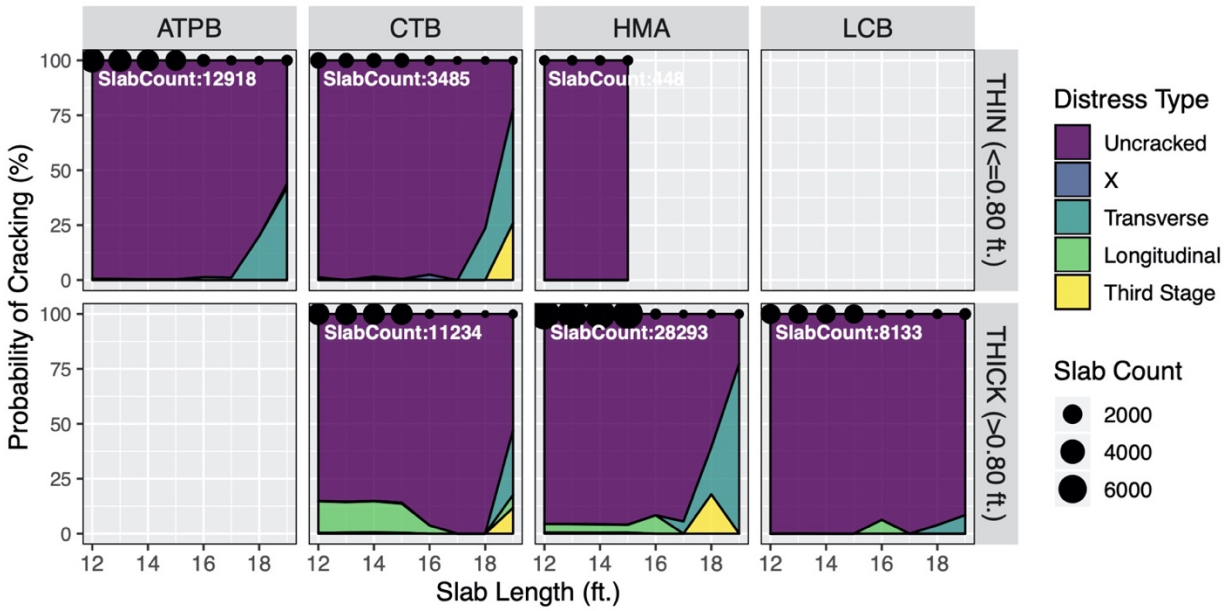

Figure 4.15: Distress type versus slab length for WRF shoulder type

4.2.2.5. Climate Region

Figure 4.16 shows the Caltrans climate region distribution. Most of the JPCP is located in the Inland Valley and South Coast, while the High Desert and Low Mountain climate regions have the fewest lane-miles of JPCP.

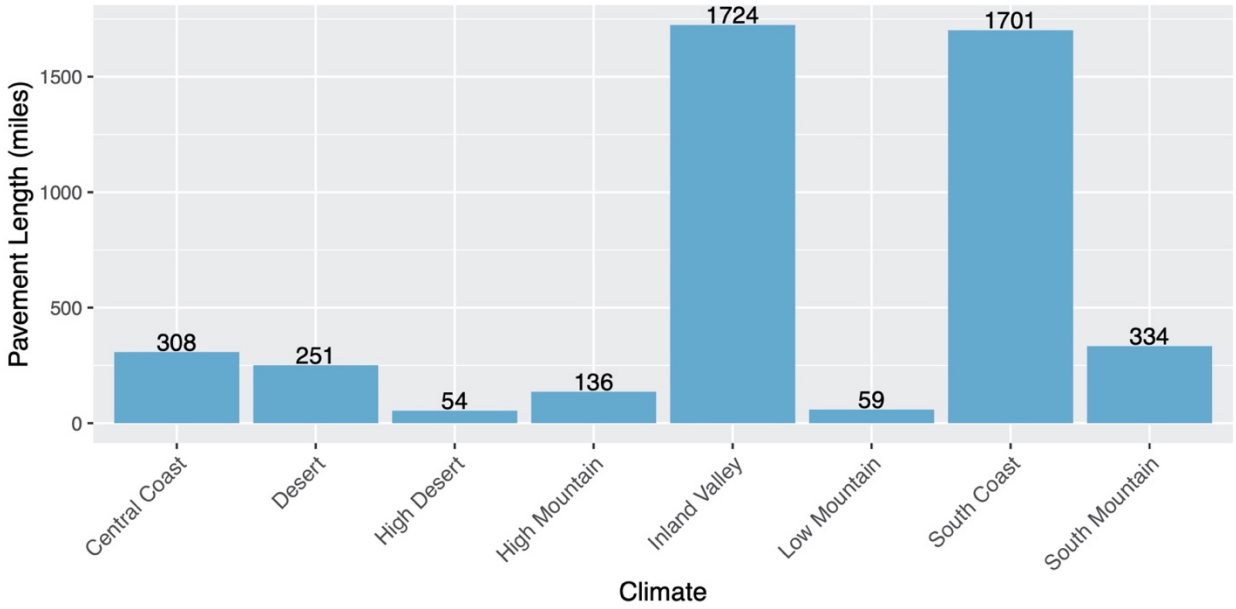

Figure 4.16: Climate region distribution

Figure 4.17 shows the JPCP performance in different climate regions. The High Desert (small amount of data), Inland Valley, Low Mountain (small amount of data), and South Mountain climate regions have

poorer performance than the others. The lane-miles of JPCP in the South Coast region appear to have excellent performance. The statistical performance model captures observations from the raw data as shown in Figure 4.18.

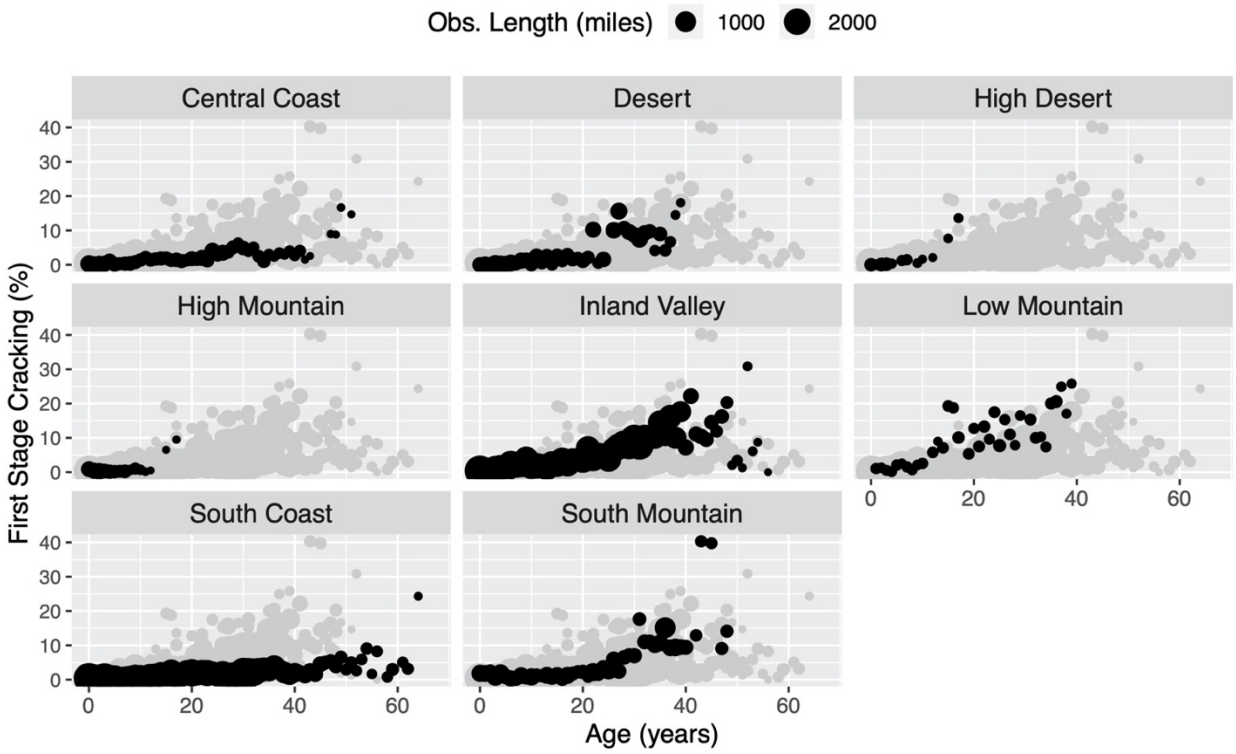

Figure 4.17: JPCP first-stage cracking for different climate regions

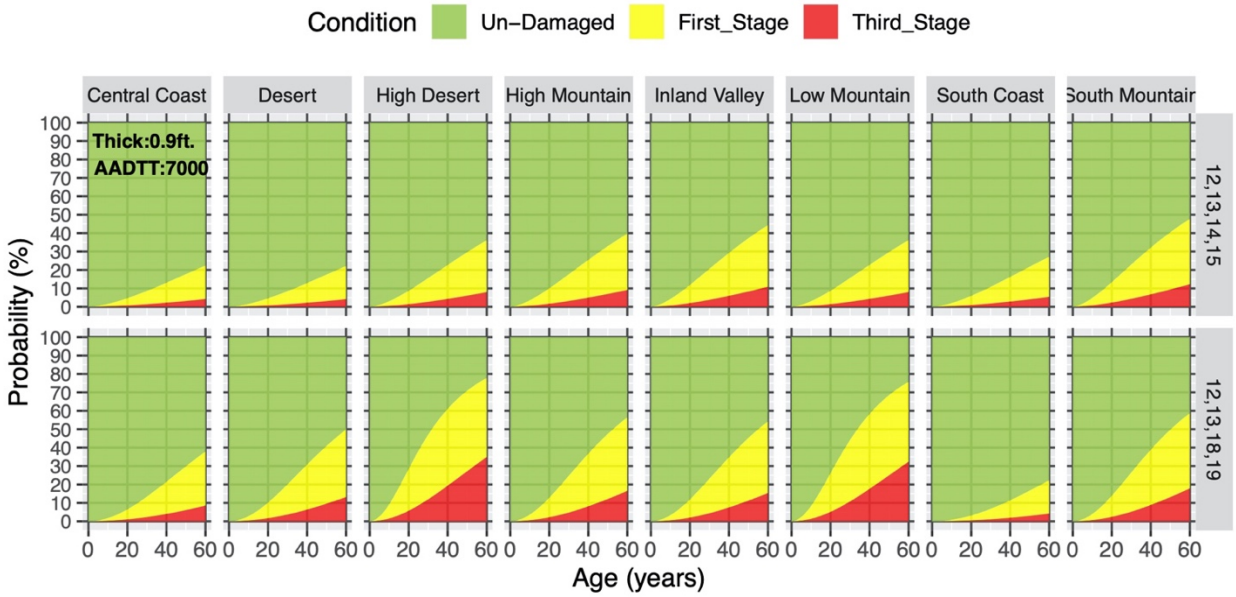

Figure 4.18: Performance model predictions for different climate regions

4.2.2.6. WIM Spectrum

Figure 4.19 shows the distribution of the lane-miles with for the five WIM spectra in the database. Higher WIM spectrum numbers correspond to heavier truck traffic loads. It can be seen that most of the JPC pavement has WIM spectra 1 and 2. This is certainly weighted by the lane-miles of inner lanes that have fewer trucks, and the trucks in those lanes tend to be smaller and lighter.

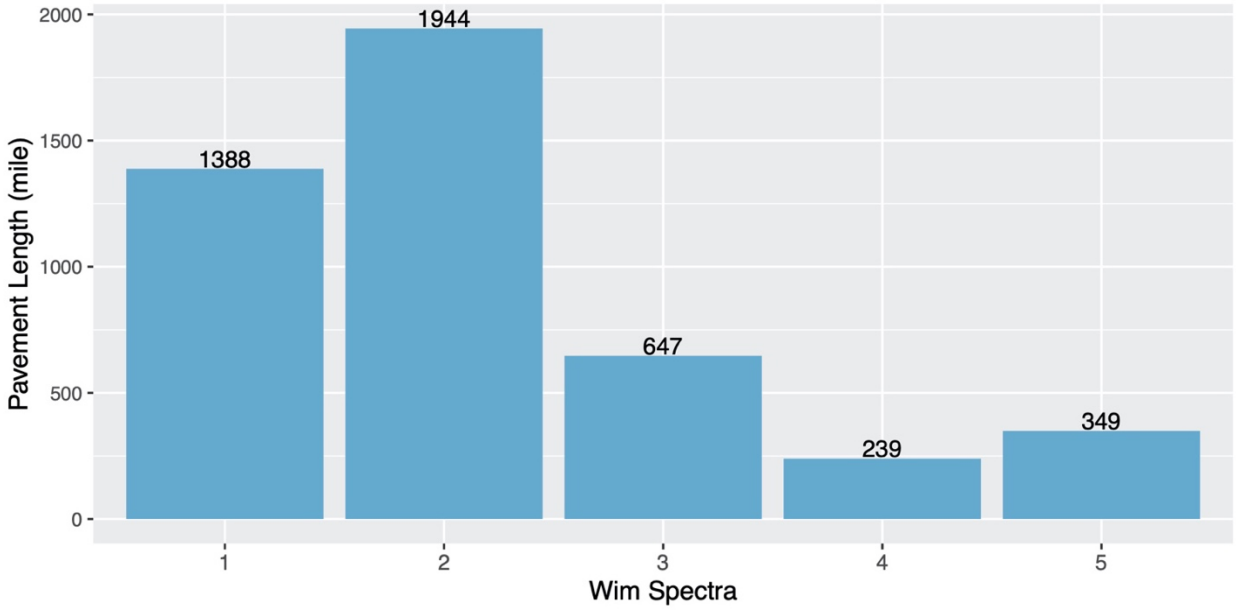

Figure 4.19: WIM spectra distribution

Figure 4.20 shows the JPCP performance for the different WIM spectra. As the WIM spectrum increases from 1 to 3, the amount of first-stage cracking increases, as expected. However, this is not the case for the heavier WIM Spectra 4 and 5, which have similar performance. Similarly, the statistical performance model did not show a consistent increase in cracking as the WIM spectrum increased, which was an unexpected outcome. The same trend was noted while developing the statistical model, and, therefore, it was decided to not include the WIM spectra variable in the cracking statistical performance model.

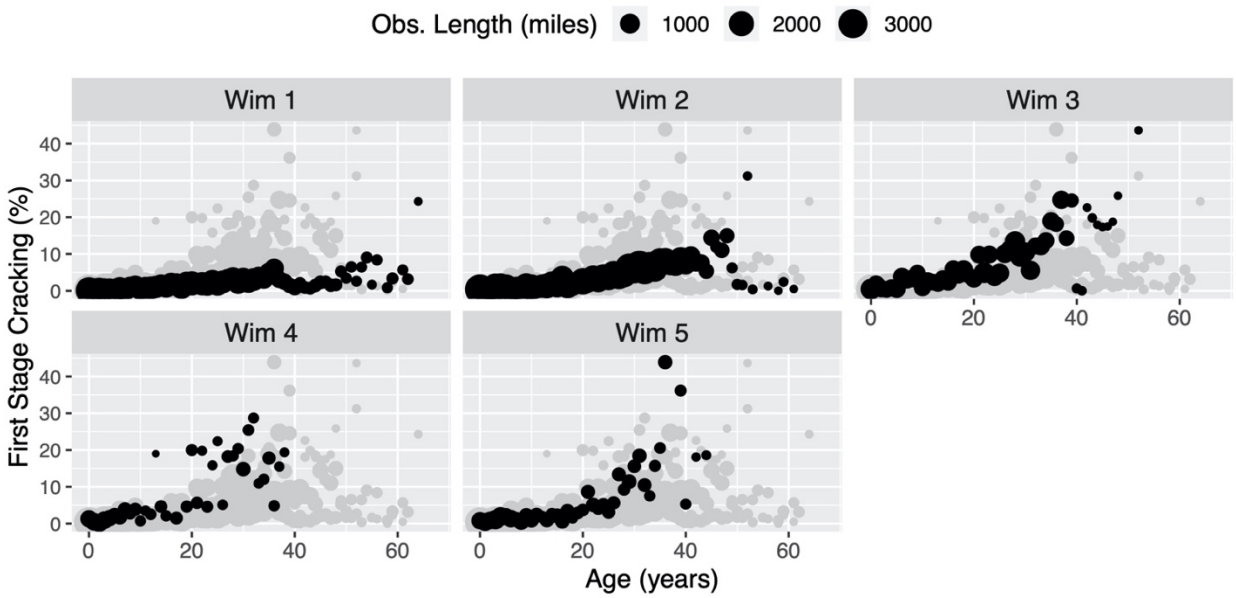

Figure 4.20: JPCP First-stage cracking for different WIM spectra

4.2.2.7. Annual Average Daily Truck Traffic (AADTT)

Figure 4.21 shows the distribution of unidirectional per lane AADTT. The X-axis shows the AADTT in thousands of trucks in 3,000 trucks-per-day increments.

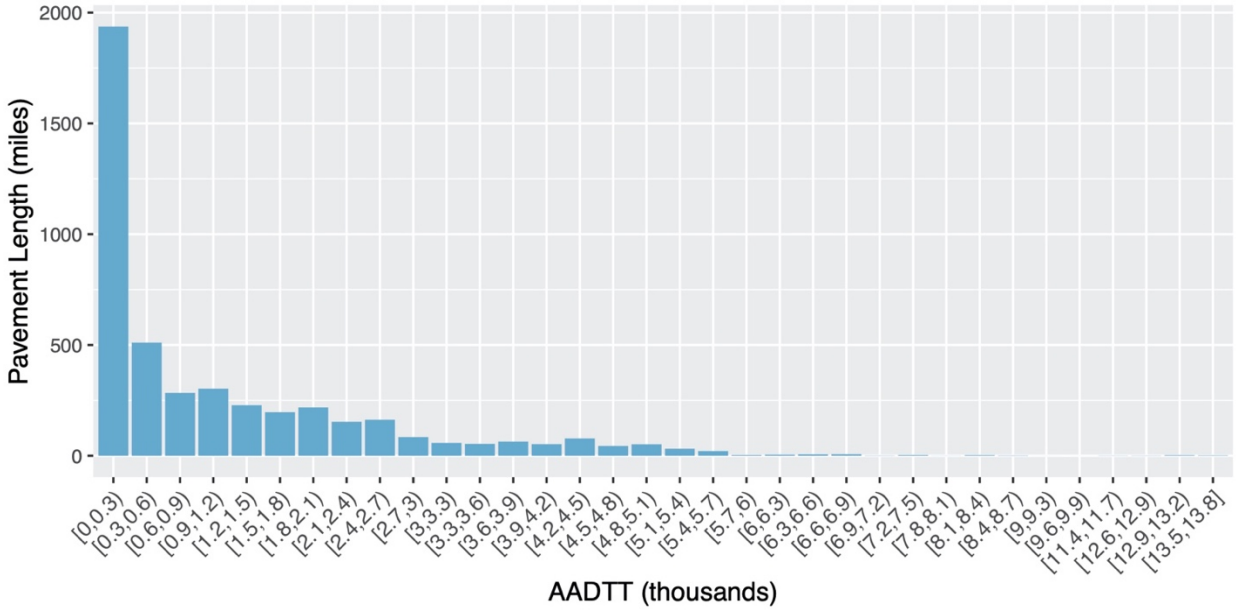

Figure 4.21: AADTT distribution

Figure 4.22 shows the performance of JPCP for different AADTTs. Each panel corresponds to a range of AADTT in thousands. As shown in the figure, as truck traffic increases, the amount of first-stage cracking

increases. The last four panels have sparse data, and drawing conclusions from them is not advised. However, predictions by the performance model support the visual observation in the data that greater AADTT causes more cracking, which was expected.

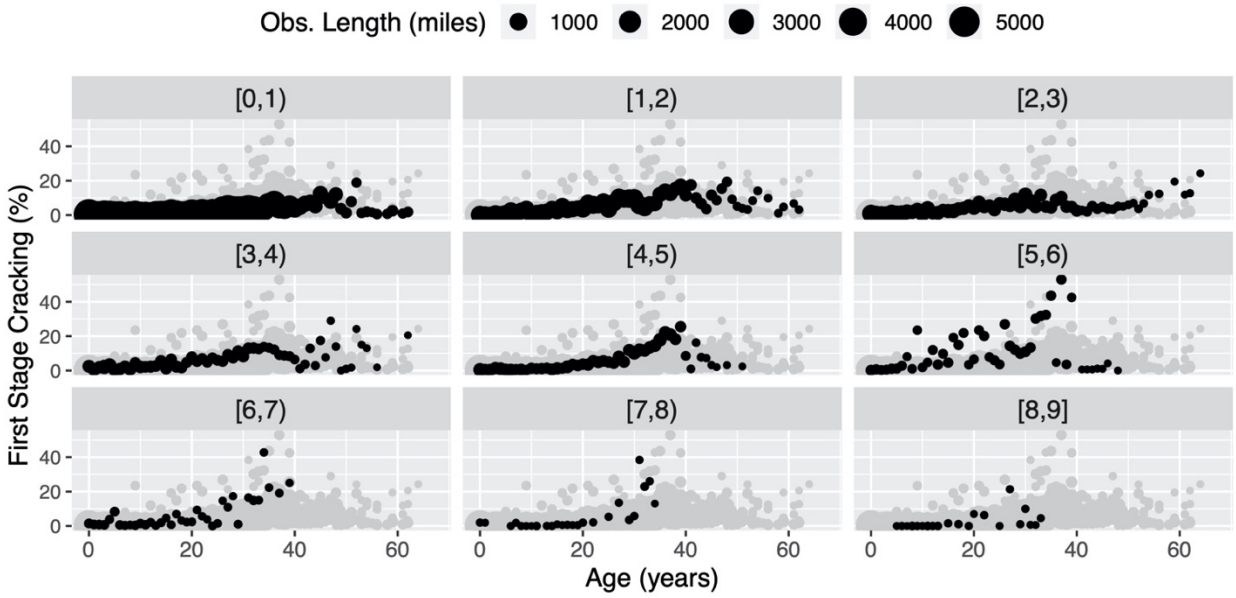

Figure 4.22: JPCP first-stage cracking for different AADTTs (thousands of trucks per day per direction per lane)

4.3. Pavement ME Performance Prediction Models for JPCP

The following three distress models are used in Pavement ME for analyzing and designing jointed plain concrete pavement (JPCP):

- Transverse cracking
- Mean transverse joint faulting
- Smoothness index (IRI)

The transverse cracking and mean transverse joint faulting models are stand-alone developed based on mechanics and statistical modeling principles. However, the IRI model was developed solely by relating the output of the transverse cracking and faulting models to IRI using statistical techniques. Each of these models is discussed further below.

4.3.1. Transverse Cracking

In Pavement ME, the structural responses of JPCP such as stress, strain, and deflection are computed using neural networks developed from a large factorial of finite element analysis results. These structural

responses are related to the damage accumulated in the pavement caused by environmental conditions and traffic loadings through Miner's law fatigue equation. The general expression for fatigue damage accumulation considering all the critical factors for JPCP transverse cracking is as follows:

$$FD = \sum \frac{n_{i,j,k,l,m,n}}{N_{(i,j,k,l,m,n)}} \tag{4.1}$$

where FD is the total fatigue damage (top-down and bottom-up), $n_{i,j,k,l,m,n}$ is the applied number of load applications at condition i, j, k, l, m, n, and $N_{(i,j,k,l,m,n)}$ is the allowable number of load applications at condition i, j, k, l, m, n. Each subscript represents different conditions, such as age, month, axle type, load level, temperature difference, traffic path, etc. The allowable number of load applications is the number of load cycles at which fatigue failure is expected (corresponding to 50 percent of slabs with transverse cracking) and is a function of the applied stress and the strength of the portland cement concrete (PCC). The allowable number of load applications is determined using the following field-calibrated fatigue model:

$$\log\left(N_{i,j,k,l,m,n}\right) = C_1 \left(\frac{MR}{\sigma}\right)^{C_2} \tag{4.2}$$

where $N_{i,j,k,l,m,n}$ is the allowable number of load applications, MR is the PCC modulus of rupture in psi, σ is the applied stress in psi, and C_1 and C_2 are equation constants that should not be changed because they have been calibrated by previous researchers and new data are not available to calibrate them.
The amount of transverse cracking observed in a JPCP section is calculated using the fatigue damage calculated by Equation (4.1) as follows:

$$CRK = \frac{100}{1 + C_4(FD)^{C_5}} \tag{4.3}$$

where CRK is the percentage of bottom-up or top-down transverse cracking appearing on the surface, FD is the fatigue damage index calculated using Equation (4.1), and C_4 and C_5 are the equation constants calibrated using field data. It should be noted that in Pavement ME, it is assumed that both top-down and bottom-up cracking can occur. Damage is calculated at the top and bottom of the slab, and the results are used to determine, respectively, top-down and bottom-up transverse cracking. Finally, top-down and bottom-up transverse cracking are regarded as two independent phenomena and are used to estimate the total transverse cracking probability:

$$CRK = CRK_{top\_down} + CRK_{bottom\_up} - CRK_{top\_down} * CRK_{bottom\_up} \tag{4.4}$$

4.3.2. Mean Transverse Joint Faulting

The faulting progression rate in JPCP increases due to poor load transfer across a joint or crack; heavy axle loads that result in increased differential deflections; and free moisture and high fines content in the layers beneath the concrete that lead to erosion and fines pumping of the base, subbase, and subgrade materials under the pavement. According to the MEPDG (NCHRP, 2003), traffic loading, slab thickness, PCC modulus of elasticity, modulus of subgrade reaction (k-value), base type, shoulder type, transverse joint spacing, and dowel diameter are among the design factors that affect transverse joint faulting.

Pavement ME uses an incremental approach to calculate faulting in JPCP. A faulting increment is determined at each month, and the current faulting level affects the magnitude of the increment. The following model—shown as Equations (4.5), (4.6), (4.7), and (4.8)—determines monthly faulting by summing the incremental faulting over the pavement life since opening to traffic:

$$Fault_m = \Sigma_{i=1}^{m} \Delta Fault_i \tag{4.5}$$

$$\Delta Fault_i = C_{34}(FaultMax_{i-1} - Fault_{i-1})^2 * DE_i \tag{4.6}$$

$$FaultMax_i = FaultMax_0 + C_7 * \Sigma_{j=1}^{m} DE_j * \log\left(1 + C_5 * 5^{Erod}\right)^{C_6} \tag{4.7}$$

$$FaultMax_0 = C_{12} * \delta_{curling} * [\log\left(1 + C_5 * 5^{Erod}\right) * \log\left(P_{200} * \frac{WetDays}{P_s}\right)]^{C_6} \tag{4.8}$$

where $Fault_m$ is the mean joint faulting at the end of month m in inches, $\Delta Fault_i$ is the incremental change in mean joint faulting on a monthly basis (during month i) in inches, DE_i is the differential deflection energy density of subgrade deformation for month i in lb/in, $FaultMax_i$ is the maximum mean transverse joint faulting in month i in inches, $FaultMax_0$ is the initial maximum mean transverse joint faulting in inches, $Erod$ is a base/subbase erodibility factor, $\delta_{curling}$ is the maximum mean monthly PCC slab corner upward deflection due to temperature curling and moisture warping, P_s is the overburden on subgrade in lbs, P_{200} is the percent subgrade material passing #200 sieve, and $WetDays$ is the average annual number of wet days (greater than 0.1 inches of rainfall). The constants C_{12} and C_{34} are defined as follows:

$$C_{12} = C_1 + C_2 * (FR)^{0.25} \tag{4.9}$$

$$C_{34} = C_3 + C_4 * (FR)^{0.25} \tag{4.10}$$

where FR is base freezing index defined as the percentage of time the temperature at the top of the base is below freezing. C_1 through C_7 in Equations (4.6) through (4.9) are the mean transverse joint faulting model constants that are calibrated against field data.

The model's functional form reflects the hypothesis that faulting potential depends on the amount of PCC slab curling, base erodibility, and the presence of fines and free water in the subgrade. Faulting potential decreases with an increase of overburden pressure on the subgrade. The faulting development rate depends on the faulting level and decreases as the cumulative faulting increases until it stabilizes to a certain level.

The process of calculating mean transverse joint faulting in Pavement ME can be summarized in the following steps:

- Process the traffic data to calculate the equivalent number of single, tandem, and tridem axles.
- Process the pavement temperature profile data to convert the hourly pavement temperature profile generated by the Enhanced Integrated Climate Model (EICM) to effective nighttime differences.
- Process the monthly relative humidity to take into account the effect of seasonal changes in moisture conditions on differential shrinkage in terms of monthly deviations in slab warping expressed in terms of equivalent temperature differential.
- Calculate initial maximum faulting.
- Evaluate joint load transfer efficiency (LTE).
- Calculate current maximum faulting.
- Determine critical pavement responses for the increment.
- Evaluate the loss of shear capacity and dowel damage.
- Calculate the faulting increment.
- Calculate cumulative faulting.

4.3.3. International Roughness Index (IRI)

According to the MEPDG (NCHRP, 2003), for a given rigid pavement with an initial smoothness, several factors combine to contribute to smoothness loss over time. The occurrence and progression of visible distresses in JPCP was found to be the main factor decreasing a pavement's smoothness after construction. JPCP smoothness decreases as the quantity and severity of distresses such as transverse cracking, mean transverse joint faulting, and joint spalling increase. The initiation and progression of such distresses result from application of traffic loads, environmental loads, loss of foundation support, and the effect of aging on the pavement materials. As shown previously, these variables' effects on the occurrence of distresses in JPCP—such as transverse cracking and mean transverse joint faulting—were taken into account using mechanistic-empirical (ME) approaches. The results from these models will be used as input data for the Pavement ME smoothness model.

In Pavement ME, smoothness is predicted as a function of the initial as-constructed profile of the pavement and any change in the longitudinal profile over time due to traffic. The following is the smoothness (IRI) model developed and used in Pavement ME:

$$IRI = IRI_0 + C_1 * CRK + C_2 * SPALL + C_3 * TFAULT + C_4 * SF \quad (4.11)$$

where IRI is the predicted roughness index in (in.)/(mi.), IRI_0 is the initial smoothness in (in.)/(mi.), CRK is the percent of slabs with transverse cracking, $SPALL$ is the percentage of joints with spalling, $TFAULT$ is the cumulative transverse joint faulting per mile in inches, SF is the site factor, and C_1 through C_4 are the equation constants that should be calibrated using field data.

Transverse cracking and faulting are calculated with the models explained earlier. The site factor is defined as the following:

$$SF = AGE * (1 + 0.556 * FR) * (1 + P_{200}) * 10^{-6} \quad (4.12)$$

where AGE is the pavement age in years, FR is the freezing index, and P_{200} is the percentage of subgrade materials passing the #200 sieve.

Transverse joint spalling is determined using the following equation:

$$SPALL = \left[\frac{AGE}{AGE + 0.01}\right]\left[\frac{100}{1 + 1.005^{-12*AGE+SCF}}\right] \quad (4.13)$$

where $SPALL$ is the percentage of spalled joints, AGE is the pavement age in years, and SCF is scaling factor based on site, design, and climate. The equation for SCF is:

$$SCF = -1400 + 350\, AC_{PCC} * (0.5 + PREFORM) + 43.4 * f_c'^{0.4} - 0.2 * \left(FT_{cycle} * AGE\right) + 43 * HPCC - 536\, WC_{PCC} \quad (4.14)$$

where AC_{PCC} is PCC air content in percent; AGE is the age of the pavement in years, $PREFORM$ is 1 if preformed sealant is present, otherwise 0, f_C' is PCC compressive strength in psi, FT_{cycle} is average annual number of freeze-thaw cycles, $HPCC$ is PCC slab thickness in inches, and WC_{PCC} is the PCC water-cement ratio.

4.4. Sensitivity Analysis

The main goal of this study is to calibrate the distress prediction models in Pavement ME for JPCP design in California. However, prior to calibration, it is necessary to review the ranges of values for input variables and then to evaluate the sensitivity to those ranges to determine which have the most significant effect on the results. The results of the sensitivity analysis identify which variables should get more attention in the design method and will be used to check the reasonableness of the model predictions, to identify problems in the software, and to understand the level of difficulty involved in obtaining the inputs.

The inputs considered for the JPCP sensitivity analysis were categorized into four groups, and a range of values for each input was selected (see Table 4.1). (Note: The values appearing in boldface in Table 4.1 are those used for the base model. In the rest of this chapter, the Pavement ME results for all cases show the predicted performance range for the range of inputs relative to the base model.) The input value ranges selected for the analysis are different than the ranges that will need consideration when developing design tools for Caltrans. In particular, the slab thicknesses needed to cover the range of designs for Caltrans conditions will include thinner and thicker slabs.

The ranges for the variables considered in this study were selected based on the historical data available in the Caltrans PMS database for variables controlled by the designer (e.g., PCC slab thickness, PCC slab length, base type, shoulder type, etc. discussed in previous section) and the UCPRC material database variables out of the control of the designer (e.g., PCC compressive strength, PCC CTE, PCC shortwave absorptivity, etc. discussed in the Appendix). Therefore, the range selected for each variable reflects the common construction practice in California and validates the sensitivity of the models' performance to the variable's change. These values were selected for the analysis to identify the reasonableness of the results from the models based on California experience, to identify which variables are most sensitive, and to identify variables for which the results are non-monotonic (that is, an increase in the input variable may result in an increase or decrease in the predicted performance depending on the input variable value). In many cases, identifying a variable's sensitivity requires the range used to check for sensitivity to be much larger than the range expected in the field.

These ranges will not be used for Pavement ME calibration. In the calibration process, the range selected for each variable will include all the values ever used for JPCP construction in in California, based on the

PMS database. The ranges studied in this chapter are a subset of those that will be used for the Pavement ME calibration that will be explained in next chapter.

As noted, the variables can be divided into those that can be determined by a pavement designer, and those that a designer cannot control. Specifically, the pavement structural design variables are primarily determined by the designer. The second group of variables, material inputs, are unknown to a designer in a design-bid-build project delivery environment, although some of the materials variables are partially constrained by specifications, such as strength, and those that are not, such as CTE. The third and fourth groups, traffic and climate, are generally known to the designer but cannot be controlled. Of course, there are many other input variables that need to be defined as part of Pavement ME runs. However, some variables were not considered due to a lack of data for them, such as shrinkage, which is also unknown to the designer. Their effects were not considered in this study, and their default values were used in the Pavement ME runs.

Table 4.1: Input variables examined in the sensitivity analysis

Input Category	Variable
Pavement structural design	PCC slab thickness: (7, **8**, 9) in inches
	PCC slab length: (12-13-14-15, **15**, 12-13-18-19) in feet
	Load transfer: (**Doweled**, Undoweled)
	Friction loss duration: (No Friction, **120**, 240) in months
	Base type: (Aggregate Base (AB), **Hot-Mix Asphalt (HMA)**, Cement-treated Base (CTB), Lean concrete base (LCB))
	Shoulder type (edge support): (Not-Tied, **Tied**, Widened)
	Subgrade type: (**Gravel&Sand (A-1a)**, Sand (A-3), Clay (A-5))
	Erodibility index: (ExtremelyErosionResistant (1), **FairlyErodible (4),** VeryErodible (5))
Pavement material	PCC compressive strength: (4,730, **5,730**, 6,730) in psi
	PCC Coefficient of Thermal Expansion (CTE): (4, **5**, 6) in 10^{-6}°F^{-1}
	PCC shortwave absorptivity: (0.65, **0.7**, 0.8, 0.9)
	PCC heat capacity: (**0.2**, 0.24, 0.28) in BTU.lb.°F
	PCC thermal conductivity: (1.0, 1.15, **1.25**, 1.5) in BTU.hr.ft.°F
	Built-in curl-warp temperature: (–15, –**10**, –5, 0) in °F
Traffic	Average annual daily truck traffic for two lanes (AADTT): (7,000, 12,000, **14,000**, 16,000, 20,000)
	WIM spectra: (1, **3**, 5)
Climate	Climate region: (Desert, High Desert, South Mountain, **Low Mountain**, High Mountain, Inland Valley, Central Coast, South Coast)

Notes:

The units used in the Pavement ME software are presented, although they are not necessarily the units used by Caltrans in design; Caltrans units and metric units [rounded to nearest 15 mm] are shown in parentheses in the initial discussion of each variable.

The values appearing in boldface were used for the base model.

To perform a sensitivity analysis of the distress prediction models for JPCP in Pavement ME, a base model was defined with a reference set of input values. The values were selected to investigate the effects of variation of input variables on the results of the Pavement ME models. The base model was defined as a pavement structure with an 8-inch (200 mm, 0.67 ft) PCC slab, a 4-inch (105 mm, 0.33 ft) HMA base, a 6-inch (150 mm, 0.5 ft) aggregate subbase, and a well-graded gravel and sand (A-1a) subgrade.

4.4.1. Pavement Structural and Design Inputs

4.4.1.1. PCC Slab Thickness

According to the Mechanistic-Empirical Pavement Design Guide (NCHRP, 2003), PCC slab thickness is one of the most critical design features from the standpoints of both performance and cost. In general, as slab thickness increases, critical bending stresses and deflections decrease, with a consequent reduction in cracking and faulting.

This sensitivity analysis considered three PCC thicknesses: 7, 8, and 9 inches (0.58, 0.67, 0.75 ft [175, 200, 230 mm]). These thicknesses were selected because most of the performance data used for the calibration came from projects with 8- to 10-inch slabs, and because of a desire to consider slabs somewhat less than 8 inches, the current minimum in the HDM, which may be used on routes with lower truck traffic volumes.

The significant effect that PCC slab thickness has on JPCP transverse cracking performance can be observed in Figure 4.23. It can be seen from the figure that decreasing slab thickness from 9 to 7 inches resulted, in this particular scenario, in an unacceptable design in terms of transverse fatigue cracking.

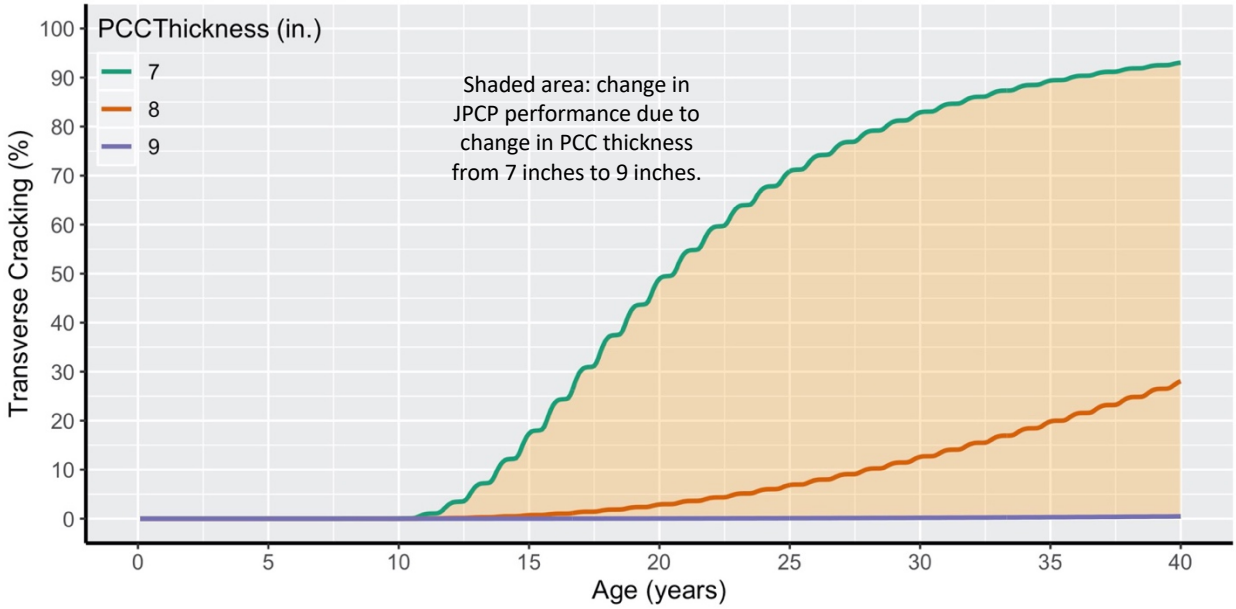

Figure 4.23: Effect of PCC slab thickness on transverse cracking with 50% reliability

Note: In all the following figures, the shaded area shows the change in JPCP performance illustrated in Figure 4.23. The shaded area is shown as a reference for comparing the effects that result from adjusting other variables. In this example, the strategy was used to compare the sensitivity of Pavement ME cracking predictions that include the rest of the variables with changes in PCC slab thickness.

Figure 4.24 shows the effect of PCC slab thickness on the JPCP faulting. These results do not match the stated expectation that thicker PCC slabs would have less faulting. Instead, this figure shows that 7-inch thick slabs have less faulting than thicker slabs. This outcome is believed to be related to the fact that dowel bar diameter was kept constant for all the PCC slab thicknesses (1.25 in.). Maintaining the same dowel diameter while increasing slab thickness results in a reduction in nondimensional dowel stiffness (JD), which is the ratio of cross-sectional steel area to total cross-sectional slab area. This in turn reduces LTE, which increases the differential energy of subgrade deformation, thus resulting in increased cumulative faulting. Therefore, a designer should increase dowel bar size with thicker PCC slabs. As shown in Figure 4.25, Pavement ME predicted faulting decreases versus slab thickness if the dowel diameter is adjusted for each slab thickness (1.0, 1.25, and 1.5 in. dowel diameter, respectively, for 7, 8, and 9 in. slab thickness). In any case, as long as a JPCP has an adequate dowel bar size at the transverse joints according to Caltrans guidelines, faulting should not be the critical path distress for long-term JPCP performance.

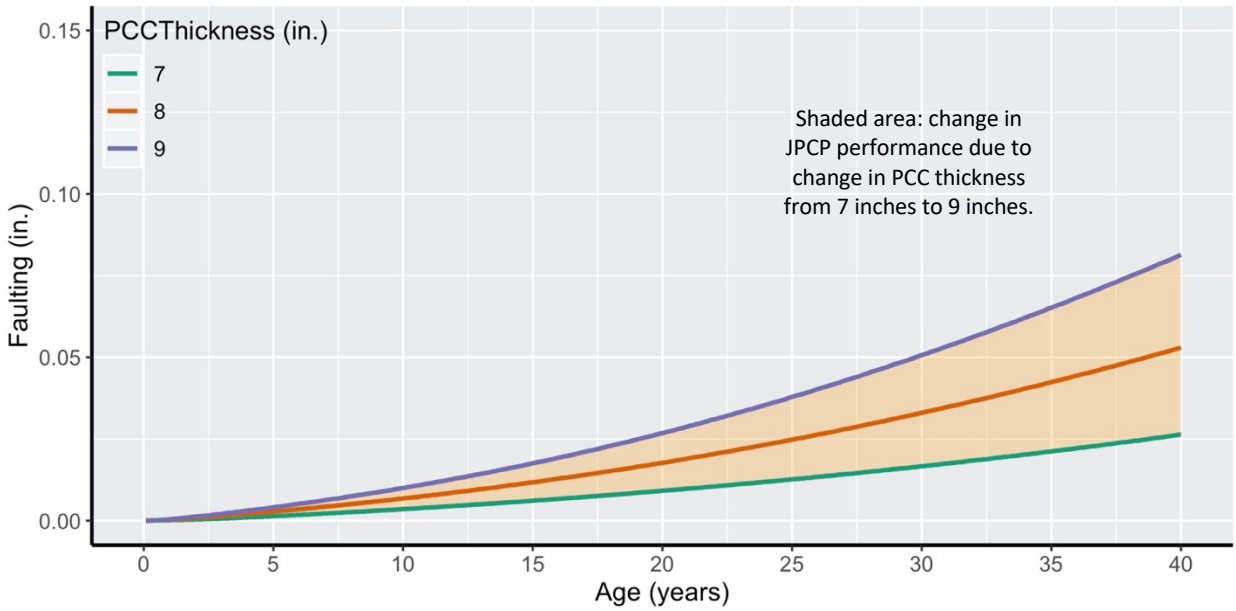

Figure 4.24: Effects of PCC slab thickness on faulting (while keeping dowel diameter constant) with 50% reliability

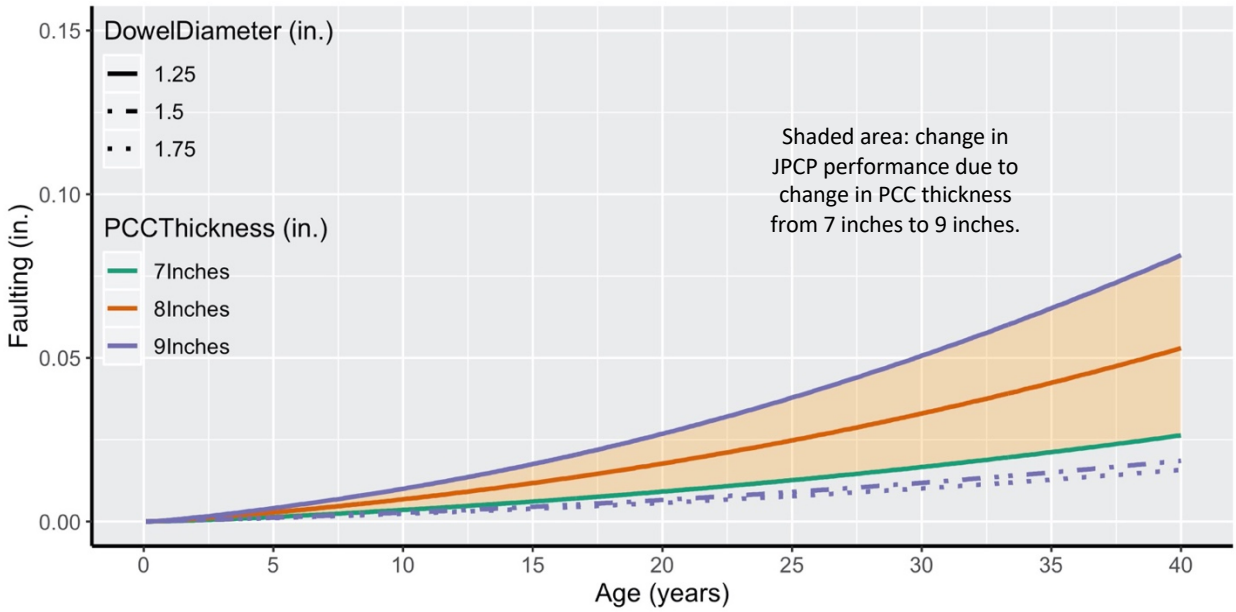

Figure 4.25: Effect of PCC slab thickness on faulting (while changing dowel diameter) with 50% reliability

The change in IRI is shown in Figure 4.26. Pavement ME determines IRI as a function of initial IRI, site conditions, transverse cracking, faulting, and spalling. Dowel diameter was adjusted for each slab thickness (1.0, 1.25, and 1.5 in. dowel diameters, respectively, for 7, 8, and 9 in. slab thicknesses) in order to produce the data shown in the figure. As expected, IRI decreased as slab thickness increased.

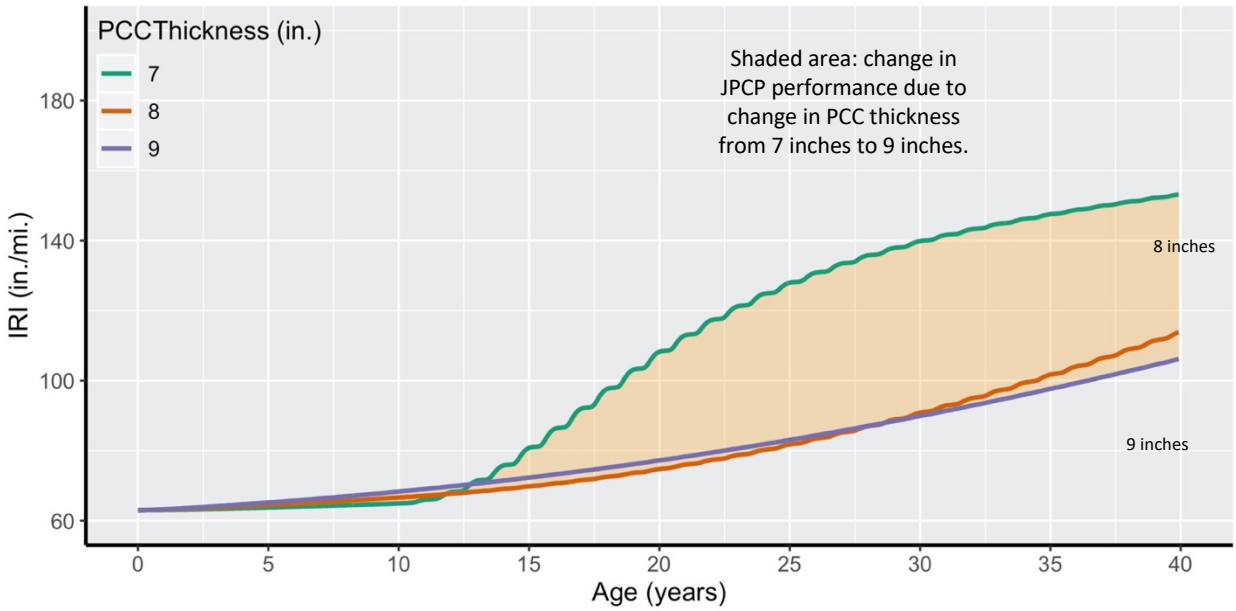

Figure 4.26: Effects of PCC slab thickness on IRI with 50% reliability

4.4.1.2. PCC Slab Length (Transverse Joint Spacing)

The MEPDG (NCHRP, 2003) states that transverse joint spacing affects transverse cracking, and to a lesser degree it also affects joint faulting. The MEPDG also states that field studies have shown that JPCPs with longer transverse joint spacing tend to be more susceptible to transverse cracking, and that therefore transverse joint spacing should be chosen within the context of JPCP design features such as PCC slab thickness, PCC slab width, PCC material properties, base type, and shoulder type.

Three different PCC slab length sets, 15 ft. (4.6 m), (12,13,14,15 ft.), and (12,13,18,19 ft.) are considered in this study. These slab lengths are (or were) the ones most commonly constructed in California, and designers who are adding or reconstructing lanes must either match the joint spacing in the adjacent lane or place an isolation joint between lanes if they are using joint spacings in the new lanes that do not match those in the existing lanes. The current version of Pavement ME cannot model random slab length. When this option is selected in the software, the mean slab length is used in cracking and faulting calculations; something similar applies to IRI. Consequently, the three slab length sets are modeled by Pavement ME as single slab lengths of 15, 13.5, and 15.5 ft. respectively.

Figure 4.27 shows the effect of transverse joint spacing on JPCP transverse cracking performance. This figure shows that longer PCC slabs have more transverse cracking than shorter ones. These results indicate that a 1 inch slab thickness change from 8 to 9 inches increases the percentage of transverse

cracking as much as a change from a joint length set of (12,13,14,15 ft.) to one with only 15 ft. joint spacing.

Figure 4.28 shows the effect of transverse joint spacing on JPCP faulting. As stated in the Pavement ME documentation, slab length is not a major factor affecting JPCP faulting. In this figure, it can be seen that over a 40-year service life, the difference in faulting is insignificant for different PCC slab lengths. The effect of transverse joint spacing is more important for IRI (Figure 4.29) than for faulting because the Pavement ME IRI model considers transverse cracking, which is sensitive to slab length.

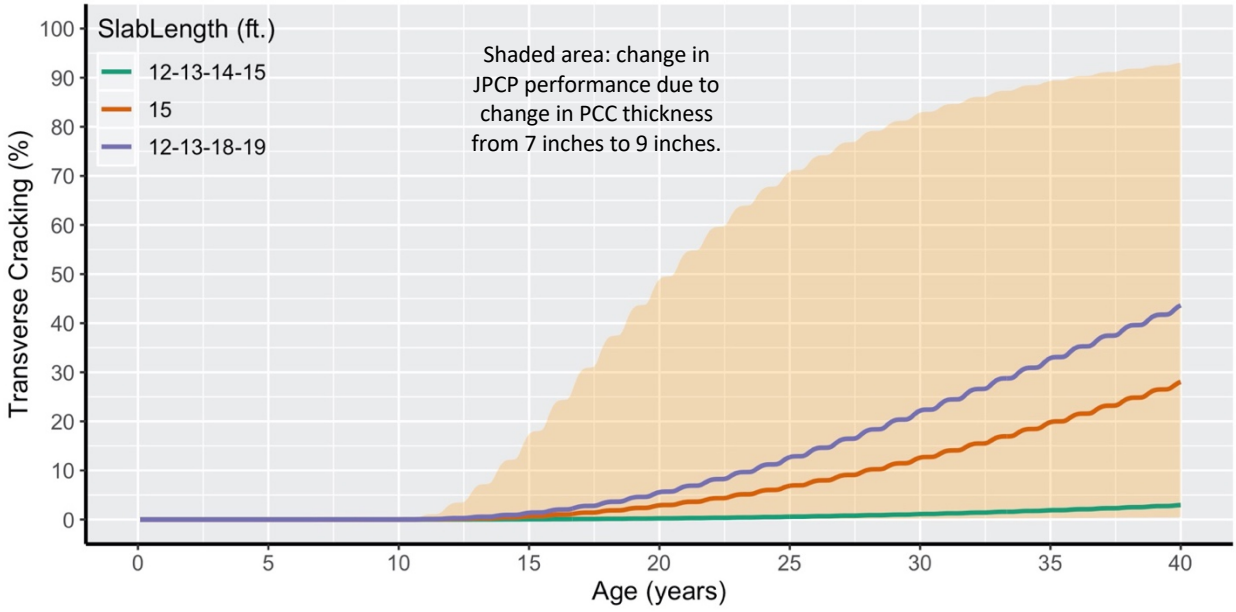

Figure 4.27: Effects of PCC slab length on transverse cracking with 50% reliability

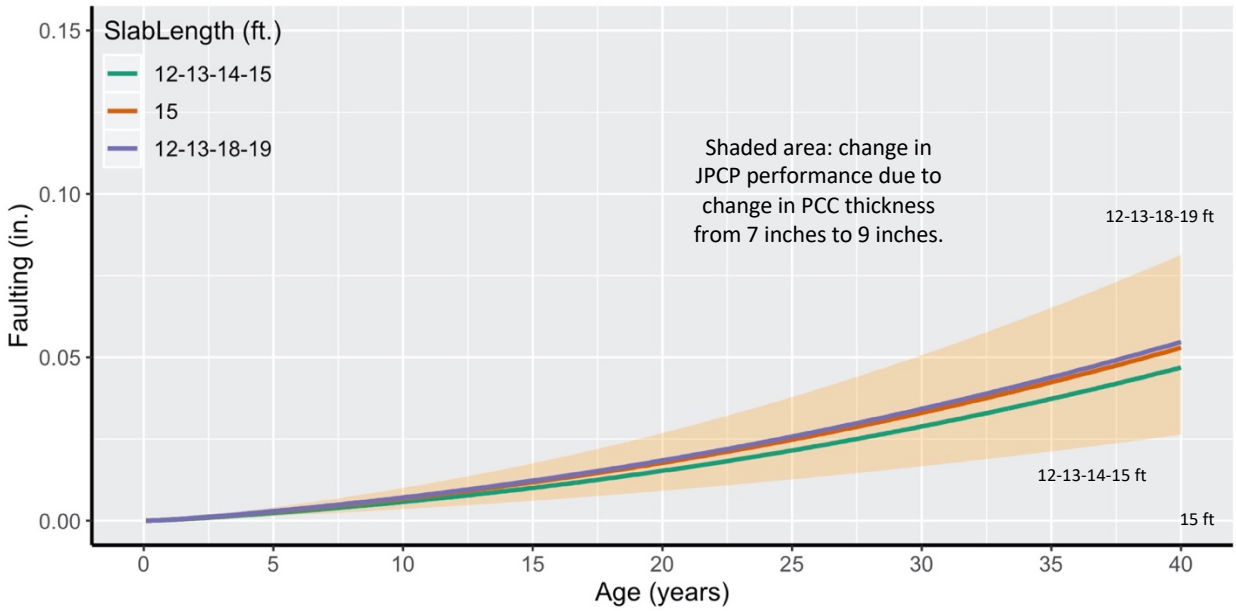

Figure 4.28: Effects of PCC slab length on faulting with 50% reliability

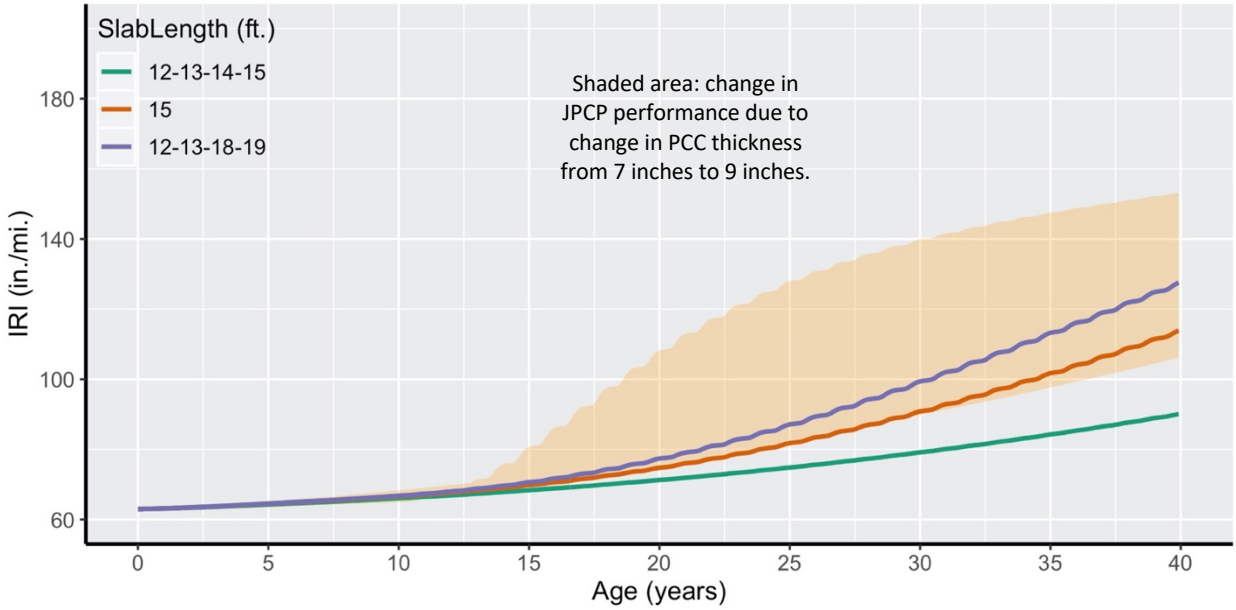

Figure 4.29: Effects of PCC slab length on IRI with 50% reliability

4.4.1.3. Load Transfer

According to the Pavement ME documentation, load transfer across transverse joints is the most critical factor controlling JPCP joint faulting and, subsequently, smoothness. The documentation also states that load transfer affects JPCP top-down cracking, and that field studies have shown that use of mechanical devices (dowels) greatly decreases the potential for transverse joint faulting, with the dowel diameter being an important factor affecting JPCP faulting. Small-diameter dowels (1 inch or less) are relatively

ineffective in preventing joint faulting, but large-diameter dowels (e.g., 1.5 inch) are highly effective. This size difference matters because the larger the dowel embedded in the concrete, the more it will spread and, therefore, reduce the compressive stresses on the concrete around it. The lower those stresses are, the better the concrete can maintain a tight fit around the dowel—and for a longer period of time.

Figure 4.30 shows the effect of using dowels on JPCP transverse cracking. This figure shows that the Pavement ME transverse cracking model is unaffected by the use dowels. However, as expected, Figure 4.31 and Figure 4.32 show the significant effect dowels have on the faulting and smoothness performance of JPCP. These figures show that undoweled JPCP will fail the faulting and smoothness criteria within almost the first five years of service life. Therefore, constructing doweled JPCP is an essential practice for having a long-lasting smooth pavement for heavier traffic.

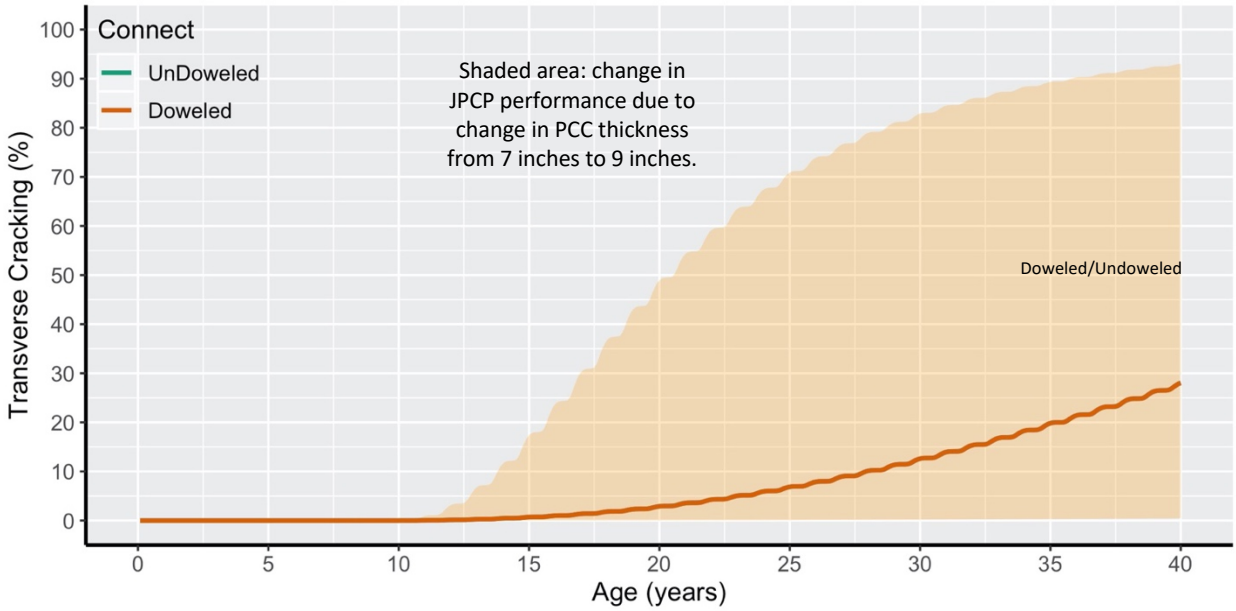

Figure 4.30: Effects of load transfer on transverse cracking with 50% reliability

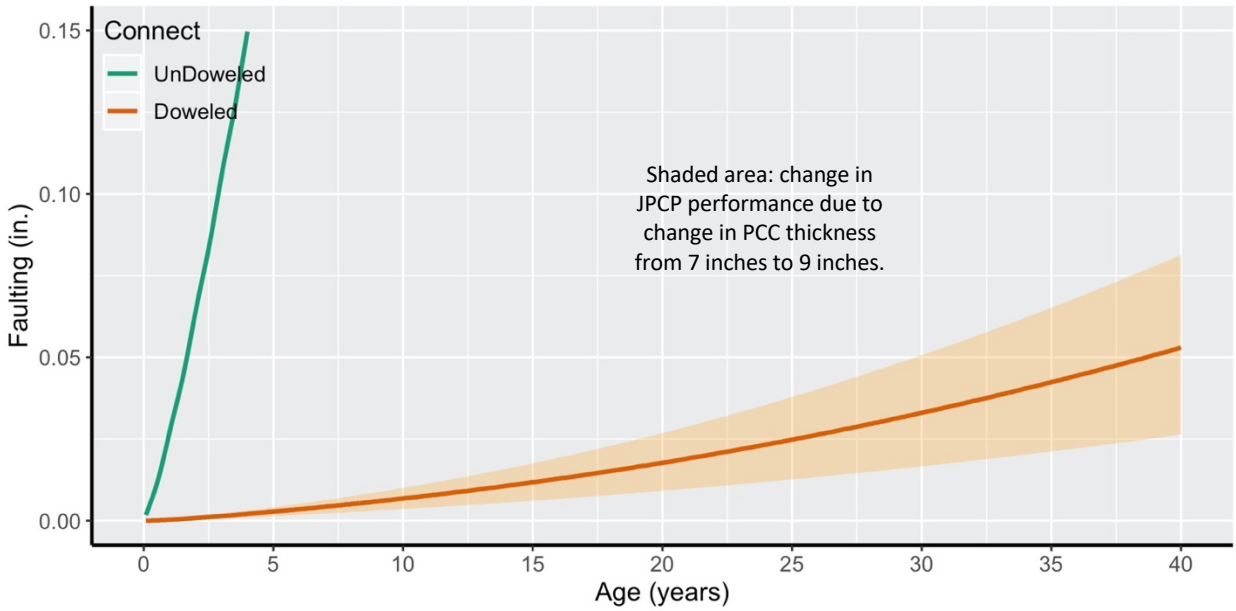

Figure 4.31: Effects of load transfer on faulting with 50% reliability

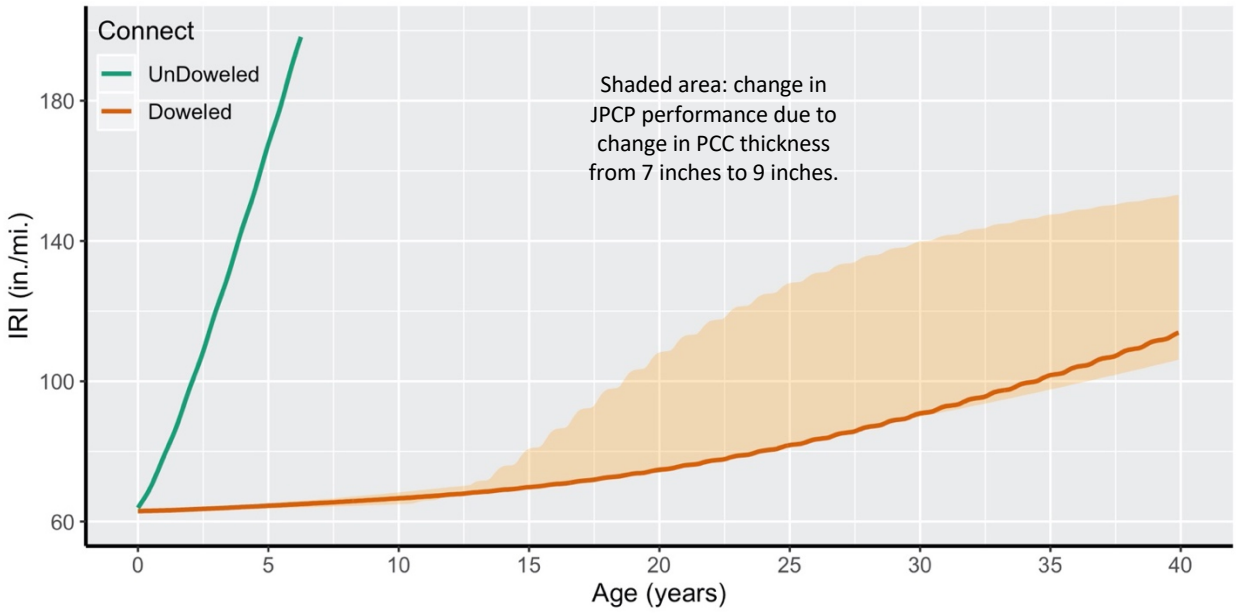

Figure 4.32: Effects of load transfer on IRI with 50% reliability

4.4.1.4. Friction Loss Duration

Base friction is an important property affecting the formation and distribution of JPCP transverse cracking. Based on the Pavement ME documentation, the interface between a stabilized base and a PCC slab can be modeled only as being either completely bonded or completely unbonded for JPCP design. The documentation also notes that the structural contribution of a stabilized base is significant if the base

is fully bonded to the slab, and much less significant if there is no bonding, with the extent of the contribution depending on the relative thicknesses of the stabilized base and PCC. A very thin stabilized base will not contribute much to structural capacity even if it is bonded because it will not shift the neutral axis substantially down in the PCC slab and therefore not cause significant reduction in tensile stress in the PCC. Full bonding is stated to be the typical condition, especially for asphalt-stabilized bases, based on an analysis of deflection testing results conducted at slab interiors. The documentation also notes that over time the effects of environmental and traffic loading tend to weaken this bond around the edges. The assumption of full bonding over the entire design period is therefore often un-conservative compared to the actual condition over the full design period.

If the initial condition is bonded, both the starting condition (bonded or unbonded) and the pavement age (month) when the debonding will occur can be input. The slab-base interface is assumed to be fully bonded up to the age when debonding occurs; after the debonding age, the interface is assumed to be fully unbonded. In this study, three different durations of loss of bonding (referred to by the software as friction) were considered: no base friction (0-month base friction), 120-month base friction, and 240-month base friction. It should be noted that all these cases shown are on an HMA base, and the results may change for a different kind of base type.

Figure 4.33 shows the effect of friction loss duration on transverse cracking for a pavement with an HMA base type. In the plot, it can be seen that the pavement shows no signs of transverse cracking before the friction loss period. Once the pavement age has passed that point, it starts showing signs of deterioration and transverse cracking. Therefore, the longer that full bonding is modeled between the PCC slab and the base, the less transverse cracking that the model will predict in the pavement during its service life.

Figure 4.34 shows that friction loss duration has no effect on JPCP faulting and that no matter what value is chosen for this variable, the pavement will have the same faulting performance during its service life. As shown in Figure 4.35, this is not the case for IRI, as IRI depends on both faulting and transverse cracking and, as a result, the longer the time to debonding, the less transverse cracking, and hence, less IRI.

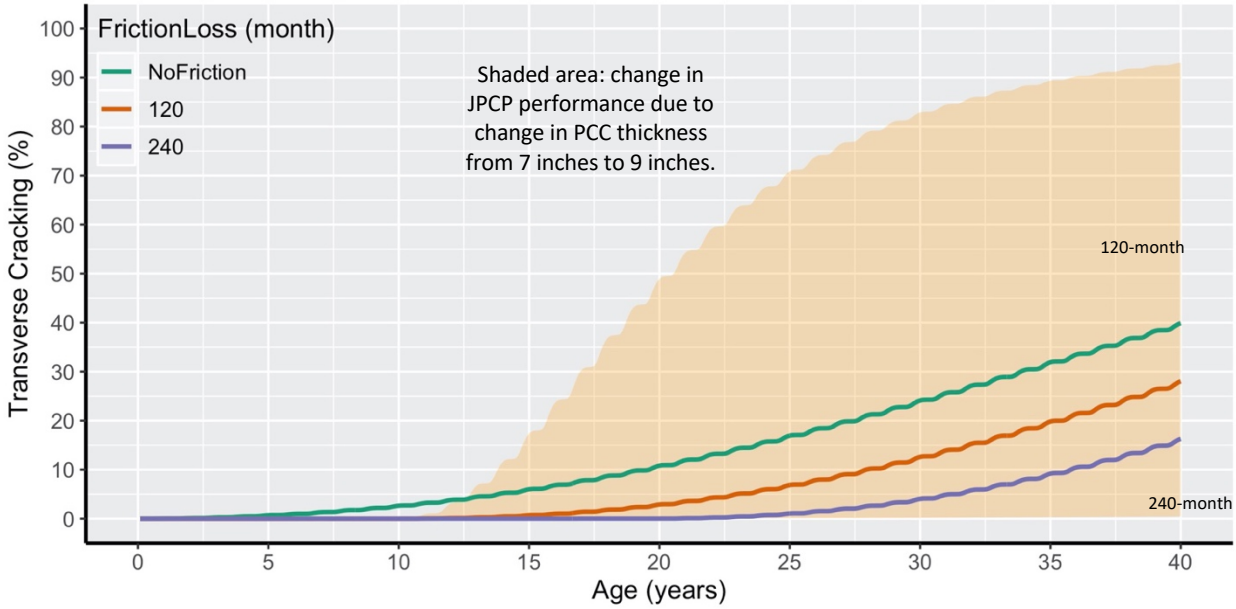

Figure 4.33: Effects of friction loss duration on transverse cracking with 50% reliability

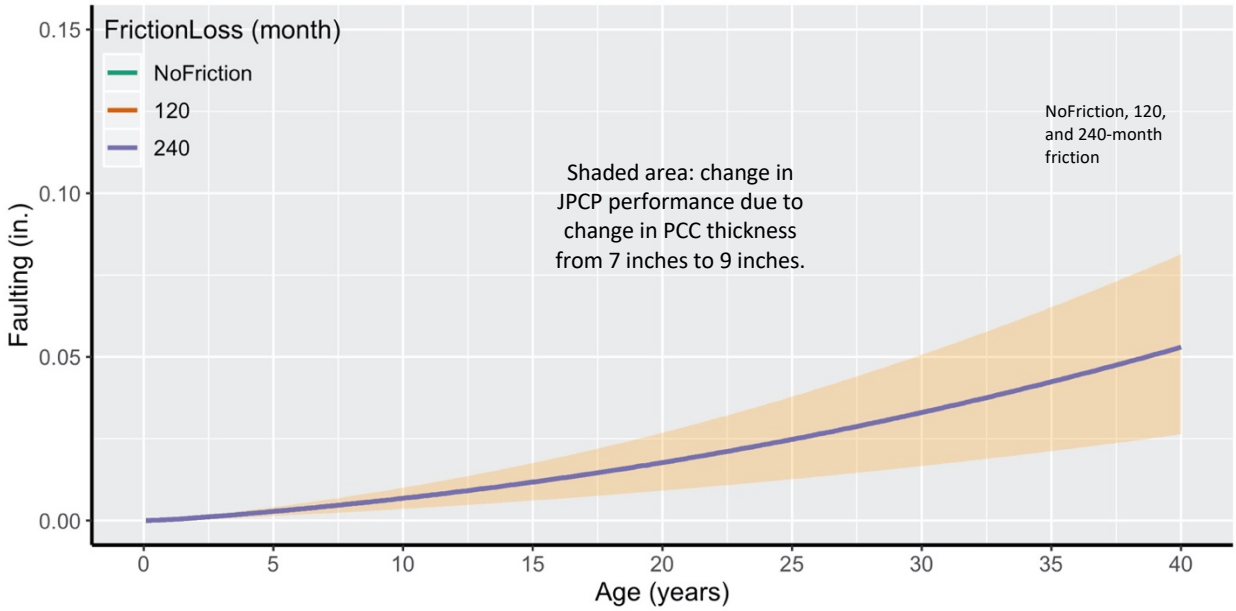

Figure 4.34: Effects of friction loss duration on faulting with 50% reliability

(Note: **The figure has three lines, one each for NoFriction, 120, and 240-month friction, that are nearly identical and hard to distinguish.)**

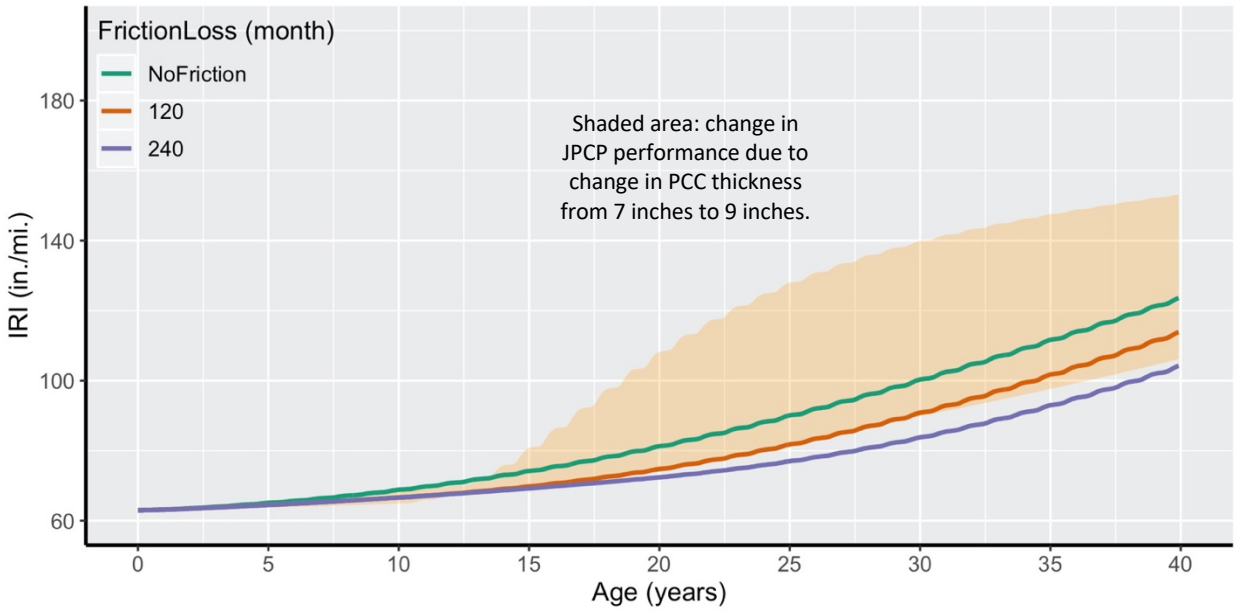

Figure 4.35: Effects of friction loss duration on IRI with 50% reliability

4.4.1.5. Base Type

According to the Pavement ME documentation, base type has been shown to affect joint faulting, smoothness, and slab cracking. A stiff stabilized base's structural contribution can be very significant if the base is bonded to the slab. However, the main purpose of providing a base course in JPCP is to provide uniform support and erosion resistance, which are critical for avoiding localized failures and faulting. The documentation states that for structural capacity, there are several other design factors (e.g., slab thickness, PCC strength, and edge support) that have a more direct and far greater impact than a stabilized base. In this study four different base types were considered: aggregate base (AB), cement-treated base (CTB), lean concrete base (LCB), and hot mix asphalt (HMA). The erodibility index was kept constant for the different base types since the erodibility index effects are specifically evaluated in previous sections.

Figure 4.36 shows the effects of these base types on JPCP transverse cracking. It should be noted that the bonding period (friction loss) for AB is zero months, as AB does not bond with the PCC slabs, and therefore the transverse cracking predicted in the pavement starts at the initial stage of service life. On the other hand, HMA, CTB, and LCB start to show transverse cracking after 12 years (120-month friction loss is the defined value for friction loss in the model). Eventually, as expected, the HMA base shows the best transverse cracking performance of the four base types, a result that aligns with the pavement condition survey data from California's state highway network.

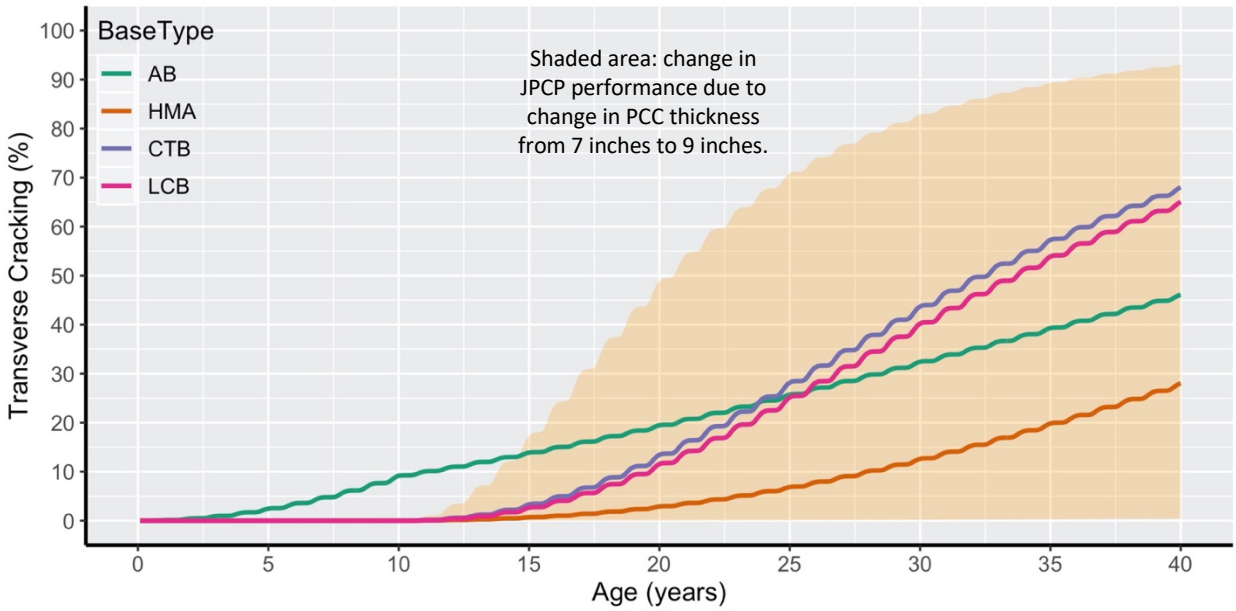

Figure 4.36: Effects of base type on transverse cracking with 50% reliability

Figure 4.37 shows that base type did not affect faulting performance as much as it affected transverse cracking performance. This figure shows that CTB and LCB have the best faulting performance, as they provide stiffer support compared to other alternatives. The differences between the different base types would have been larger if the erodibility index had been adjusted for each material. LCB and HMA can provide an erodibility index of 1 (extremely erosion resistant) and HMA can provide an index value of 2 (very erosion resistant), while an erodibility index of 4 (fairly erodible) can be expected from a crushed aggregate base. Figure 4.38 shows that HMA provided the best smoothness performance among the base types studied in this report because it had less transverse cracking than the others.

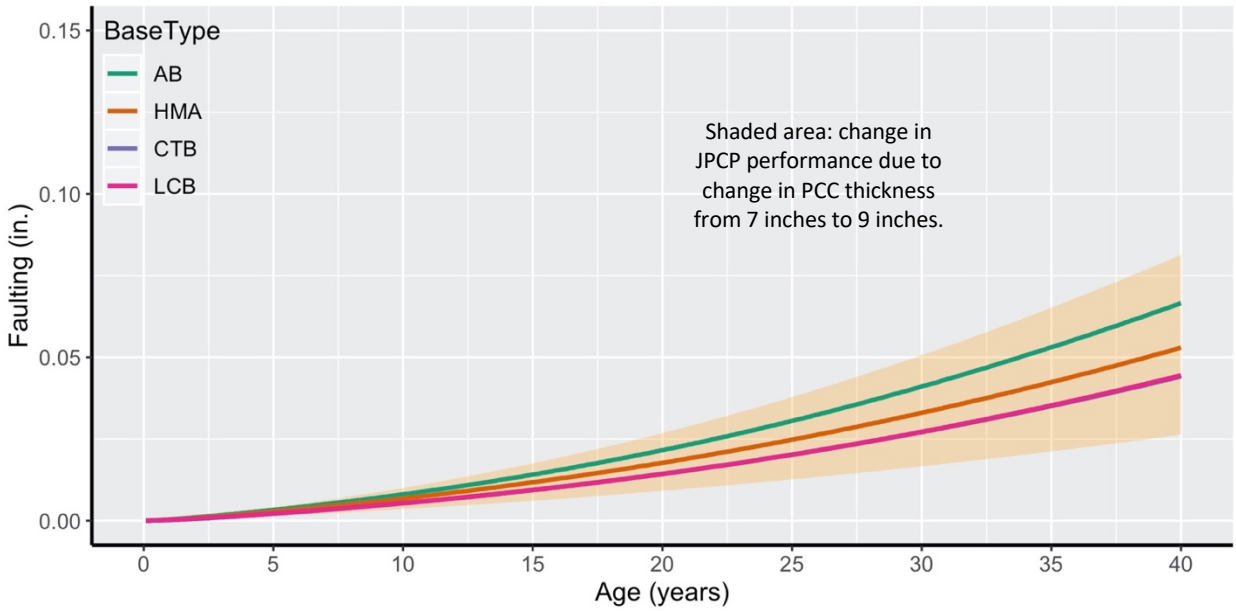

Figure 4.37: Effects of base type on faulting with 50% reliability

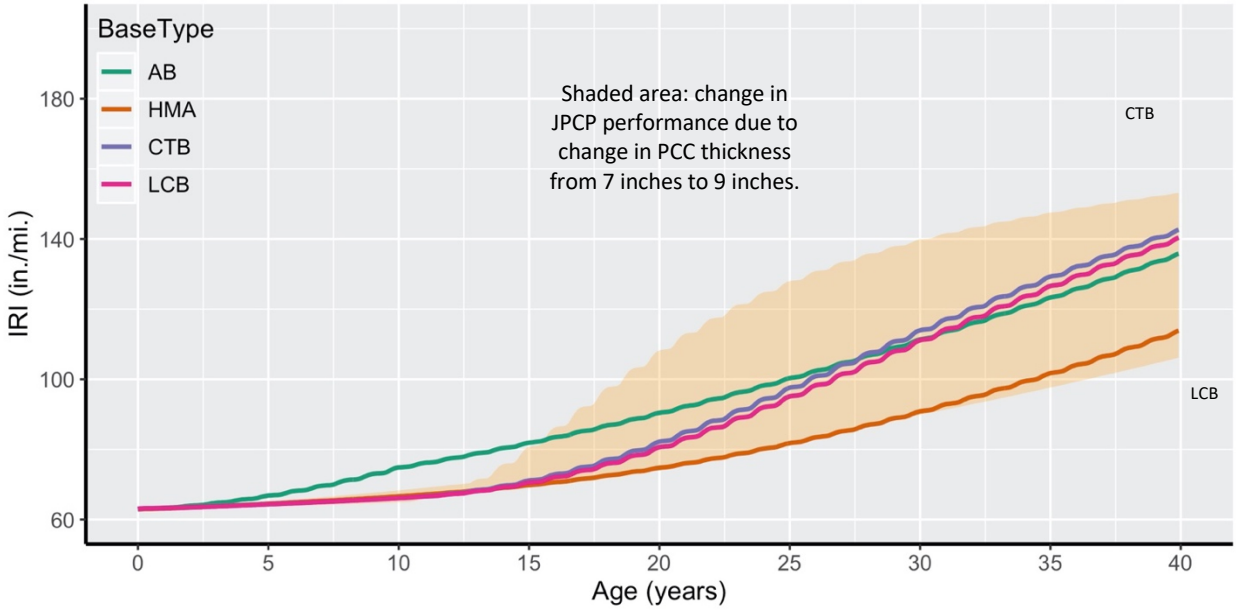

Figure 4.38: Effects of base type on IRI with 50% reliability

4.4.1.6. Shoulder Type (Edge Support)

According to the Pavement ME documentation, tied PCC shoulders and widened slabs can significantly improve JPCP performance by reducing critical deflections and stresses along the edge. Shoulder type also affects the amount of moisture infiltrating the pavement structure. The effects of moisture infiltration are considered in determining the unbound layers' seasonal moduli values. In this analysis, three shoulder

types (edge supports) are considered: not-tied, tied, and widened. Not-tied JPCP, where there is an asphalt or gravel shoulder, does not support any load transfer between the PCC slabs and shoulder.

When a tied PCC shoulder is built, the PCC slabs are tied to the concrete shoulders. In models for these types of shoulders, the long-term load transfer efficiency (LTE) between the lane and the shoulder is an input value, which in this study was assumed to be the default value of 50 percent. LTE is defined as the ratio of deflections of the unloaded and loaded slabs. The higher the LTE, the greater the support provided by the shoulder to reduce critical responses of the mainline slabs.

Widened slabs improve JPCP performance by effectively moving the mean wheelpath away from the pavement edges where the critical loadings occur, and thereby reduce the risk of transverse cracking. The design input for widened slab is slab width, which can range from 12 to 14 ft. This study assumed the default value of 14 ft.

Figure 4.39 shows the effectiveness of edge support (shoulder type) on the JPCP's transverse cracking performance. As stated earlier, and as shown in the figure, the widened slabs and tied-shoulder slab types have better performance than the not-tied shoulder type. Similar trends can be observed in Figure 4.40 and Figure 4.41 for faulting and IRI, respectively.

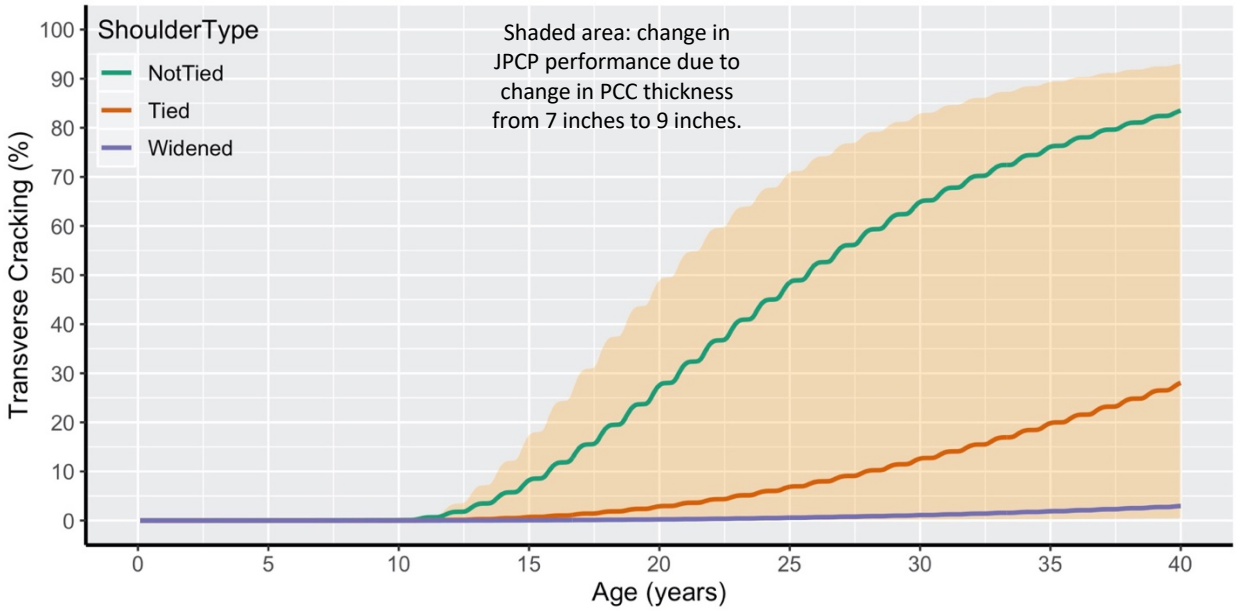

Figure 4.39: Effects of shoulder type on transverse cracking with 50% reliability

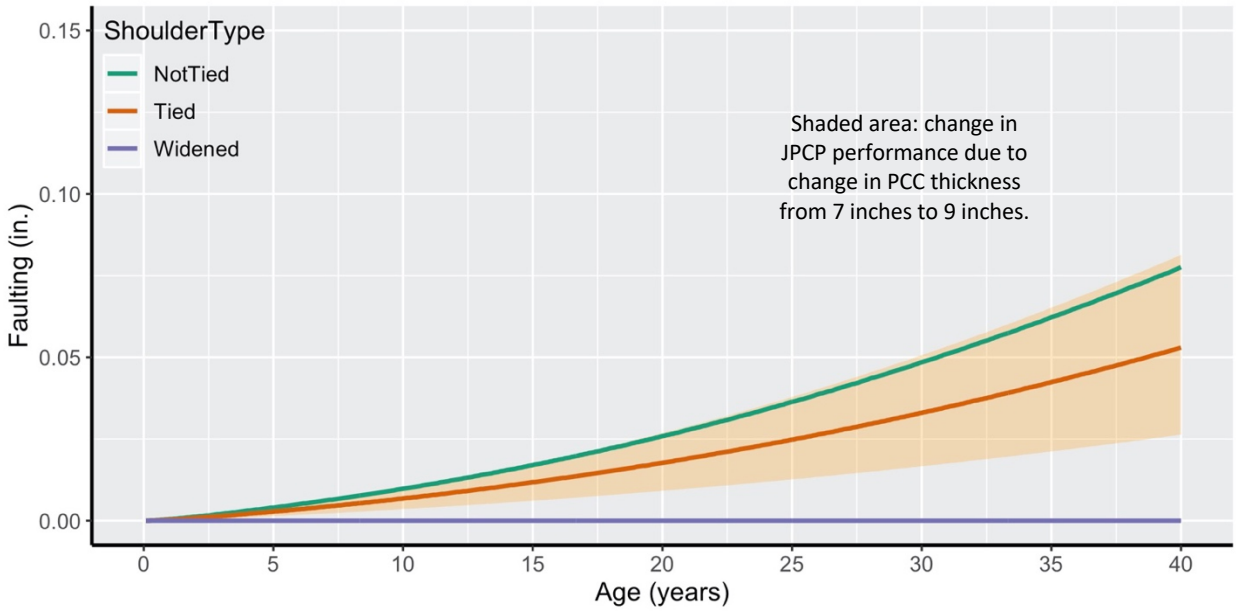

Figure 4.40: Effects of shoulder type on faulting with 50% reliability

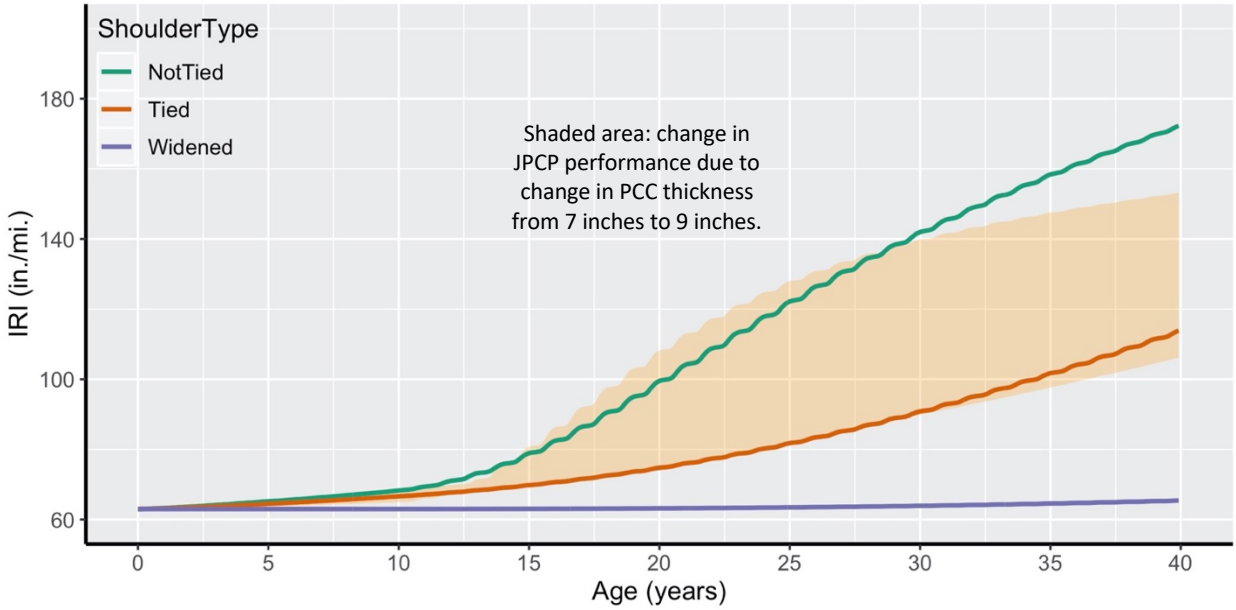

Figure 4.41: Effects of shoulder type on IRI with 50% reliability

4.4.1.7. Subgrade Type

In Pavement ME, subgrade and unbound pavement layers are characterized using their resilient moduli. For rigid pavement design, the subgrade k-value needed for the structural analysis is obtained through a conversion process that transforms the actual pavement structure into an equivalent structure that consists of a PCC slab, base, and an "effective dynamic k-value" for all the layers underneath the base. The effective dynamic k-value represents the compressibility of all the layers beneath the PCC slab and base

course. The effective dynamic k-value of the subgrade is calculated for each month of the year and utilized directly to compute critical stresses and deflections in the incremental damage accumulation over the design life of the pavement. Factors such as water table depth, depth to bedrock, and frost penetration depth (frozen material) can significantly affect the effective dynamic k value.

In this study, three types of subgrade were considered: clay (A-5), gravel and sand (A-1a), and sand (A-3). Figure 4.42 shows the effects of subgrade on the transverse cracking of JPCP. It can be seen that the gravel and sand, and the sand subgrades had nearly identical performance, and the clay subgrade performed the best. However, Figure 4.43 and Figure 4.44 show that the clay subgrade had higher values for both faulting and IRI.

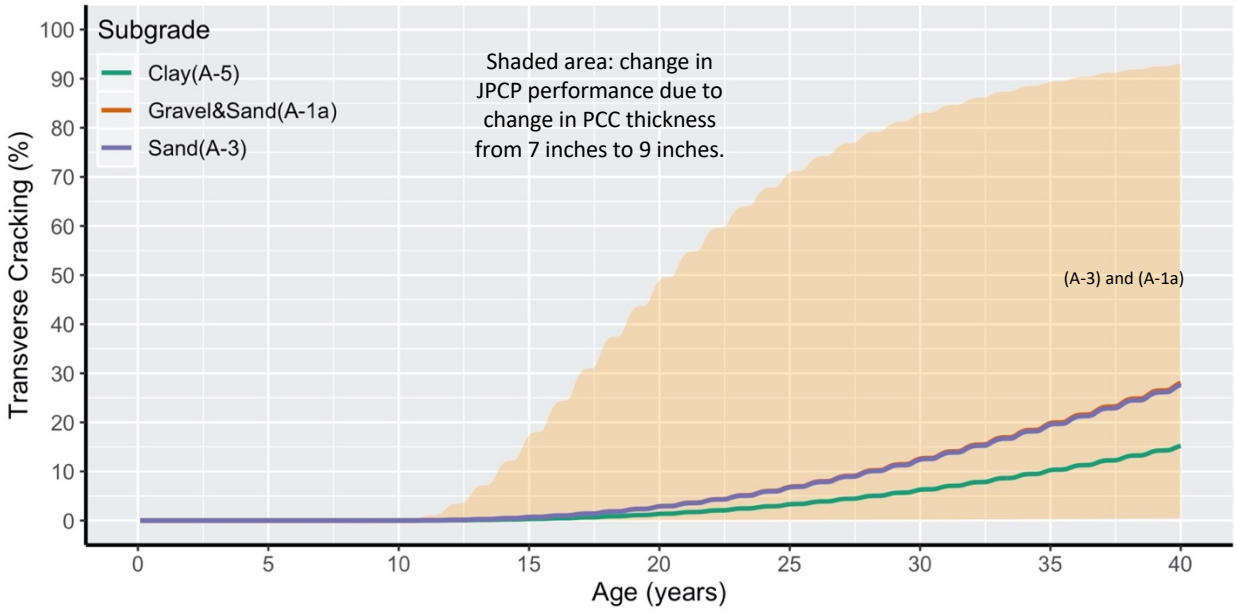

Figure 4.42: Effects of subgrade type on transverse cracking with 50% reliability
(Note: **The figure has two lines, one for A-3 and one for A-1a, that are nearly identical.)**

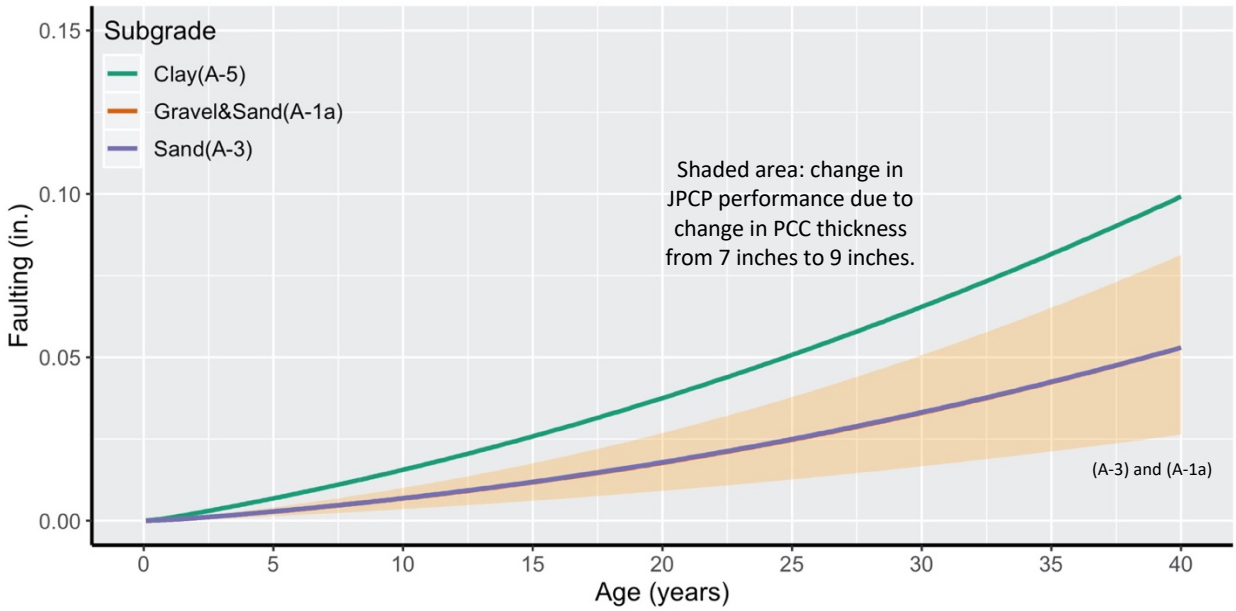

Figure 4.43: Effects of subgrade type on faulting with 50% reliability

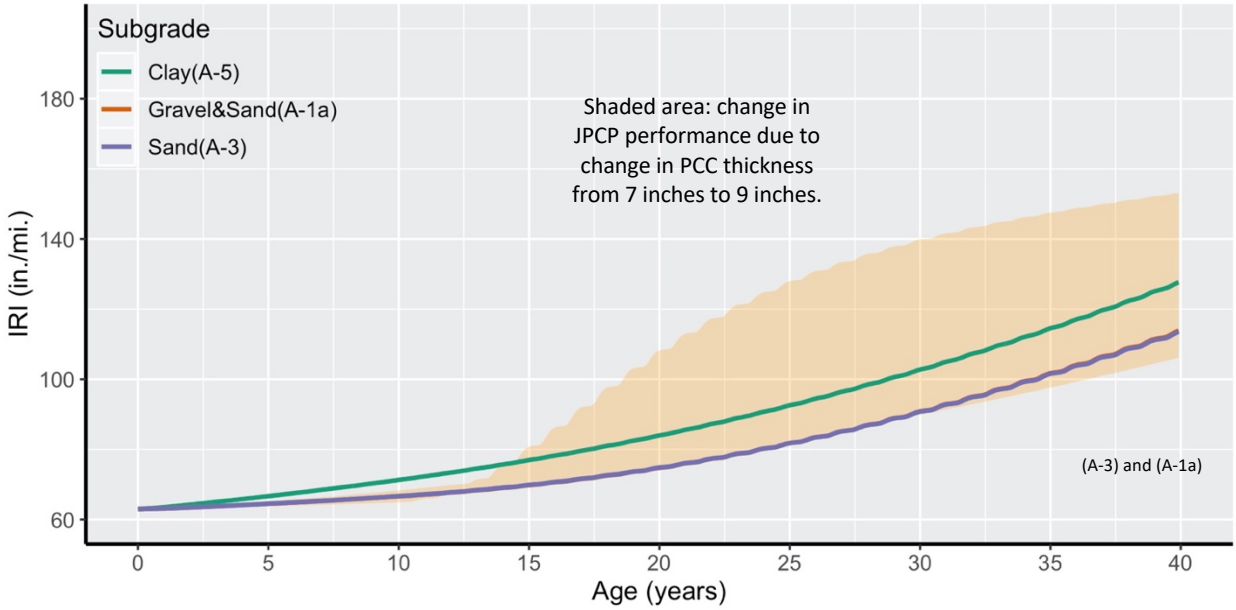

Figure 4.44: Effects of subgrade type on IRI with 50% reliability
***(Note:* The figure has two lines, one for A-3 and one for A-1a, that are nearly identical.)**

4.4.1.8. Erodibility Index

According to the Pavement ME documentation, the erosion potential of the base or subbase (the layer directly beneath the PCC layer) has a significant impact on the initiation and propagation of pavement distress. Different base types are classified based on long-term erodibility behavior as follows:

- Class 1: Extremely erosion-resistant materials

- Class 2: Very erosion-resistant materials
- Class 3: Erosion-resistant materials
- Class 4: Fairly erodible materials
- Class 5: Very erodible materials

In this study, Classes 1, 2, and 4 were considered. Class 1 is applicable to cement-treated base (CTB) and hot mix asphalt (HMA), Class 2 to CTB, and Class 4 to aggregate base (AB). Figure 4.45 shows that the erodibility index has no effect on transverse cracking performance, as expected. As also expected, Figure 4.46 and Figure 4.47 show that the base with more erodible material will cause more faulting in JPCP and, consequently, will result in a rougher pavement.

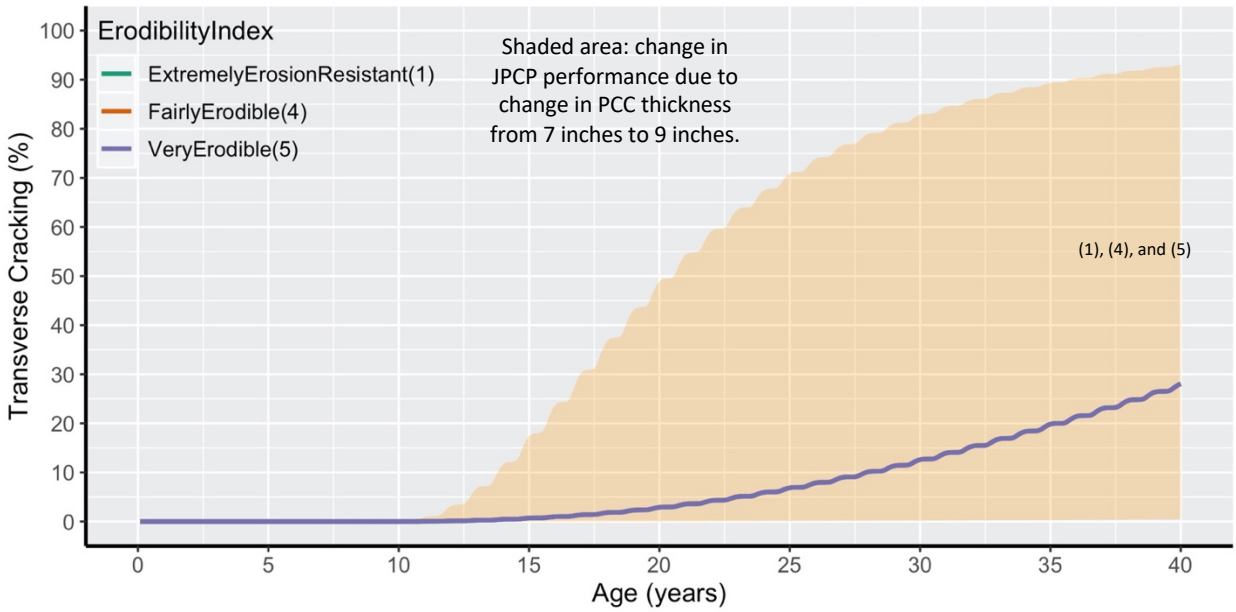

Figure 4.45: Effects of erodibility index on transverse cracking with 50% reliability.
(Note: **The figure has three lines, one each for (1), (4), and (5), that are nearly identical and indistinguishable.)**

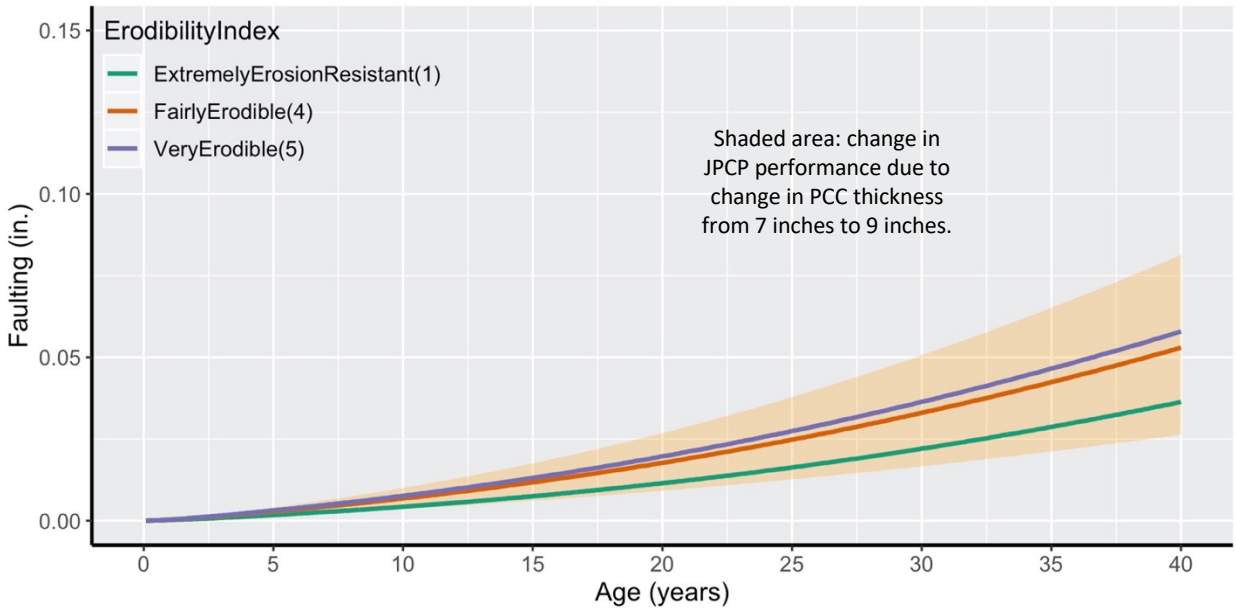

Figure 4.46: Effects of erodibility index on faulting with 50% reliability

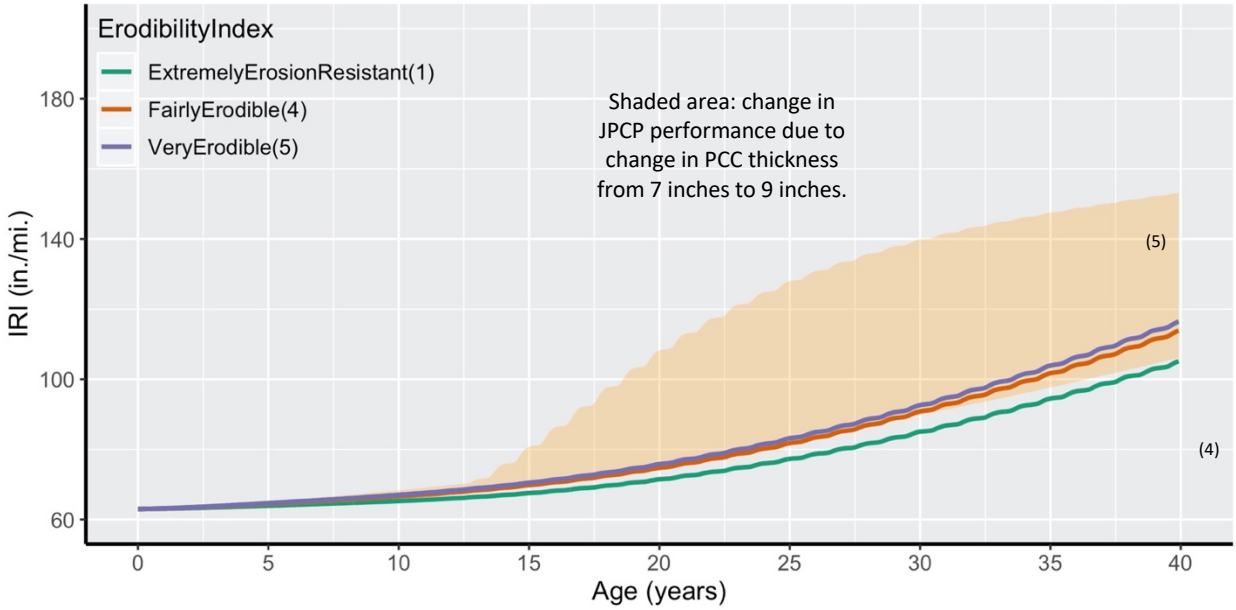

Figure 4.47: Effects of erodibility index on IRI with 50% reliability

4.4.2. Pavement Material Inputs

Pavement material inputs are the variables generally unknown to a designer at the design stage and are not readily available for most of the JPCP projects constructed in California. This makes calibrating Pavement ME against the Caltrans PMS data a challenge. However, over the past few years, the UCPRC has obtained some material input data by sampling from various research projects with JPCP construction sites. Data from these projects can be used to understand the distribution of pavement material variables

and their within-project and between-project variabilities to calibrate Pavement ME more efficiently. The material inputs data collected were PCC compressive strength, PCC modulus of elasticity, PCC coefficient of thermal expansion (CTE), PCC surface absorptivity, and PCC density.

Five data sources were used to set up the material input database.

- Ground penetrating radar (GPR) data. The objective of an earlier UCPRC GPR study was to create a lane-based pavement structure inventory database consisting of layer thickness and material types for the entire state highway network. The data collected as part of this project were used to establish fixed management sections for network-level and project-level PMS operations. As part of this project, some Blind Verification Sections (BVS) were established to provide additional quality assurance, and a large number of cores were taken that were later tested for CTE. In this current report, PCC CTE was the project-specific variable obtained from this GPR study.
- Previous MEPDG calibration data. These data were obtained from cores taken from different pavement sections across the California as part of an earlier UCPRC MEPDG calibration project (Kannekanti et al., 2007).
- Alkali-silica reaction (ASR) data. The objective of an earlier UCPRC ASR project was to look for the presence of alkali-silica reaction in California's pavements and bridges by evaluating the core samples taken from the pavement sections across the state (Li et al., 2016).
- Stantec data. These data were obtained by drilling core specimens to study the influence CTE on JPCP cracking (Kohler et al, 2008).
- Caltrans CTE database. After the 2006 sensitivity analysis that showed a very high sensitivity of transverse cracking in the MEPDG models to CTE, Caltrans required contractors to test and report CTE for several years. This database has the CTE test results taken from the JPC pavements while under construction during that period.

Further discussion on pavement material inputs is provided in the appendix.

4.4.2.1. PCC Compressive Strength

The compressive strength of PCC materials can used to estimate the elastic modulus, flexural strength, and indirect tensile strength if no directly measured information for these properties are available as inputs. In Pavement ME, the processed inputs for PCC strength and modulus properties are the monthly strength and modulus values for the entire design period. According to the Pavement ME documentation, an increase in PCC compressive strength, which is used to model commensurate increases in flexural

strength, leads to lower fatigue damage; however, since the PCC modulus of elasticity also increases with increased compressive strength, the bending stress due to shrinkage and thermal gradients will also increase. Thus, the reduction in fatigue damage is not as dramatic as might be expected when PCC strength (flexural strength estimated from compressive strength) is increased. In addition, a higher-strength PCC obtained through increased cement content may result in greater shrinkage of the hardened mixture, although this is not modeled in Pavement ME. If this higher shrinkage occurs, it will lead to greater warping, which will increase tensile stresses at the top of the slab and, consequently, top-down cracking.

The compressive strengths were measured on cores taken at least several years and often many years after construction. The values were converted from the long-term strengths to equivalent 28-day strengths based on Pavement ME formula, which include the ACI formula that relates flexural (MR) and compressive strength, a default time evolution function for flexural strength, and a default 1.2 ratio between 20-year and 28-day flexural strength. In practice, all flexural strength values were divided by 1.2 in order to estimate the 28-day flexural strength, regardless of concrete age. For any given time, the ratio between MR and 28-day MR is a function of age; thus, applying a 1.2 factor to all projects regardless of age is a simplification. The Pavement ME default time function is logarithmic. It increases very quickly at the beginning and very slowly after a few years (as expressed in actual concrete mechanical properties). For example, for 3-year-old concrete, the ratio between MR and 28-day MR is 1.16, which is very close to 1.2. In other words, the age correction of field specimens can be simplified by applying a 1.2 factor as soon as the project is a few years old. Finally, the 28-day flexural strength values were converted back to compressive strengths using the ACI formula.

A hierarchical input level in the MEPDG input scheme allows a designer to categorize their knowledge of an input parameter into one of three levels, and in this way the catalog can determine the input values for most of the material and traffic parameters. The following defines each hierarchical input level that a designer can use:

- Input Level 1: This input parameter is measured directly; it is site- or project-specific. This level represents the greatest knowledge about the input parameter for a specific project, but the testing and data collection costs for determining this parameter's input value are the highest of the three possible levels. Level 1 should be used for pavement designs that have unusual site features, materials, or traffic conditions that are outside the inference-space used to develop the correlations and defaults included for Input Levels 2 and 3.

- Input Level 2: This input parameter is estimated from correlations or regression equations. The input value is calculated from other site-specific data or parameters that are less costly and/or easier to measure than they are for Level 1. Input Level 2 can also represent measured regional values that are not project specific.
- Input Level 3: This input parameter is based on "best-estimated" or default values. Level 3 inputs are based on global or regional default values—the median value from a group of data with similar characteristics. This input level reflects the least knowledge about the input parameter for the specific project, but it has the lowest testing and data collection costs.

Level 3 was selected for concrete strength/stiffness properties. This means that the only input is the 28-day compressive strength. Then Pavement ME uses the ACI formula to estimate 28-day flexural strength and modulus of elasticity, and a default time evolution function applicable to both flexural strength and modulus of elasticity.

In this study, three different values were considered for PCC compressive strength. These values were chosen based on the PCC compressive strength data distribution shown in the appendix.

Figure 4.48 shows the transverse cracking model's sensitivity to changes in the compressive strength of the PCC slab (and the associated changes in flexural strength and modulus of elasticity). It can be seen that increasing the slab's compressive strength from 4,730 psi to 6,730 psi (32.6 MPa to 46.4 MPa) decreased the transverse cracking from 70 percent to about 8 percent in a 40-year service life.

Figure 4.49 shows that the faulting model is less sensitive to changes in PCC strength (and the associated changes in flexural strength and modulus of elasticity) than the transverse cracking model was. Figure 4.50 shows that increasing the PCC compressive strength decreased the IRI, as less transverse cracking occurred with a stronger PCC.

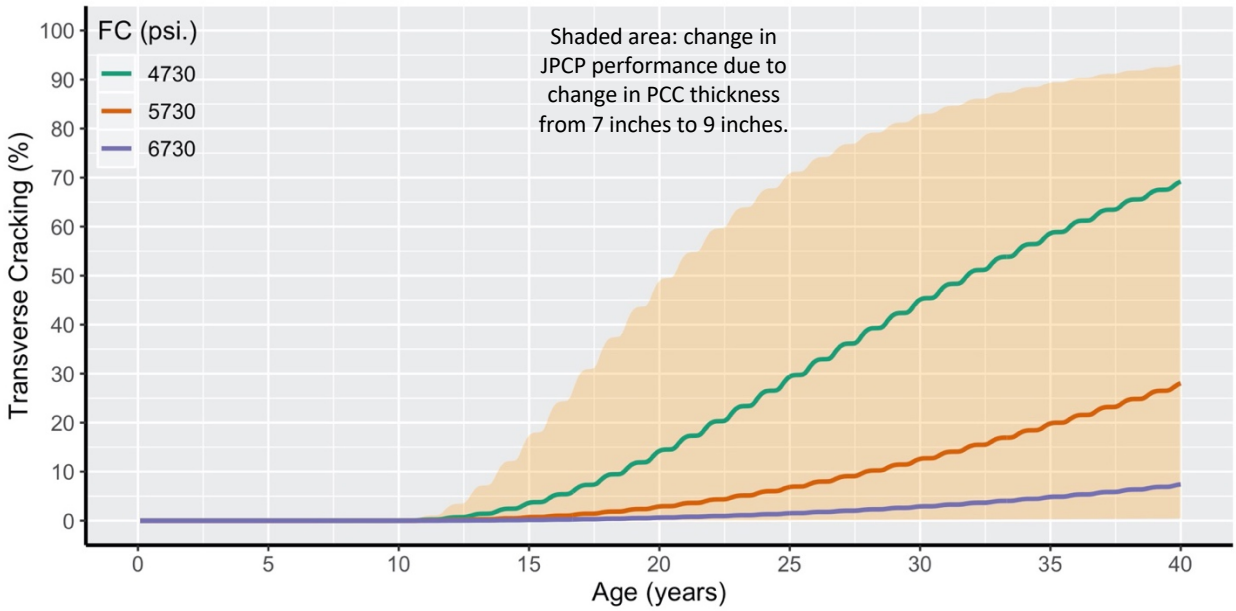

Figure 4.48: Effects of PCC compressive strength and associated assumptions regarding flexural strength and stiffness on transverse cracking with 50% reliability

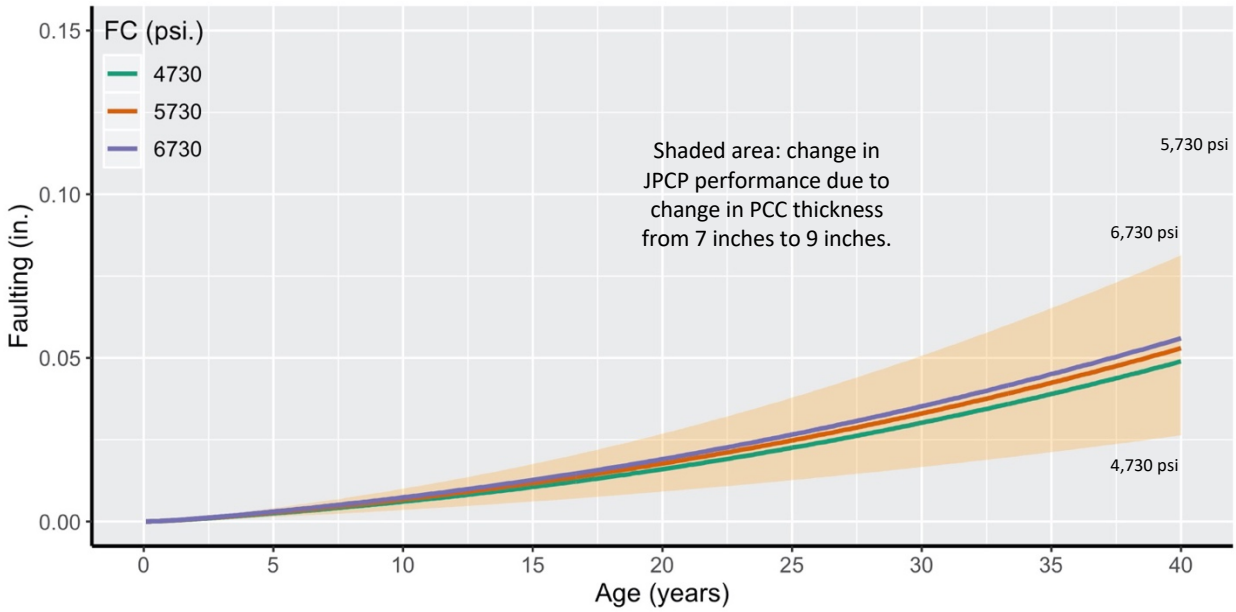

Figure 4.49: Effects of PCC compressive strength and associated assumptions regarding flexural strength and stiffness on faulting with 50% reliability

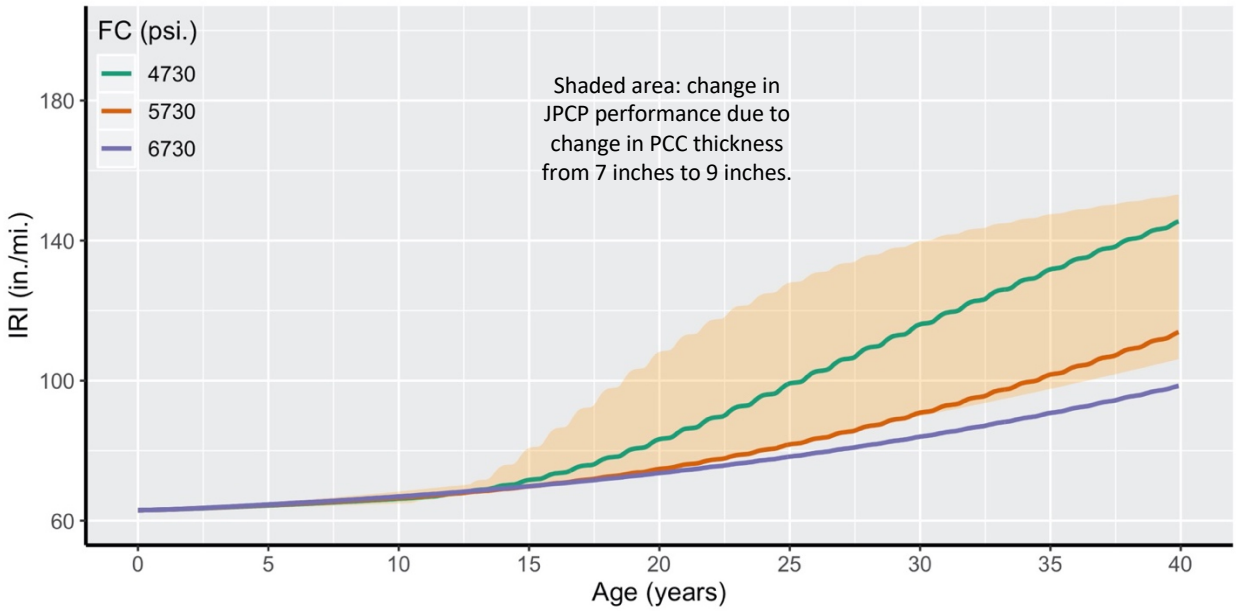

Figure 4.50: Effects of PCC compressive strength and associated assumptions regarding flexural strength, and stiffness on faulting on IRI with 50% reliability

4.4.2.2. PCC Coefficient of Thermal Expansion

The coefficient of thermal expansion (CTE) is defined as the change in unit length per degree of temperature change. CTE affects both critical slab stresses and transverse joint openings. The magnitude of calculated curling stress (caused by temperature difference through the slab thickness) is very sensitive to CTE. According to the MEPDG (NCHRP, 2003), under certain exposure conditions, curling stresses can comprise 50 percent or more of the critical stress experienced by a loaded JPCP slab, which thereby affects transverse cracking significantly.

This study considered three CTE values that were chosen using the CTE data distribution shown in Figure A.17 in the appendix: 5 microstrain/°F-1, which is close to the median value shown in the appendix, and one standard deviation above and below. Figure 4.51 shows the significant effect CTE has on the transverse cracking performance of JPCP. Figure 4.52 and Figure 4.53 also show that increasing CTE in JPCP will cause a significant increase in both faulting and IRI because of greater curling.

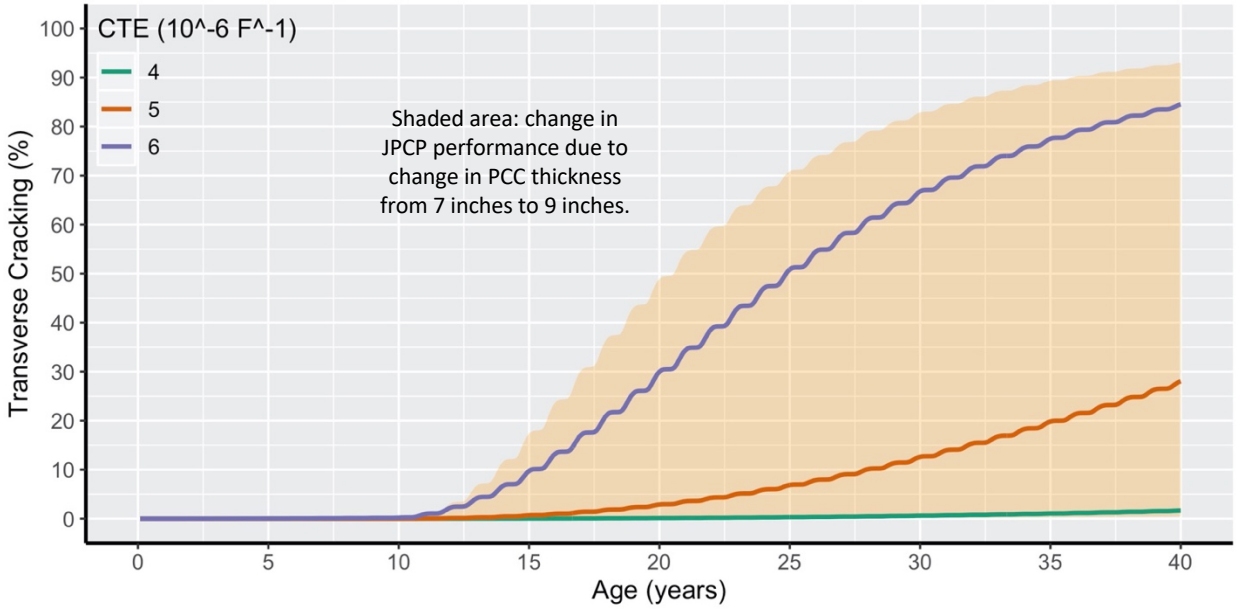

Figure 4.51: Effects of PCC CTE on transverse cracking with 50% reliability

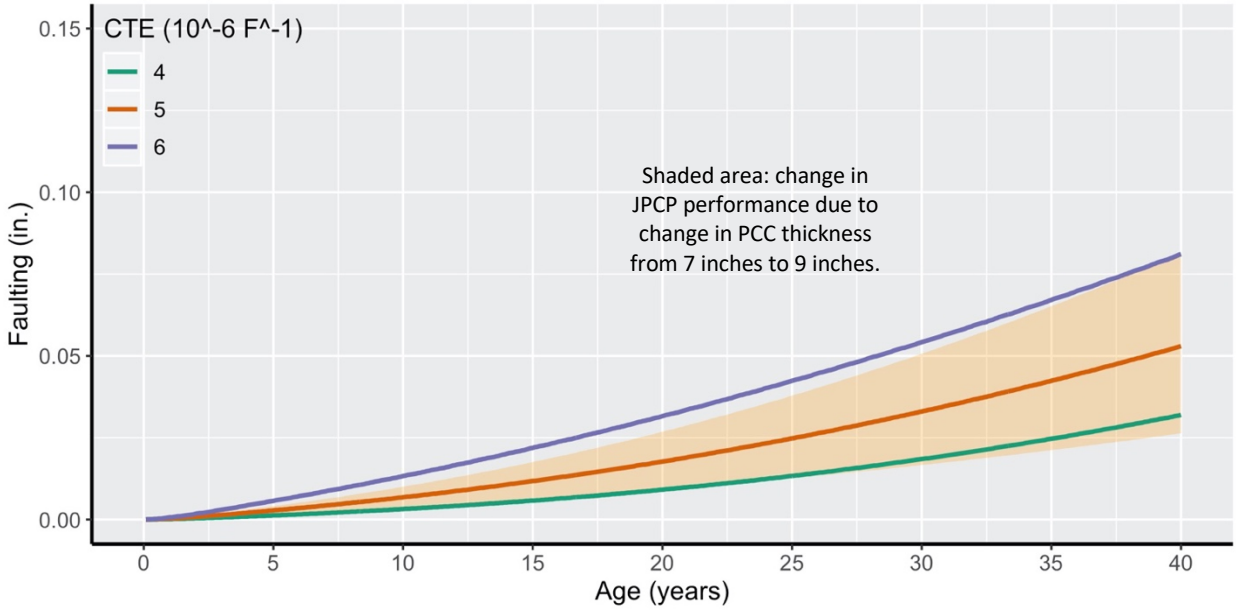

Figure 4.52: Effects of PCC CTE on faulting with 50% reliability

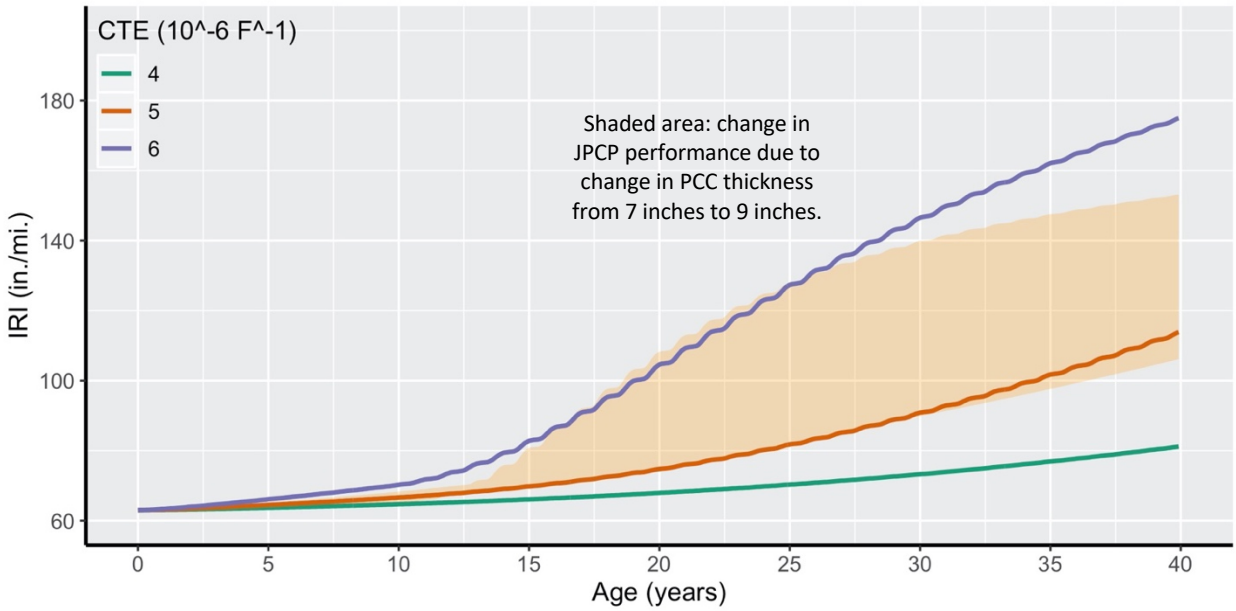

Figure 4.53: Effects of PCC CTE on IRI with 50% reliability

4.4.2.3. PCC Shortwave Absorptivity

The shortwave absorptivity of a pavement surface depends on its pavement composition, color, and texture. Shortwave absorptivity is the ratio of the amount of solar energy absorbed by the pavement surface to the total energy the surface was exposed to, and it naturally affects the temperature regime within the pavement structure and its associated structural response. This input ranges from 0 to 1. The more reflective a surface is, the lower its shortwave absorptivity will be.

The shortwave absorptivity range recommended by the Pavement ME software is between 0.5 to 1.0. In this study, four values for PCC shortwave absorptivity were considered, 0.65, 0.7, 0.8, and 0.9, based on the shortwave absorptivity data distribution in Figure A.20 in the appendix and the Pavement ME-recommended range. The default value in Pavement ME is 0.85. The shortwave absorptivity data distributions provided in the appendix were obtained from just three projects, which have all been in service for many years, and were therefore expected to show high values. The average of the shortwave absorptivity data in the appendix was 0.91, and this is why the top of the shortwave absorptivity range was set to 0.9. The rest of the values were considered since the JPCP at its initial service life had lower shortwave absorptivity values. Figure 4.54 shows the effect that PCC shortwave absorptivity had on results from the transverse cracking model. It can be seen from the figure that reducing the PCC shortwave absorptivity from 0.9 to 0.65 had a large impact on transverse cracking performance, an impact similar to the one resulting from an increase in PCC slab thickness from 7 inches to 9 inches. Figure 4.55

and Figure 4.56 show the impact of PCC shortwave absorptivity on faulting and IRI, which in both cases is significant.

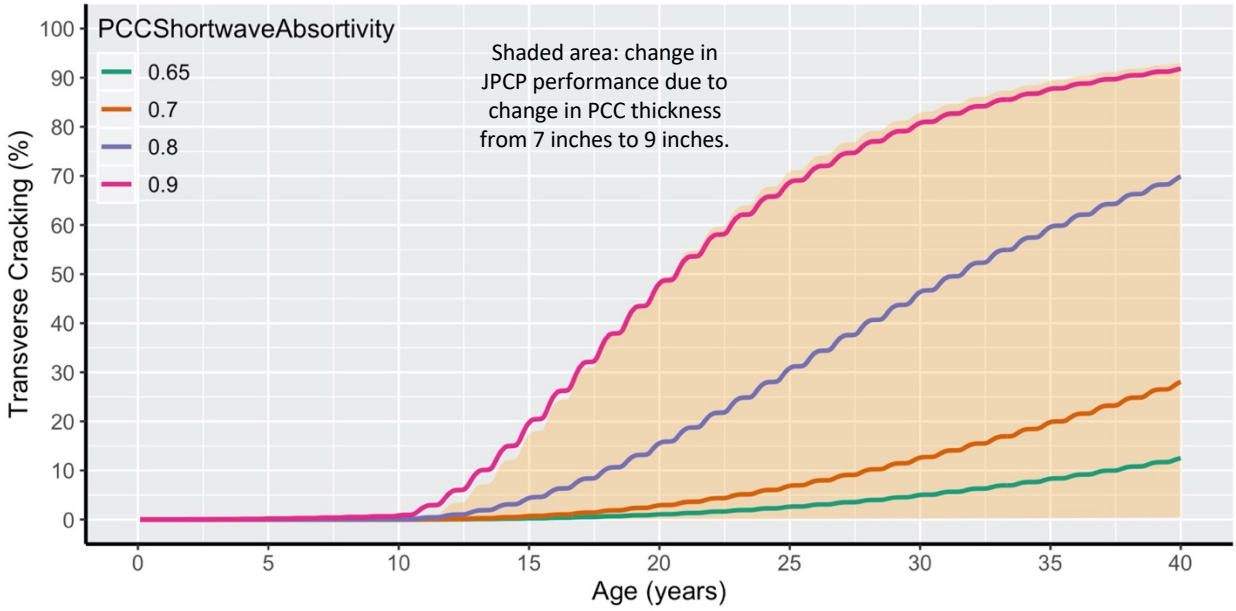

Figure 4.54: Effects of PCC shortwave absorptivity on transverse cracking with 50% reliability

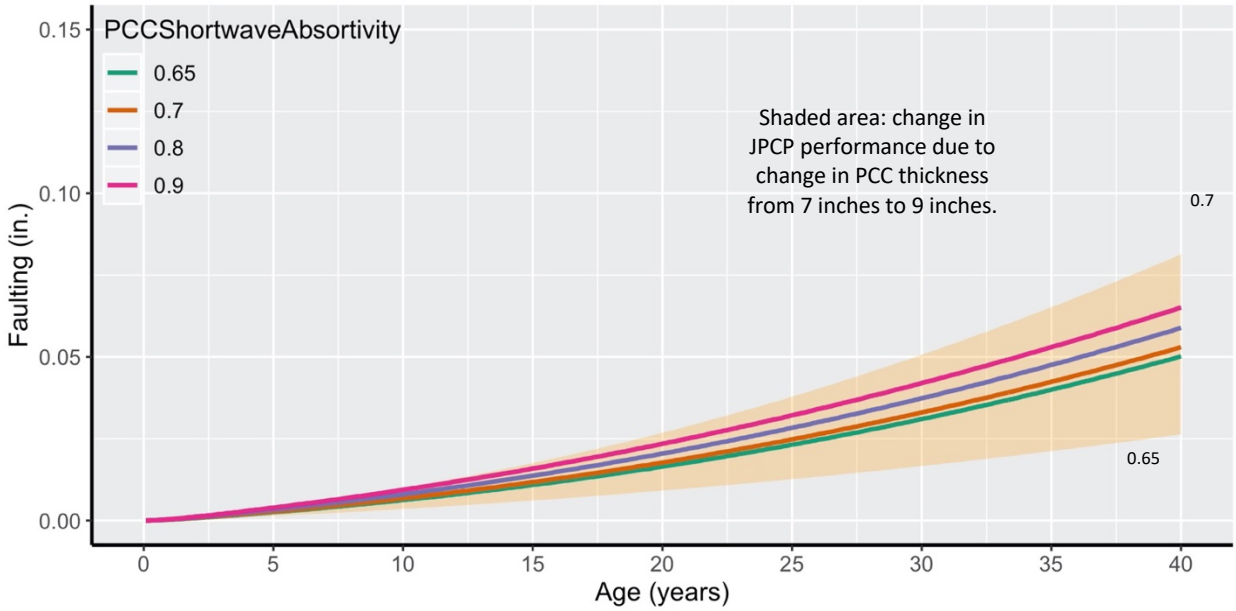

Figure 4.55: Effects of PCC shortwave absorptivity on faulting with 50% reliability

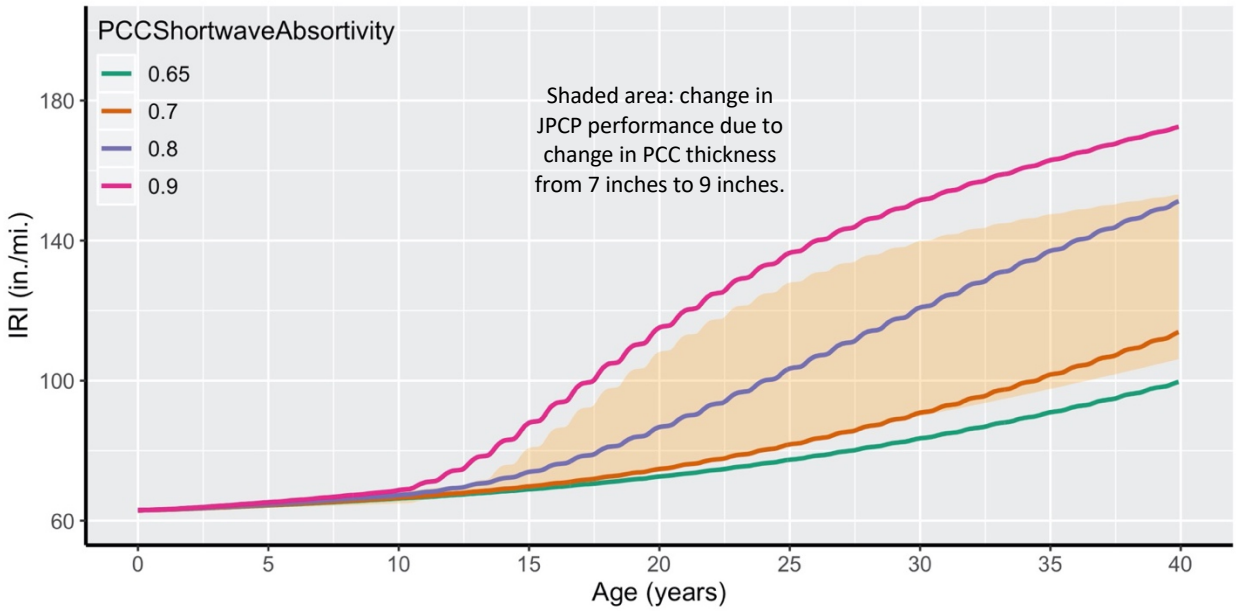

Figure 4.56: Effects of PCC shortwave absorptivity on IRI with 50% reliability

4.4.2.4. PCC Heat Capacity

PCC heat capacity is the heat required to raise the temperature of a unit mass of material by a unit temperature. No PCC heat capacity data are available in the UCPRC database. The heat capacity range recommended by the Pavement ME software is between 0.1 to 0.28. Based on that recommendation, this study considered three values: 0.2, 0.24, and 0.28 (Pavement ME default value). It was found that values less than 0.2 did not produce a result in Pavement ME. The figures below show that this variable does not have much of an effect on the transverse cracking, faulting, and IRI models.

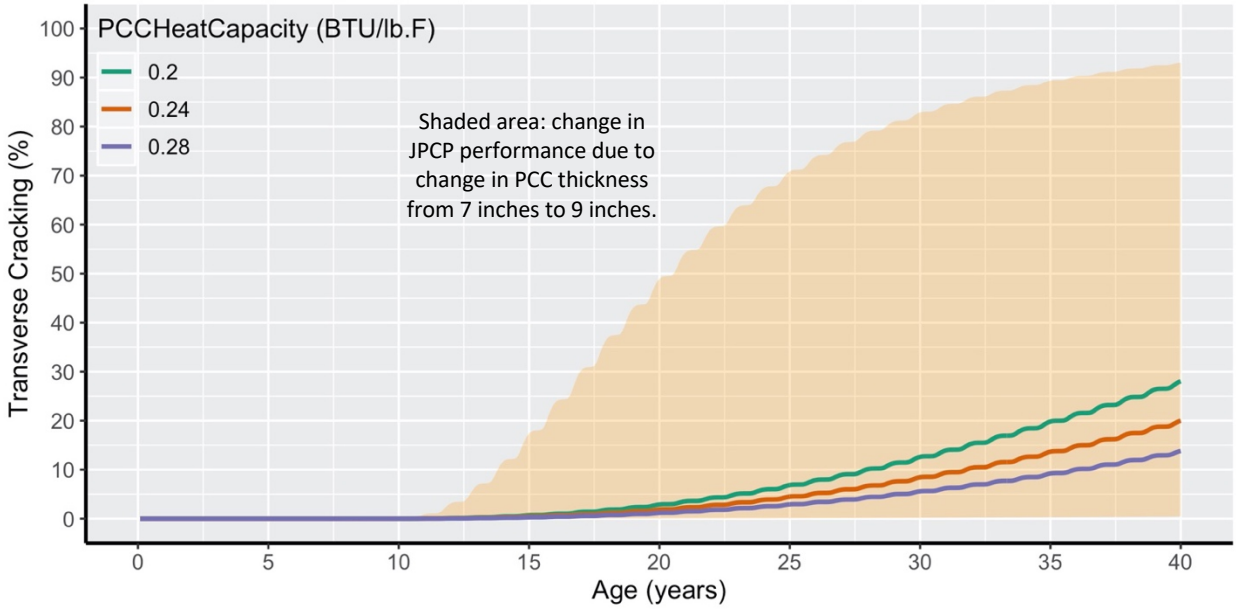

Figure 4.57: Effects of PCC heat capacity on transverse cracking with 50% reliability

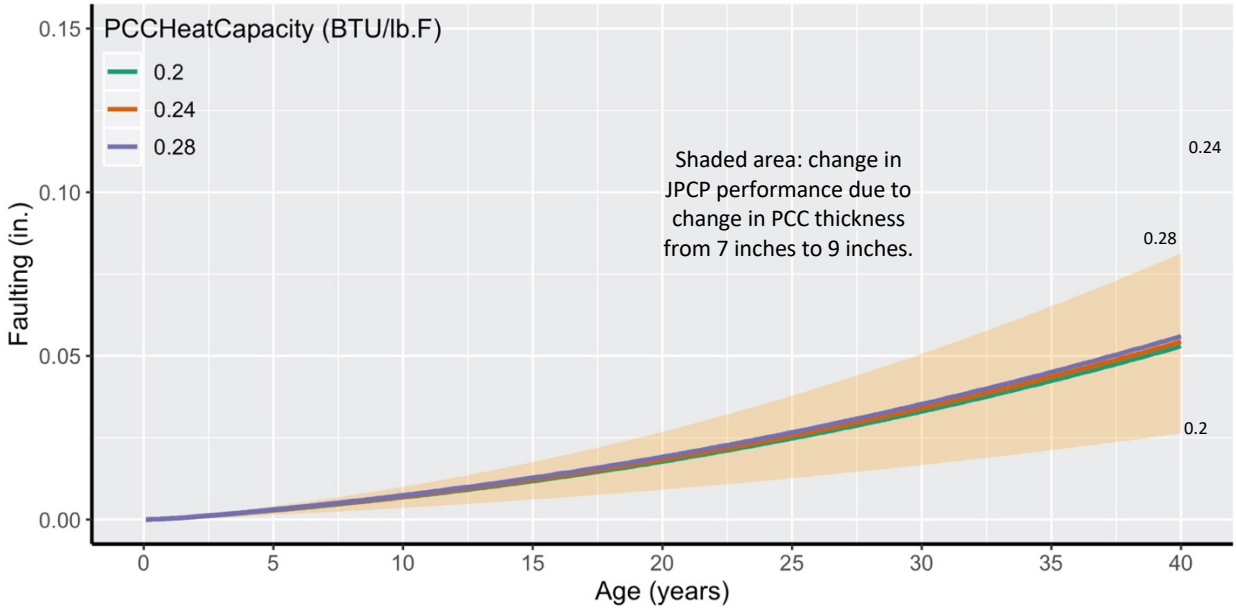

Figure 4.58: Effects of PCC heat capacity on faulting with 50% reliability

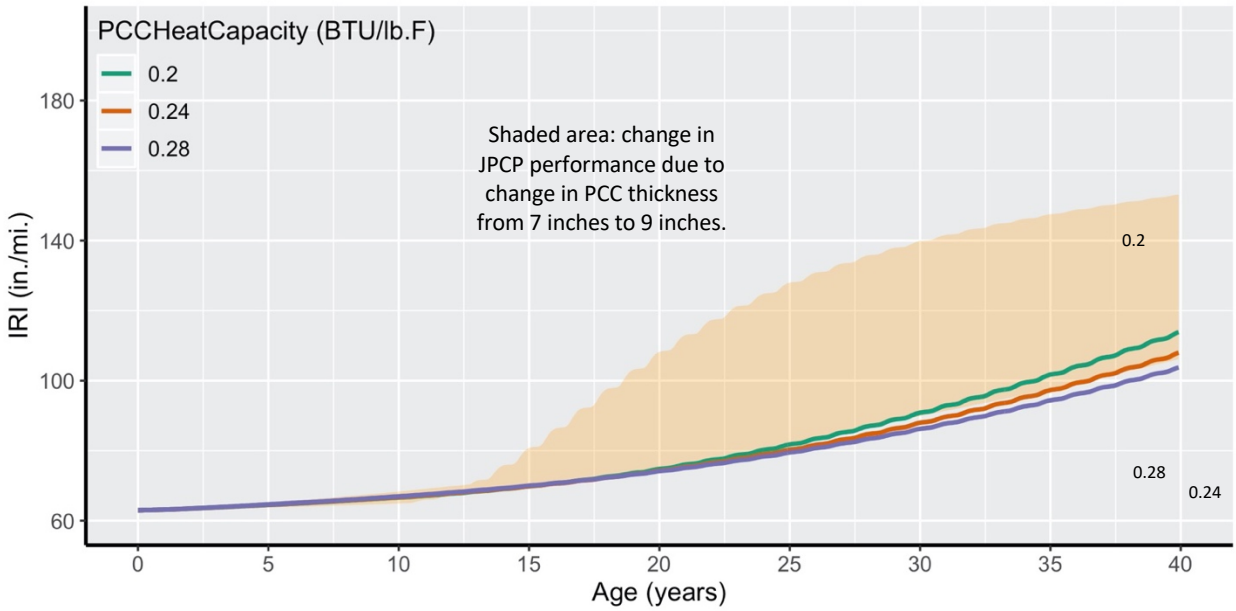

Figure 4.59: Effects of PCC heat capacity on IRI with 50% reliability

4.4.2.5. PCC Thermal Conductivity

Thermal conductivity is the quantity of heat that flows normally across a surface of unit area per unit of time and per unit of temperature gradient. No PCC thermal conductivity data are available in the UCPRC database. Pavement ME recommends a range of 1.0 to 1.5 for this variable, and therefore this study considered four PCC thermal conductivity values: 1.0, 1.15, 1.25 (the Pavement ME default value), and 1.5 BTU/(hr.ft.°F). Figure 4.60, Figure 4.61, and Figure 4.62 show that thermal conductivity has a significant impact on JPCP transverse cracking and smoothness performance but does not affect faulting much. However, there is not a monotonic relationship between thermal conductivity and Pavement ME predicted cracking, faulting, and IRI. This outcome was not unexpected since the implications of thermal conductivity are complex, and one should not expect a monotonic relation between this variable and Pavement ME distress outputs.

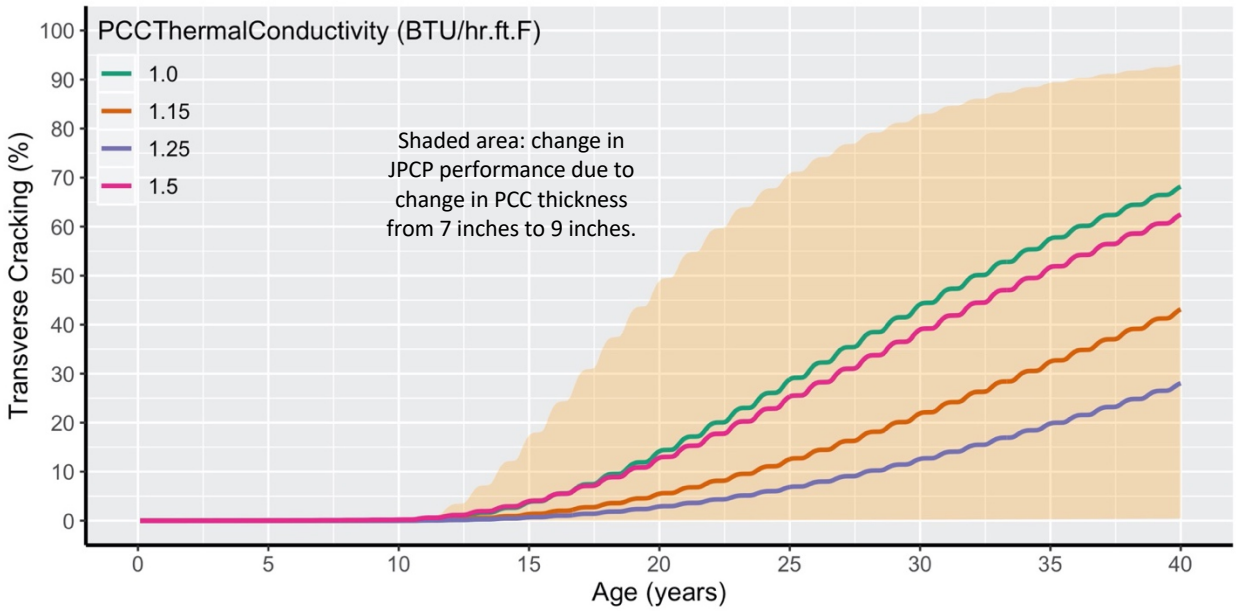

Figure 4.60: Effects of PCC thermal conductivity on transverse cracking with 50% reliability

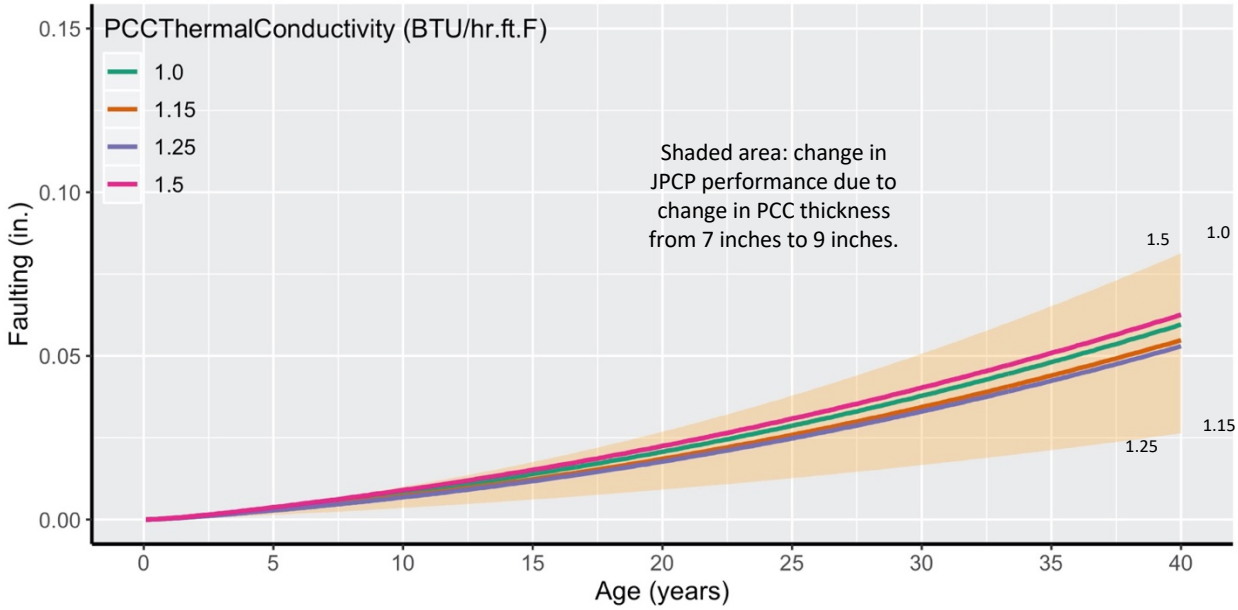

Figure 4.61: Effects of PCC thermal conductivity on transverse cracking with 50% reliability

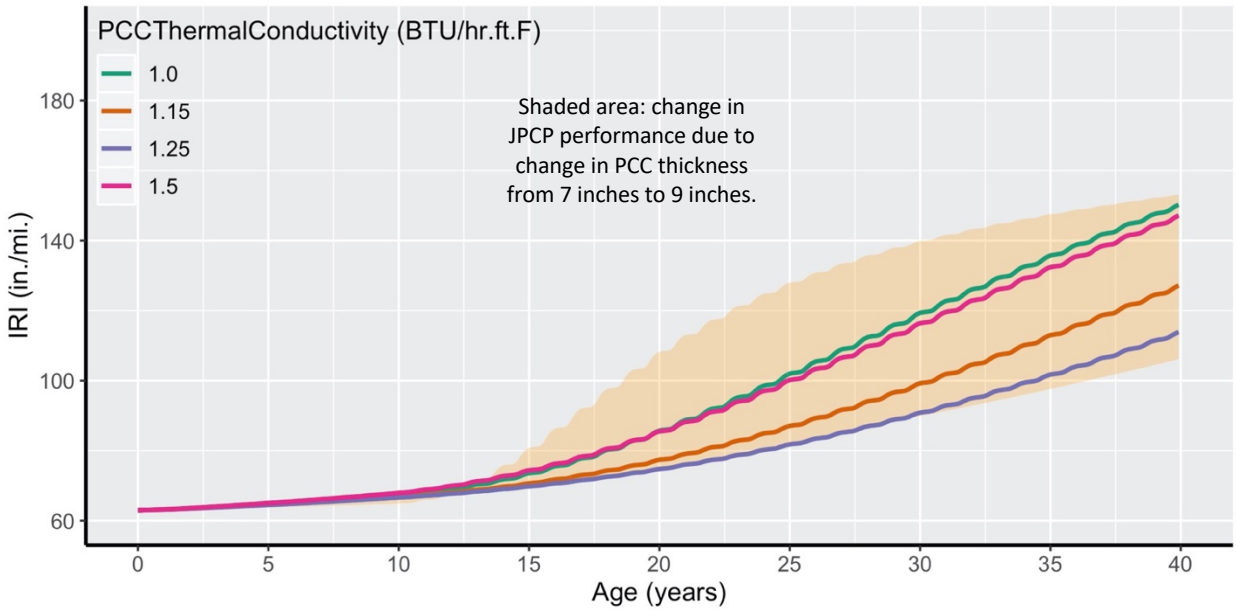

Figure 4.62: Effects of PCC thermal conductivity on IRI with 50% reliability

4.4.2.6. PCC Built-In Curl-Warp Temperature

According to the Pavement ME documentation, PCC paving is often performed during the morning on hot, sunny days, in conditions that tend to expose the newly paved PCC slabs to a high positive temperature difference from intense solar radiation. Therefore, the PCC slabs are flat when they harden, but they are hardening when there is a large positive temperature gradient (the upper portion of the slab is much warmer than the bottom). This temperature gradient has been termed the zero-stress temperature gradient. Whenever the temperature gradient in the slabs falls below, the zero-stress gradient locked into them at the time of construction, the slabs will curl upward, causing tensile stress at the top of the slab that can lead to top-down cracking of JPCP. Thus, to prevent, reduce, or eliminate the upward curling, the slabs are constructed to take advantage of several factors that act to reduce the built-in effective negative temperature gradient: the slab self-weight, dowels, and the weight of any base course bonded to the slab. These factors affect the amount of actual permanent curl, as well as the amount of creep relaxation that may take place. The Pavement ME documentation states that if PCC paving is performed later in the afternoon or at night, so that the highest temperature from the heat of hydration does not correspond with the most intense solar radiation, the temperature gradient at the time of hardening will be much lower and could potentially even be negative.

Differential shrinkage (top versus bottom of the slab) also produces permanent warping that is superimposed on the zero-stress thermal gradient and is modeled in the same way as permanent curling. The permanent components of curling and warping are, therefore, considered together. It is important to

note that only a portion of permanent curl/warp actually affects pavement response, because the PCC creep and slab foundation permanent deformation that occur over time negate some of the effects of the permanent curvature present in PCC slabs.

No PCC built-in curl-warp temperature data are available in the UCPRC database. However, Pavement ME recommends a range of 30 to 0°F, so this study considered four built-in curl-warp temperature values: 0, 5, 10 (Pavement ME default value), and 15°F. Decreasing the built-in curl-warp equivalent temperature gradient (cooler-on-top), which the Pavement ME models assume comes from a combination of the drying shrinkage gradient and the thermal gradients when the concrete sets, results in larger tensile stresses at the top of the slab (which entails more top-down transverse cracking) and larger corner deflections (which entails larger differential deflection energy and, consequently, more faulting). Pavement ME cracking, faulting, and IRI predictions for the different built-in curl-warp temperatures are shown in Figure 4.63, Figure 4.64, and Figure 4.65, respectively. Figure 4.63 shows the significant impact of the built-in curl-warp temperature on JPCP transverse cracking. However, while a monotonic relationship between this variable and both top-down and bottom-up cracking is expected, the same is not true for total cracking. The reason is that total cracking is a combination of top-down and bottom-up, with the former worsening and the later improving as the built-in curl temperature increases (in absolute value). As shown in Figure 4.63, the total cracking reaches a minimum when the built-in curl is –10°F, and it increases when this variable either decreases or increases. However, as expected, a monotonic relationship existed between the built-in curl temperature and both top-down and bottom-up cracking independently of each other, as shown in Figure 4.66. That figure shows the effects of built-in curl temperature on bottom-up, top-down, and total (bottom-up + top-down) cracks separately.

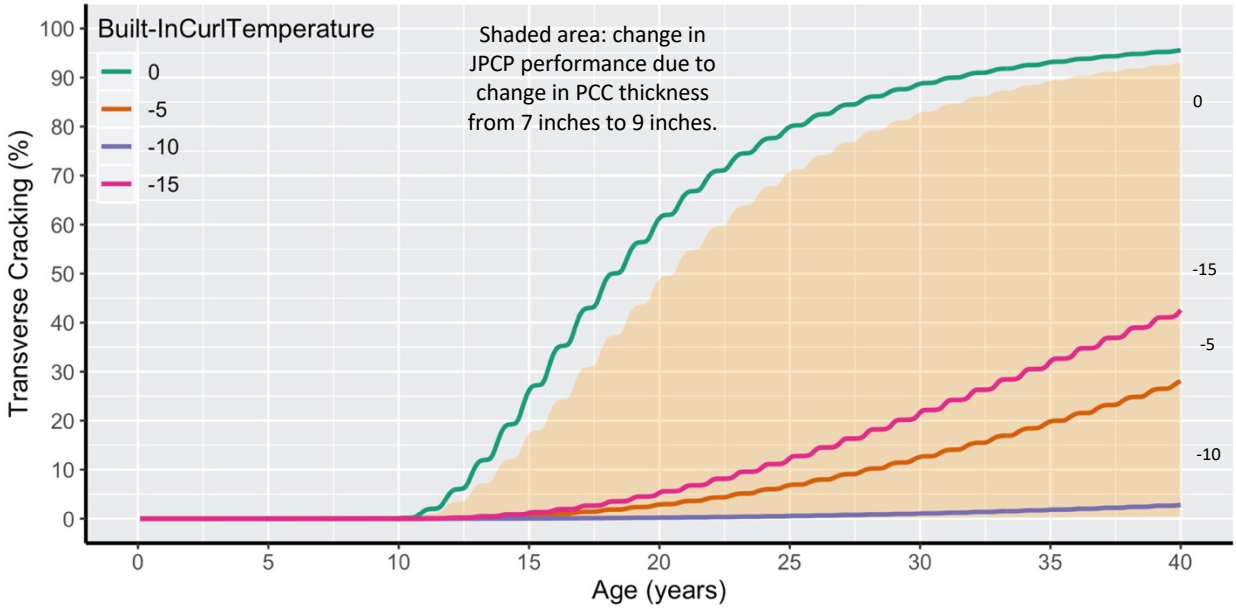

Figure 4.63: Effects of built-in curl-warp temperature on transverse cracking for 8-inch slabs with 50% reliability

The relationship between faulting and built-in curl-warp temperature (Figure 4.64) is as expected. The larger the built-in curl-warp, the larger the deflections and the differential deflections and, consequently, the larger the differential deflecting energy and the subsequent faulting. The relationship between built-in curl-warp temperature and IRI is more complicated, as IRI is a function of both faulting—to which built-in curl-warp is monotonically related—and transverse cracking—to which built-in curl-warp is not monotonically related.

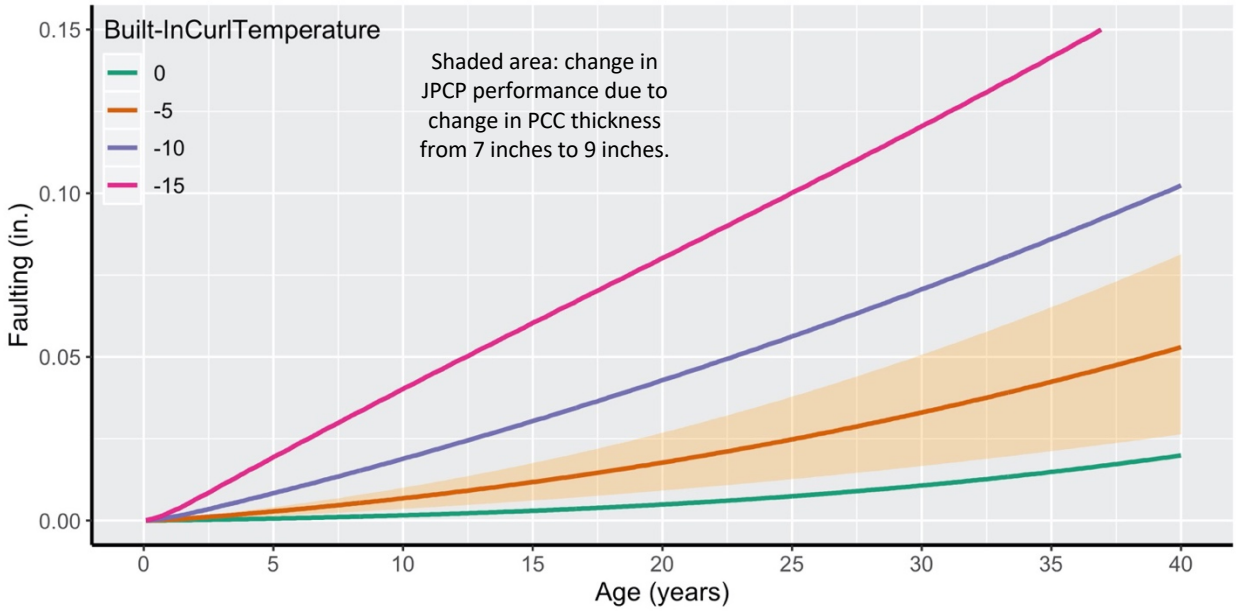

Figure 4.64: Effects of built-in curl-warp temperature on faulting with 50% reliability

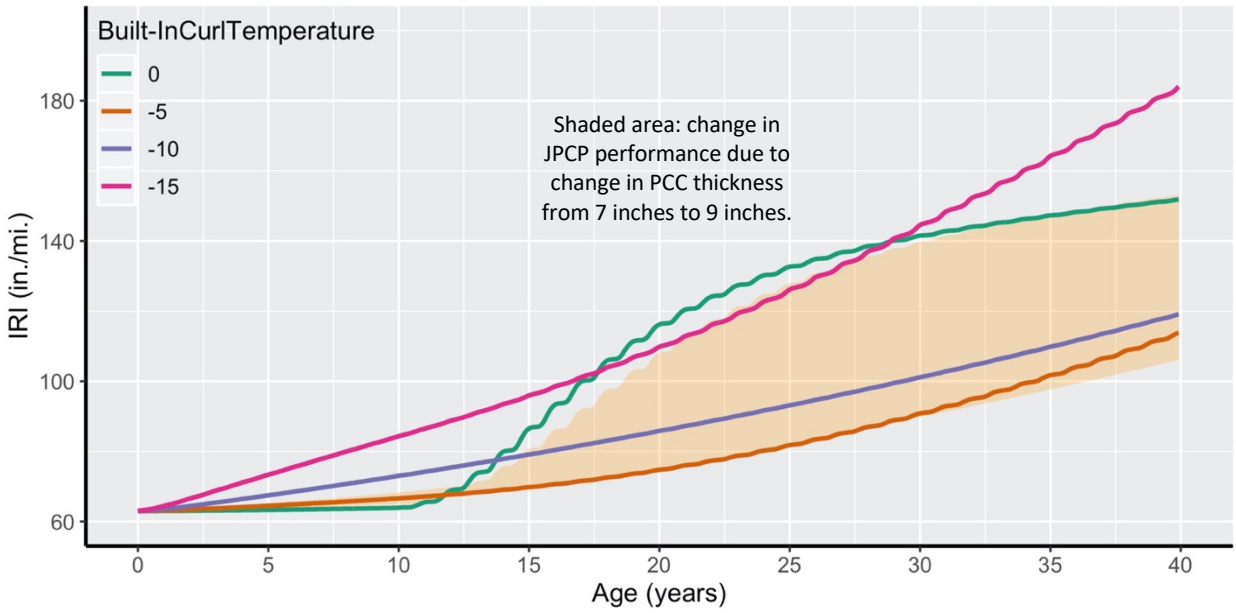

Figure 4.65: Effects of built-in curl-warp temperature on IRI with 50% reliability

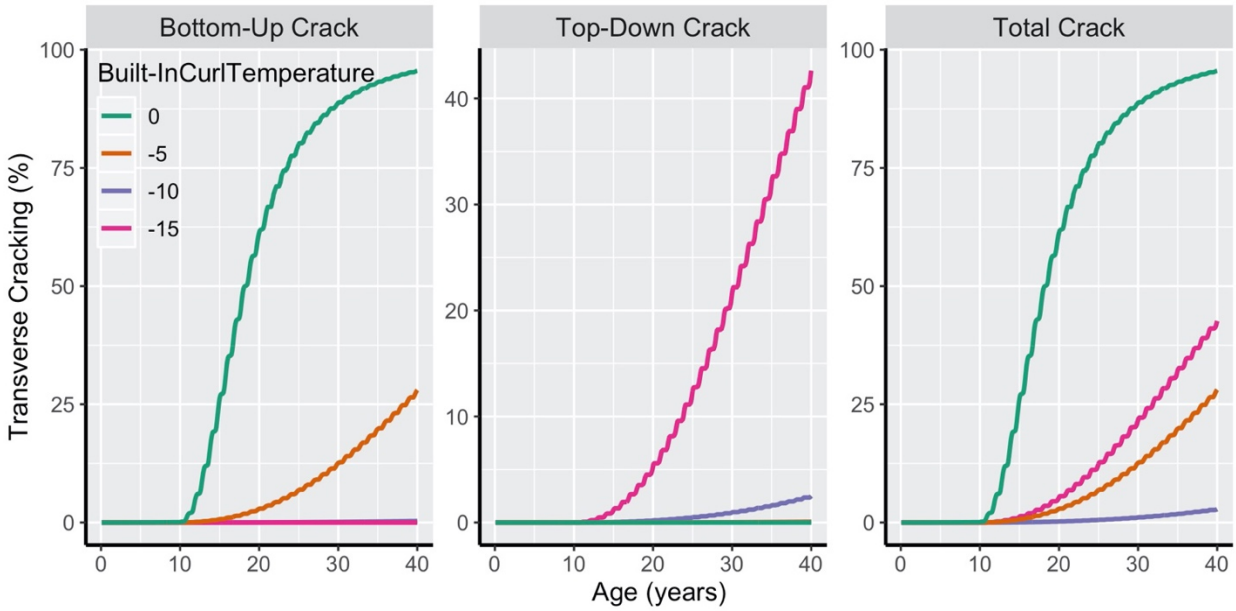

Figure 4.66: Effects of built-in curl-warp temperature on bottom-up, top-down, and total transverse cracking for 8-inch slabs with 50% reliability

4.4.3. Traffic Inputs

4.4.3.1. Average Annual Daily Truck Traffic

Traffic data are one of the key data inputs required for the analysis and design of pavement structures. The Pavement ME software considers truck traffic loading in terms of axle load spectra and average

annual daily truck traffic (AADTT), which is the bidirectional average annual daily truck traffic for two lanes.

This study considered five AADTT values, 7,000, 12,000, 14,000, 16,000, and 20,000, and assumed WIM Spectra 3 (WIM 3) as the default spectrum. The AADTT values are bidirectional with two lanes in each direction. These values were picked based on the AADTT distribution shown in previous section. These heavy truck traffic values were chosen to be high to evaluate the sensitivity to traffic. The directional and truck lane distribution factors were assumed to be 50 and 95 percent, respectively. Five WIM spectra characterize the truck loads for the different highways in the Caltrans road network. Each WIM spectra (1 through 5) includes a particular distribution of truck classes and axle load distributions for each truck class and axle type. The use of WIM spectra constitutes Level 2 traffic inputs in Pavement ME. The WIM spectra are described in the appendix. Using the Caltrans method of calculating equivalent single axle loads (ESALs), the truck traffic levels included in this sensitivity analysis along with the WIM 3 assumption translate to 40-year ESALs of x, y, z, k, and j respectively, which represent Caltrans Traffic Index values of 15, 16, 16, 16.5, and 17 when rounded to the nearest 0.5. It must be made clear that ESALs are not used in Pavement ME. Instead, an axle load spectra must be used with truck classification count data.

Figure 4.67, Figure 4.68, and Figure 4.69 show that as AADTT increased, transverse cracking, faulting, and IRI increased, as expected. This sensitivity is such that a doubling of truck traffic from 7,000 to 14,000 trucks per day resulted in approximately the same increase in transverse cracking as reducing the slab thickness from 9 to 8 inches when the AADTT is 14,000.

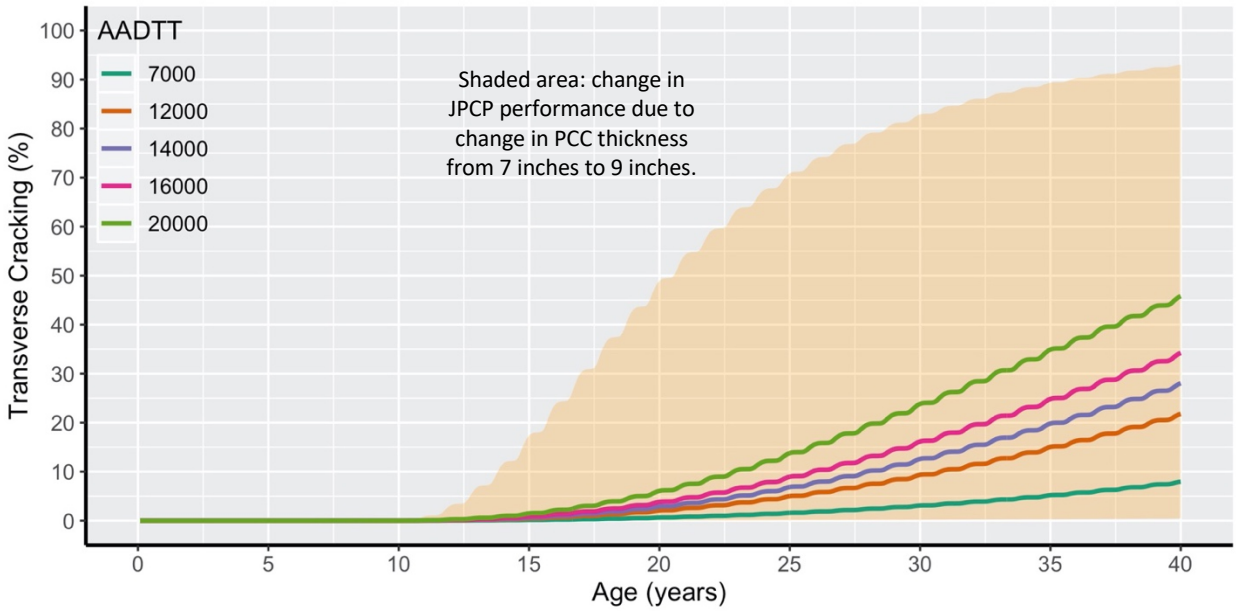

Figure 4.67: Effects of AADTT on transverse cracking with 50% reliability

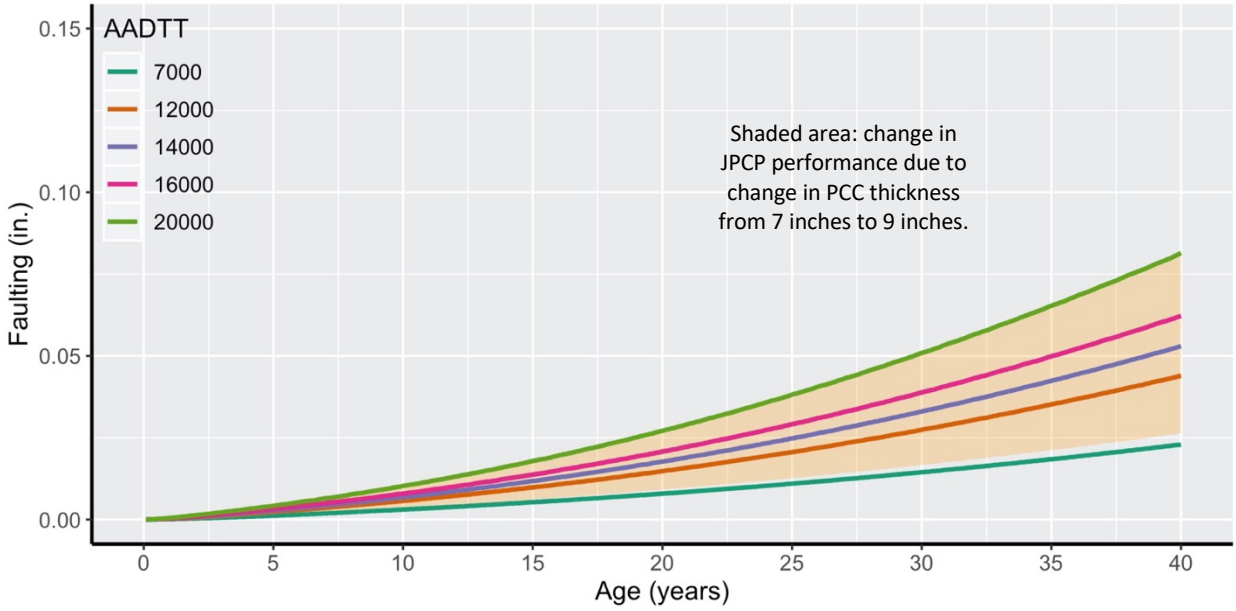

Figure 4.68: Effects of AADTT on faulting with 50% reliability

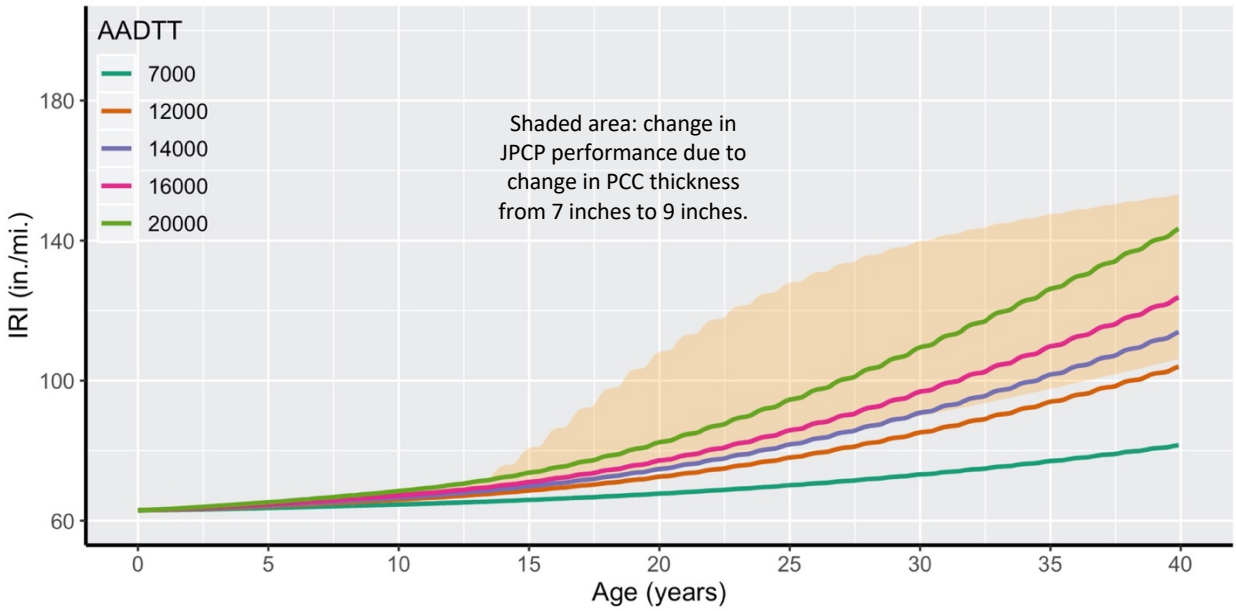

Figure 4.69: Effects of AADTT on IRI with 50% reliability

4.4.3.2. Weigh-in-Motion (WIM) Spectra

Weigh-in-motion data are a tabulation of the vehicle type and the number, spacing, and weight of axles for each vehicle weighed over a period of time. WIM data are used to determine the normalized axle load distributions or spectrum for each axle type within each truck class. In other words, the load spectrum for an axle type is the percentage of loads in each load category for a given number of axles of that type. There are five WIM groups in California, three of which are considered in this study: Spectra 1, Spectra 3, and Spectra 5 (9). In general, axles get heavier as the WIM spectra changes from Spectra 1 to Spectra 5 (called "spectra" here because there is a spectrum for each axle type in each set) and therefore, more distress is expected under higher-numbered WIM groups.

Figure 4.70, Figure 4.71, and Figure 4.72 show the effect of WIM spectra on Pavement ME–predicted transverse cracking, faulting, and IRI, respectively. It was expected that an overall heavier WIM spectra, represented by a higher WIM spectra number, would result in larger predicted distresses. However, the Pavement ME–predicted cracking, faulting, and IRI were not particularly sensitive to the WIM spectra. This is because the different WIM spectra differ from one another in the middle and low load ranges, as shown in Figure 4.73; however, these load levels produce very little damage to the JPCP. On the contrary, the three WIM spectra are very similar to one another for equivalent single axle loads above 18 kips, which produce most JPCP damage, and that explains why the three result in similar cracking, faulting, and IRI. For similar reasons, one should not necessarily expect Pavement ME–predicted distresses to increase systematically as WIM spectra increases.

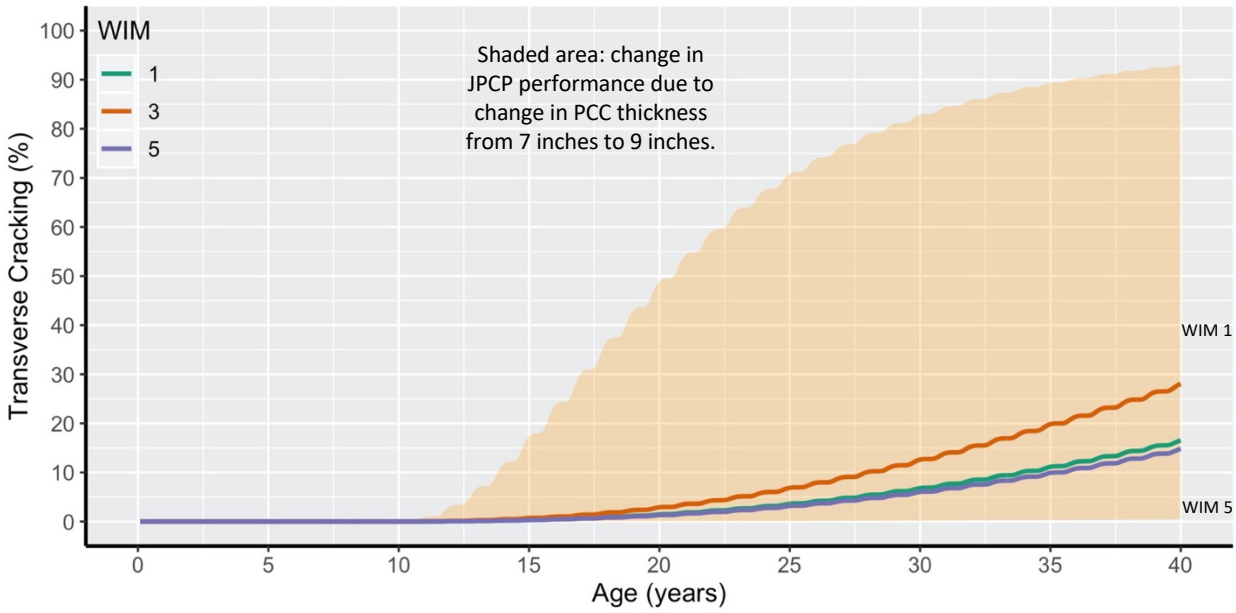

Figure 4.70: Effects of WIM spectra on transverse cracking with 50% reliability

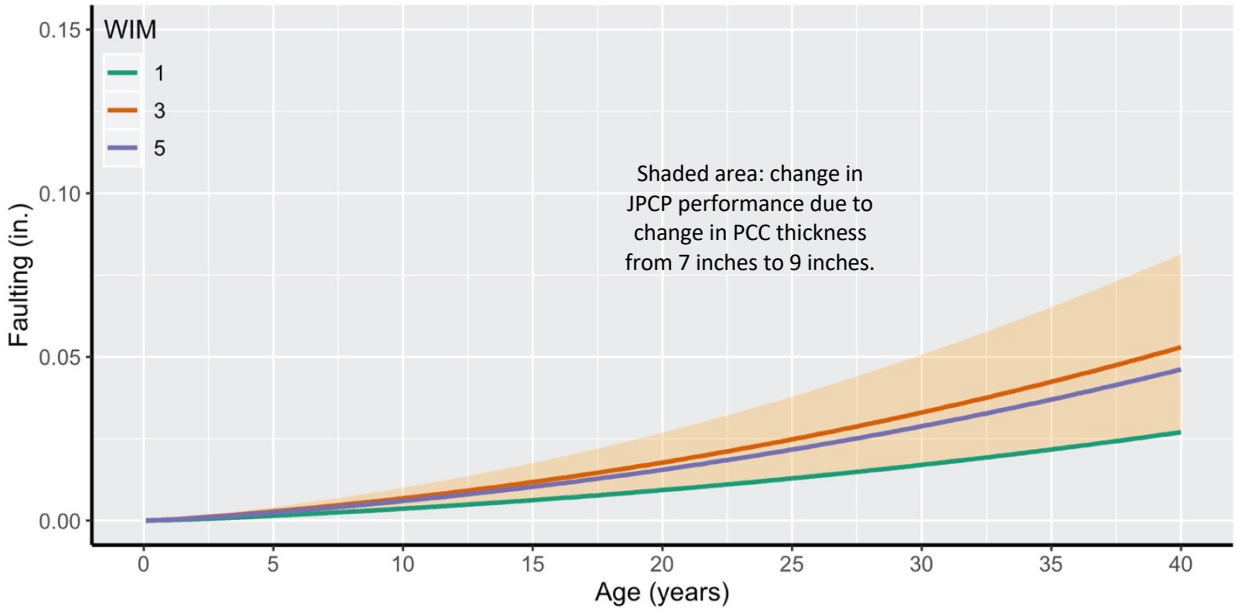

Figure 4.71: Effects of WIM spectra on faulting with 50% reliability

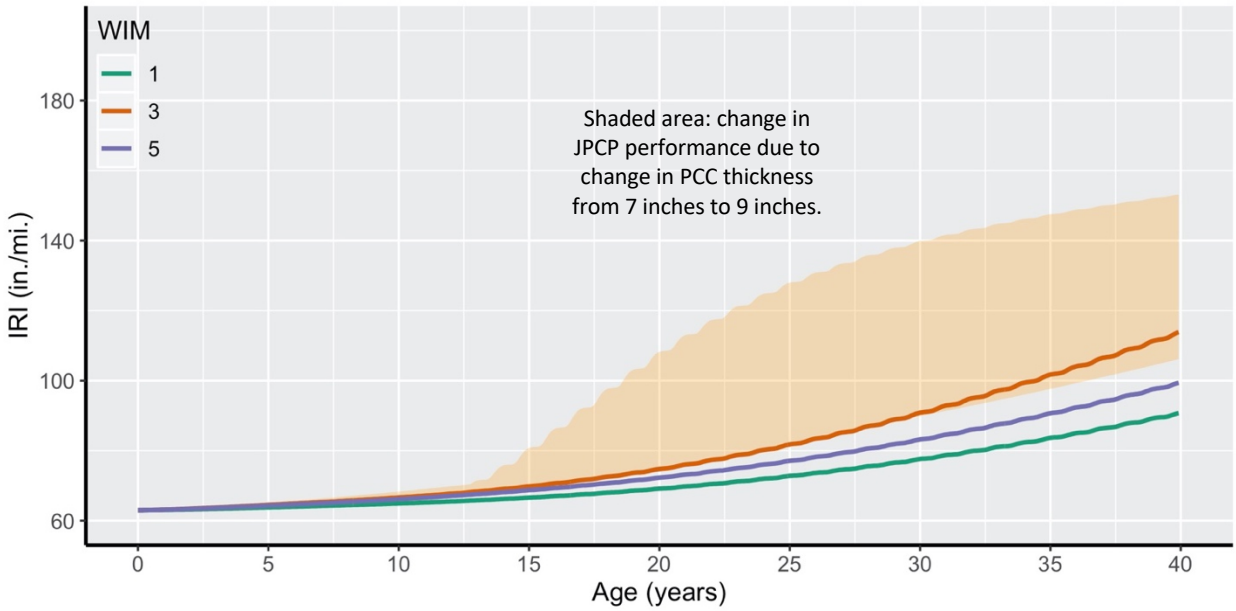

Figure 4.72: Effects of WIM spectra on IRI with 50% reliability

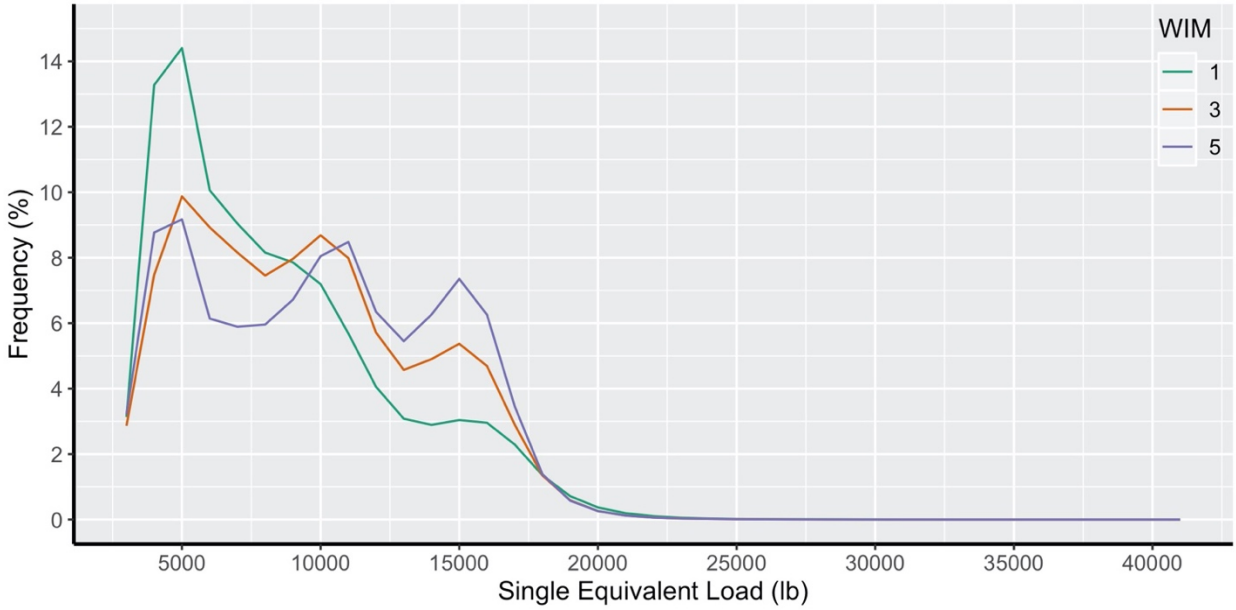

Figure 4.73: Equivalent single axle loads associated to WIM spectra

(Note: **The *single equivalent load* is the result of splitting tandem axles in two and tridem axles in three [e.g., one tandem becomes two singles with half the load each]. The use of single equivalent axles is a simplified way to determine the similarity between different WIM spectra. It does not impact the actual spectra being used in Pavement ME.)**

4.4.4. Climate

According to the MEPDG, environmental conditions have a significant effect on the performance of rigid pavements. The interaction of climatic factors with pavement materials and loading is complex. Factors such as precipitation, temperature, freeze-thaw cycles, and depth to water table affect pavement and

subgrade temperature and moisture content, which, in turn, directly affect the pavement layers' load-carrying capacity and ultimately pavement performance.

This study considered California's nine climate regions. The weather stations used to represent each climate region are shown in Table 4.2.

Table 4.2: Climate Regions and Corresponding Weather Stations

Climate Region	Representative Weather Station in Pavement ME	Weather Station Identification Number
Central Coast	San Francisco	23234
Desert	Riverside	03171
High Desert	Reno	23185a
High Mountain	Emigrant Pass	23225c
Inland Valley	Sacramento	23232
Low Mountain	Santa Rosa	23213
North Coast	Arcata/Eureka	24283
South Coast	Los Angeles	23174
South Mountain	Palm Springs	3104d

Figure 4.74, Figure 4.75, and Figure 4.76 show that all the distress models are significantly affected by climate region. The transverse cracking results are somewhat unexpected with respect to the South Coast region, which might be considered a relatively benign climate region based on the observed performance data, but which had the third-most cracking of all the regions, and the harsher High Desert region, which showed the least amount of cracking.

However, appearances can be deceptive. In a study conducted as part of the earlier Pavement ME calibration, temperature gradients were calculated using (a) the stand-alone version of the Enhanced Integrated Climate Model (EICM) coded into Pavement ME and 30 years of climate data (Ongel and Harvey, 2004) and (b) six of the current nine climate regions that Caltrans designs for; the High Mountain, South Mountain and Low Mountain regions were not included in the calculations at first but were added later. Further, the North Coast region was not included in this sensitivity analysis because there are few concrete pavements there.

In Figures 25 and 26 in Reference (Ongel and Harvey, 2004), the ranking in terms of distributions of positive temperature gradients that would contribute to bottom-up transverse cracking showed that the South Coast, Inland Valley, and Desert regions had similar high positive gradients, while the High Desert and Central Coast regions had similar low positive gradients. The ranking in terms of distributions of negative temperature gradients that would contribute to top-down transverse cracking were the High

Desert, Desert, and Inland Valley regions with similar high negative gradients, while the Central Coast and South Coast regions had similar low negative gradients. Based on the temperature gradients from the previous study, the region with both low positive and negative gradients is the Central Coast, and it had the second lowest amount of cracking of the regions common to both studies, as shown in Figure 4.74. The regions with the highest positive temperature gradients common to both studies were the Desert, South Coast, and Inland Valley, which are the three regions with the most cracking, as shown in Figure 4.74. The anomaly in the results is the High Desert, which has the least cracking, but which also has high negative gradients. A comparison of cracking trends for the different climate regions in the PMS data will help identify whether the Pavement ME results match field performance with respect to ranking of cracking for the different climate regions.

The results for faulting are more consistent with the expectation that climate regions with greater negative temperature gradients would be expected to have more faulting.

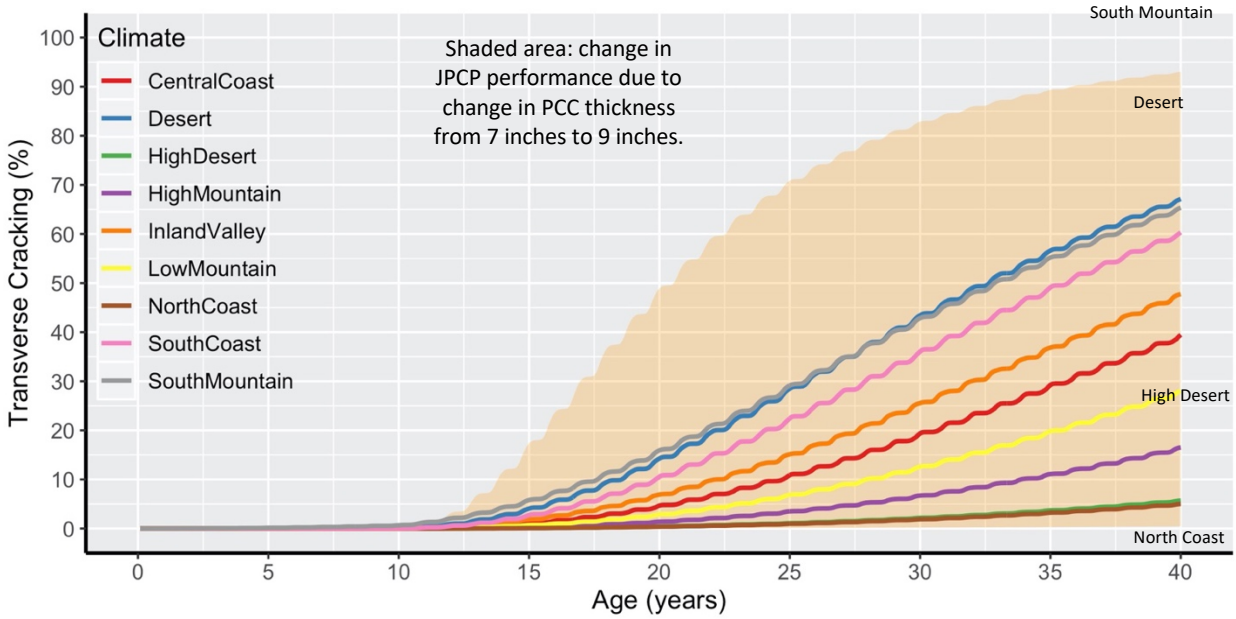

Figure 4.74: Effects of climate on transverse cracking with 50% reliability

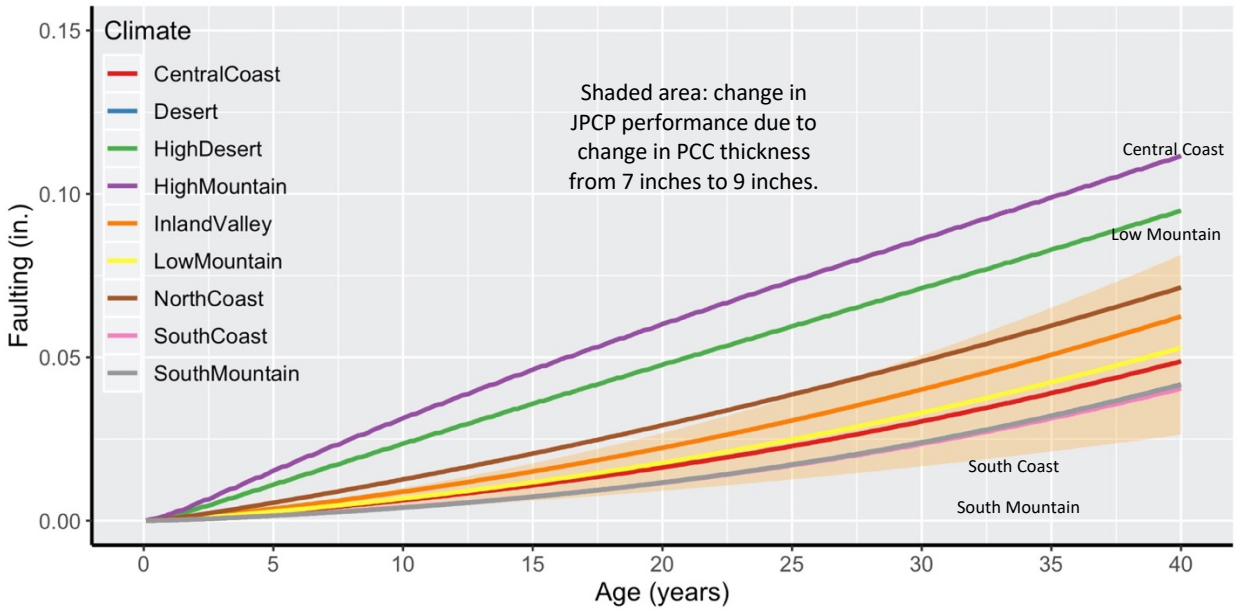

Figure 4.75: Effects of climate on faulting with 50% reliability

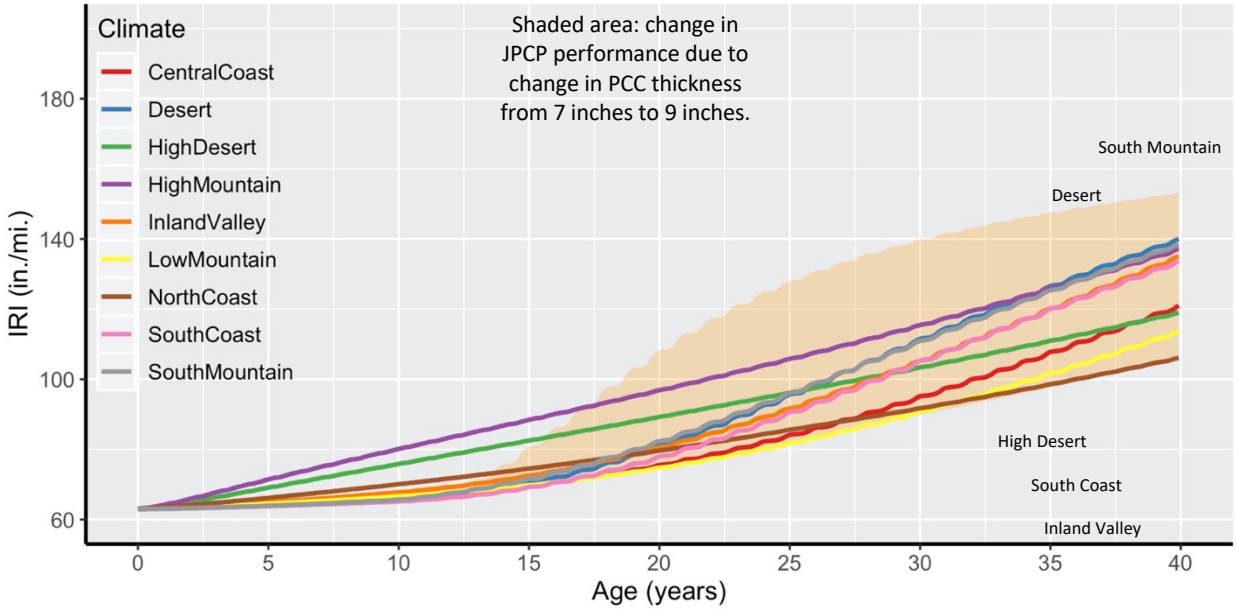

Figure 4.76: Effects of climate on IRI with 50% reliability

4.5. Summary and Conclusions

In this study, a sensitivity analysis study was performed as a first step in the calibration of Pavement ME. This is part of a project undertaken to provide Caltrans with updated tools for the design and analysis of jointed plain concrete pavements (JPCPs) in California. The sensitivity analysis identified the importance of different input variables and their effects on the outputs generated by Pavement ME's performance models for transverse cracking, faulting and IRI. These results were also used to check the reasonableness

of the model predictions, to identify problems in the software, and to understand the level of difficulty involved in obtaining the inputs.

The study considered different inputs grouped as pavement structural design variables, pavement materials variables, traffic variables, and climate variables. With some exceptions, the range chosen for each of the variables generally corresponded to one of two categories. The first was the typical range of variation of the corresponding variable in the historical Caltrans road network for the time period of the projects to be used for calibration. The second category included some cases, such as AADTT, that represented values more extreme than those found in the historical database; this approach was taken to identifying sensitivity where it would not otherwise have been observable. As stated earlier, it is important to note that the historical ranges and the more extreme values chosen for each of the variables in this study are not the ranges that will be used for developing the design catalog. Figure 4.77 through Figure 4.79 summarize the sensitivity analysis for the Pavement ME transverse cracking, mean transverse joint faulting, and smoothness index (IRI) models, respectively. The red line in the figures represents the model results for the base case inputs, and each boxplot shows the effect of varying the specific variables on the distress. Therefore, boxplots with greater height identify a variable with a greater effect on the distress for the range of inputs considered. Based on these figures, the following variables were found to be the ones with the greatest influence on JPCP design. They are ranked from most to least influential:

- Transverse cracking
    - PCC slab thickness
    - Built-in curl-warp temperature
    - PCC coefficient of thermal expansion (CTE)
    - PCC shortwave absorptivity
    - PCC compressive strength, which was used with American Concrete Institute (ACI) equations implemented in Pavement ME to predict PCC flexural strength and modulus of elasticity
    - Shoulder type
- Mean transverse joint faulting
    - Load transfer* (use of dowels)
    - Built-in curl-warp temperature
    - Shoulder type
    - Climate
    - AADTT
    - PCC coefficient of thermal expansion

- PCC thickness
- Subgrade type

- Smoothness index
  - Load transfer* (use of dowels)
  - Shoulder type
  - Coefficient of thermal expansion
  - PCC shortwave absorptivity
  - Built-in curl-warp temperature
  - AADTT
  - PCC thermal conductivity
  - PCC thickness

*Load transfer (use of dowels) is not shown in Figure 4.78 and Figure 4.79 as its high values for the undoweled case do not allow for an effective comparison of results.

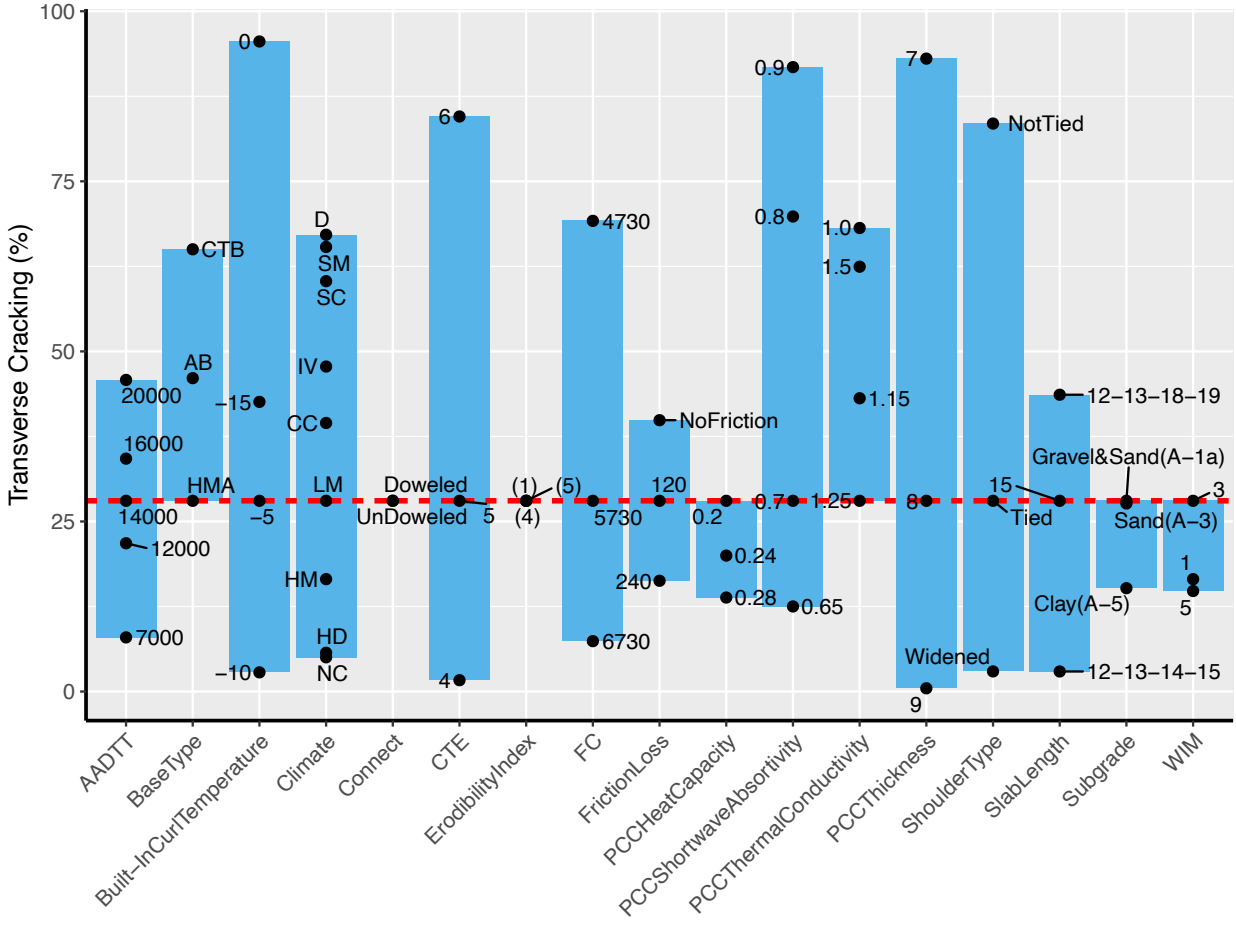

Figure 4.77: Overall sensitivity analysis of the transverse cracking model in Pavement ME

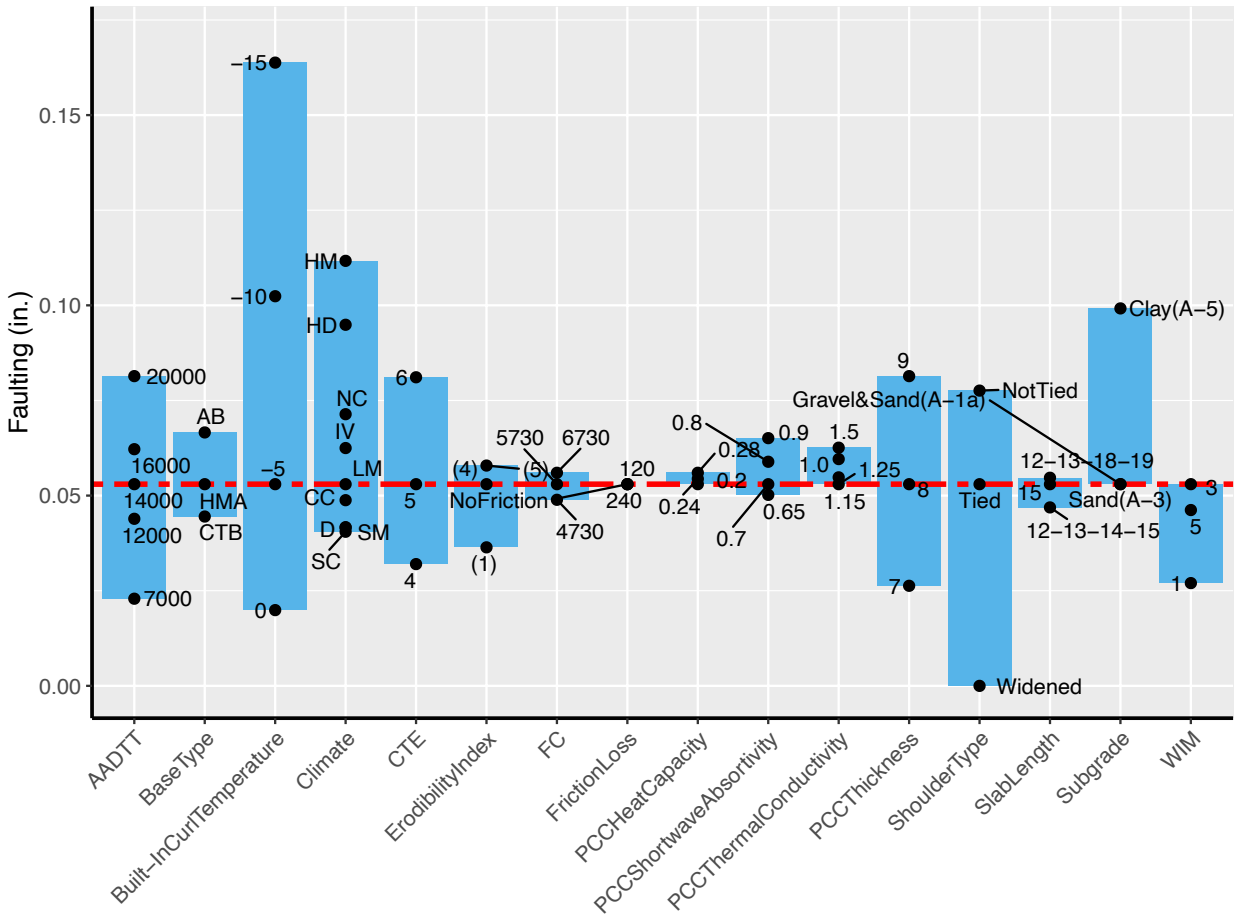

Figure 4.78: Overall sensitivity analysis of the faulting model in Pavement ME

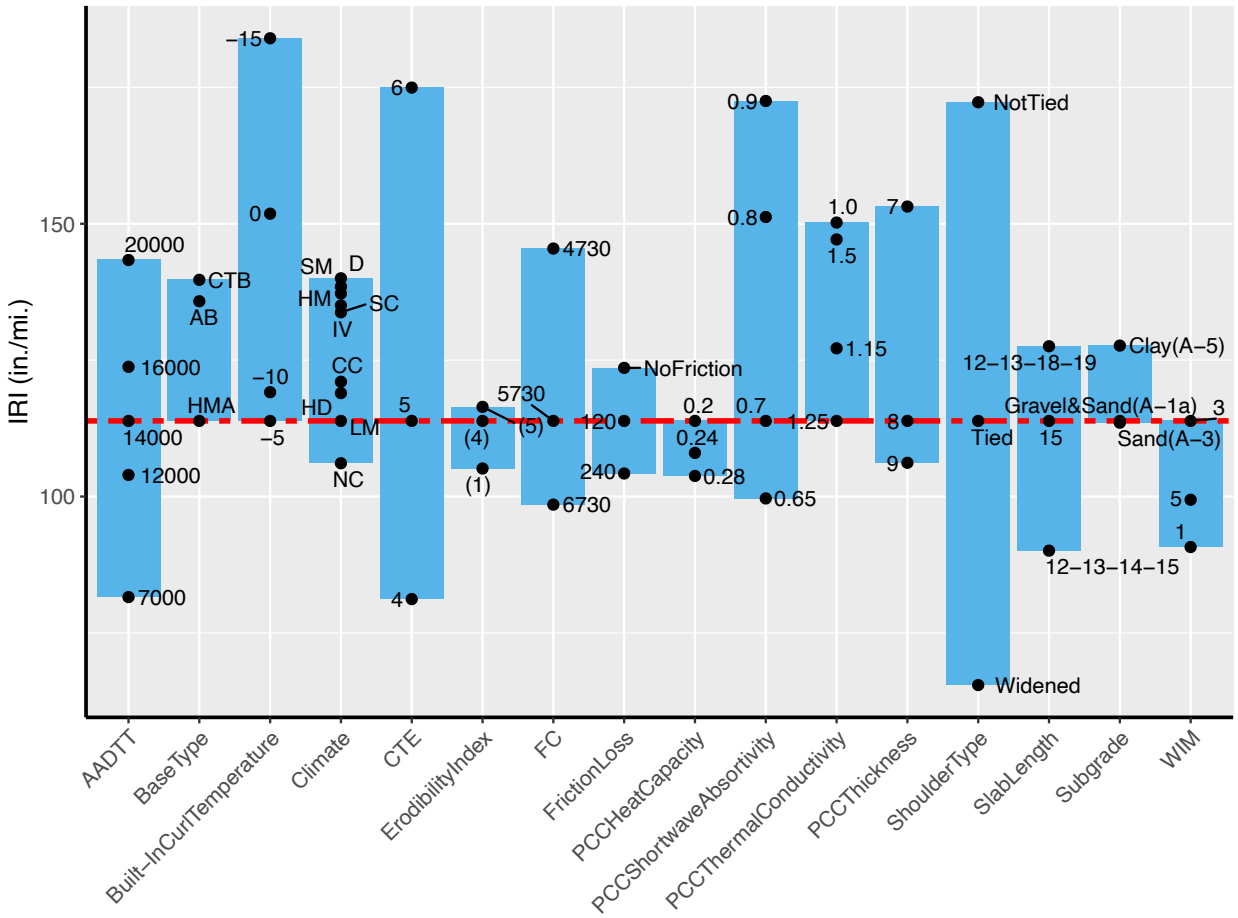

Figure 4.79: Overall sensitivity analysis of IRI model in Pavement ME

The sensitivity analysis shows that the overall JPCP performance predictions by Pavement ME are reasonable. Pavement ME–predicted distresses did not show any important unexpected trends versus any of the variables considered in this sensitivity analysis. Further, over the course of the study, no major issues were found in the running of the Pavement ME software.

Calibration of Pavement ME, the next step in this project, will proceed as planned because, except for the material inputs, the Caltrans PMS database currently includes all the other required design inputs. To help a designer overcome the lack of material inputs at the time of design, the calibration will include median values for these based on historical Caltrans projects; these should provide reasonable results and a representative "best estimate" calibration. Even so, designers will still need to keep in mind that the calibration will still include some variability due to differences in the materials supplied by different contractors on different projects (i.e., the between-project variability). This sensitivity analysis study also identified the within-project variability of construction-related variables such PCC compressive strength,

PCC modulus of elasticity, and PCC CTE. The appendix at the end of this report shows the data used for the analysis.

CHAPTER 5. Pavement ME Calibration

5.1. Introduction

5.1.1. Previous Calibration and Design Catalog Development

The American Association of State Highway and Transportation Officials (AASHTO) 2002 Mechanistic-Empirical Pavement Design Guide (MEPDG) was calibrated using Long-Term Pavement Performance (LTPP) sections throughout the United States, including some from California (NCHRP, 2003). However, it was recommended by the MEPDG development team that nationally calibrated models be validated using local data and, if necessary, recalibrated. This makes sense for California because nearly all the state's climate zones are drier and warmer than those of most of the sections in the national calibration set. In addition, the aggregate used in the state's concrete is primarily of igneous origin, while that of much of the national data set is concrete with limestone aggregate, and these igneous aggregates often have a greater coefficient of thermal expansion (CTE) than limestone aggregates. The dry climate and igneous aggregates tend to respectively increase the drying shrinkage gradients and the effects of thermal gradients, increasing the tensile stresses that cause cracking. California also does not have the prolonged periods of freezing and thawing that are accounted for in the national calibration. It was known to UCPRC researchers in 2006 from discussions with the MEPDG development team that they had override the default values used for some variables for a number of California sections that were outliers during the national calibration process, which they believed was necessary due to greater drying shrinkage and thermal stresses.

Therefore, there was a need to validate the models in the MEPDG based on the performance of California pavements and to recalibrate the models if necessary. In addition, the reliability approach used in Pavement ME is based on the national calibration and does not explicitly address typical local deviations of important variables. (Note: in this report the design guide is referred to as MEPDG and the software as Pavement ME.) Once models are locally calibrated, updated design tools then need to be developed based on the calibrated software. The first step in this process is to perform a sensitivity analysis study to check the reasonableness of the models' predictions, to identify potential software issues, and to help identify and understand the inputs that significantly affect the models' outputs.

In 2006, the University of California Pavement Research Center (UCPRC) performed a research study that included an initial sensitivity analysis of jointed plain concrete pavements (JPCP) distress prediction models in the MEPDG (Kannekanti and Harvey, 2006). That study identified the most important

variables affecting predicted performance and studied a design variable that was found to be the most important for the predicted performance of JPCP in California—the time to loss of bonding between the concrete and the base (Kannekanti and Harvey, 2007). After that calibration, the software was used to produce a preliminary design catalog for the Caltrans Highway Design Manual (HDM); Caltrans adjusted that catalog further to produce the one in the current HDM. The assumptions and results for that preliminary design catalog are documented in Sample Rigid Pavement Design Tables Based on Version 0.8 of the Mechanistic-Empirical Pavement Design Guide (Kannenkanti and Harvey, 2006). In 2019, the UCPRC performed another sensitivity analysis study of JPCP distress prediction models in Pavement ME (v2.5.3) (Saboori et al., 2019) which was discussed in the previous chapter. In this study, the important variables affecting the predicted transverse cracking performance were found to be portland cement concrete (PCC) slab thickness, built-in curl-warp temperature, PCC coefficient of thermal expansion, PCC shortwave absorptivity, and PCC compressive strength.

Pavement ME is the current version of the software developed from the MEPDG models. This software uses the MEPDG models to produce transverse cracking, faulting, and International Roughness Index (IRI) predictions.

PaveM, the California pavement management system (PMS), manages jointed plain concrete pavement based on third-stage cracking, rather than transverse cracking. First-stage cracking is defined as the first crack that divides a slab into two pieces. A first-stage crack can be a transverse crack, the only type of cracking modeled by Pavement ME, or a longitudinal crack, which also occurs on Caltrans JPCP (Harvey et al., 2000). Third-stage cracking is defined as a state of cracking that divides a slab into three or more pieces. In California, a transverse crack is one of the cracks that commonly creates a third-stage crack along with a longitudinal crack, although, less frequently, third-stage cracking is also created by two transverse cracks or two longitudinal cracks.

The traditional approach for validating and calibrating mechanistic-empirical design methods is to collect all input data—including performance, as-built, and detailed materials data—from tens of sections within a state and to compare the predicted and measured performances for those few sections. For the national calibration of Pavement ME, this was done on the scale of several hundred LTPP sections across the United States.

The previous California calibration of an early version of Pavement ME (Kannekanti and Harvey, 2007) followed the traditional approach to ME method calibration and involved only 52 JPCP and 43 crack,

seat, and overlay sections. On those sections the amounts of first-stage transverse and longitudinal cracking and third-stage cracking were unavailable from the pavement management system data, and they were measured at the time of coring and deflection testing for those sections that had not been overlaid with asphalt. To develop better transverse cracking histories for those sections and for the overlaid sections, it had to be estimated whether the measured third-stage cracking had begun as a first-stage transverse crack or longitudinal crack to produce a transverse cracking history starting from each section's time of construction. Because there were insufficient data and the locations of the sections did not cover the entire state well, a model predicting whether a third-stage crack began as a transverse or longitudinal crack could not be developed. Instead, a range of potential transverse cracking histories was produced for each section, with the maximum of the range assuming that all third-stage cracks began as transverse cracks and the minimum assuming that they all began as longitudinal cracks. This added uncertainty to the calibration.

Soon after that calibration, Caltrans asked for a transfer function that could predict third-stage cracking from transverse cracking predictions; this function was developed and used in the creation of the preliminary design tables that were the basis for the design tables included in the 2007 HDM. The development of that transfer function has not been published.

5.1.2. Overview of New Calibration and Design Development

In 2010, Caltrans developed a capacity for Automated Pavement Condition Survey (APCS) data collection from the state highway network, and as a result a much larger and more reliable pavement condition database is now available in PaveM. Due to a considerable effort on the part of Caltrans, the database now includes as-built data such as pavement structure, base type, shoulder type, slab length, and construction year—items that were scarce in the previous study but are now available for almost every project built since 1990, and many built prior to that year. These data provide the capability to validate and calibrate Pavement ME using thousands of performance data observations and to use the explanatory data in the as-built database. In addition to the data in PaveM, the UCPRC has collected, detailed data for Caltrans for more than 100 projects sampled in the early 2000s and 2010s. Those data are for variables—such as concrete materials properties and the stiffnesses of underlying layers—not in the as-built database in PaveM.

Since 2006, new versions of Pavement ME software have been released with many improvements in both models and software implementation. These updates and improvements, combined with the increased amount and higher quality of data now in PaveM, have created the opportunity to perform a new JPCP

prediction model sensitivity analysis and calibration specifically for California. In this study, the latest version of Pavement ME (v.2.5.5) is used. It should be noted that an earlier version of Pavement ME (v2.5.3) was used for the sensitivity analysis study. However, after careful investigation it was found that the Pavement ME model predictions have remained unchanged.

A new approach was used for the calibration process, whose results were checked against all the data available in PaveM. This new approach recognizes that in the design-bid-build (low-bid) contracting environment used in California, a designer does not actually know the detailed materials properties when a design is being created. Therefore, the calibration used median values of the detailed materials properties and recognized the variability caused by different contractors' when a design is built. The calibration also used the detailed information available from PaveM regarding layer types, thicknesses, slab dimensions, shoulder types, dates of construction, and performance data, along with detailed climate and traffic data, to find the coefficients in Pavement ME that on average produce the best match between predicted performance and observed performance. The distribution of differences between the predicted and observed performance also provide information needed for introducing reliability into the future design tools.

In this research, Pavement ME was calibrated to the transverse cracking estimated from first-stage cracking. To achieve this a new model was developed that gives the probability that the first-stage crack is longitudinal or transverse. This effort used the APCS 2011–2012 data, which accurately separated transverse and longitudinal cracking on all JPCP across the entire state and thus provided sufficient data to produce a model. This model was then used to predict the rate of transverse and longitudinal cracking development for all JPCP performance data in the historic PMS database. The model included consideration of explanatory variables such as shoulder type, climate region, and slab thickness and dimensions, among others.

The model was able to relate the development of transverse cracking to the subsequent development of third-stage cracking. This can be used to set transverse cracking failure levels for the development of design tools and to relate predicted transverse cracking from Pavement ME to the third-stage cracking used in PaveM.

The calibration of the Pavement ME empirical model transverse cracking coefficients C_4 and C_5 was made using the predicted portion of transverse cracking in the observed first-stage cracking. The model was also able to identify situations where longitudinal cracking was expected. Associated design guidance

will be developed from this model to help designers limit the possibility of early failure. That guidance is not included in this report. Pavement ME was not developed to predict longitudinal cracking because it seldom occurs outside of the dry climate regions that are predominant in California and some other western states, a condition that is not typical of the rest of the United States.

The steps followed in the calibration process are as follows:

1. Identify roadway segments
2. Prepare PMS data
3. Develop statistical performance model
4. Estimate median values for unknown variables
5. Run Pavement ME for each cell of data
6. Analyze nationally calibrated model error
7. Identify within-project variability (WPV) and between-contractor variability (BCV) and find calibrated C_5
8. Identify between-project variability (BPV) and find calibrated C_4
9. Find C_4 corresponding to 95 percent reliability
10. Analyze calibrated model error

The results presented in this report demonstrate the new calibration procedure for the Pavement ME JPCP transverse cracking model based on use of the extensive data in the pavement management system database. The set of calibrated model coefficients will be used to develop Caltrans JPCP design catalog.

In section 5.2, a performance model for first- and third-stage cracking is developed. Also, a transfer model is developed to predict the portion of first-stage cracking data being transversely cracked. In section 5.3, the new calibration procedure is presented. Section 5.4 presents the summary and conclusions of the study and recommendations for future studies.

5.2. Pavement Management System and JPCP Cracking Statistical Performance Model

Pavement management is the process of using available financial resources as efficiently as possible to ensure the highest overall functional performance of a road network, both spatially and over time, while maintaining the structural condition of the pavements to protect the initial investment in construction. As such, to perform pavement management, it is necessary to capture the current functional and structural condition of the network and to predict its future condition for different management scenarios.

Historically, a team of Caltrans pavement raters conducted a pavement condition survey (PCS) at various locations along the state highway system (SHS) once a year as part of a manual pavement condition survey. The pavement raters visually inspected the outer highway lanes for both directions of travel using systematic sampling techniques. Pavement condition assessments were extrapolated for each section of the entire SHS based on those sample locations.

The boundaries of pavement management sections across the network changed annually, as did the locations where surveys occurred. Because the same location was not sampled each year, building performance histories was difficult for the 2006 Pavement ME calibration. Changing section boundaries from year to year also meant that a given pavement location could be included in different sections in any year. On jointed plain concrete pavements (JPCP) the sections were typically around one mile long.

Between 2011 and 2012, Caltrans began testing and transitioning from the manual PCS to the Automated Pavement Condition Survey (APCS). The APCS can efficiently collect, evaluate, and analyze pavement conditions for all lanes on the SHS. It utilizes vehicles equipped with an array of on-board high-definition cameras, laser sensors, Global Positioning System trackers, and other measurement devices that quickly collect pavement data at highway speeds. The information collected includes geographical locations of the highways, downward-looking pavement surface images, forward right-of-way images, and pavement surface profiles. The data are collected for every 26.4-foot section, referred to as an element, for asphalt pavement and continuously reinforced concrete pavement and every concrete slab for JPCP. Data are aggregated to calculate a weighted average of the pavement condition of larger segments for management or reporting purposes.

Because evaluating condition, especially functional condition, can be subjective, agencies have generally settled on trying to identify and quantify specific distresses. A distress is a measurable phenomenon on the surface of a pavement, such as observable cracking, changes in ride quality (smoothness/roughness), or rutting. Distress is the result of internal deterioration within the pavement, typically either cracking or permanent deformation of materials, or in the case of JPCP permanent changes in vertical alignment on the two sides of joints. Deterioration, in turn, is the result of internal damage within the materials, which is not observable. This might include particle movement, breaking of bonds, or other atomic/microscopic changes. These damage processes take place at different rates at different locations in the pavement because of variability in the materials, construction processes, traffic, drainage, and underlying subgrade soil type, among many possible sources. As a result, distress is observed to accumulate at different rates

along the road surface, even within a section that is nominally uniform with regard to all of the variables mentioned above.

This chapter outlines the pavement structure, climate, and traffic variables along with distress measures available in California's pavement management system (known as PaveM) database. It also briefly discusses the qualitative effects of different variables on the performance of the JPCP over its service life. The condition survey distress data from both the PCS and APCS were used to develop empirical performance models for PaveM, and these models were in turn used to calibrate Pavement ME, as shown in the next chapter. An empirical performance model is a statistical model based on the data obtained through the pavement condition surveys. The model predicts the future performance (condition) of the pavement—which in this study is the percentage of cracking—based on input variables such as pavement structure (i.e., portland cement concrete [PCC] slab thickness, PCC slab length, base type, and shoulder type) and nonstructural variables such as climate and truck traffic spectra category. In Section 2.5, a model (transfer function) is developed that gives the probability that a first-stage crack is longitudinal or transverse. This model is later used to determine the portion of first-stage cracked pavements having transverse cracking. Adding the result to third-stage cracking data will be used to calibrate the Pavement ME transverse cracking model.

5.2.1. Structural Distress Measures in JPCP

5.2.1.1. Concrete Slab Cracking

Cracking is the primary distress in JPCP due to traffic loading and environmental conditions. Each pass of traffic loading results in damage-causing stress in the concrete slabs. The minor damage from each load accumulates with thousands to hundreds of millions of load passes until eventually it results in failure in the form of fatigue cracking. Environmental conditions, such as curling caused by vertically differential temperatures in the slab and warping caused by vertically differential shrinkage, also create stresses that contribute to damage in the concrete slab.

Cracking in concrete slabs can be categorized into three main types: transverse cracking, longitudinal cracking, and corner cracking. Transverse cracks appear perpendicular to the pavement centerline and extend across the entire slab from one longitudinal edge to the other. Longitudinal cracks appear parallel to the pavement centerline and extend along the entire slab from one transverse joint to the other. Corner cracks occur in one quadrant of a slab and have one endpoint on a longitudinal joint and the other on a transverse joint. Other types of cracking are also possible, such as diagonal cracks or "deformed"

transverse or longitudinal cracks, but these are uncommon and are caused by localized issues, such as subsidence.

Typically, a combination of repeated loads combined with thermal and shrinkage stresses causes transverse cracking in concrete slabs. There are two mechanisms for initiation and progression of transverse cracking, referred to as bottom-up and top-down cracking. When truck axles are near the longitudinal edge of a slab, midway between the transverse joints, a critical tensile stress occurs at the bottom of the slab with its maximum value in the longitudinal direction. The presence of a high positive vertical temperature gradient (the top of the slab is warmer than the bottom of the slab) through the slab thickness causes additional tensile stress at the bottom of the concrete slab and loss of slab support near its longitudinal edges, midway between transverse joints. Both of these stresses contribute to bottom-up cracking.

Alternatively, the combined effect of two heavy truck axles, frequently steering and drive axles, simultaneously loading the opposite ends of a slab results in tensile stresses at the top of the slab that may cause top-down fatigue transverse cracking. Top-down transverse cracking is accelerated by high negative temperature gradients (the top of the slab cooler than the bottom of the slab) and differential drying shrinkage (the top of the slab has contracted more than the bottom), which cause tensile stress at the top of the slab and loss of slab support at its corners.

Longitudinal cracking in California is primarily caused by high differential drying shrinkage that causes high tensile stresses at the top of the slab and loss of slab support at its corners, which (with the combined effect of left and right wheels of the truck axles) result in top-down cracking.

Corner cracking is also caused by a top-down mechanism, where load repetitions at the corner of the slab combine with poor joint and shoulder load transfer, loss of slab support from the underlying layers, and curling (cooler on top than the bottom of the slab) and warping stresses. The lack of support and poor load transfer may be due to the pumping of underlayer material or loss of load transfer between the adjacent concrete slabs, such as undoweled concrete pavement that does not have tied concrete shoulders.

Once a slab has cracked, its geometry changes and the locations of critical loads and distress on it changes. Because cracks are more random than constructed joints, the process of cracking from this point onward becomes more chaotic and difficult to analyze. In some cases, a first-stage transverse crack might

act as an additional joint, and the slab will show little further distress. In other cases, a first-stage crack might result in a cascading failure as the slab transitions to a more aggressive failure mode.

Caltrans has traditionally categorized the cracking in JPCP in terms of its severity into two main groups: first-stage and third-stage cracking. In the official Caltrans definition, first-stage cracking is a crack that breaks the concrete slab into two pieces; this crack can be a transverse, longitudinal, or diagonal crack. Third-stage cracking is defined as a set of two or more intersecting longitudinal or transverse cracks that divide the concrete slab into two or more pieces. However, despite these written definitions, Caltrans raters have long used the simpler definitions that a slab has first-stage cracking if it is divided into two pieces and it has third-stage cracking if it is divided into three or more pieces. Corner cracking is not considered in any of these two definitions and is defined and measured separately.

Caltrans measures cracking as the percent of cracked slabs in a pavement section. Caltrans historically has collected data on first- and third-stage cracking only, without defining whether the first-stage cracking is transverse or longitudinal. However, as part of the APCS data collection in 2011–2012 and 2018, transverse and longitudinal cracking data were also collected as individual measures. Therefore, the amount of transverse and longitudinal cracking data in the APCS database comes only from these years and is much less than the amount of data that consists of only first- and third-stage cracking.

5.2.1.2. Transverse Joint Faulting

Faulting is the difference in elevation across a transverse joint between two adjacent concrete slabs or across a transverse crack. It is primarily caused by poor load transfer and is therefore usually an issue with undoweled JPCP.

The main mechanism that causes faulting is movement of fine material from under the leave concrete slab to under the approach slab. This is caused by large differences in deflection between the loaded slab and the unloaded slab, which reverse as wheels travel across the joint and create a pumping action. Dowel bars significantly decrease relative deflections across transverse joints under load, thus reducing faulting development and further deterioration of joints and corner cracks.

Caltrans measures both average fault height and faulting as the percent of transverse joints in a pavement section with faults greater than a threshold value of 0.15 inches. Average fault height is used in the Mechanistic-Empirical Pavement Design Guide (MEPDG) and other federal pavement management metrics, but it is difficult to measure because small fault heights cannot be measured reliably and are

rounded down to zero in the averaging. There is some disagreement over the measurement of faulting at transverse cracks and if these should be included in these metrics. Typically, they are included in MEPDG and similar metrics by the automated algorithms that analyze and report faulting from the measured data.

5.2.1.3. International Roughness Index (IRI)

Pavement roughness is generally defined as an expression of irregularities in the pavement surface that adversely affect the ride quality of a vehicle and thus the user. Roughness is an important pavement characteristic because it affects not only ride quality but also vehicle maintenance costs, fuel consumption, and freight damage. Roughness in PaveM data is quantified using the International Roughness Index, which defines a characteristic of the longitudinal profile of a traveled wheel track. IRI constitutes a standardized roughness measurement and is measured in units of inches/mile in PaveM.

5.2.2. Statistical Performance Model for First- and Third-Stage Cracking

JPCP performance data can be considered a time series panel dataset, where the panels are the individual pavement sections that are defined as discrete lengths of pavement with similar factor levels for all the variables at different locations within projects. The variable of interest is the pavement state, an ordinal variable. There are three cracked pavement states: (1) undamaged, (2) first stage, and (3) third stage. This variable obviously is not a continuous, normally distributed variable. A generalized linear model is thus required, and in this case an ordered logit model (or ordered logistic regression) seems appropriate. In addition, because the data are nested panel data, a mixed- effects model is required, which allows each panel to have different regression parameters (the intercept in this model) to account for unexplained variability. The nested panel data (longitudinal data) are multidimensional data involving measurements over time, which in this case are cracking performance measures obtained from condition surveys in different years. In this context, this unexplained variability is called between-project variability (BPV), and it is caused by parameters such as material properties (e.g., PCC compressive strength, PCC thermal conductivity, and PCC coefficient of thermal expansion) that are unknown to designers prior to construction and variables that are not included in the database, such as subgrade soil stiffness. This type of model is known as a cumulative link mixed model (CLMM), a specialized form of a generalized linear mixed model accounting for ordinal data, whose generalized form is:

$$\mathbf{g}\big(\mathrm{p}(\mathbf{y} < j)\big) = \boldsymbol{\eta} = \theta_j + \mathbf{X}\boldsymbol{\beta} + \mathbf{Z}\boldsymbol{\gamma} + \boldsymbol{\epsilon} \tag{5.1}$$

where:
$\mathbf{y}$ = vector of outcomes
$\mathbf{g}(\cdot)$ = link function
$\boldsymbol{\eta}$ = latent predictor $\sim N(\mathbf{0}, \mathbf{I})$
θ_j = threshold for level j
$\mathbf{X}$ = matrix of predictor variables
$\boldsymbol{\beta}$ = vector of fixed effect regression parameters
$\mathbf{Z}$ = matrix of design variables (panel variables)
$\boldsymbol{\gamma}$ = vector of random effects $\sim N(\mathbf{0}, \mathbf{I}\boldsymbol{\xi})$
$\boldsymbol{\epsilon}$ = vector of random errors

In this case, the link function is the logistic function, which is the natural logarithm of the odds that an event occurs, and the probability distribution of the outcomes is treated as a binomial distribution at each transition. Because the outcomes have a known distribution, the error of the latent variable must be scaled to have a unit normal distribution. Without scaling the latent variable to a unit normal distribution, there will be infinite solutions (fitted models). Notice that the only variable that changes with each threshold is θ_j, so that the transitions from one level to the next are not independent. The major advantage of this structure is that it accounts for the fact that the first-stage cracking evolution can inform the growth of third-stage cracking. This is particularly useful in this study because, for most JPCP sections, the first-stage cracking percentage reaches values that are much larger than those of third-stage cracking.

To fit the CLMM, the data were first structured so that each pavement section was a single sample, with the project level variables (e.g., PCC slab thickness, PCC slab length, shoulder type, base type, and climate) repeated for each section. In this approach, each observation (pavement section) can have any of three conditions—undamaged, first-stage cracked, or third-stage cracked—with a column determining the length of the section. Equivalently, the data within each project can be treated as a percentage of pavement sections that are in each of the three categories, and the fit weighted by the number of pavement sections. These two approaches are equivalent and produce identical results.

Several different predictor variables were tried in the fitting process. Based on the results from different models and visual inspection of the data, the following CLMM was used for calibration of the transverse cracking model:

$$\text{logit}\big(p(Y_i < j)\big) = \theta_j - \beta_1 \log(age_i) - \beta_2 \log(\text{age}_i) * AADTT\_lane_i - \beta_3 slab\_pattern_i * PCC\_thickness_i - \beta_4 \log(age_i) * slab\_pattern_i - \beta_5 base\_type_i - \beta_6 shoulder\_type_i - \beta_7 climate_i * slab\_pattern_i - u(project_i) \quad (5.2)$$

The proposed model includes a $log10$ transform of age (in years), which is consistent with the observed effect of age and has been used in many other pavement models (Saboori et al., 2018 and Tseng, 2012). This selection results automatically in zero probability of cracking when age is zero. Because Caltrans pavement design thicknesses are expressed in US feet, the thickness variable was not changed to millimeters. During the model's development, it was found that the doweled/undoweled variable had no impact on the cracking status of the pavement, and therefore the variable was discarded. The WIM spectra variable did not have the expected effect, i.e., WIM Spectra 4 and 5 (heavier traffic) did not cause more cracking, and hence was not considered in the model. This likely points to issues with the WIM spectra assignment rather than the cracking data and will be investigated in future research.

This model estimates the probability of the i^{th} observation falling in the j^{th} category or below, where i is the index for observations (pavement section) and j is the index for the response categories, which in this model are undamaged, first-stage, and third-stage cracking. The explanatory variables are:

- age: age of the pavement section in years
- $AADTT\_lane$: Average Annual Daily Truck Traffic in thousands
- $slab\_pattern$: slab length that is a categorical variable with levels 12,13,14,15 ft or 12,13,18,19 ft
- $PCC\_thickness$: PCC slab thickness in feet
- $base\_type$: type of base that is a categorical variable with levels aggregate base (AB), hot mix asphalt (HMA), asphalt-treated permeable base (ATPB), lean concrete base (LCB), and cement-treated base (CTB)
- $shoulder\_type$: type of pavement shoulder that is a categorical variable with levels not applicable (NAP), meaning an inner lane, untied flexible shoulder (FLX), tied concrete shoulder (RIG), and widened concrete shoulder (WRF)
- $climate$: one of the climate regions that exists in California

θ_j is the threshold coefficient or cut point between either uncracked and first-stage cracking or first- and third-stage cracking. β_1, β_2, β_3, β_4, β_5, β_6, and β_7 are model coefficients. Project effects were considered to be random with normal distribution $u(project_i) \sim N(o, \sigma^2)$. The random effect is considered on a

project level and represents the between-project variability that is due to variables, such as material properties, that are unknown to a designer prior to construction. The difference between these unknown variables—while all the other design variables, traffic, and climate are the same—will lead to different pavement performance. This is unexplained by the variables that could be included in the model and accounted for by random effects in the CLMM. The random effect for each project is initially chosen randomly, however, final results are obtained by iteratively maximizing the log of the likelihood function. The CLMM2 function in the ordinal package in R was used to fit the model (Christensen, 2015). Table 5.1 to Table 5.3 show the results of the model fit to the data. Looking at the p-values, some variables became insignificant, however, their interactions with other variables are significant. In the statistical model fitting, each individual variable is an intercept term and should be included in the model, as ignoring an intercept term may cause the fitting process to force the model through zero, which is not necessarily correct.

Table 5.1: Mixed-effects cracking performance model random effect parameter

Random Variable	Variance	Standard Deviation
Project	1.32856	1.152632

Table 5.2: Mixed-effects cracking performance model location (fixed) parameters

Coefficient	Estimate	Std. Error	z-value	p-value
log10(Age)	1.1134	0.0650	17.1332	< 2.22e-16
slab_pattern (12,13,18,19)[1]	-0.2141	1.5338	-0.1396	0.889000
pcc_thickness	-1.8864	1.4091	-1.3387	0.180682
base_type (ATPB)[2]	0.9241	0.3956	2.3357	0.019508
base_type (CTB)	-0.1939	0.2486	-0.7800	0.435400
base_type (HMA)	0.3148	0.3330	0.9453	0.344484
base_type (LCB)	1.9887	0.3675	5.4111	6.2636e-08
shoulder_type (FLX)[3]	0.2841	0.0372	7.6288	2.3697e-14
shoulder_type (RIG)	-1.4978	0.0772	-19.3954	< 2.22e-16
shoulder_type (WRF)	0.2849	0.1499	1.9007	0.057336
climate (Desert)[4]	0.2200	0.6973	0.3155	0.752355
climate (High Desert)	0.2256	1.3702	0.1646	0.869229
climate (High Mountain)	1.1428	0.7080	1.6140	0.106527
climate (Inland Valley)	1.2008	0.5376	2.2337	0.025505
climate (Low Mountain)	0.8263	1.3733	0.6017	0.547389
climate (South Coast)	0.2657	0.5388	0.4931	0.621925
climate (South Mountain)	1.3493	0.6532	2.0657	0.038857
log10(age)*AADTT_lane	0.1224	0.0035	35.2560	< 2.22e-16
slab_pattern (12,13,18,19)*pcc_thickness	-0.1833	1.7065	-0.1074	0.914476

log10(age)*slab_pattern (12,13,18,19)	0.4582	0.0762	6.0121	1.8316e-09
slab_pattern (12,13,18,19)*climate (Desert)	-0.6564	0.8341	-0.7870	0.431281
slab_pattern (12,13,18,19)*climate (High Desert)	0.4981	1.7792	0.2800	0.779515
slab_pattern (12,13,18,19)*climate (High Mountain)	-1.2651	1.5402	-0.8214	0.411417
slab_pattern (12,13,18,19)*climate (Inland Valley)	-1.1382	0.6472	-1.7587	0.078623
slab_pattern (12,13,18,19)*climate (Low Mountain)	0.7469	1.4870	0.5023	0.615480
slab_pattern (12,13,18,19)*climate (South Coast)	-1.2499	0.6633	-1.8845	0.059503
slab_pattern (12,13,18,19)*climate (South Mountain)	-1.7031	0.7515	-2.2662	0.023436

[1]Reference category: 12,13,14,15 ft
[2]Reference category: AB
[3]Reference category: NAP
[4]Reference category: Central Coast

Table 5.3: Mixed-effects cracking performance model threshold parameters

Threshold Coefficients	Estimate	Standard Error	z-value
Undamaged >> First-Stage	6.7784	1.2109	5.5980
First-Stage >> Third-Stage	8.7319	1.2113	7.2090

Since the model is fairly complicated and has many interactions between different variables, it is difficult to understand the effect of each variable (coefficient in the model) on the cracking performance of the JPCP. Therefore, a sensitivity analysis on the model predictions is presented below. The predictions from the model are presented for a set of input variables so that reasonableness of the model's predictions and the effects of each variable on the JPCP performance can be evaluated.

Figure 5.1 shows the effects of PCC slab thickness on the cracking performance of JPCP. Each panel represents a PCC slab thickness. Panels are plotted for 0.6-, 0.9-, and 1.2-foot thick slabs with the short slab pattern 12,13,14,15 ft. The X-axis represents age of the pavement and the Y-axis represents the probability of each state (undamaged, first-stage cracking, and third-stage cracking). This graph is plotted for the Central Coast climate region, with no shoulder, LCB, and AADTT per lane of 4,000. It can be seen that as the PCC slab thickness increases (looking from left to right in the panels) the green area becomes bigger and yellow and red areas shrink. This means that the thicker PCC slabs show less first- and third-stage cracking, which matches what was expected from the qualitative analysis of the data presented at the beginning of this chapter.

Figure 5.1: Mixed-effects cracking performance model predictions for different PCC slab thicknesses

Figure 5.2 shows the effects of slab pattern on the JPCP cracking performance. This graph is plotted for the Central Coast climate region, with no shoulder, LCB, 0.9-foot PCC slab thickness, and AADTT per lane of 4,000. The performance model predicts much more first- and third-stage cracking for the long slab pattern 12,13,18,19 ft than for the short one 12,13,14,15 ft.

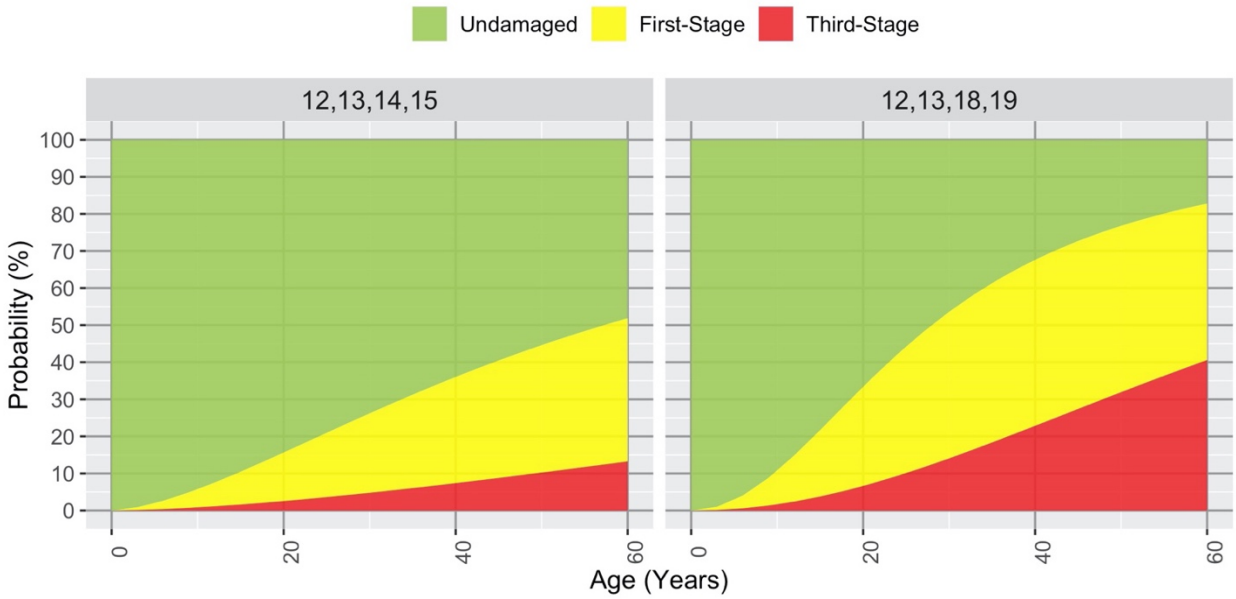

Figure 5.2: Mixed-effects cracking performance model predictions for different PCC slab patterns

Figure 5.3 shows the effects of different base types on the cracking performance of JPCP. This graph is plotted for the Central Coast climate region, with no shoulder, 0.9-foot PCC slab thickness, short slab pattern 12,13,14,15 ft, and AADTT per lane of 4,000. This graph shows that the conclusion drawn from Figure 4.10, which shows that CTB has the worst cracking performance of the five base types considered, was not correct as it considered only one variable (base type) on the performance of JPCP. The performance model used for Figure 5.3 considers all the variables and their interactions at the same time and predicts that the JPCP with LCB has the worst cracking performance, while the JPCP with CTB and HMA bases have the best cracking performances. (In the Pavement ME calibration process, the ATPB and HMA base types will be combined into one category, as ATPB has not been defined in Pavement ME software.)

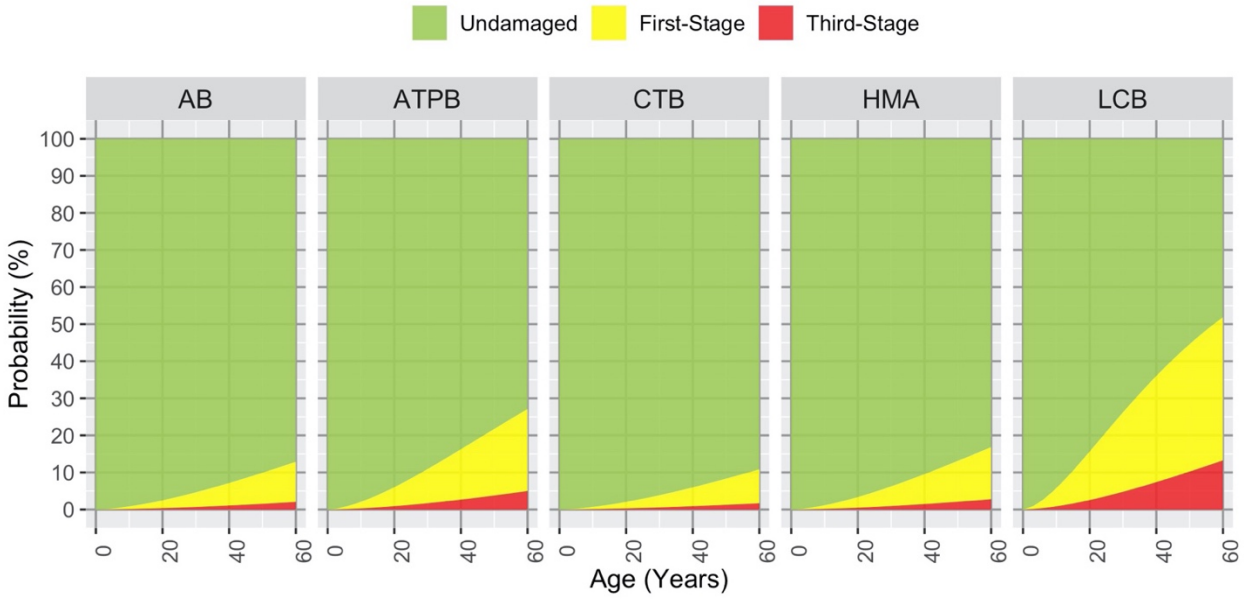

Figure 5.3: Mixed-effects cracking performance model predictions for different base types

Figure 5.4 shows the effects of shoulder type on JPCP cracking performance. This graph is plotted for the Central Coast climate region, with LCB, 0.9-foot PCC slab thickness, short slab pattern 12,13,14,15 ft, and AADTT per lane of 4,000. In the figure below, NAP represents no shoulder (i.e., interior lanes), FLX is untied flexible shoulder, RIG is tied concrete shoulder, and WRF is widened concrete shoulder. The graph shows that the JPCP with tied concrete shoulder performs the best and the JPCP with flexible and widened shoulders equally perform poorly. The widened slabs were historically constructed with 14-foot slabs (2 feet of shoulder) to mitigate the problem with transverse cracking; however, as shown in Figure 4.13, this shoulder type results in nearly the same JPCP cracking performance as the flexible shoulder.

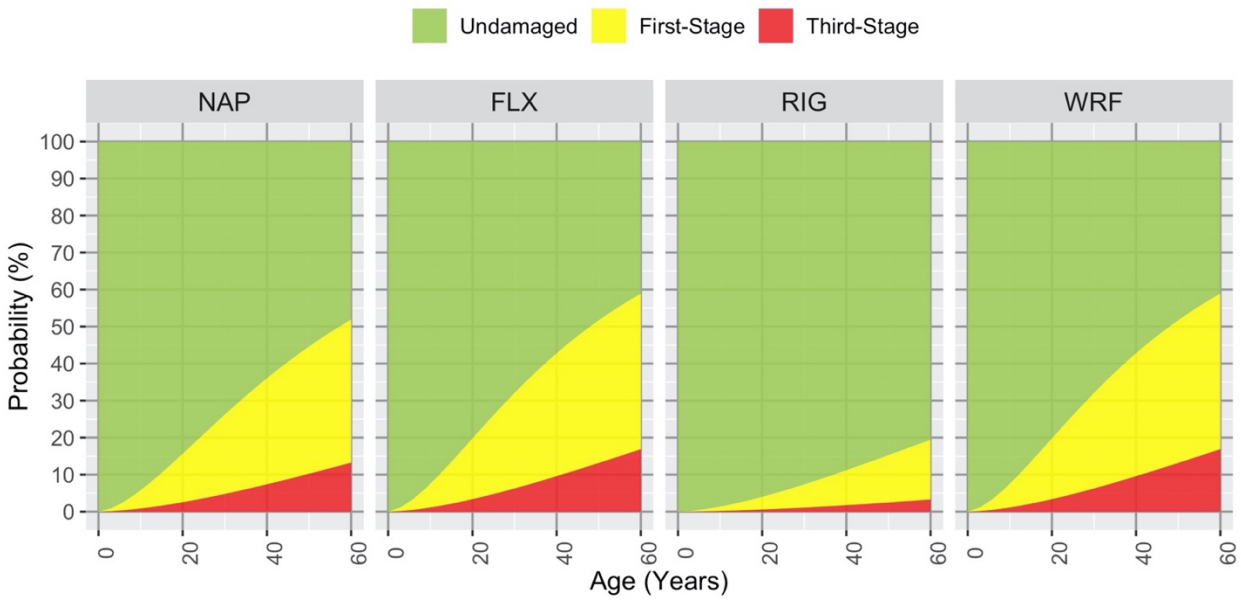

Figure 5.4: Mixed-effects cracking performance model predictions for different shoulder types

Figure 5.5 shows the effects of climate region on JPCP cracking performance. This graph is plotted for JPCP pavement with no shoulder, LCB, 0.9-foot PCC slab thickness, short slab pattern 12,13,14,15 ft, and AADTT per lane of 4,000. The JPCP in the Inland Valley, High Mountain, and South Mountain climate regions have the worst performances among all climate regions. The best performances occur in the South Coast, Central Coast, High Desert, and Desert regions, with the Low Mountain region falling in between. (The North Coast climate region does not appear in Figure 5.5, as the database used for the development of the statistical performance model does not contain JPCP for that region.)

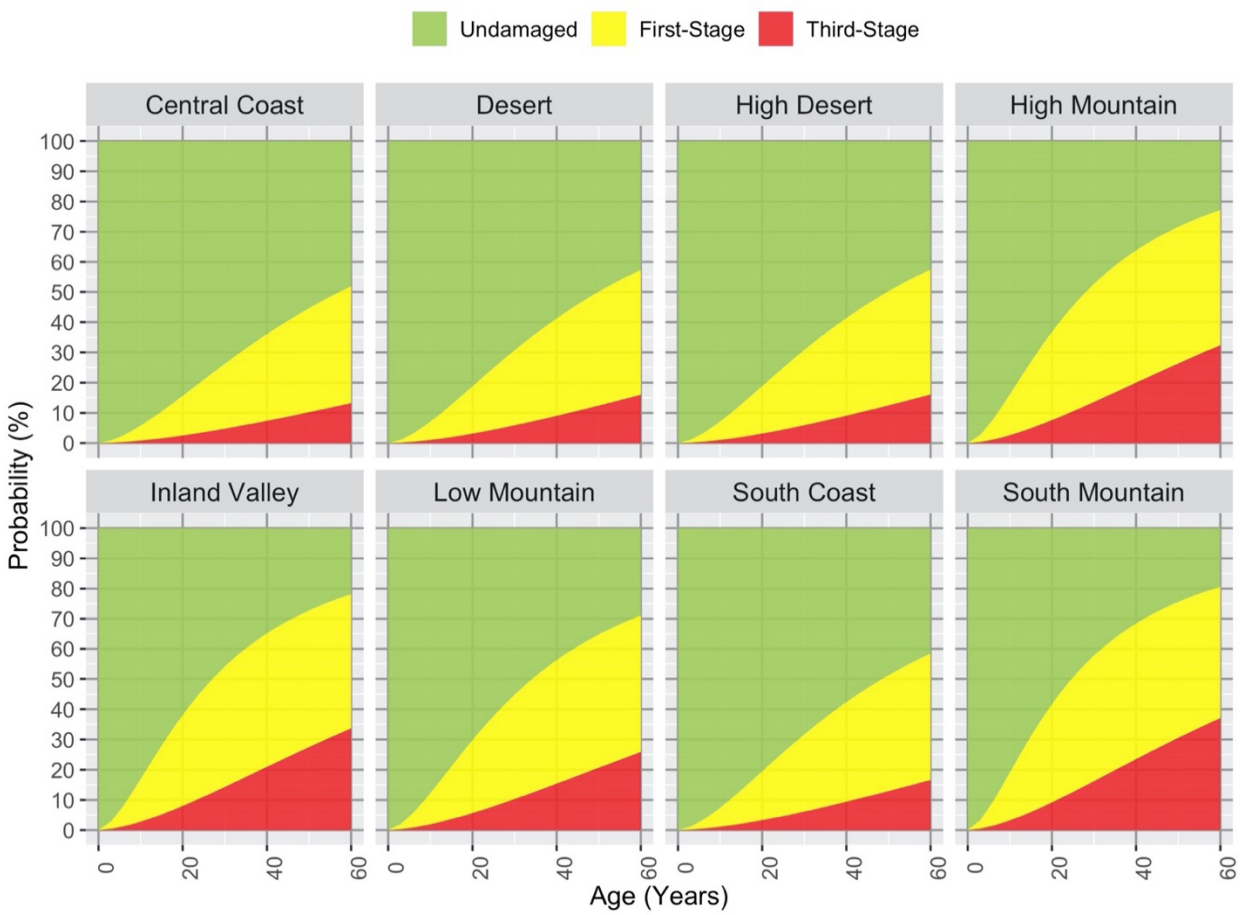

Figure 5.5: Mixed-effects cracking performance model predictions for different climate regions

Another informative output from the model, besides the coefficients, is the between-project variability (BPV) parameter, which has a standard deviation of 1.15. BPV is defined as the random effects in the CLMM model. In order to understand the concept of BPV and how it is accounted for in the CLMM, Figure 5.6 includes actual performance data and corresponding model predictions for three projects in a cell of data in the PaveM pavement management system (PMS) database. A cell of data is a set of performance data that could be collected from different projects but that have the same values for all design variables (pavement structure, traffic, and climate). The cell of data presented in Figure 5.6 corresponds to the Desert climate zone, CTB, FLX shoulder, long slab pattern 12,13,18,19 ft, 0.75-foot PCC slab thickness, and AADTT per lane of 1,000. The Y-axis represents the total cracking (first- plus third-stage cracking) percentage and the X-axis represents the time under service (age) of the JPCP. The faded gray data points are the actual raw performance data. The data points in color show the results after data aggregation.

The performance data for this cell have been collected from three different projects, and all data points corresponding to a specific project are distinguished with a specific color. Although all these projects have the same pavement structure, traffic, and climate, they have shown different cracking performance. This difference in performance is due to other sources of variability that are unavailable (unknown to designer) such as material properties (i.e., PCC compressive strength and CTE), model limitations, and error in input parameters. The dashed line is the model prediction (expected/average) without considering BPV, and the colored lines correspond to model predictions for each project (sharing the same color as its data points) considering BPV. Therefore, it is expected that after removing the BPV parameter from each project, the colored lines lie on the dashed line. In the example shown in Figure 5.6, the individual project lines are all above the cell model average. In other cells the project lines may be above or below the cell model average, and across all cells and ages the cell model average should match the median performance of the entire database. This is a very important concept that will be used in the next chapter in order to calibrate the Pavement ME transverse cracking model.

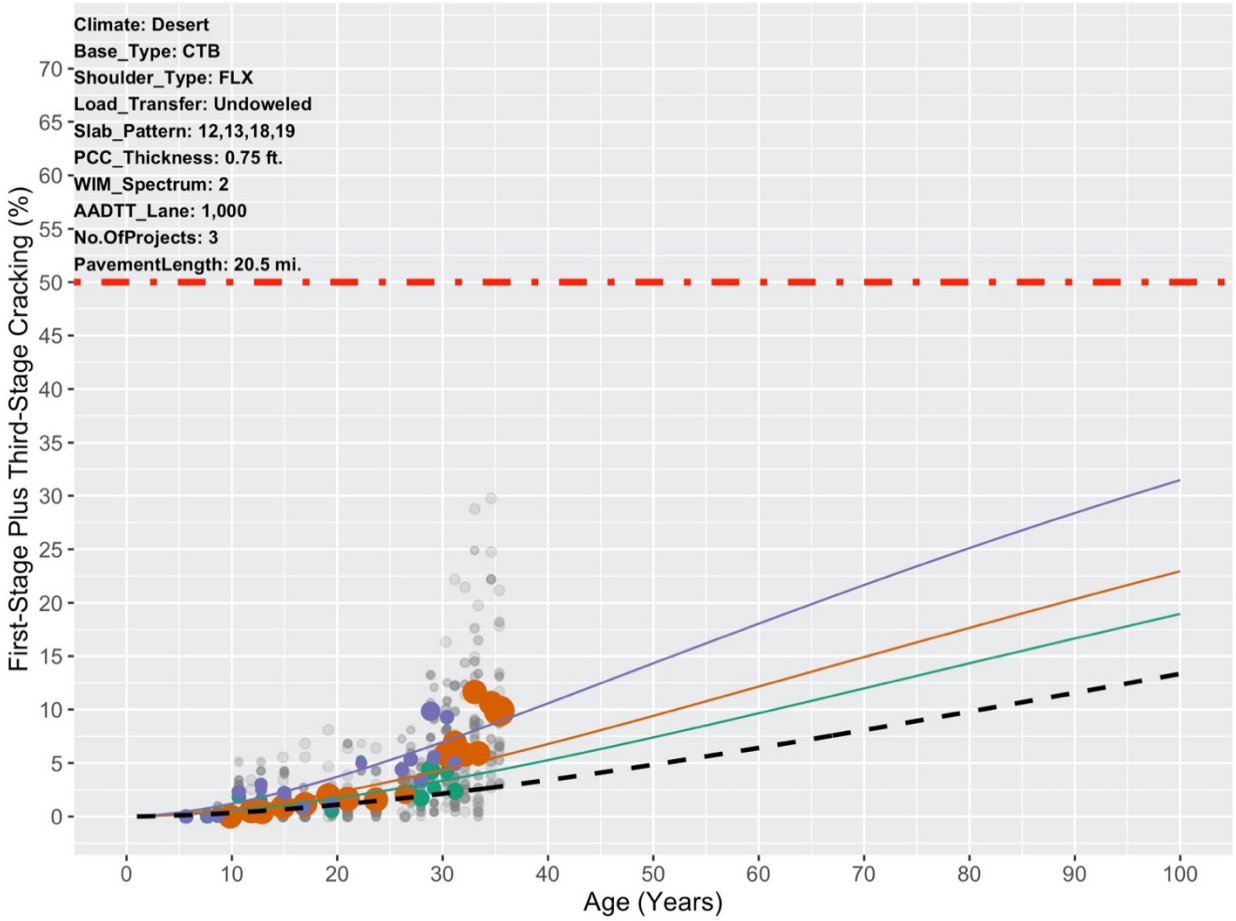

Figure 5.6: Mixed-effects cracking performance model predictions for a cell of data

5.2.3. First-Stage to Transverse Cracking Model

As detailed above, Caltrans has historically collected JPCP cracking data in terms of first-stage and third-stage cracking. However, the Pavement ME transverse cracking model predicts only the percentage of transverse cracking in JPCP. Since there are only a few years of first-stage cracking data in the PaveM database that separate transverse and longitudinal cracking, it was decided to develop a model that can predict the portion of first-stage cracking that is transverse cracking. In this study, it is assumed that 100 percent of the slabs with third-stage cracking have at least one transverse crack. This assumption together with the model allow the use of the PaveM performance database for Pavement ME calibration.

APCS 2011–2012 is the only survey that currently has per-slab data in the PaveM database. This database contains information on pavement structure, traffic, climate, and slab condition (undamaged, transversally cracked, longitudinally cracked, or X-cracked, defined as cracks that did not meet the definitions of transverse, longitudinal, or corner cracks) needing separation to identify transverse cracking (corner cracking was recorded separately). These data have been used to develop a model that can predict the portion of first-stage cracking that is transverse cracking, which was then applied to all of the APCS and PCS data Caltrans has collected since 1978 to create a transverse cracking database for Pavement ME calibration.

The data were first structured so that each slab is a single sample. The dependent variable (outcome) is a binary variable stating whether or not the slab is cracked transversely. The goal was to develop a model with the highest accuracy possible. Many different models—from those that are highly interpretable but low in accuracy (such as a logistic regression model) to machine-learning black-box models with high accuracy and low interpretability (such as random forest, gradient boosting, and neural network)—were developed. Among all these models, the gradient boosting model had the best performance, more reasonable predictions, and least time for fitting. Performance was evaluated by the percentage of transverse cracked slabs that were predicted correctly (recall) and the overall accuracy. Eighty percent of the data was randomly chosen to develop the model, and the model predictions were evaluated on the remaining 20 percent (unseen to the model) of the data. Recall is the ratio of the total number of transverse cracked slabs predicted by the model to the total number of transverse cracked slabs available in the data, and overall accuracy is the ratio of total number of correct model predictions to total number of instances.

The idea of boosting comes from the question of whether a weak learner can be modified to become better. A *weak learner* is defined as one whose performance is at least slightly better than random chance.

Boosting is the idea of filtering observations, leaving those observations that the weak learner can manage and focusing on developing new weak learners to manage the remaining difficult observations. The gradient boosting model involves three elements:

1. Loss function: the loss function should be optimized. The loss function depends on the type of problem being solved. For regression problems the squared error is used, and for classification problems the log loss function is used. In this model the log loss function was used, as it is a binary classification problem.
2. Weak learner: weak learners are mathematically (parametric or non-parametric) simple models that make predictions. Decision trees are used as the weak learner in gradient boosting.
3. Additive model: this model is used to add up the weak learners to minimize the loss function. Trees are added one at a time, and existing trees in the model are not changed. The output for each new tree is then added to the output of the existing sequence of trees in an effort to correct or improve the final output of the model. A fixed number of trees are added, or training stops once loss reaches an acceptable level or no longer improves on an external validation dataset.

A gradient boosting model was developed with the following predictors and parameters:

$$condition \sim f(PCC\_thickness, PCCSlab\_length, shoulder\_type, base\_type, climate, doweled, WIM) \quad (5.3)$$

- Max depth: 31
- Number of leaves: 137
- Number of trees: 4,000
- Learning rate: 0.005

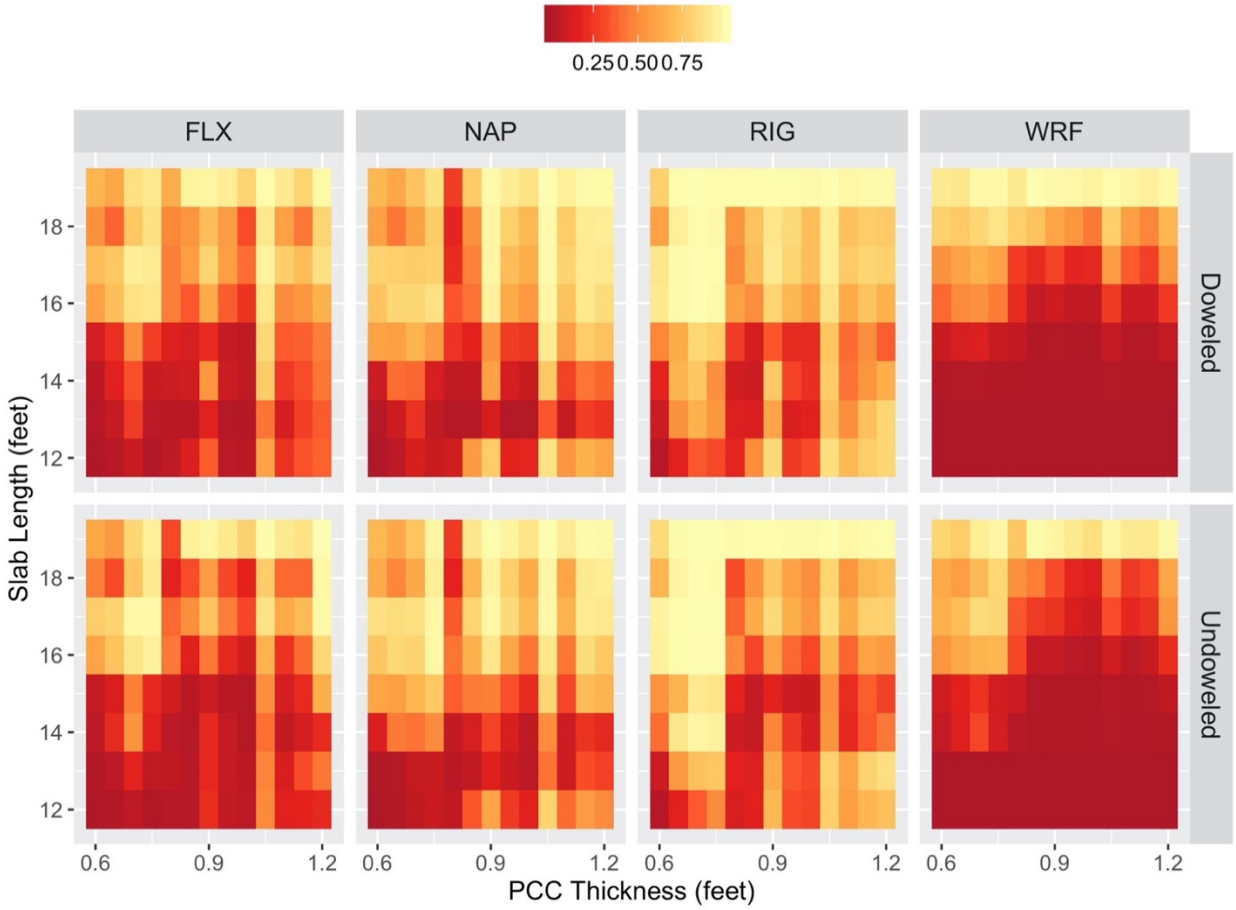

Figure 5.7: First-stage cracking to transverse cracking model predictions for different shoulder types

This model has a recall of 87.5 percent, which means that 87.5 percent of slabs with transverse cracking were identified correctly. The precision is 81.8 percent, which means out of all transverse cracking predictions done by the model, 81.8 percent were correct. Figure 5.7 shows model predictions for different pavement variables. These plots correspond to pavements in the Inland Valley climate zone, with HMA base, and under WIM Spectra 1. Each panel in the graph corresponds to a shoulder type with either doweled or undoweled load transfer. The Y axis represents the PCC slab length in feet, the X-axis represents the PCC slab thickness in feet, and the color shows the transverse cracking percentage (a lighter color indicates more transverse cracking, and a darker color indicates more longitudinal cracking. This graph shows that the model adequately predicts greater percentages of transverse cracking as the slab length increases. It also shows that the model predicts less transverse cracking for shorter slabs with widened concrete shoulder, which is in accordance to what was discussed in Section 4.2.2.4. It is also clear that for widened shoulders, the doweled pavement shows more longitudinal cracking than the

undoweled pavement, which verifies a study done on the development of a longitudinal cracking fatigue damage model for JPCP (Lederle, 2014).

Figure 5.8 shows model predictions for doweled pavements, with CTB, FLX shoulder, and WIM Spectra 1. Each panel in the graph corresponds to a different climate region. The model predicts that the Desert climate region has more transverse cracking, whereas the South Mountain region has more longitudinal cracking.

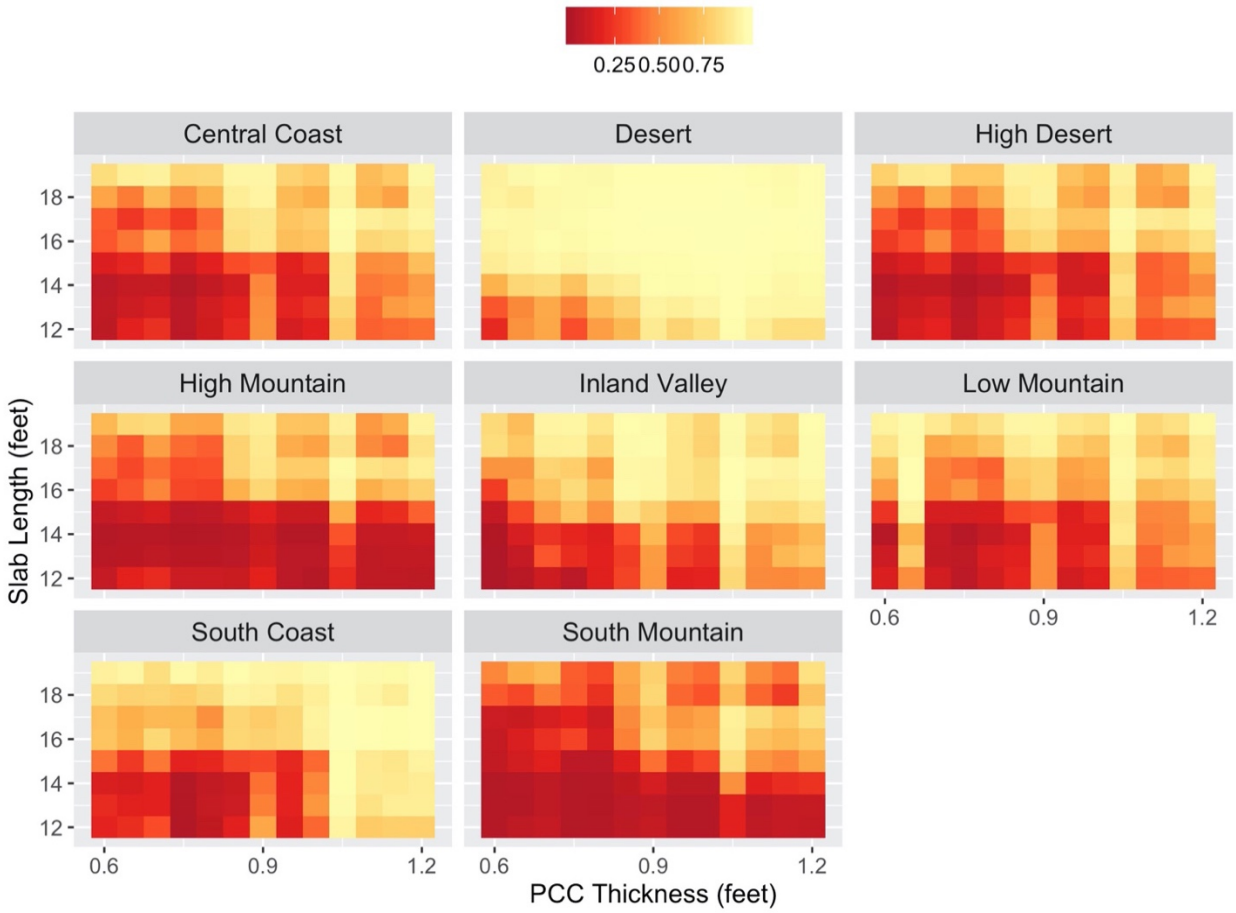

Figure 5.8: First-stage cracking to transverse cracking model predictions for different climate regions

This model separates the first-stage cracking into an estimate of transverse cracking data. Separating the first-stage cracking is done by multiplying the outcome of this model by the percentage of first-stage cracking, which results in the best estimate of the amount of transverse cracking in the JPCP. However, this amount represents the start of transverse cracking and should be added to third-stage cracking in order to obtain the total amount of transverse cracking over the full history, because third-stage cracking has at least one transverse crack. Finally, the total amount of transverse cracking is the performance

measure that will be used for Pavement ME calibration. The next chapter discusses the calibration process in detail.

5.3. Pavement ME Calibration

Pavement ME software uses three distress models for jointed plain concrete pavements (JPCP) analysis and design under traffic and environmental loads. These three distress models are transverse cracking, transverse joint faulting, and International Roughness Index (IRI). The transverse cracking and transverse joint faulting models are stand-alone models that have been developed based on the principles of mechanics and statistical models and are therefore called mechanistic-empirical models. The IRI model was developed by fitting a statistical model to the predictions of the transverse cracking and transverse joint faulting models.

The goal of this section is to calibrate the Pavement ME transverse cracking model with the performance data available in the PaveM pavement management system (PMS) database. Calibrating this model consists of determining a set of model coefficients to optimize (minimize) the model prediction errors. The performance data in the PaveM database measured faulting as percentage faulted transverse joint within a pavement section, which, when combined with the previously discussed varying section lengths and locations in the survey, resulted in data unsuitable for modeling. Caltrans built JPCP without dowels, except for a few test sections, from the late 1940s until 1998 and experienced faulting and poor ride quality on much of its concrete network until dowels were introduced.

A study in 1967, after Caltrans had switched to plant-mixed CTB with greater cement content to try and reduce faulting, showed that faulting still typically occurred within 4 million equivalent single axle loads (ESALs) of traffic after construction (Macleod and Monismith, 1979). (It is interesting to note that the same study showed a switch on test sections on US 101 from 97 percent transverse cracking and 3 percent longitudinal cracking with the less stiff pre-1967 CTB to 40 percent transverse cracking and 60 percent longitudinal cracking with the stiffer CTB, an early indication of the effects of changing from CTB to LCB seen in the previous chapter of this report). A survey of JPCP with high traffic levels in 1999 indicated that faulting was prevalent on the majority of the pavement surveyed (Harvey et al., 2000).

Caltrans mandating the use of dowels in JPCP construction since 1998 has had a significant impact on mitigating the faulting distress in California. As a result, the roughness caused by faulting has ceased to be much of an issue on JPCP; the low IRI on doweled JPCP appears to be primarily controlled by construction smoothness (NCSHRP, 2003).

The calibration of the Pavement ME faulting model in 2007 (Kannekanti and Harvey, 2007) on undoweled JPCP, using faulting measurements made by the University of California Pavement Research Center (UCPRC) with a high-speed profiler moving at slow speeds, showed that the national faulting model for undoweled pavement did a good job of predicting performance on California pavements. This is likely due in part to the fact that a large part of the calibration of that model was done on California sections, which were used because most other states had switched to using dowels much earlier than California. For the following reasons only the transverse cracking model was calibrated in this study:

- There were not enough sections with good faulting history data (built prior to 1998), and there are generally no available faulting data on JPCP built since 1998, according to the Automated Pavement Condition Survey (APCS) data in the PaveM database.
- Caltrans now constructs doweled JPCP exclusively, and faulting is not a major problem for doweled JPCP.
- The faulting model in the Mechanistic-Empirical Pavement Design Guide (MEPDG) matched well with Caltrans data in 2006 for undoweled concrete. The model coefficients have changed since a calibration study in 2007 (Kannekanti and Harvey, 2007); however, the current model predictions have changed very slightly since the last calibration.
- IRI on doweled concrete pavement is primarily a function of the IRI achieved in construction.

5.3.1. Traditional Pavement ME Calibration Process

The goal of transverse cracking model calibration is to find a set of model coefficients that minimizes the model prediction error. Traditionally, ME models, including the Pavement ME models, have been calibrated with a small number of JPCP sections (hundreds at the national level, tens at the state level) for which all the design and non-design (material properties) variables were known or collected. UCPRC calibrated the MEPDG in 2007 with 52 rigid and 43 crack, seat, and overlay (CSOL) sections (Kannekanti and Harvey, 2007). The national calibration of the MEPDG used data from fewer than 200 Long-Term Pavement Performance (LTPP) sections, with a total length of about 20 miles (NCHRP, 2003).

In the context of this report, design variables are those—such as portland cement concrete (PCC) slab thickness, PCC slab length, base type, shoulder type, traffic, and climate—that can be determined by the pavement designer prior to construction. The non-design variables are those—such as PCC compressive

strength, PCC modulus of rupture, and PCC coefficient of thermal expansion—whose exact values are unknown to the designer at the time of design. Design and non-design variables were discussed in the Pavement ME Sensitivity Analysis (NCHRP, 2003). According to traditional Pavement ME calibration, data for all the design and non-design variables must be collected, either by extracting them from as-builts or coring specimens, by running laboratory tests, or by conducting field tests. Once these data are obtained, in the traditional Pavement ME calibration, the following steps are taken to calibrate the distress models (AASHTO, 2010):

1. Select hierarchical input level for each input parameter
2. Develop local experimental plan and sampling template
3. Estimate sample size for specific distress prediction models
4. Select roadway segments
5. Extract and evaluate distress and project data
6. Conduct field and forensic investigations
7. Assess local bias of global calibration factors
8. Eliminate local bias of distress prediction models
9. Assess the standard error of estimate (SEE)
10. Reduce the SEE
11. Interpret results

For a more detailed description of each step, refer to Guide for the Local Calibration of the Mechanistic-Empirical Pavement Design Guide (AASHTO, 2010).

Pavement management systems have much more performance data than has been used for traditional mechanistic-empirical model calibration. The Caltrans PaveM database used for the calibration of Pavement ME transverse cracking model presented in this report consists of 30,155 pavement sections with a combined length of approximately 4,380 lane-miles and with 265,033 performance observations. This is 150 times more pavement sections and more than 200 times more lane-miles than those used for the national calibration.

Traditional Pavement ME calibration has limitations that do not allow the use of the kind of “big performance data” that was used in PaveM for the model calibration presented in this report. Specifically, the traditional calibration does not consider the variabilities involved in pavement performance and therefore may predict reasonable average performance while underestimating variability. (The variabilities involved in pavement performance will be explained in the following sections.) Another

limitation of the traditional calibration procedure is the requirement to determine all inputs, including non design variables. This means field sampling and material testing are needed to determine inputs, which limits the number of roadway segments that can be included in the calibration and therefore may lead to underestimation of model error and input error. The residual errors in past calibration efforts can be attributed to two causes: the model adopted has a significant amount of error and/or the inputs to the model have errors. To overcome these shortcomings, in this project, a new approach was developed to calibrate Pavement ME. The new approach uses the big performance data from the Caltrans PaveM while accounting for the different sources of pavement performance variability.

In this section, the step-by-step procedure for Pavement ME calibration is discussed in detail, as well as the calibrated transverse cracking model coefficients obtained from the procedure.

5.3.2. Variability Affecting Pavement Performance

Different sources of variability in pavements cause differences in their performance behaviors, such as their rates of section deterioration and crack progression. The sources of these performance variabilities may be due to variabilities in known design variables, to external conditions such as traffic loads and climate, or to unknown variables such as material properties. A good calibration process will take all these variabilities into account to render a more reliable calibration. However, before the new Pavement ME calibration procedure is presented, it is necessary to have a good understanding of the different components of the variabilities involved in pavement performance.

Like any other structure, pavements are not uniform. Theoretically, a pavement's performance is determined by external factors such as climate and traffic and by internal factors such as pavement structure and material properties. Each of these factors can be characterized as a random variable, and together they form a random vector. For ease of reference, the random vector can be designated as X, and it can be called pavement variable inputs because it is essentially a collection of the selected inputs believed to have significant effects on pavement performance.

The performance of a pavement regarding certain failure mechanisms can be expressed as the time history of the percentage of pavement failed by the mechanism under consideration. Consider, for example, a JPCP pavement condition survey that monitors percent slabs with transverse cracking. In the following equation, Y denotes transverse cracking—which is a function of pavement age (t) and input variable X—and can be expressed mathematically as:

$$Y = Y(t) = P\left(t_f \leq t|X\right) = Y(t;X) \tag{5.4}$$

where P is the probability of failure and t_f is the time to failure (when the slab is cracked transversely). $Y(t;X)$ is a function of time t with parameter X and is essentially the cumulative distribution function (CDF) of failure time t_f for a given performance input X. As shown in Equation 5.4, pavement performance is a time history affected by the input vector X. The variabilities in performance come from the variabilities in X.

For pavements in a large network (as in a PMS database), performance is understandably different. This is because the mean values of X are different between projects. This could be due to differences in PCC slab thickness, PCC slab length, PCC compressive strength, PCC coefficient of thermal expansion (CTE), traffic load, etc. The variability in pavement performance caused by a change in the mean value of X is referred to as *between-project variability* (BPV). The unexplained part of this variability, i.e., the part that cannot be explained by the model's inputs, is introduced as random effects in the mixed-effects cracking performance model used for this calibration.

Alternatively, consider a specific project in which X is nominally the same throughout. Of course, "nominally the same" does not mean "exactly the same." Statistically, two variables are nominally the same when they have the same distribution. The following are some examples of variables that are nominally the same:

- Concrete materials are nominally the same if they are produced by the same plant following the same mix design, use the same sources for raw materials, and are placed by the same contractor under the same conditions and consistently following the same practices. However, concrete properties such as modulus of rupture may vary in different locations of a single project, and this variation may cause different rates of deterioration—and hence different cracking performance—in different slabs within the project.
- PCC slab thicknesses are nominally the same in the overall project based on the design thickness. However, not all slabs are constructed with the exact same thickness. Their thickness may slightly vary over the project, which will eventually result in different cracking rates.
- Climate conditions are nominally the same if they are classified into the same climate zone, but temperature, humidity, and other climate conditions may differ along one project, and this variation may cause different cracking performance along the project.

Given the random nature of X, pavement distresses are expected to develop at different rates within one project even if X is nominally the same. This type of variability in pavement performance is referred to as *within-project variability* (WPV). In other words, a project can be divided into many segments, with each segment representing a random sample of X, and the values of X in the segments are likely to be different from each other. This results in different pavement performance.

There is a third type of variability that is caused by the change in the variability (standard deviation) of X. There are many scenarios in which the variability of X can change. However, changes in variability of X are typically accompanied by changes in its mean value as well. One scenario that can lead to minimal change in the mean value of X while allowing the variability of X to change is a change of the contractor. Different contractors have different quality-control tolerances and hence different variability in X. For example, Contractor A may have rigorous quality control and produces a PCC whose flexural strength after 28 days has a mean value of 643 psi and a standard deviation of 25 psi, while Contractor B may not follow such rigorous quality control and produces a PCC with the same mean flexural strength (643 psi) but with much larger standard deviation, e.g., 60 psi. These two contractors will have different *between-contractor variability* (BCV) even if they are using the same materials at the same project location. The same contractor's results under different conditions may change over time and from project to project as well, which is also captured by between contractor variability, since contractors were not tracked in this study.

5.3.3. Effects of Different Variabilities on Pavement ME Transverse Cracking Transfer Function

To illustrate the effects of different variabilities on the Pavement ME transverse cracking transfer function, a simplified example of a project in which all the variables that have an effect on pavement performance (such as pavement structure, material properties, traffic loads, and climate) is considered. The only parameters that may change over the entire project are PCC modulus of rupture (MR) and the stress applied on the pavement under loading (σ). Further, to make the calculation simple, it is assumed that there is only bottom-up cracking and no top-down cracking. These simplifications are referred to as the simple project assumption.

It is assumed that both MR and σ are random variables that follow normal distributions (the exact type of distribution is irrelevant since it does not change the results). Together, MR and σ form the input random vector X discussed in the previous section.

According to the Pavement ME documentation, concrete fatigue life N_f is determined by the modulus of rupture MR and the applied tensile stress σ through the following equation:

$$log_{10}(N_f) = C_1 \cdot \left(\frac{MR}{\sigma}\right)^{C_2} \tag{5.5}$$

where $C_1 = 2.0$ and $C_2 = 1.22$. The applied stress depends on various factors, such as traffic and structure. The fatigue damage DI_f, accumulated following Miner's Rule, is:

$$DI_f = \Sigma_{\text{ijklmno}} \frac{n_{ijklmno}}{N_{ijklmno}} \tag{5.6}$$

where the subscripts $ijklmno$ indicate the permutations of various factors affecting the applied stress, and $n_{ijklmno}$ is the number of traffic load applications corresponding to the stress level. Once the fatigue damage is known, the percent of slabs cracked, denoted as CRK, can be calculated using the following equation:

$$CRK = \frac{100}{1 + C_4(DI_f)^{C_5}} \tag{5.7}$$

C_4 and C_5 are the model coefficients that should be calibrated separately with each region's separate condition. The nationally calibrated values for these coefficients are $C_4 = 0.52$ and $C_5 = -2.17$. These values are used in this section to describe the effects of different variabilities on transverse cracking model predictions. Figure 5.9 illustrates the correlation between accumulated damage and the number of slabs cracked using Equation 5.7. This equation is called the *transfer function*. It converts mechanistic damage to pavement distress through an empirical correlation.

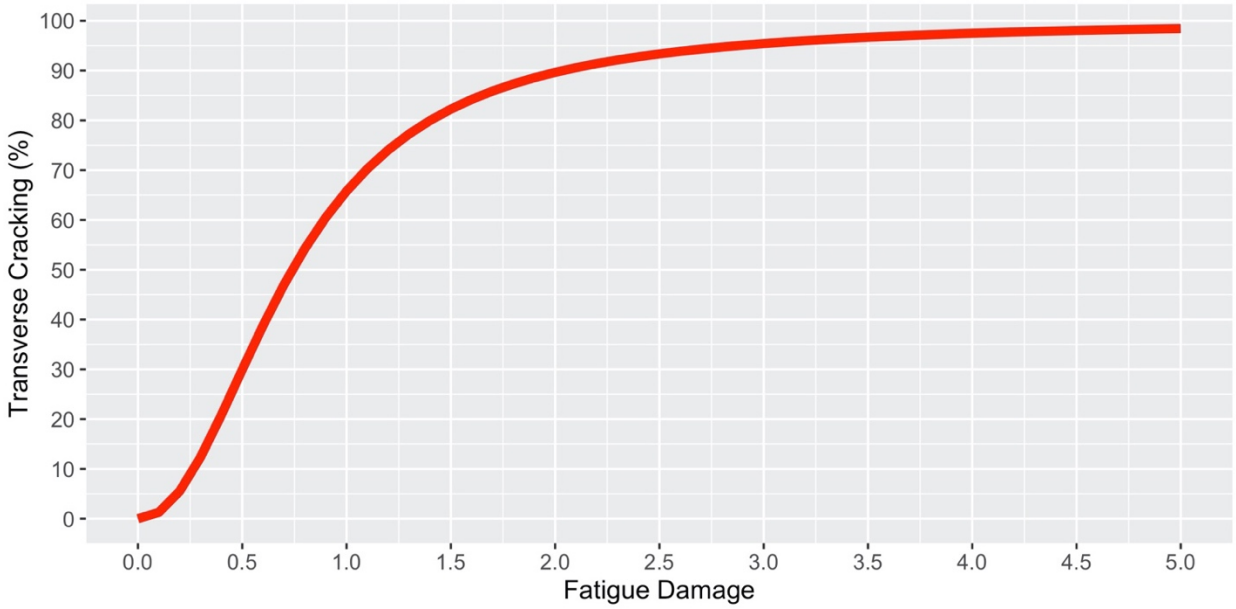

Figure 5.9: Pavement ME transverse cracking transfer function

It is assumed that a project can be divided into contiguous segments in which the material properties (MR in this case) and loading (σ in this case) are uniform and constant along each individual segment. For simplicity, it is also assumed that the segments are equal in length. This scenario is referred to as the *uniform segmentation assumption*.

Within the uniform segmentation assumption, the values of MR and σ for any specific segment within a simple project are random samples of the corresponding distributions. The percent of slabs cracked in a particular segment can be calculated with Equation 5.5 to Equation 5.7. The percent of slabs cracked over the whole project is then the average of the values over all segments:

$$CRK_{project}(t) = \frac{1}{m}\Sigma_{i=1}^{m} CRK_i(t) = \frac{1}{m}\Sigma_{i=1}^{m} CRK(t; MR_i, \sigma_i) \quad (5.8)$$

where m is the number of equal-size segments within the simple project, MR_i and σ_i are the values of MR and σ respectively for segment i, and t is the time since the project opened to traffic. The value $CRK_{project}\ (t)$ represents the percent of slabs expected to have cracked at any given time t. In other words, Equation 5.8 calculates the probability that any slab will crack by time t. This suggests that $CRK_{project}\ (t)$ is the CDF of slab cracking life.

Similarly, the transfer function defined in Equation 5.7 represents the percent of slabs expected to have cracked for any given level of fatigue damage DI_f. Since DI_f is a monotonic function of time, the transfer function is also a CDF of slab cracking life, albeit in the damage space. In other words, the link from damage to cracking is not deterministic. In fact, cracking can occur at any damage level, although more damage corresponds to a greater probability of cracking. This is why not all slabs within a segment crack at the same time even though their calculated damage is the same.

Following the simple project assumption and the uniform segmentation assumption, a project is made up of many uniform segments. Each segment is uniform in terms of the calculated fatigue damage DI_f if the same properties are assumed for all slabs in the segment. Therefore, each segment shows a different rate of cracking due to the variability in loading and material properties. These concepts and definitions will be used in the following sections of this chapter to show the effects of different variabilities on predicted transverse cracking and to explain how the different sources of variability can be accounted for in the calibration process. They will also be used in the development of the Caltrans JPCP design catalog and in the use of Pavement ME to design a pavement.

5.3.3.1. Monte Carlo Simulation Procedure

Following the simplified example introduced in the previous section of this chapter, a Monte Carlo simulation is used to illustrate the different types of variability involved in pavements. The steps below are followed for conducting Monte Carlo simulations:

1. Determine the simulation duration in terms of maximum number of traffic loadings, N_{max}.
2. Select a set of number of traffic applications and form an array $n = \{n_1, n_2, \dots, n_m\}$, where $n_i \in [0, N_{max}]$. This array is referred to as the traffic history array. Each value in the array represents a point in time.
3. Determine the number of segments n_{sg} for the simple project.
4. Generate n_{sg} random samples for MR and σ independently and assign one set of values for each segment.
5. For each segment in the project
    a. Calculate the concrete fatigue life N_f using the MR and σ values corresponding to the current segment.
    b. Calculate the damage history corresponding to the traffic history array n, using Equation 5.6
    c. Convert the damage history into percent cracking history using Equation 5.7

6. For every value in the traffic history array n, calculate the following statistics across all segments:
    a. Average damage
    b. Median damage
    c. Average of percent slab cracked
    d. Median of percent slab cracked

5.3.3.2. Within-Project Variability (WPV)

To illustrate the meaning of within-project variability, continuing with the simplified example presented above, a simple project is assumed with 1,000 segments of pavement. For the simplified pavement systems described in the previous sections, WPV comes from the random nature of both MR and σ. To illustrate WPV, it is assumed that MR in a project follows normal distribution with a mean value of $5.5\ MPa$ and a standard deviation of $0.5\ MPa$, i.e., $MR \sim N(5.5,0.5)$, where $N(\mu, \epsilon)$ indicates a random variable following the normal distribution with mean μ and standard deviation ϵ. Similarly, it is assumed that the stress applied in a project follows a normal distribution with a mean value of 2.0 MPa and a standard deviation of $0.3\ MPa$, i.e., $\sigma \sim N(2.0,0.3)$.

Figure 5.10 shows the histories of accumulated damages for the 1,000 segments as well as the overall average. As expected, different small segments show different rates for damage accumulation depending on the ratio between MR and σ. Damage accumulates rapidly in some segments and slowly in others. Due to the simple project assumption of the same randomly sampled stress being repeated in a given segment, damage always accumulates at a constant rate for a given segment, which results in straight lines for damage time histories.

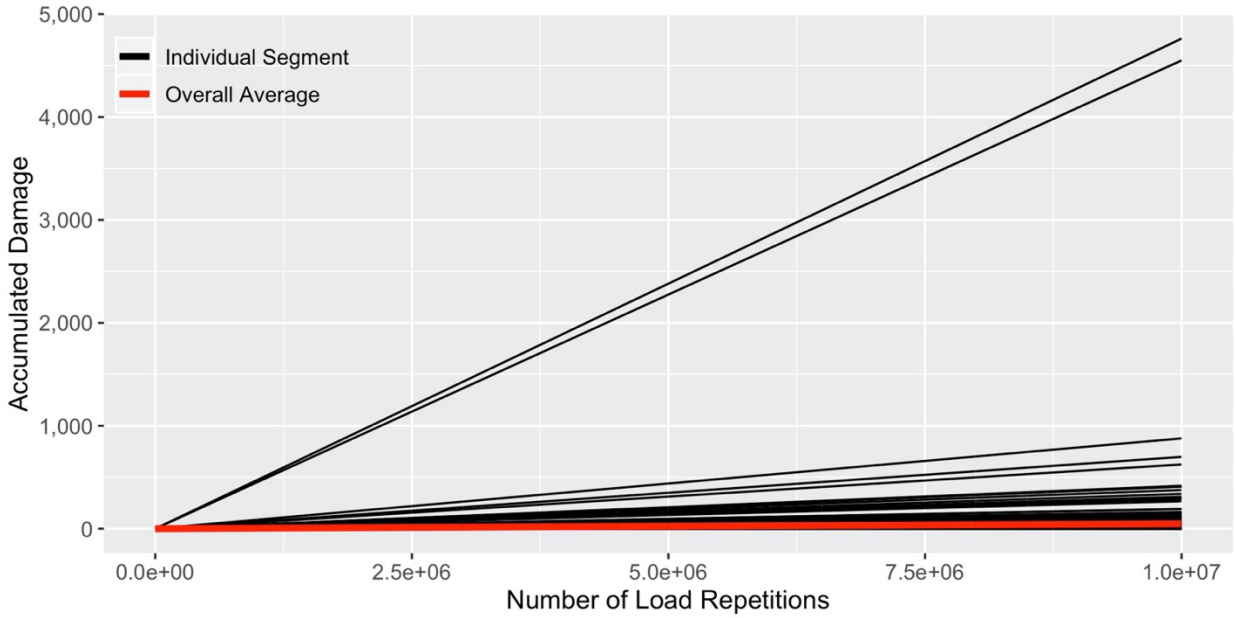

Figure 5.10: Accumulated damages versus number of load repetitions for 1,000 pavement segments

Figure 5.11 shows the percent transverse cracking histories for different segments within the simple project. Some segments reach 100 percent cracking very quickly while other segments last much longer. The large difference between different segments of the project illustrates the WPV. As discussed earlier, the percent cracking history for each individual segment is the CDF of cracking life for that particular segment.

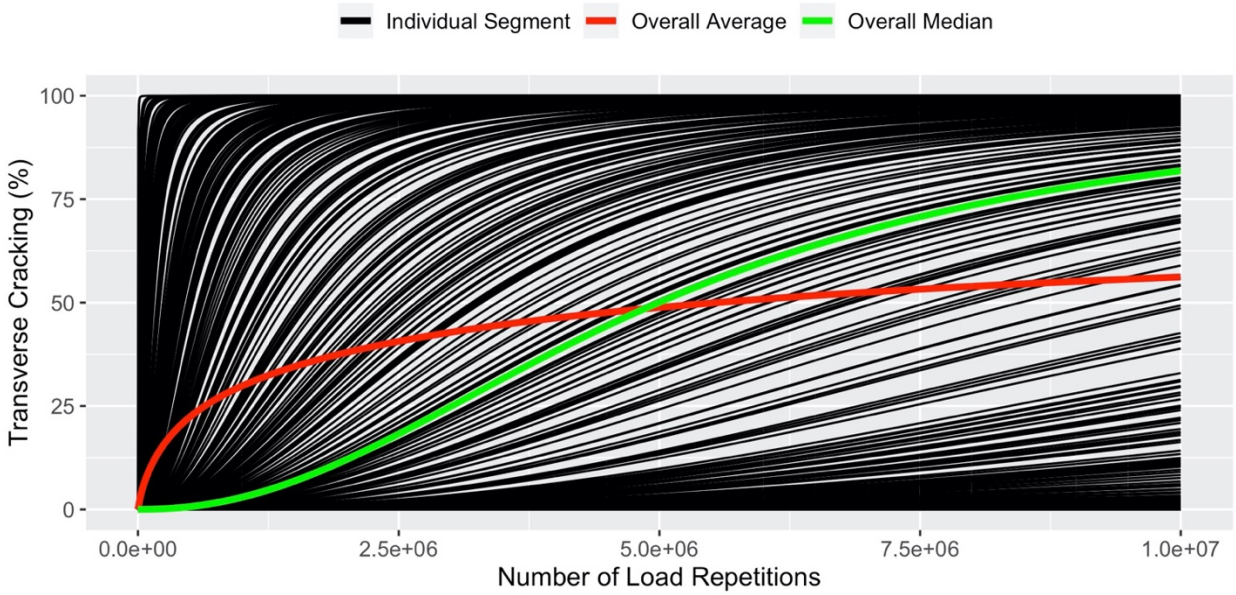

Figure 5.11: Transverse cracking (percent of slabs transverse cracked) versus number of load repetitions for 1,000 pavement segments

Figure 5.11, the history of overall average percent cracking is shown as a red curve. The overall average represents the aggregation over the 1,000 segments in the project as if pavement cracking data were collected from a series of pavement condition surveys. The overall average percent cracking history is the CDF of cracking life for any randomly selected segment within the project.

Figure 5.11 indicates that the shape of percent cracking history for individual segments is very different from the one for the overall project (i.e., the overall average). This is expected because the shape of the overall average depends on the amount of WPV while the shape for any individual segment depends only on the specific value of X assigned to the segment. This is a very important observation because it means that trends observed from individual uniform segments are not applicable to the relatively long and non-uniform project.

In Figure 5.11, the overall median cracking curve for all the pavement segments is shown as a green curve. The overall median cracking curve is determined by finding the median of percent cracking among all segments at any given time. Unlike the overall average, the overall median has the same shape as the individual segments. This is because the histories for individual segments have the same shape and do not cross each other. This observation is universally applicable because of some intrinsic properties of pavement systems. Namely, pavement performance is a monotonic function of different inputs. This property is referred to as the monotonic property.

In the case of the simple project under discussion here, the monotonic property refers to the fact that surface cracking is a monotonic function of both MR and σ. Specifically, surface cracking is a strictly decreasing function of MR and a strictly increasing function of σ. As a result, the cracking history that results from input of the median of MR and σ leads to the median of percent slabs cracking at any given time t (or, interchangeably, any number of traffic cycles applied n):

$$\widetilde{CRK}(t) = CRK\left(t; \widetilde{Mr}, \tilde{\sigma}\right) = \frac{100}{1 + C_4 \cdot \left[DI_f\left(t; \widetilde{Mr}, \tilde{\sigma}\right)\right]^{C_5}} \tag{5.9}$$

where $\widetilde{((.))}$ indicates taking the median value of a quantity. According to Equation 5.9, the overall median percent cracking history is determined by the median values of MR and σ, and therefore is essentially the CDF of cracking life for a segment with median input X and should have the same shape as the percent cracking history for each individual segment.

Equation 5.9 also suggests that the relation between overall median percent cracking $(\widetilde{CRK})(t)$ and overall median damage $\left(\widetilde{DI_f}\right)(t)$ (which is equal to $DI_f(t; \widetilde{(Mr)}, \tilde{\sigma})$ due to the monotonic property) follows the transfer function.

Figure 5.11 shows that overall average and overall median are typically different when a project is non-uniform. However, overall average will converge to the overall median as the variabilities in MR and σ both decrease to zero. Figure 5.11 also shows an important finding: the overall average and overall median reach 50 percent at exactly the same time. This is not a coincidence. To explain this further, first denote the point of intersection as P_{50}. Given that the overall average cracking history represents the CDF of cracking life, the X-coordinate of this point represents the median cracking life, which depends only on the median values of MR and σ due to the monotonic property. In other words, although changing the variability of MR and σ will change their shape, all overall average curves will have to go through point P_{50} as long as the mean values for MR and σ are the same.

5.3.3.3. Between-Contractor Variability (BCV)

To illustrate between-contractor variability, an example can be looked at where the mean values of MR and σ are fixed at 5.5 MPa and 2.0 MPa, respectively, indicating same material and same slab thickness, while their standard deviations are set to different values, indicating different contractor variability for material strength and slab thickness. Figure 5.12 shows the BCV caused by changing the standard deviation of MR from 0 to 0.4 MPa while keeping σ fixed at 2.0 MPa. Figure 5.13 shows the BCV caused by changing the standard deviation of σ from 0 to 0.01 MPa while keeping MR fixed at 5.5 MPa. Figure 5.14 shows the BCV caused by changing standard deviations for both MR and σ. In Figure 5.12 to Figure 5.14, the Y-axis shows the overall average of percent slabs with transverse cracking among all segments within a project.

Figure 5.12 to Figure 5.14 confirm that the time (or, interchangeably, the number of traffic cycles applied, n in this case) needed for 50 percent of a pavement to reach cracking failure remains the same no matter what the standard deviations are for MR and σ.

As shown in Figure 5.12 to Figure 5.14, a higher standard deviation causes the curves to rise faster initially, but these curves flatten more after 50 percent cracking, which means that there are more slabs that have either very short or very long cracking lives. In other words, higher standard deviations of MR

and σ cause slab cracking life to spread out more, which is expected. The range of this spread reflects the amount of BCV.

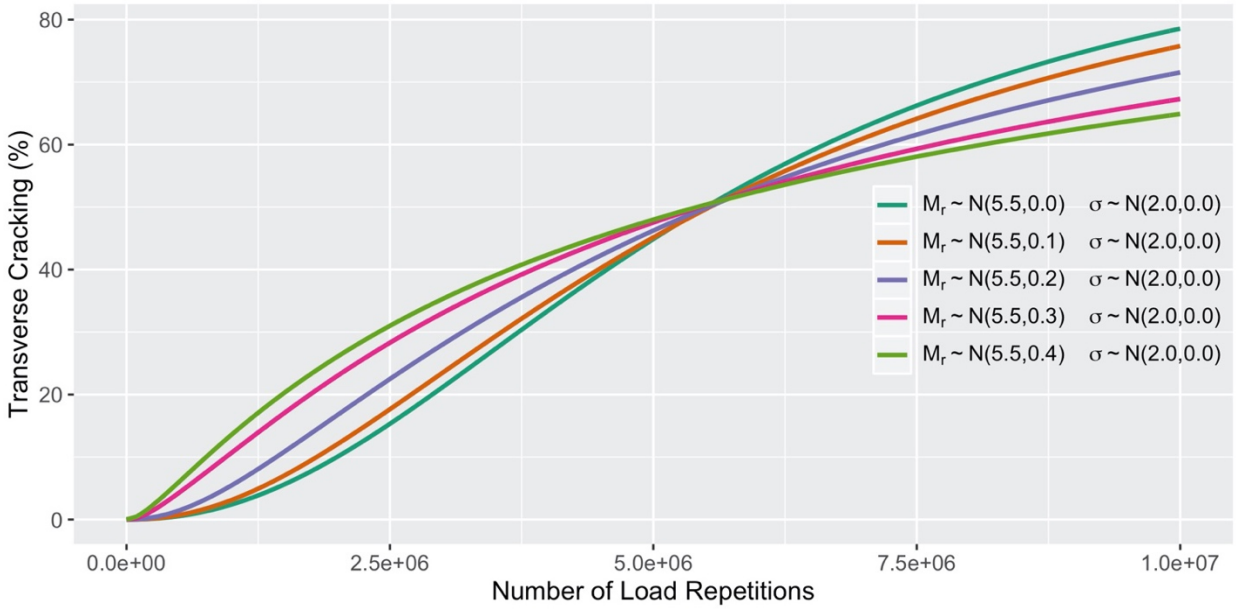

Figure 5.12: Transverse cracking histories for projects with different standard deviation in modulus of rupture

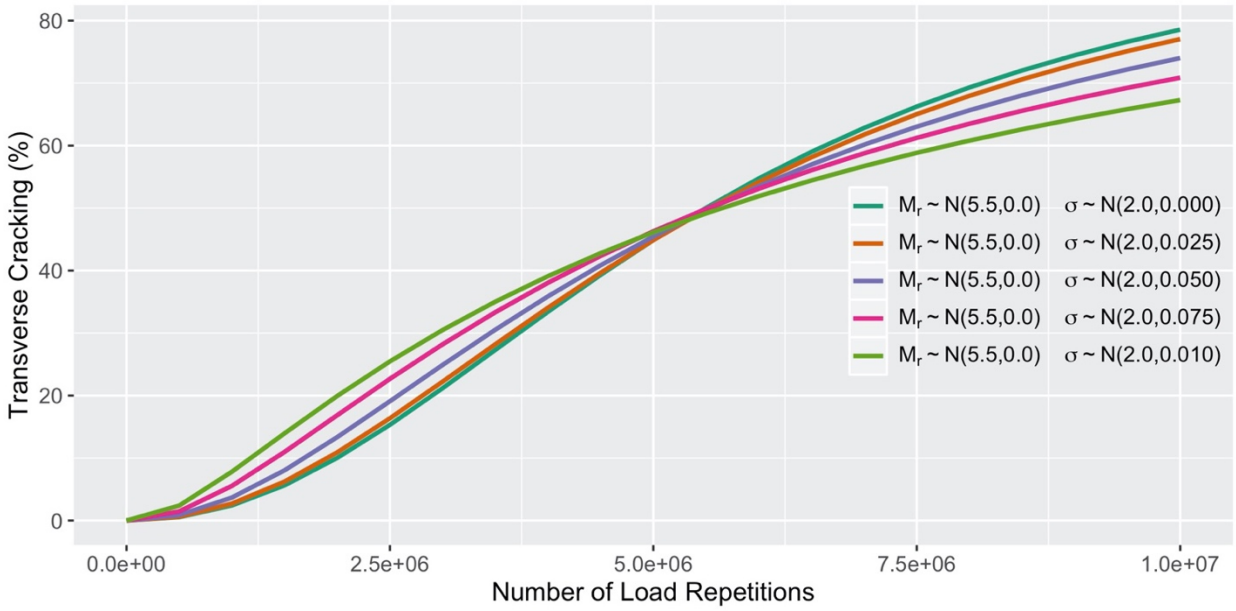

Figure 5.13: Transverse cracking histories for projects with different standard deviation in applied stress

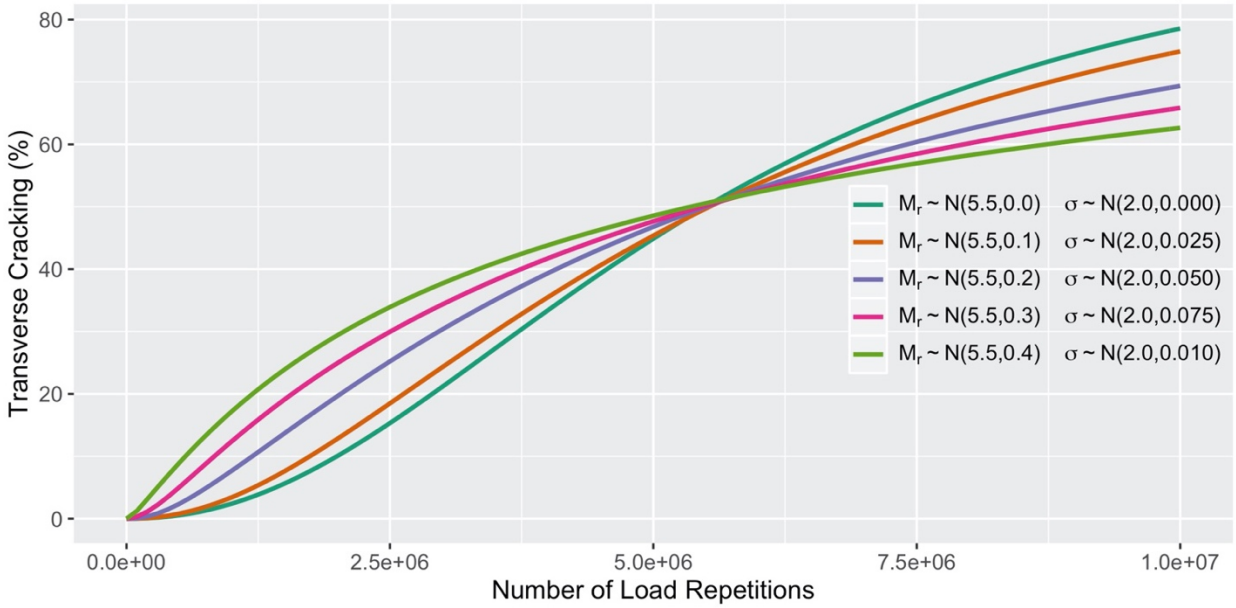

Figure 5.14: Transverse cracking histories for projects with different standard deviations in modulus of rupture and applied stress

5.3.3.4. Between-Project Variability (BPV)

To illustrate between-project variability, Monte Carlo simulations were conducted by varying the mean values for MR or σ while keeping their standard deviations at zero. Results are shown in Figure 5.15. In this figure, the Y-axis shows the overall average of percent slab cracking. Despite the lack of variability in MR and σ, all segments within a project perform the same, and as a result the overall median and overall average are the same.

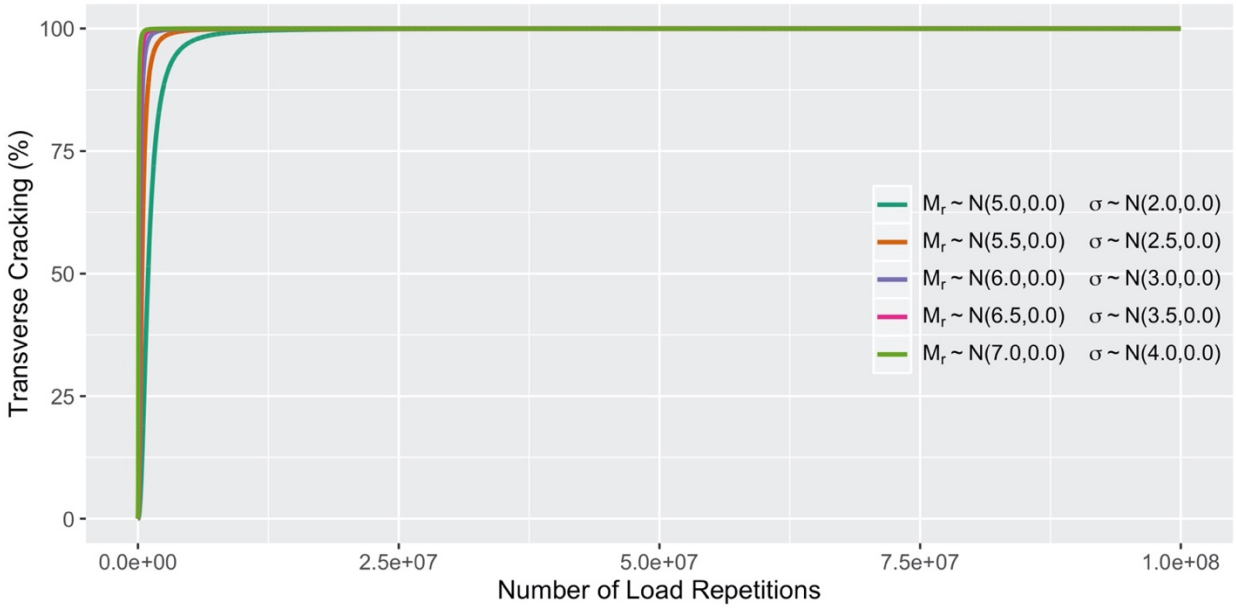

Figure 5.15: Transverse cracking histories for projects with different mean values and zero standard deviation in modulus of rupture and applied stress

Figure 5.15 shows the percent cracking histories for projects with different mean values for both MR and σ. Figure 5.16 shows the same graph but with the X-axis in log scale in order to make the plot more readable. As expected, cracks develop faster as the ratio $\frac{\sigma}{MR}$ increases.

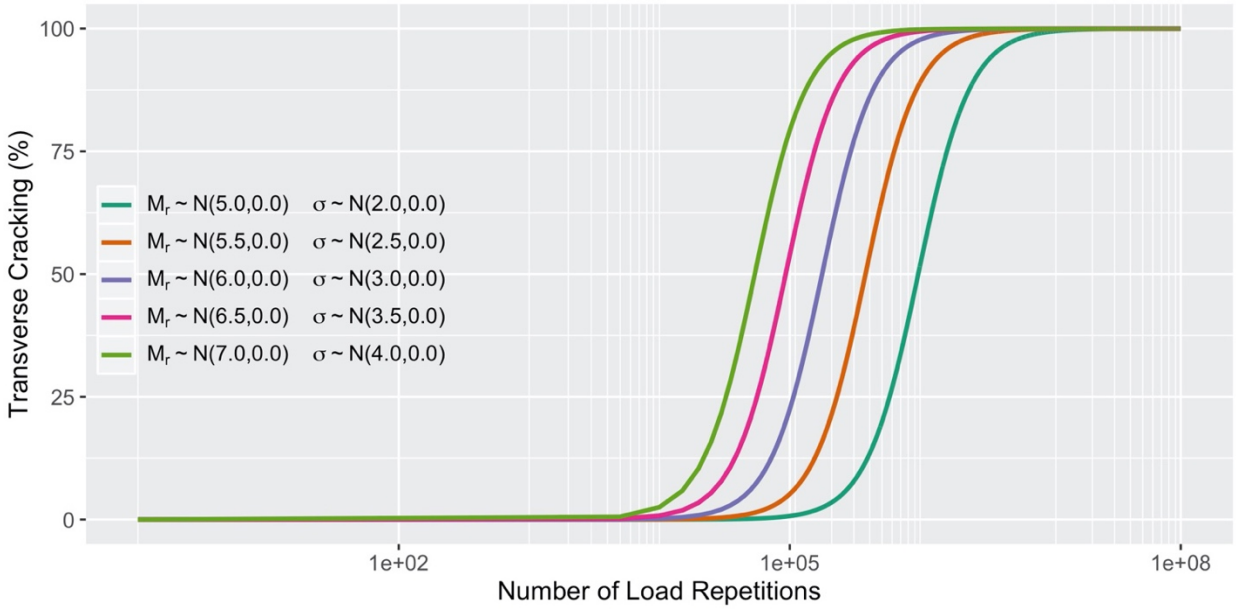

Figure 5.16: Transverse cracking histories for projects with different mean values in modulus of rupture and applied stress in a semi-log plot

Figure 5.16 shows that the shapes of percent cracking histories are the same with the X-axis in log scale, and the differences between them can be removed by applying a project-dependent scale factor on the time axis. This observation is not a coincidence and it is due to another fundamental property of pavement performance. Specifically, damage in a given pavement project follows the same pattern of damage versus time, regardless of the actual value of various factors affecting performance, but with the patterns shifted in time (the X-axis in Figure 5.16 when the mean values change). This is because the damage pattern is determined by traffic pattern (for traffic-induced damage), which is fixed for a given pavement project. Mathematically, this means:

$$DI_f(t; X_1) = DI_f(t; X_2) \cdot f(X_2, X_1) \tag{5.10}$$

where $DI_f(t; X)$ is the fatigue damage at time t for a given input X, and $f(X_2, X_1)$ is a function that depends only on inputs X_1 and X_2. The proof for this equation is shown in the following.

According to Equation 5.6:

$$DI_f(t; X_1) = \Sigma_{\text{ijklmno}} \frac{n_{ijklmno}(t)}{N_{ijklmno}(X_1)} \tag{5.11}$$

This can be recast as:

$$DI_f(t; X_1) = N(X_1)^T n(t) \tag{5.12}$$

where N is a vector with $N_{ijklmno}$ as the elements and n is a vector with $n_{ijklmno}$ as the elements. Note that n represents the division of traffic into different traffic loading cases (such as combination of axle type, axle load, and tire pressure) and in general:

$$n(t) = \text{n}(t) \cdot \hat{n} \tag{5.13}$$

where $\hat{n}$ is a unit vector representing the traffic load spectrum while $n(t)$ is the accumulated traffic volume at time t. With this, the following holds:

$$\frac{DI_f(X_1;t)}{DI_f(X_2;t)} = \frac{N(X_1)^T n(t)}{N(X_2)^T n(t)} = \frac{N(X_1)^T \hat{n}}{N(X_2)^T \hat{n}} \tag{5.14}$$

which means that Equation 5.10 holds. This feature of the transverse cracking model is referred to as the scalability property. It should be noted that no WPV has been included in the proving of the scalability property. Another way to think about this is to assume that Equations 5.10 to 5.14 are being applied to a segment that has uniform inputs X.

The scalability property means that pavements will have the same shape of damage versus time (same damage rate with time) no matter how good or how bad their materials are, as long as their traffic histories (volumes and spectra) are the same. Although it requires the use of Miner's Rule to prove, the scalability property makes sense for pavement performance in general. For the projects used to illustrate BPV in this section, the scalability property is illustrated in Figure 5.17, which shows the accumulated damage histories for projects with different mean values for both MR and σ. As shown in the figure, the histories of accumulated damage are all straight lines in a log-log plot, indicating that their difference can be removed by applying a project-dependent scale factor on the Y coordinate (i.e., accumulated damage).

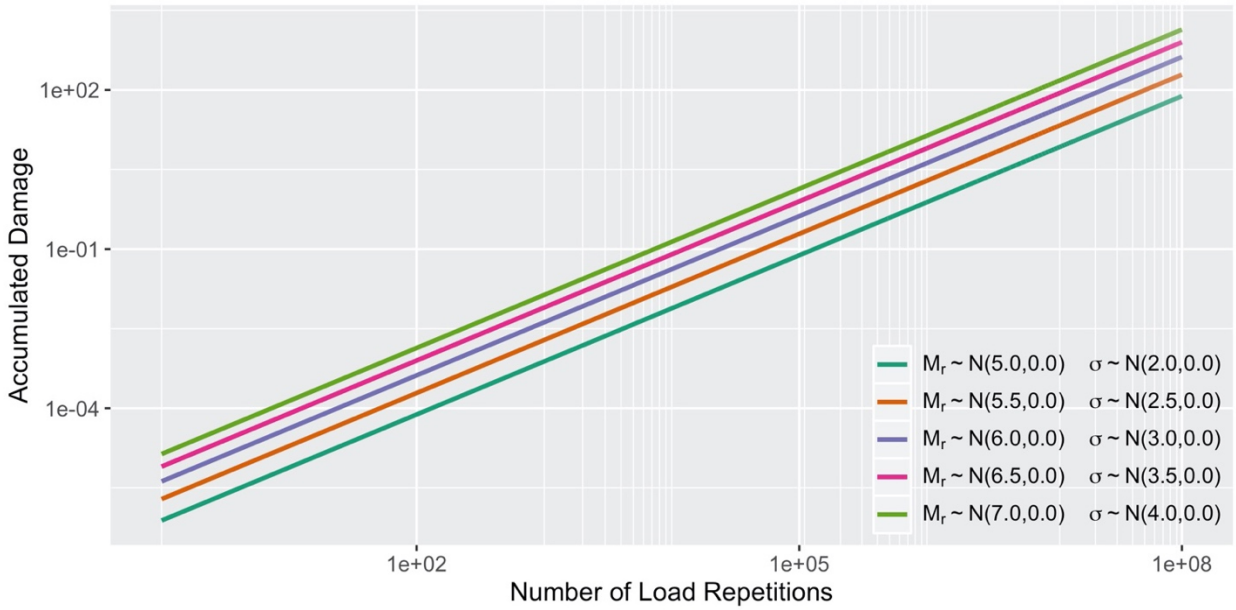

Figure 5.17: Accumulated damage histories for projects with different mean values in modulus of rupture and applied stress in a log-log plot

The illustrations of WPV, BCV, and BPV in the above sections show how each source of variability affects pavement performance. To summarize:

- The amount of WPV affects the shape of the observed cracking history (i.e., overall average), but it does not affect the overall median cracking history.
- The amount of WPV determines the amount of deviation between overall average (mean) and overall median cracking. As WPV decreases to zero, the overall average converges to the overall median.
- The amount of BCV affects the range of variation of the overall average.

- BPV affects only the rate of damage accumulation versus time but not the shape of damage versus time.

All the findings in this section will be used in the next section to separate the three different variabilities.

5.3.4. Step-by-Step Procedure for Pavement ME Transverse Cracking Calibration Using PaveM Database

As discussed earlier, the new Pavement ME calibration procedure considers two properties of pavement systems:

- *Monotonic property*: pavement performance is monotonically related to various relevant factors. For example, pavement lasts longer if one increases MR of the concrete while keeping everything else equal.
- *Scalability property*: damage in a given pavement project shares the same relationship of damage versus time (or traffic loading) regardless of the actual value of various factors affecting performance. This is because the damage versus traffic relationship is determined by the traffic loading as expressed by the axle load spectrum for traffic-induced damage, which is fixed for a given pavement project. In other words, any change in the traffic load spectrum will cause a change in the damage pattern. An increase or decrease in the amount of traffic will result in a shift in the relationship along the time axis. The same is true for environment-induced damage in terms of the temperature and shrinkage spectrum for concrete pavement.

The monotonic property implies that median inputs correspond to median performance. This allows to link at least one set of input—vector X—with its corresponding performance for the roadway network under calibration. Therefore, instead of sampling and testing each individual calibration segment, one needs only to determine the median input vector X for a given roadway network under calibration to produce the median performance, or the median input vector for a sub-set of the roadway network to produce the median performance for the subset, such as a subset with same median slab thickness, base type, shoulder type, and joint length.

The scalability property implies that one can use the median input—vector X—to determine the damage pattern over time. The true damage can be obtained by further applying a scale factor. The value of the scale factor reflects how different the actual input vector is from the median input vector. The distribution of the scale factor indicates the BPV of the road network.

Among all the variables included in input vector X, some are typically known to designers at the time of design while others are not. The known variables are referred to as *design inputs*, while others are *non-design inputs* in this approach. Typical design inputs for rigid pavements include:

- Traffic (volume and spectrum)
- Climate
- PCC slab thickness
- PCC joint spacing
- Doweled/undoweled
- Base type (AB, HMA, LCB, CTB, etc.)
- Shoulder type (FLX, NA, RIG, WRF, etc.)

Typical non-design inputs include:

- Modulus of rupture (MR)
- Modulus of elasticity (E)
- Coefficient of thermal expansion (CTE) and other thermal properties
- Shrinkage properties
- Albedo

The division of design and non-design inputs may change between one road agency to another. For example, one agency might specify the maximum value for CTE and change it from a non-design input into a design input.

A design program needs to provide the performance estimation for a given set of design inputs while accounting for the uncertainties in the non-design inputs. If the known inputs for calibration do not match the given design inputs, the calibration models for transverse cracking can be adjusted by adding or removing BCV and BPV for non-overlapping inputs. For example, modulus of rupture (MR) is typically assumed to be a design input, yet in reality it is a non-design input because its actual value for any given project is typically unknown prior to construction of the project. The BPV of MR should be determined as part of the calibration to explain part of the variability in observed performance.

In Pavement ME, pavement distress prediction is a two-step process. In the first step, pavement damage is determined based on pavement response and accumulated over time. In the second step, the damage is

converted into the corresponding pavement distress through an empirical correlation that is referred to as a transfer function. The first step is mechanistic, and the second step is empirical. The mechanistic step reflects the known factors about various pavement behaviors, while the empirical step reflects the unknown or unaccounted-for factors. It is assumed that the mechanistic step is more or less correct, and only the empirical step needs to be calibrated. The calibration procedure should determine how each uncertainty in various components of the pavement affects the empirical step. This is only partially true for the national calibration, because its authors had no direct measurements of damage and were required to manually separate the calibration of the mechanistic component and the transfer function.

For the transverse cracking model, the corresponding pavement damage is denoted as DI_f. The objective of the calibration is to determine coefficients for the transfer function defined by Equation 5.7, namely C_4 and C_5. The variabilities involved in pavement performance—namely BPV, WPV, and BCV—should be accounted in the calibration process.

As stated in Section 5.3.3.4, BPV is caused by differences in average input variables—such as PCC modulus of rupture, PCC compressive strength, and PCC CTE—between different projects. BPV shifts the transverse cracking horizontally as shown in Figure 5.15 and Figure 5.16. In Equation 5.7, C_4 is responsible for BPV and shifts the transverse cracking in the horizontal direction. Figure 5.18 shows the effect of different C_4 values on the transfer function while keeping C_5 constant. As the C_4 value increases, the model shifts to the right and predicts less transverse cracking (note the damage corresponding to 50 percent cracking for different curves) for a given amount of accumulated damage. Therefore, the effect of BPV should be reflected in the C_4 coefficient.

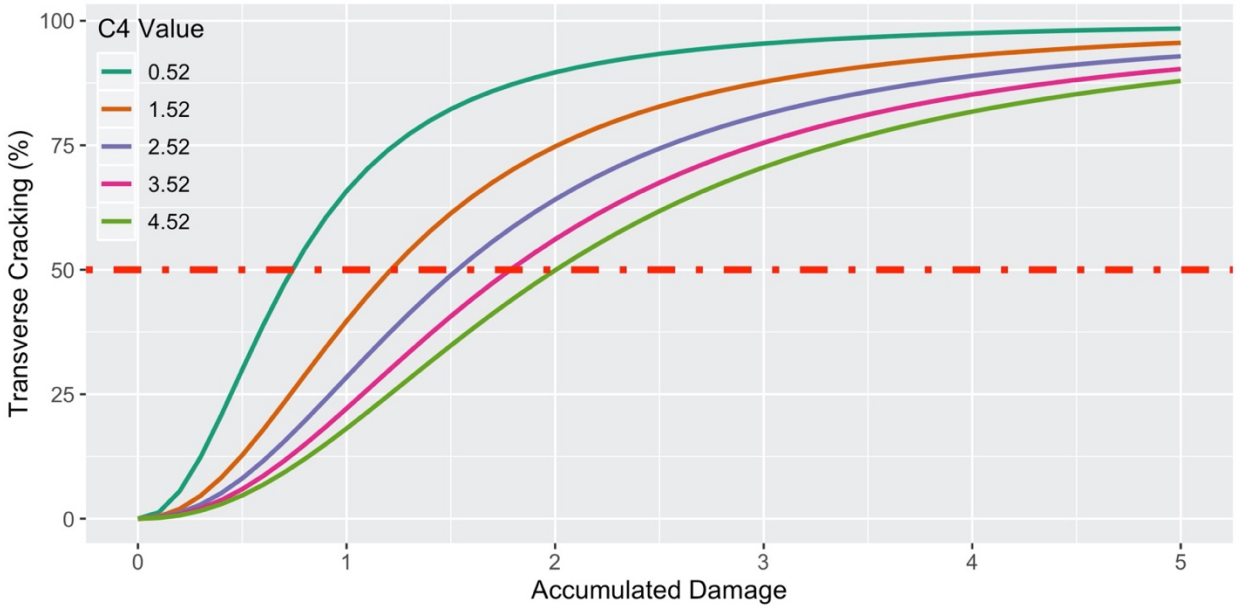

Figure 5.18: Effects of C_4 coefficient on Pavement ME transfer function

Figure 5.19 is a schematic representation of transverse cracking for 50 different projects. Each black line represents the cracking performance of a single project. These projects show different cracking performances due to the differences in their nominal input variable values (those such as PCC compressive strength and PCC CTE that are unknown to the designer). Figure 5.19 illustrates that these projects show a wide range of cracking performance that is caused by BPV. The green line represents a performance for which 50 percent of projects perform worse (50 percent reliability), and the red line represents a performance for which 95 percent of projects perform worse (95 percent reliability).

Theoretically, calibrating the Pavement ME transverse cracking model to each of the black lines results in a distribution of C_4 values. Choosing 50 and 95 percentiles, C_4 values from that distribution correspond to the green and red lines, respectively. However, this is not a feasible action in this study, since important non-design variables are not available for each project. In Sections 5.3.4.8 and 5.3.4.9, a detailed procedure showing how to account for BPV using the statistical random-effects performance model developed in Section 5.2.2 and how to obtain the C_4 values for 50 and 95 percent reliabilities will be explained.

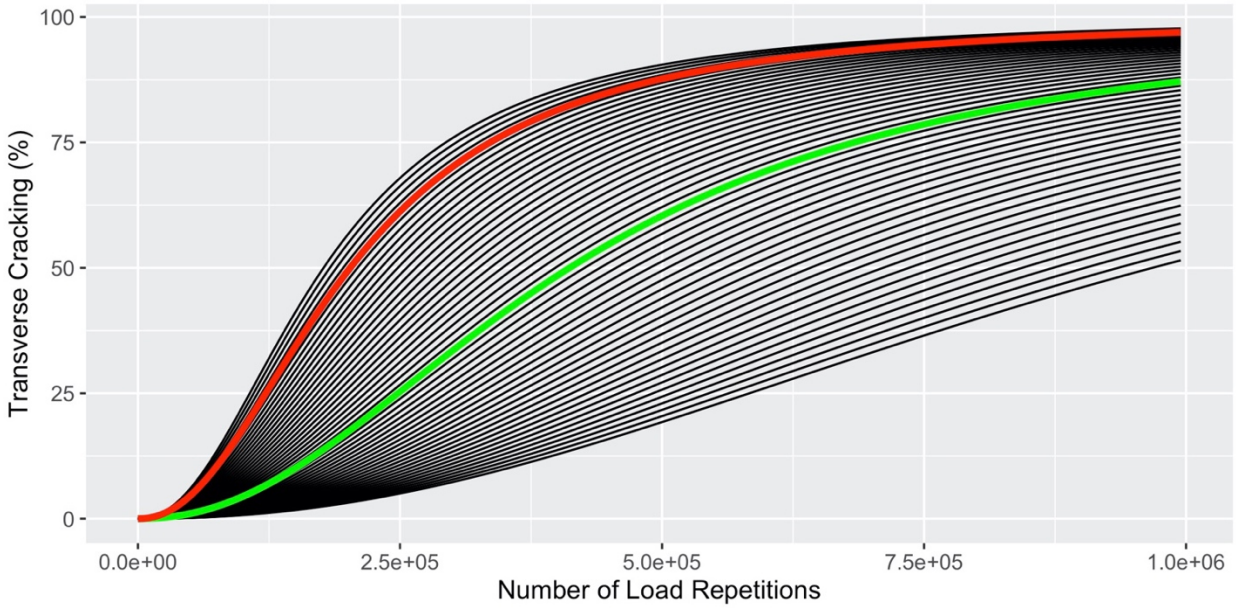

Figure 5.19: Schematic representation of BPV

WPV and BPV are caused by variations in the standard deviation of average input variables such as PCC modulus of rupture, PCC compressive strength, and PCC CTE within each project. WPV and BCV affect the shape of transverse cracking curves as shown in Figure 5.12 to Figure 5.14. In Equation 5.7, C_5 is responsible for WPV and BCV and changes the shape of the transverse cracking curve. Figure 3.12 shows the effect of different C_5 values on the transfer function while keeping C_4 constant. As the C_5 value becomes more negative, the model predicts higher rates of cracking at the beginning, but the curve becomes flatter as more damage occurs. Figure 5.20 shows how C_5 values spread the curve and hence reflect the effects of WPV and BCV. In order to account for these variabilities in determining the C_5 value, a Monte Carlo simulation will be performed on a set of important non-design variables that will be explained in detail in Section 5.3.4.7.

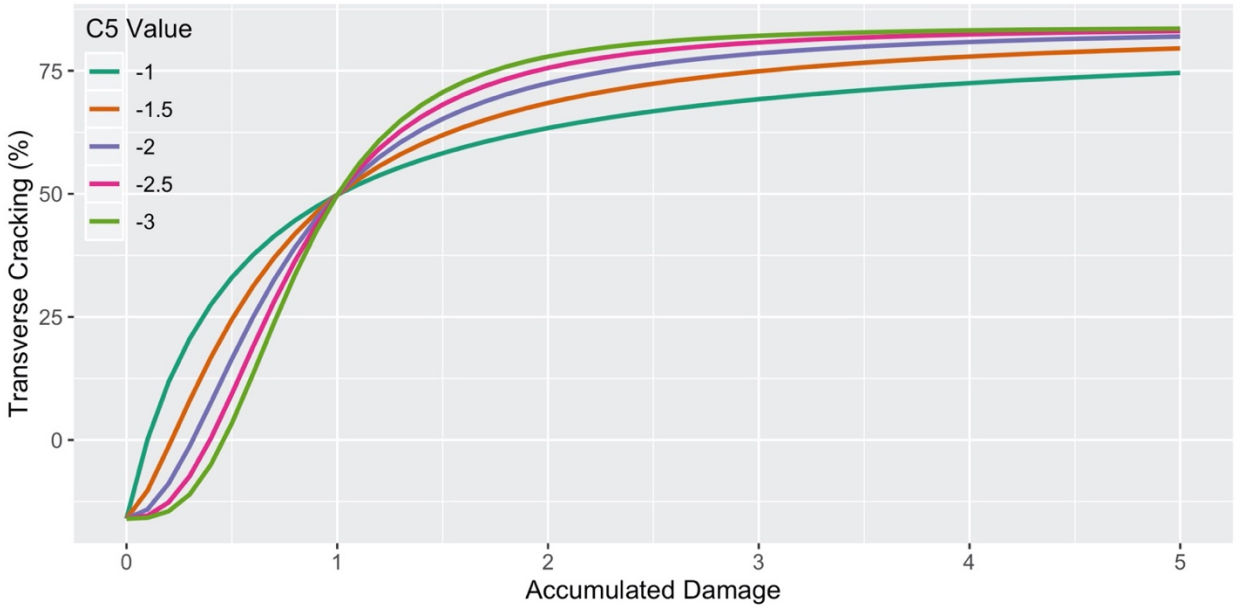

Figure 5.20: Effects of C_5 coefficient on Pavement ME transfer function

The following sections of this chapter explain step-by-step the procedure for calibrating the transverse cracking model in Pavement ME using the PaveM database.

5.3.4.1. Step 1: Identify Roadway Segment

In Step 1, the criteria for identifying roadway segments for calibration outlined in *Guide for the Local Calibration of the Mechanistic-Empirical Pavement Design Guide* (hereafter referred to as the "local calibration guide") should be followed (AASHTO, 2010). In general, there should be a reasonable amount of observed distress both in terms of number of observations and the extent of distress. In the local calibration guide, Step 4 discusses how roadway projects are selected while Step 7 discusses how to use the data from roadway segments to access local bias. There is no requirement on the length of roadway segments.

5.3.4.2. Step 2: Prepare PMS Data

In Step 2, anomalies and obvious measurement errors are removed from the condition survey data. Since the condition surveys collect first- and third-stage cracking, these measurements are converted to transverse cracking (the cracking type that Pavement ME predicts) using the model proposed in Chapter 4.

5.3.4.3. Step 3: Develop Statistical Performance Model

In addressing Step 3, recognize that performance data for an individual pavement project may be scattered. Since performance data are panel data and collected from different projects, a mixed-effects model that can capture the BPV is developed. The equation for the statistical performance model and a detailed discussion on its coefficients can be found in Chapter 4.

5.3.4.4. Step 4: Estimate Median Values for Non-Design Variables

As stated in Section 5.3.3, for variables unknown to the designer— variables also referred to as non-design variables in this report—the median value should be used for each of the inputs in order to predict median performance. The resulting set of inputs are referred to as the *golden reference inputs*. Pavement ME Sensitivity Analysis (Saboori, 2020) discusses these variables and their effect on transverse cracking model predictions. The following is a list of unknown variables and their summary statistics. These distributions were obtained from previous tests carried out by UCPRC as part of different projects funded by Caltrans.

- PCC compressive strength:
  - Mean: $4{,}539\ psi$
  - Median: $4{,}458\ psi$
  - Standard deviation of within-project standard deviation (BCV): $400\ psi$
- PCC CTE:
  - Mean: $4.91 \times 10^{-6}\ °\mathrm{F}^{-1}$
  - Median: $4.8 \times 10^{-6}\ °\mathrm{F}^{-1}$
  - Standard deviation of within-project standard deviation: $0.275 \times 10^{-6}\ °\mathrm{F}^{-1}$
- PCC density
  - Mean: $147\ pcf$
  - Median: $147\ pcf$
  - Standard deviation of within-project standard deviation: $1.64\ pcf$

Among the three variables shown above, PCC density does not have a significant effect on transverse cracking. Therefore, its effects on WPV and BCV will not be considered in Section 5.3.4.7.

5.3.4.5. Step 5: Run Pavement ME for Each Cell of Data

As stated in Section 5.2.2, a cell of data is a set of performance data that could be collected from different projects but that have the same values for all design variables. These variables are PCC slab thickness, PCC slab length, base type, shoulder type, weigh-in-motion (WIM) spectra, Average Annual Daily Truck Traffic (AADTT) lane, and climate. Figure 5.21 shows an example of performance data for a cell of data from the PaveM database.

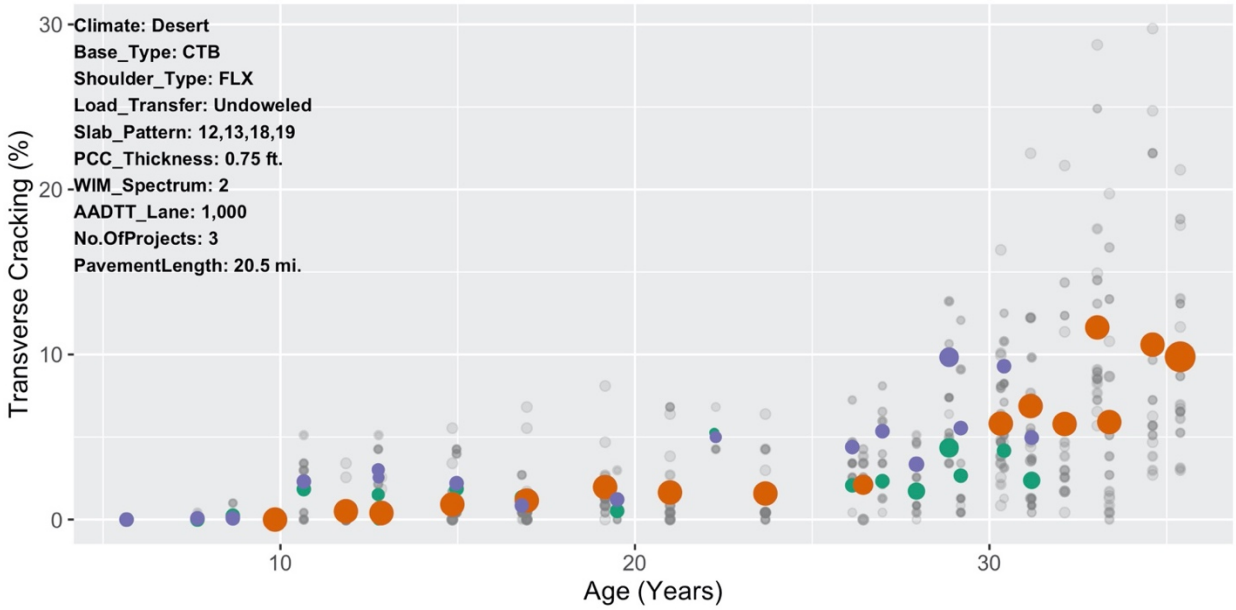

Figure 5.21: A cell of data of cracking performance used for Pavement ME calibration in PaveM database

Figure 5.21 shows the amount of transverse cracking observed from three different projects that are in a cell of data. The X- and Y-axes represent the age of the pavement and the percent of transverse cracking, respectively. Each project is represented with a different color. The size of each data point indicates the amount of data (pavement lane-miles) available for that specific observation; therefore, the bigger the data point the more lane-miles of pavement data it represents. On the left top corner, the variables corresponding to the cell of data are presented. The total length of pavement included in this graph is 20.5 lane-miles. The shaded gray points are the raw data from the PaveM database; after they were aggregated, these data became the colored data points that were used for the calibration. Figure 5.21 shows a clear increasing trend in the amount of transverse cracking for each project, which was expected.

Not all the cells in the PaveM database have multiple projects with this much data. For example, Figure 5.22 shows a cell of data with one project and 0.7 lane-miles of pavement.

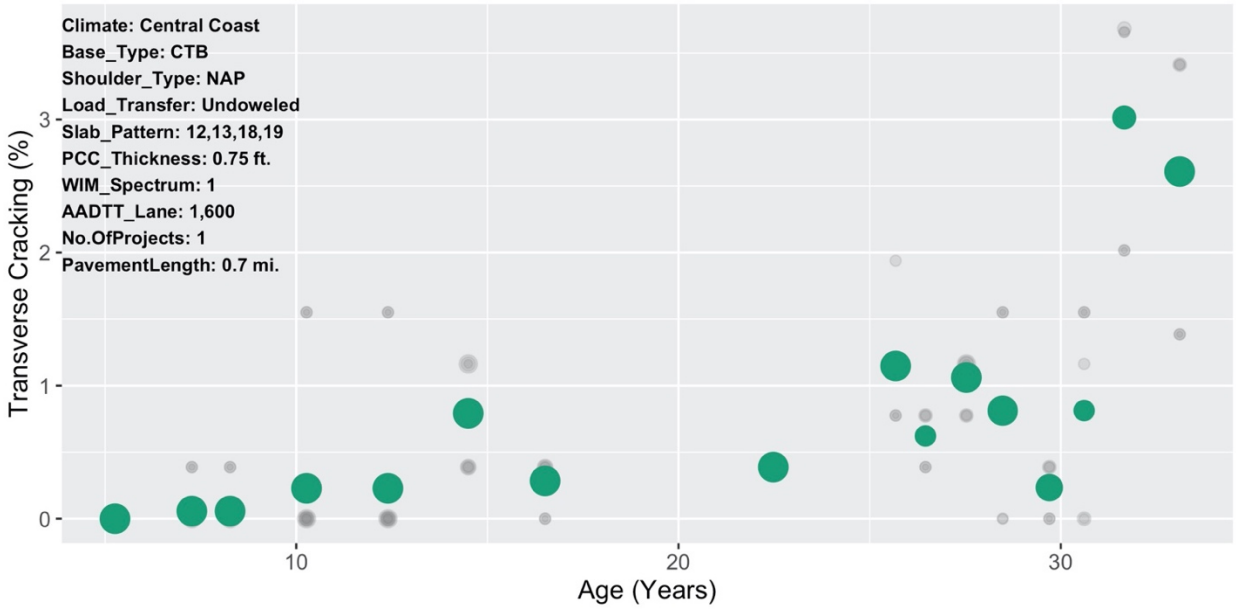

Figure 5.22: An example of a cell of data with limited observations

There are 1,646 cells of data, corresponding to different combinations of design, climate, and traffic variables, available in the PaveM database. The list of factor levels of all variables that constitutes the 1,646 cells of data is as follows:

- PCC thickness: 0.60 foot to 1.2 feet with 0.05-foot increment
- Slab pattern: 12,13,14,15 ft and 12,13,18,19 ft
- Base type: aggregate base (AB), asphalt-treated permeable base (ATPB), hot mix asphalt (HMA), cement-treated base (CTB), and lean concrete base (LCB)
- Shoulder type: no shoulder (NAP), untied flexible (FLX), tied concrete (RIG), and widened concrete (WRF)
- Load transfer: doweled and undoweled
- WIM spectra: WIM_1, WIM_2, WIM_3, WIM_4, and WIM_5
- AADTT per lane: 100 to 13,200 with 100 increment
- Climate region: Central Coast, Desert, High Desert, High Mountain, Inland Valley, Low Mountain, South Coast, South Mountain

Pavement ME should be run for each of these cells. However, since the slab pattern is a categorical variable in the database with two levels—12,13,14,15 ft and 12,13,18,19 ft—a decision was made to run Pavement ME four times (once for each of the slab lengths within the slab pattern category) and use the average of the results for calibration. For example for a 12,13,14,15 ft slab pattern, Pavement ME is run

separately for 12-foot, 13-foot, 14-foot, and 15-foot slab lengths, and the average predicted results of these runs are used for calibration. As a result, 6,584 (1,646 × 4) Pavement ME runs are executed.

After running Pavement ME for each cell, the output files that contain the data pertaining to the amount of bottom-up and top-down damage versus age are stored separately, for use in the calibration.

5.3.4.6. Step 6: Analyze Nationally Calibrated Model Error

Looking at the predictions of the Pavement ME transverse cracking model using the nationally calibrated coefficients $C_4 = 0.52$ and $C_5 = -2.17$, it was found that there is a significant difference between the amount of error for short 12,13,14,15 ft compared with long 12,13,18,19 ft slab patterns. Figure 5.23 is a decision tree model fit on the errors made by the nationally calibrated Pavement ME transverse cracking model versus the PaveM performance data. In each blue box the upper number is the bias (average error) of the national model compared to the California performance data in terms of the difference in percent slabs cracked between the model prediction and the performance data; the lower number is the portion of the total calibration data for that variable factor level.

The top blue box shows that, considering 100 percent of the data, the nationally calibrated model has a 13 percent overall bias. This indicates that on average the national model overpredicts the amount of transverse cracking in California projects by 13 percent. One of the goals of this calibration project is to reduce this number to as close to zero as possible. Going one level down, the branch on the right is divided by slab pattern, which indicates that the model prediction error is considerably different between two types of slab patterns. It can be seen that the national model on average makes a 6 percent error (overprediction) on shorter slabs, whereas it makes 33 percent error (overprediction) on longer slabs. This significant difference between model predictions for different slab patterns suggested that two sets of calibration coefficients were needed to handle the model errors properly. As shown in the following steps, the calibration was done for the two slab patterns separately and as a result, there are two sets of calibrated C_4s and C_5s.

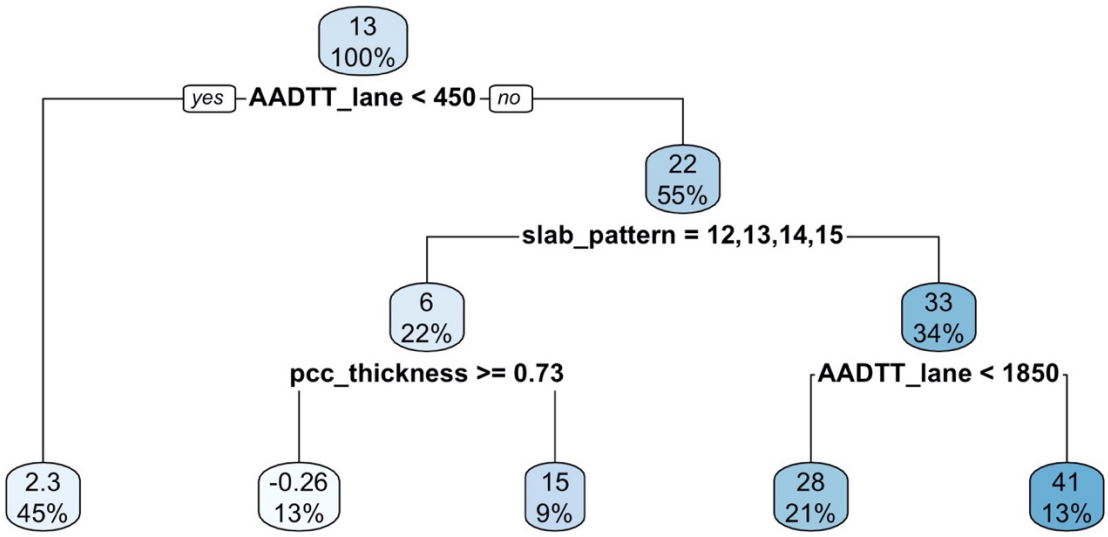

Figure 5.23: Decision tree fitted on the nationally calibrated Pavement ME transverse cracking model prediction error for all data

(Note: **in each blue box the upper number is the bias (average error) of the national model compared to the California performance data in terms of the difference in percent slabs cracked between the model prediction and the performance data; the lower number is the portion of the total calibration data for that variable factor level.)**

Figure 5.24 shows a decision tree model fit on the errors made by the nationally calibrated Pavement ME transverse cracking model versus the PaveM performance data only for short slab pattern JPCPs. It shows that the nationally calibrated Pavement ME model overpredicts the amount of transverse cracking for the short slab pattern by 3.3 percent. Going down the tree, it can be seen that the model performs worse for PCC slabs thicker than 0.68 foot compared to thinner ones.

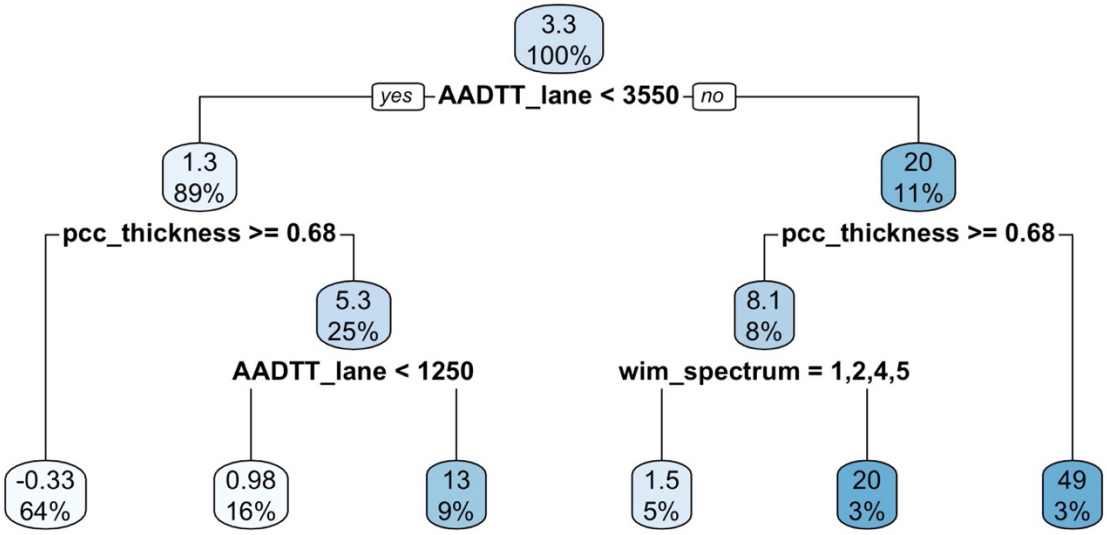

Figure 5.24: Decision tree fitted on the nationally calibrated Pavement ME transverse cracking model prediction error for only short slab pattern 12,13,14,15 ft

Figure 5.25 and Figure 5.26 show examples of Pavement ME transverse cracking model predictions compared to actual data and their corresponding errors. The dashed line represents the nationally calibrated Pavement ME transverse cracking model prediction. Figure 5.25 shows that the model significantly overpredicts the amount of transverse cracking occurring in longer slabs, while in Figure 5.26 there is less overprediction for shorter slabs.

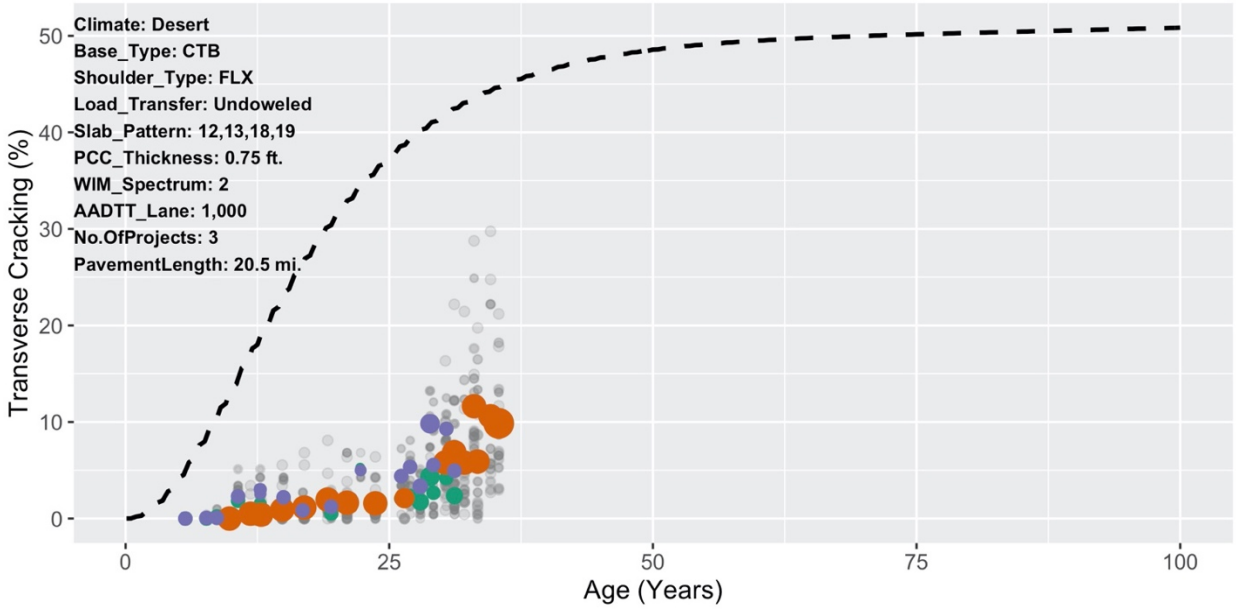

Figure 5.25: An example of long slab pattern performance data compared with Pavement ME transverse cracking model prediction showing overprediction error

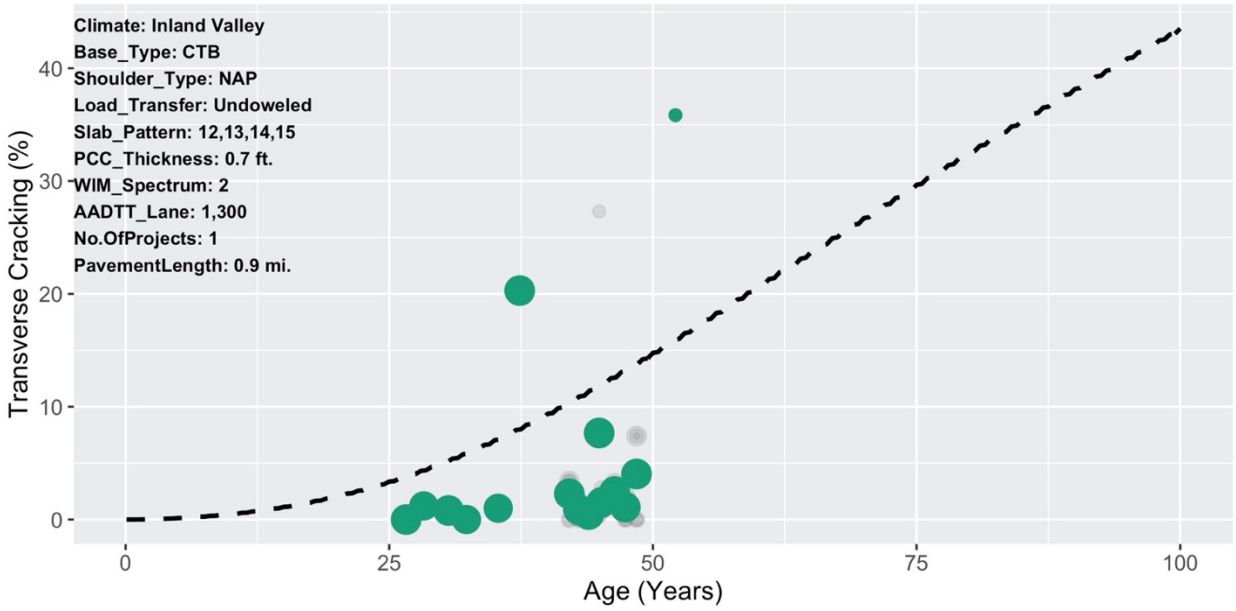

Figure 5.26: An example of short slab pattern performance data compared with Pavement ME transverse cracking model prediction showing overprediction error

Figure 5.27 shows an example of Pavement ME transverse cracking model predictions for the short slab pattern that underpredicts the pavement performance.

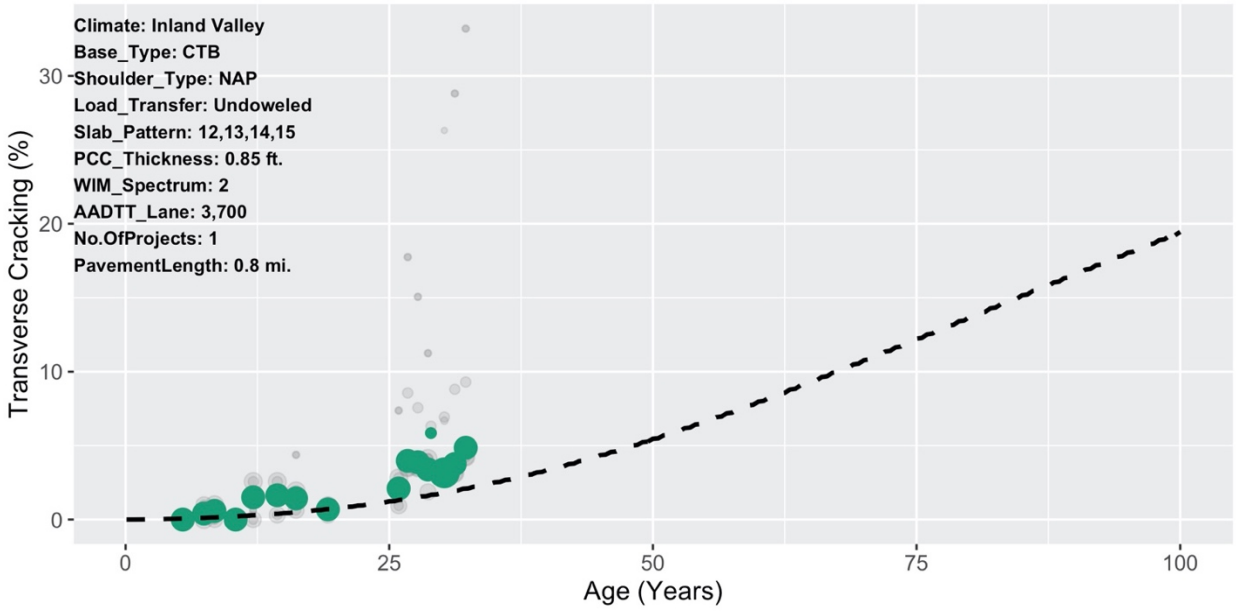

Figure 5.27: An example of short slab pattern performance data along with Pavement ME transverse cracking model prediction showing underprediction error

5.3.4.7. Step 7: Identify WPV and BCV and Find Calibrated C_5

For determining WPV and BCV, those input variables that have significant effect on the transverse cracking prediction were used. Variables and their effects on the model prediction were investigated in the Pavement ME Sensitivity Analysis (Saboori, 2020). Three variables—PCC slab thickness, PCC compressive strength, and PCC CTE—that were believed to have a significant impact on the Pavement ME transverse cracking model prediction were selected to simulate WPV and BCV using the Monte Carlo simulation method discussed earlier in this chapter.

Based on the discussion in Section 5.3.3.1, a Monte Carlo simulation was performed on a few cells (not all cells, due to computational constraints) of data using variations in the three input variables mentioned above. The distributions for PCC compressive strength and PCC CTE were shown in Section 5.3.4.4. The standard deviation of within-project standard deviation for PCC slab thickness, SS_x, used to perform BCV is 0.03 foot. This variable was not discussed in Section 5.3.4.4 as it was not a non-design variable. However, it has variability in its measurements, and since it has significant effect on the Pavement ME transverse cracking model, it was included in the Monte Carlo simulation. For each variable two distributions were considered to choose random values as follows:

- $N(X, \sigma_x - SS_x)$
- $N(X, \sigma_x + SS_x)$

in which $N(.)$ represents the normal distribution, X is the median of the variable under study, σ_x is the standard deviation of the variable representing WPV, and SS_x is the standard deviation of within-project standard deviation of the variable representing the between-contractor variability. Therefore, there will be eight combinations of variable distributions from which 100 (corresponding to 100 uniform segments) inputs are randomly drawn. Choosing randomly from these distributions simulates 8 different projects that have the same median values for the variables of interests—which here are PCC compressive strength, PCC CTE, and PCC slab thickness—with different WPV.

Figure 5.28 shows an example of a Monte Carlo simulation performed on a cell of data. Each gray line represents the Pavement ME transverse cracking model prediction for randomly chosen values from 8 combinations of input distributions mentioned above. It can be seen that the lines cover a wide range of performance due to WPV and BCV. Some segments show a rapid increase in the rate of cracking in the first few years of service life, whereas on the other side of spectrum some show barely any cracking in 100 years. The lines are shown with transparency in order to better illustrate their density.

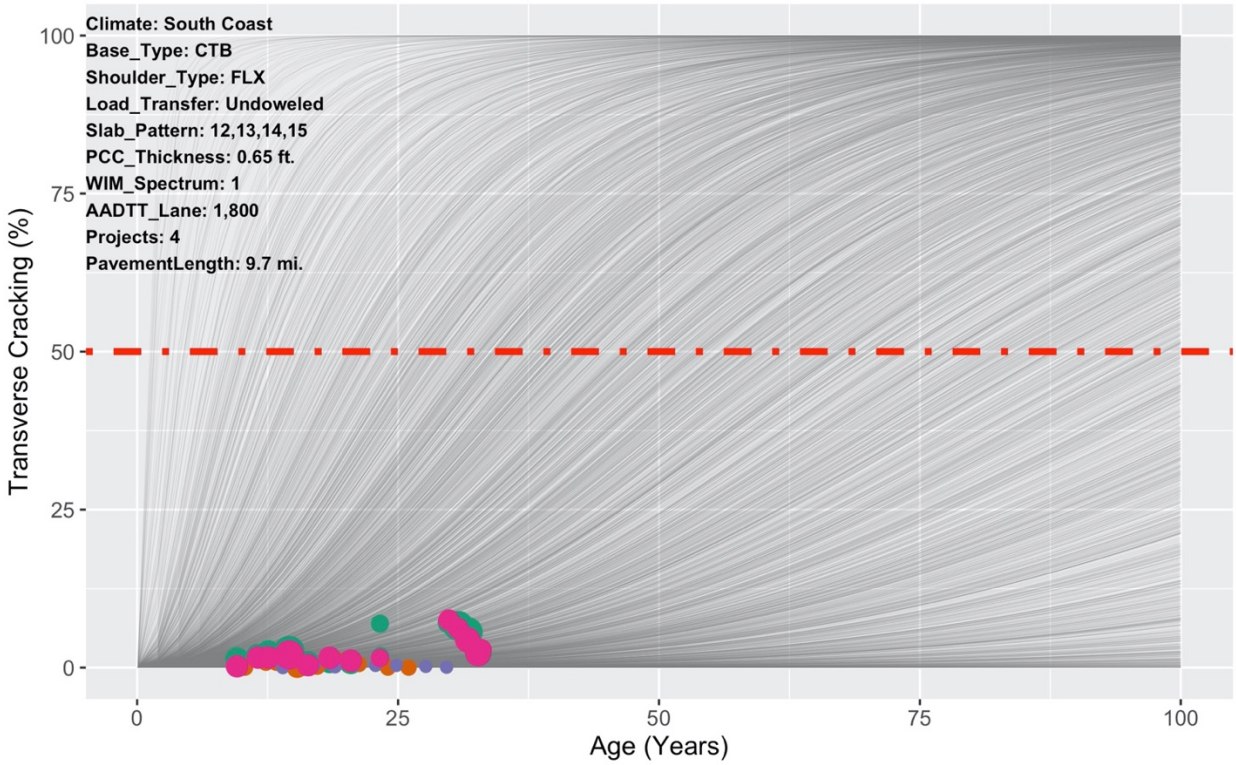

Figure 5.28: An example of a Monte Carlo simulation on a cell of data

In the Figure 5.28 each line represents a specific slab length and input value. As mentioned earlier, 100 randomly selected sets of input variables were sampled from the distributions for concrete strength, CTE, and thickness as part of the Monte Carlo simulation; these correspond to 100 uniform segments of pavement. Taking the average performance from these 100 samples for each specific length and distribution, one would expect them to cross over the 50 percent cracking, as shown earlier in this chapter.

Figure 5.29 shows eight lines for each slab length, passing through 50 percent transverse cracking, after averaging the 100 runs. Each line corresponds to a combination of the three random input distributions used in this section to run Monte Carlo simulation. The pink, purple, orange, and green lines correspond to 15-foot, 14-foot, 13-foot, and 12-foot slab lengths, respectively.

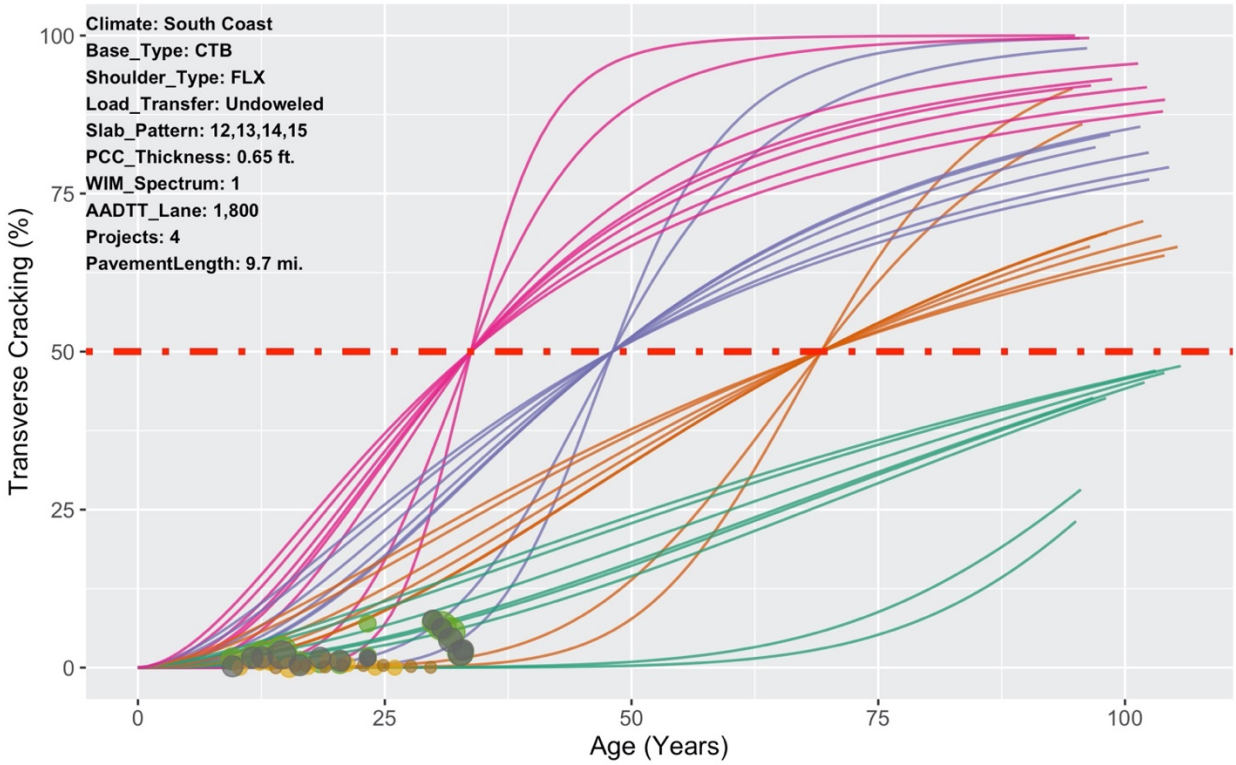

Figure 5.29: An example of Monte Carlo simulation on a cell of data grouped by slab length

The C_5 coefficient directly affects the shape of the transfer function in Pavement ME and hence accounts for WPV and BCV. Therefore, running Monte Carlo simulation helps find the distribution for the C_5 values by using the median value as the calibrated coefficient. In order to find the distribution for the C_5 coefficient for each Monte Carlo run, the time to 50 percent cracking (t_{50}) is obtained using the damage calculated by Pavement ME. For each combination of input variables—PCC slab thickness, PCC CTE, and PCC compressive strength—100 input variables were chosen randomly. Therefore, there are 100 different t_{50} corresponding to these runs. It is assumed that each run is a step function for a slab, and the t_{50} is the time that failure occurs as shown in Figure 5.30. Each black line is a step function that shows the time at which the slab transversely cracked (corresponding to t_{50}). A logistic regression (which has an S shape) is fit to the data using t_{50} as a point on the logistic regression. The red line in Figure 5.30 is the logistic regression model fitted to the black step lines. Having this logistic regression, the C_5 coefficients and their distributions can be obtained by performing simple mathematical operations.

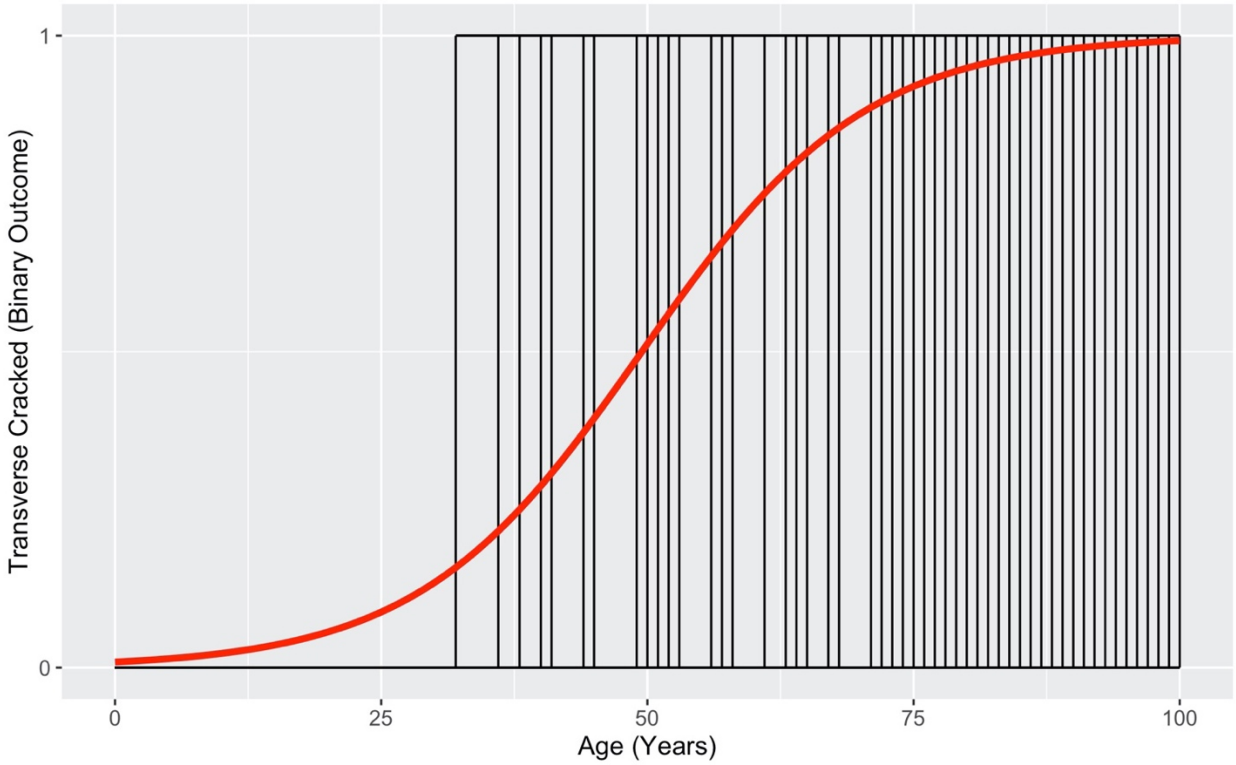

Figure 5.30: Schematic representation of cracked slabs and fitted logistic regression model

The C_5 coefficient for short slabs has a median of -2.37 and a standard deviation of 2.18, and the C_5 for long slabs a median of -2.56 and a standard deviation of 2.39. As these coefficients are fairly similar, a decision was made to use a single C_5 coefficient with a median of -2.37 for both slab patterns. This value is very close to -2.17, the nationally calibrated coefficient.

5.3.4.8. Step 8: Identify Between-Project Variability and Find Calibrated C_4

In Section 5.2.2, the statistical performance model and how it estimates between-project variability was discussed. This statistical performance model will be used to account for BPV and to calibrate the Pavement ME transfer function for C_4.

Figure 5.31 is repeated here from Section 5.2.2 (Figure 5.6) to illustrate the procedure followed to obtain the calibrated C_4 coefficient while accounting for BPV. Figure 5.31 is a cell of data that contains three different projects shown in different colors. It is clear that these projects have different cracking performance caused by errors in the estimation of the design variables and/or effects that cannot be explained with the design variables shown on the top left of the figure. This randomness in cracking performance is considered in developing the statistical model by assigning a random variable to each project and by estimating the random project variable by iteratively maximizing the log of likelihood. The

colored lines are the statistical model predictions for each project considering the individual fit of the random effect between projects (BPV) due to some unknown variables (i.e., PCC compressive strength, PCC CTE, etc.) and the dashed line is the expected (average) behavior of a pavement section with this random effect (BPV) removed and replaced by the median value for those unknown variables. For the cell shown, all three projects had worse performance than when median properties are assumed for the unknown variables. Therefore, to account for BPV, this unknown source of randomness should be accounted for in C_4 calibration.

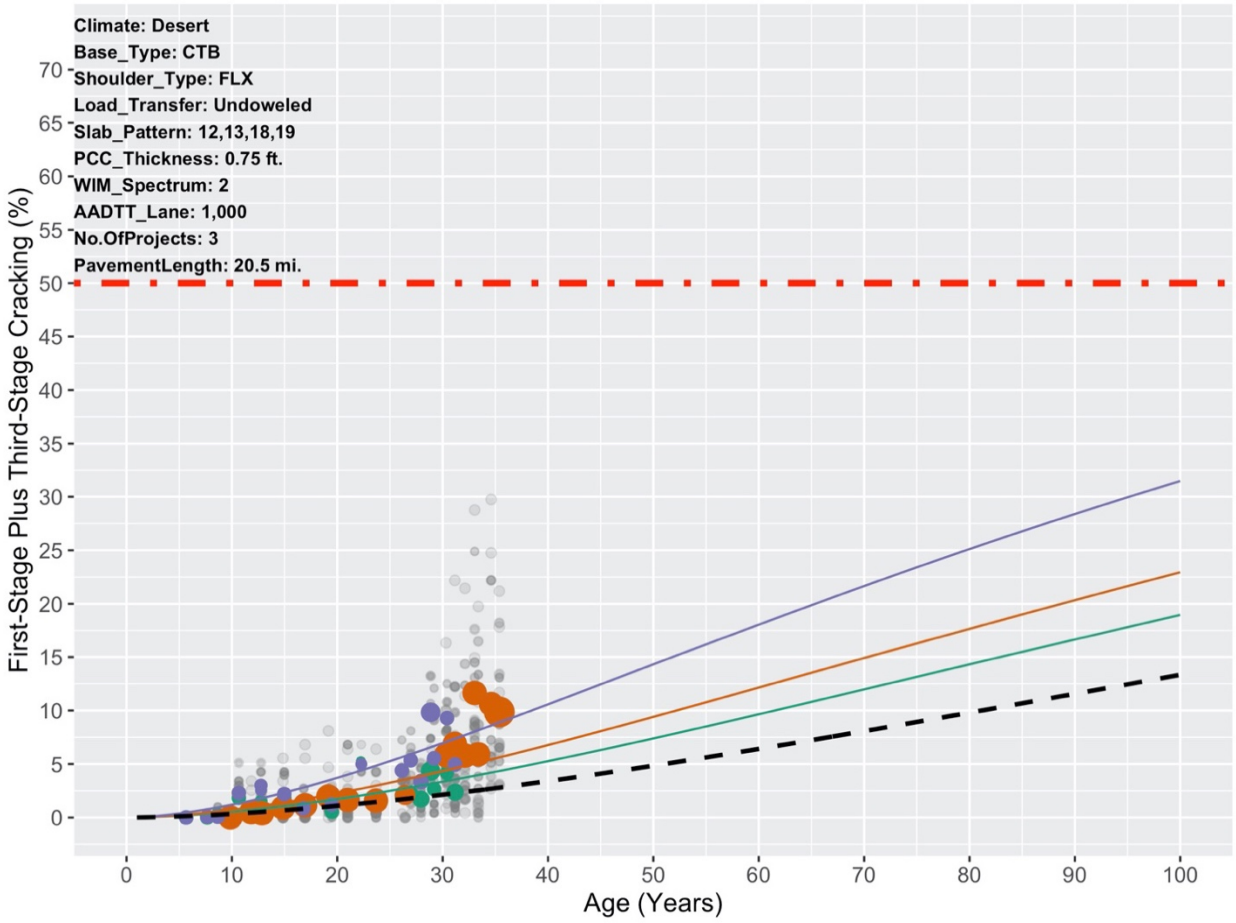

Figure 5.31: Mixed-effects cracking performance model predictions for a cell of data

To achieve this goal, the colored lines should be shifted so that they lie on the dashed line. Therefore, time to 50 percent cracking ($t_{50-expected}$) as a reference point was calculated for the dashed line using the statistical model developed in Section 5.2.2. The same procedure was followed to find $t_{50-project}$ for each individual project. Having these values, the scale factors (the amount of shift specific to each project) are used to shift each individual project to match the expected performance using the median values for the unknown variables. The scale factors can be calculated as:

$$SC_i = \frac{t_{50-expected}}{t_{50-project_i}} \quad (5.15)$$

in which SC_i is the scale factor corresponding to project i, $t_{50-expected}$ is the expected time (without BPV) to 50 percent cracking for a pavement with known variables such as PCC thickness, slab pattern, base type, shoulder type, AADTT per lane, and climate used in the statistical performance model, and $t_{50-project_i}$ is the time (with BPV) to 50 percent cracking for a pavement in project i.

For the data shown in Figure 5.31, $t_{50-expected}$ is about 190 years, and $t_{50-project_i}$ for the projects are about 90, 122, and 144 years. Using these numbers, the scale factors for these projects are 2.11, 1.55, and 1.31 respectively. These scale factors are used to account for BPV to shift each project performance to match the expected performance. Figure 5.32 shows the performance data after BPV adjustment. It can be seen that all the data along with colored lines (statistical model performance prediction with BPV) are shifted and lie along the expected performance prediction (dashed line).

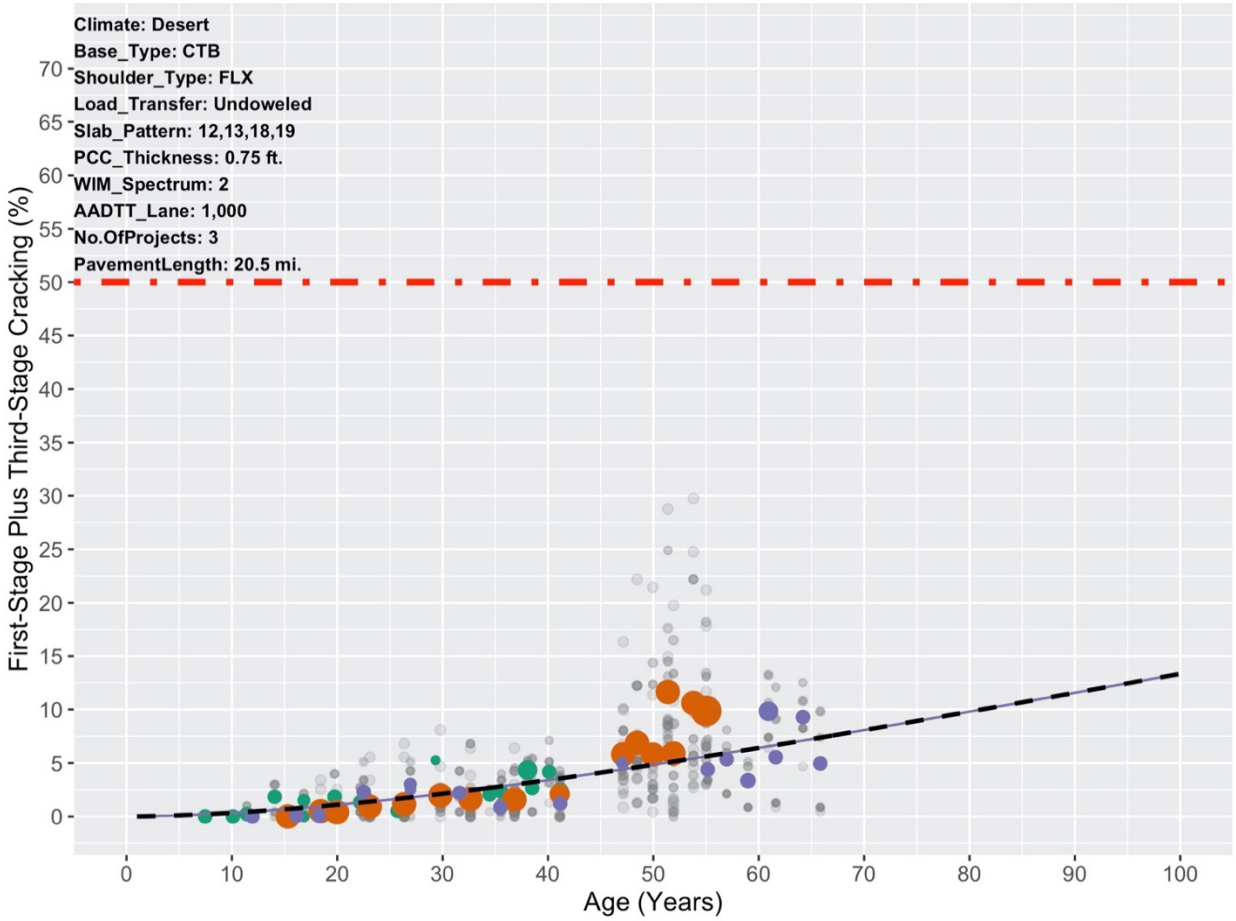

Figure 5.32: The expected (average) performance of the pavement after removing BPV

Using this process, BPV has been removed from the data, which is a preliminary step for C_4 calibration. One should note that the C_4 obtained through this process corresponds to 50 percent reliability, as the scale factors shift the data to the expected (average) performance using the statistical model. With BPV removed, the data will be used to minimize the Pavement ME transverse cracking model prediction bias shown below:

$$Bias = \Sigma(y_i - \hat{y}_i) \tag{5.16}$$

in which y_i is the actual transverse cracking percentage measured from the field (PaveM data) and $\hat{y}_i$ is the predicted transverse cracking value by Pavement ME model.

As stated earlier, two sets of calibrated C_4 are computed for the two slab patterns due to the significant difference in their transverse cracking performance. Following are the C_4 coefficients calculated corresponding to 50 percent reliability.

Table 5.4: Calibrated C4 for 50 Percent Reliability

Slab Pattern	Calibrated C_4 for 50 Percent Reliability
12,13,14,15 ft	4.129
12,13,18,19 ft	468.755

5.3.4.9. Step 9: Find C_4 Corresponding to 95 Percent Reliability

Looking at the statistical model developed in Section 5.2.2 and shown in Equation 5.2, the $u(project_i)$ is the between-project variability (BPV) assigned to each project in the model. In fitting the model, this random effect is assumed to have a normal distribution $u(project_i) \sim N(0, \sigma)$. The standard deviation was calculated to be 1.15.

In the previous step, in order to account for BPV, all individual project data were shifted to the average (expected value) performance. Applying the expected value function $(E(.))$ to Equation 5.2 also resulted in the average performance. This is because the $E\big(u(project_i)\big) = 0$; therefore, randomness is accounted for in the calibration process and the resulting function corresponds to 50 percent reliability.

To find the C_4 that corresponds to 95% reliability, the performance data should be adjusted (shifted) to a project such that 95% of projects had better cracking performance. This was be done by looking at the distribution of BPV $u(project_i)$ in the statistical model and using the value that 95% of the random

effect variables fall below. Figure 5.33 shows the distribution of this variable obtained from the statistical model.

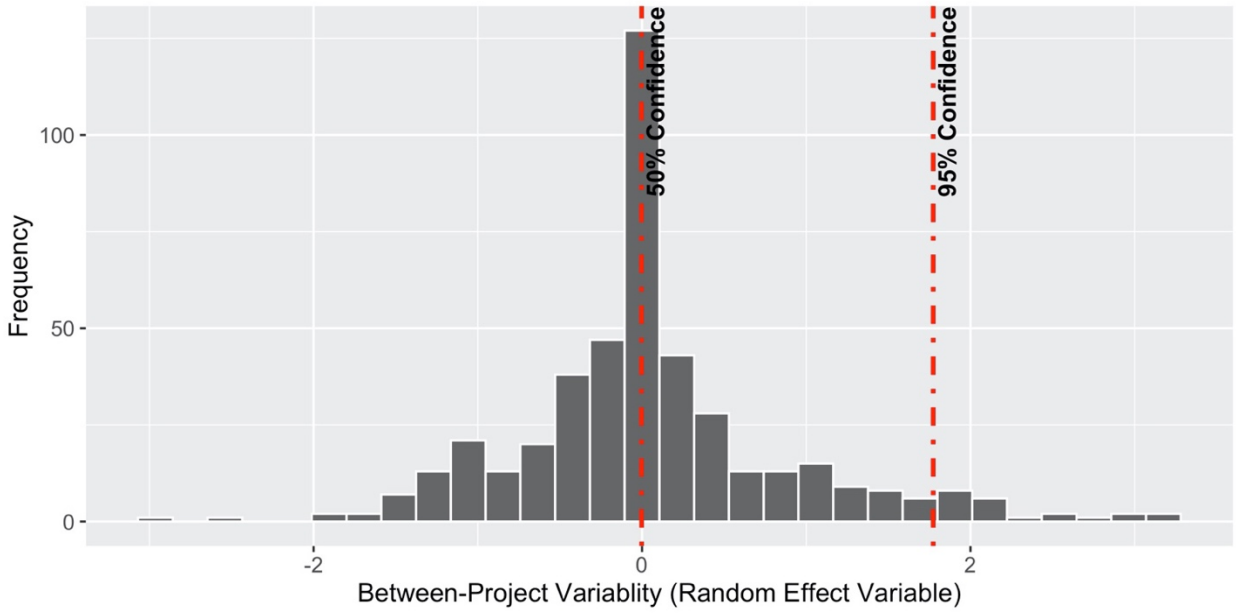

Figure 5.33: Distribution of random effect variable in mixed-effects cracking performance model

Having BPV correspond to the project at which 95 percent of the projects in the PaveM database had better performance, the $t_{50-95\%conf}$ for each cell of data can be calculated using the first- and third-stage cracking performance model. Using $t_{50-95\%conf}$, the scale factor equation becomes:

$$SC_i = \frac{t_{50-95\%conf}}{t_{50-project_i}} \tag{5.17}$$

in which $t_{50-95\%conf}$ is the time to 50 percent cracking for the project that performed worse than 95 percent of the rest of the projects in the PaveM database. Using this scale factor, the rest of the calibration process for 95 percent reliability is the same as the previous step. The following are the C_4 coefficients calculated corresponding to 95 percent between-projects reliability.

Table 5.5: Calibrated C4 for 95 Percent Between-Projects Reliability

Slab Pattern	Calibrated C_4 for 95 Percent Between-Projects Reliability
12,13,14,15 ft	0.217
12,13,18,19 ft	33.172

Figure 5.34 shows that a Pavement ME prediction for a 50 percent reliability nationally calibrated model (dashed line) and for 50 percent (solid black line) and 95 percent (red line) reliability locally calibrated models, for one specific PaveM long slab cell of data.

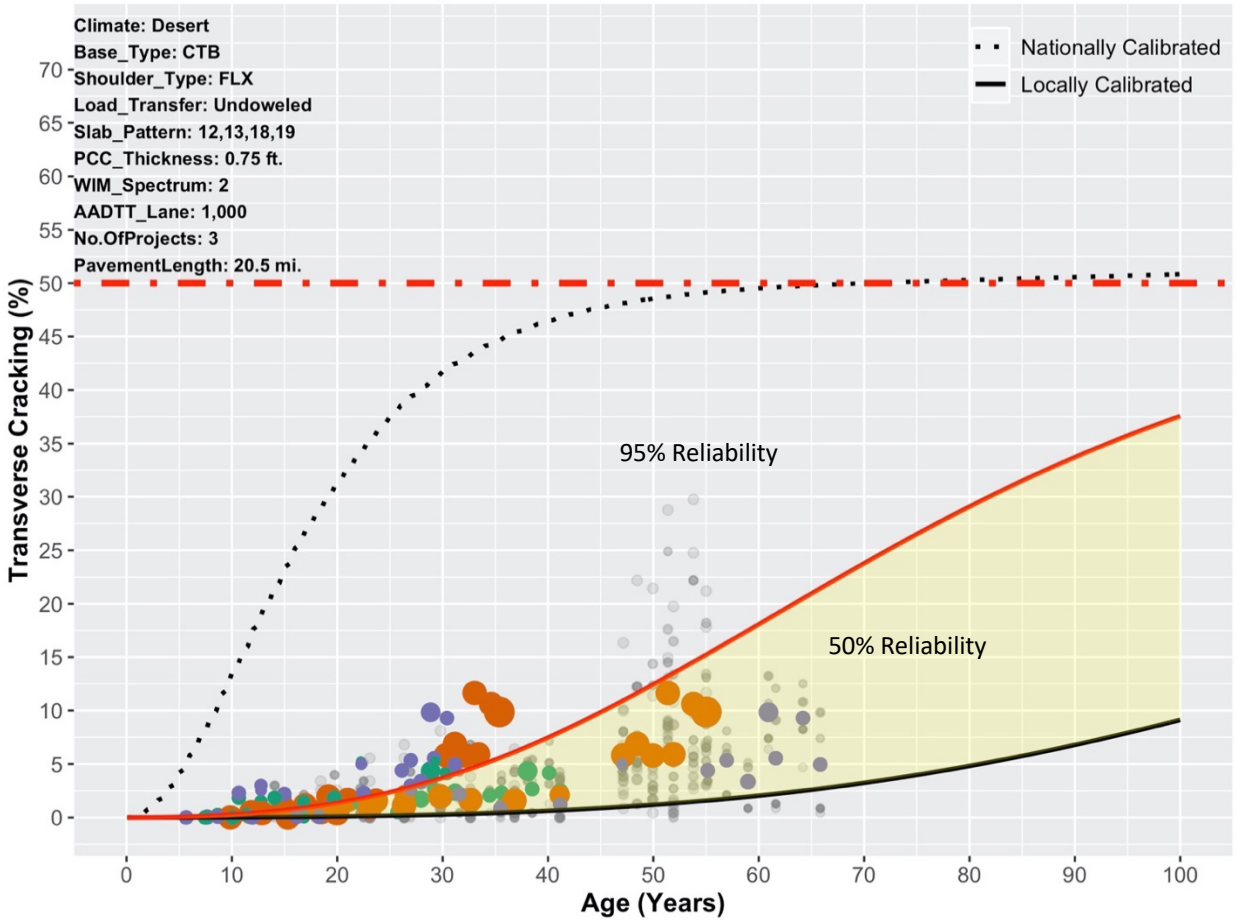

Figure 5.34: Example of locally calibrated Pavement ME transverse cracking model prediction with 50 percent and 95 percent reliabilities for long slab pattern for one cell

Figure 5.35 shows an example of Pavement ME calibrated model prediction for short slab pattern.

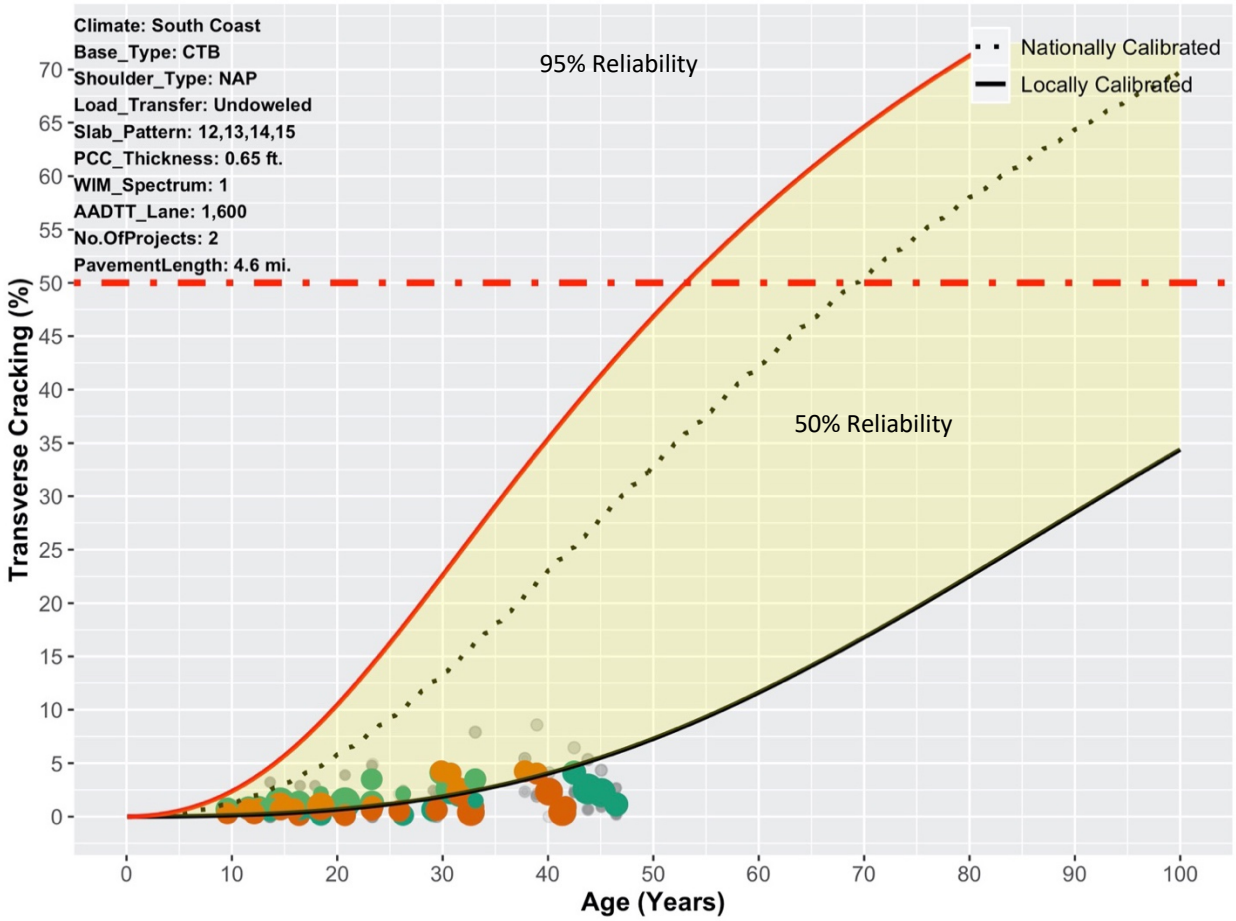

Figure 5.35: Example of locally calibrated Pavement ME transverse cracking model prediction with 50 percent and 95 percent reliabilities for short slab pattern for one cell

5.3.4.10. Step 10: Analyze Calibrated Model Error

Figure 5.36 and Figure 5.37 show the Pavement ME transverse cracking predictions (50 percent reliability) against the actual data collected from the field. The size of each data point represents the amount of data it contains in lane-miles. It is clear that the nationally calibrated Pavement ME tends to overpredict the amount of transverse cracking, as most of the data lie above the line of equality (red line). After calibration the bias has decreased from 13.3 percent to 0.039 percent, and it can be seen in Figure 5.37 that the data is now well distributed around the equality line. The standard error has also significantly decreased from 23.03 percent to 5.62 percent.

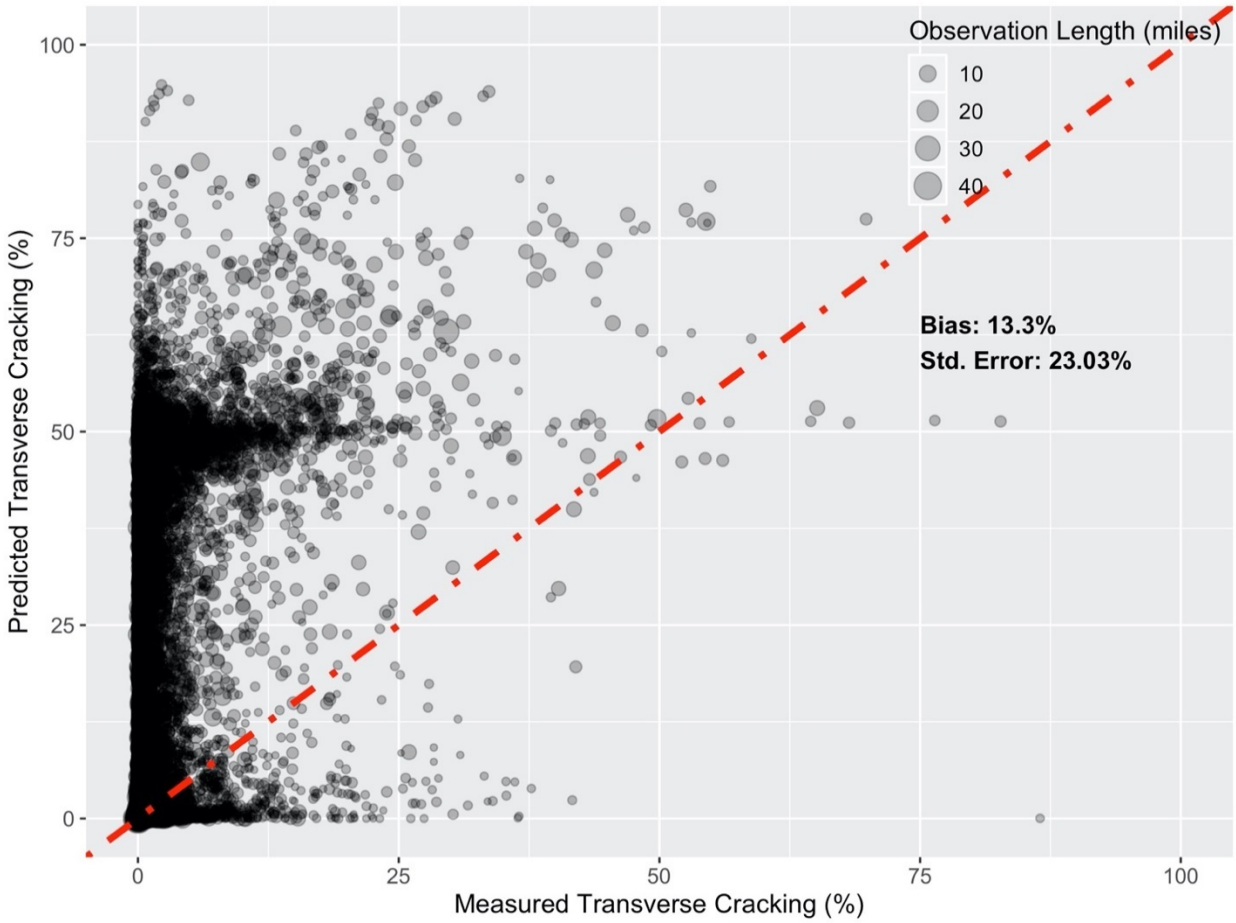

Figure 5.36: Predicted transverse cracking from nationally calibrated Pavement ME transverse cracking model versus measured transverse cracking

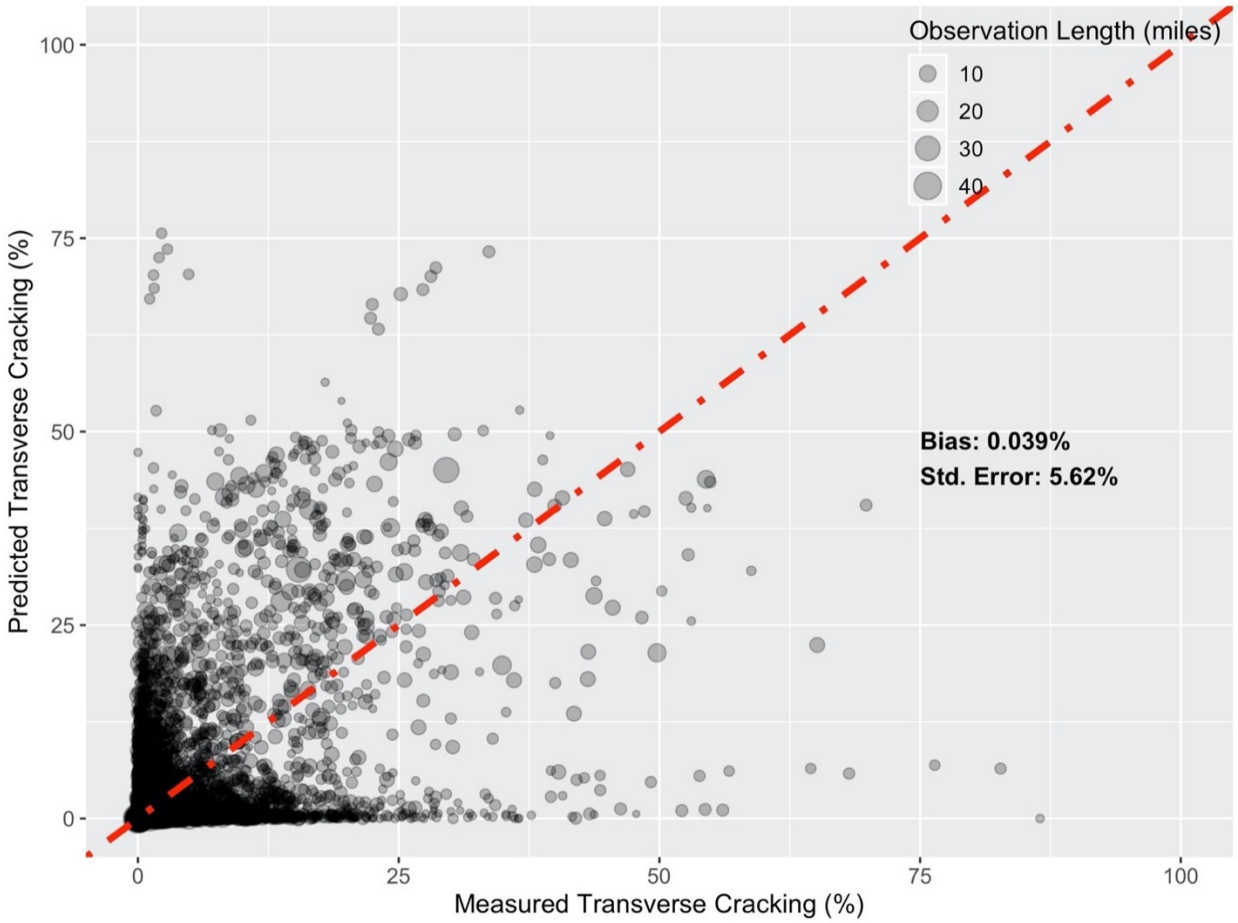

Figure 5.37: Predicted transverse cracking from locally calibrated Pavement ME transverse cracking model versus measured transverse cracking

5.4. SUMMARY, CONCLUSIONS, AND RECOMMENDATIONS

5.4.1. Summary

In this study, the Pavement ME (V2.5.5) transverse cracking model for jointed plain concrete pavements was calibrated. A very large performance database with data collected from California's highway network as part of the annual condition survey was used for the calibration.

The calibration of the Pavement ME faulting model in 2007 (Kannekanti and Harvey, 2007) on undoweled jointed plain concrete pavements (JPCP) and using faulting measurements made by the University of California Pavement Research Center (UCPRC) with a high-speed profiler moving at slow speeds showed that the national faulting model for undoweled pavement did a good job of predicting performance on California pavements. This is likely due in part to the fact that a large part of the calibration of that model was done on California sections, which were used because most other states had

switched to using dowels much earlier than California. For the following reasons, only the transverse cracking model was calibrated in this study:

- There were not enough sections with good faulting history data (built prior to 1998), and JPCP built since 1998 generally does not have faulting according to the Automated Pavement Condition Survey (APCS) data in the PaveM pavement management system (PMS) database.
- Caltrans constructs doweled JPCP exclusively, and faulting is not a major problem for these pavements.
- The faulting model in Mechanistic-Empirical Pavement Design Guide (MEPDG) matched well with Caltrans data in 2006 for undoweled concrete. The model coefficients have changed since a calibration study in 2007 (Kannekanti and Harvey, 2007), however, the current model predictions have changed very slightly since last calibration.
- IRI on doweled concrete pavement is primarily a function of the IRI achieved in construction.

Historically, Caltrans collected first- and third-stage cracking data as part of its manual pavement condition surveys. Caltrans defines first-stage cracking as a single crack that divides a slab into two pieces. This crack can be either transverse or longitudinal. Third-stage cracking is defined as a state of cracking that divides a slab into three or more pieces. Almost all third-stage cracking in California consists of either two transverse cracks or a transverse and a longitudinal crack. The Pavement ME transverse cracking model predicts only the amount of transverse cracking that will occur in JPCP. Therefore, a model was needed to predict the portion of first-stage cracking that is transverse cracking.

The APCS 2010–2011 has per-slab information on first-stage, transverse, and longitudinal cracking data. A model was developed based on this dataset to predict the transverse cracking percentage of pavements with first-stage cracking. Using this model, the amount of transverse cracking could be computed from first-stage cracking data. The computed transverse cracking will be added to third-stage cracking (which has at least one transverse crack) to calculate total transverse cracking. Total transverse cracking data will be used to calibrate the Pavement ME transverse cracking model.

In addition to the first-stage–to–transverse-cracking model, a performance model was developed to predict the amount of first- and third-stage cracking. This model was used to account for variabilities involved in JPCP performance, and these variabilities were used in the new calibration approach.

The goal of Pavement ME transverse cracking model calibration was to find a set of model coefficients that minimizes model prediction error with observed cracking data. Traditionally, Pavement ME models

have been calibrated with a small number of JPCP sections (hundreds) for which all the design and non-design variables were known (or collected). Design variables are those such as portland cement concrete (PCC) slab thickness, PCC slab length, base type, shoulder type, etc. that can be determined by the pavement designer prior to construction, and non-design variables such as PCC compressive strength, PCC modulus of rupture, PCC coefficient of thermal expansion, etc. are those that are unknown to the designer.

Traditional Pavement ME calibration has limitations that do not permit the use of very large performance databases from pavement management systems such as California's PaveM. It does not include consideration of the independent variabilities between projects and within projects of pavement performance, and therefore the traditionally calibrated models predict reasonable average performance while they underestimate the variability. Another limitation of the traditional calibration procedure is the requirement of using project-specific inputs that in practice are not known to the designer and are not present in the pavement management system database. This means field sampling and material testing are needed to determine inputs. This limits the number of roadway segments that can be included in the calibration and therefore may lead to underestimation of model error and input error. Despite the use of design variable inputs, large residual errors are typically encountered in past calibration efforts. These large errors may be attributed to two reasons: first, the model adopted has significant amount of error; and/or second, the inputs to the model have errors. Both of these reasons seem highly likely. With these challenges, and the very large data set that Caltrans has built into PaveM, a new calibration approach was introduced in this study that uses the extensive Caltrans performance database while accounting for the variabilities caused by unknown (non-design) variables.

The new approach considers the variabilities involved in JPCP performance—such as between-project variability, within-project variability, and between-contractor variability—to produce more reliable results. These variabilities will be used in the Pavement ME transverse cracking model predictions in the forthcoming Caltrans JPCP design catalog. After calibrating the Pavement ME transverse cracking model, the model's average error for the percent of slabs cracked has been reduced from 13.3 to 0.039 for predicted versus observed transverse cracking.

An updated design catalog was developed based on the design variable factorial that were determined by consulting with Caltrans to meet its future JPCP design needs. The design catalog was calibrated using Pavement ME transverse cracking model predictions with 50 percent and 95 percent reliabilities (Mateos et al., 2022).

5.4.2. Conclusions

- During development of a first- and third-stage cracking performance model, the following were found from the performance data:
    - JPCP with thicker and shorter slabs performs much better than JPCP with thinner and longer slabs, as was previously known and expected.
    - Neither the presence nor the absence of dowels in a JPCP impacts its transverse cracking performance.
    - Among JPCP base types, lean concrete base (LCB) has the poorest cracking performance, and CTB and HMA have the best.
    - JPC pavements with untied flexible (FLX) shoulders and with no shoulders (NAP) show more transverse cracking than JPCPs with tied concrete shoulders (RIG). JPCP with widened concrete shoulders (WRF) do not perform well, and the statistical model predicts performance similar to FLX shoulders. This is because widened shoulders, which are susceptible to longitudinal cracking, were also mostly used with the more recent practice of 14-foot slabs, which are less prone to transverse cracking than previous slab lengths.
    - The JPCP in the Inland Valley, High Mountain, and South Mountain climate regions have the worst performance among all the California climate regions. The best JPCP performance occurs in the South Coast, Central Coast, High Desert, and Desert regions, and the Low Mountain region falls between those.
    - The weigh-in-motion (WIM) spectra effect does not follow the expected trend of higher WIM levels causing more cracking. WIM Spectra 3 and 4 cause more cracking than WIM Spectra 5.
    - The model predicts more cracking under higher Average Annual Daily Truck Traffic (AADTT) per lane, as expected.
- The Pavement ME transverse cracking model tends, in general, to overpredict the amount of transverse cracking by about 13%. This bias is 19% for JPCPs with the long slab pattern but just 3.3% for those with the short slab pattern. Therefore, due to these distinct trends in Pavement ME transverse cracking model predictions, two separate sets of model coefficients were obtained for the different slab patterns.

5.4.3. Recommendations

- There are two important variables—PCC CTE and PCC compressive strength (as a surrogate for flexural strength)—that were not available for calibration and that had a significant impact on the Pavement ME transverse cracking model prediction. The designer of a JPCP project does not know these variables prior to construction and knows only the minimum specified values. Use of the minimum specified values in the calibration will tend to impart additional unquantifiable conservatism into the designs. The distribution of measured strengths, translated to flexural strengths, was considered in the calibration, and will be considered in the updated Caltrans JPCP design catalog. The new approach presented in this study accounts for the uncertainties produced by these unknown factors by incorporating different types of variabilities in the calibration process and hence different levels of reliabilities in the model predictions. However, having better data for these variables from projects in California in the future will definitely reduce the calibrated model errors for future calibrations.
- The WIM spectra that were believed to have a significant impact on JPCP performance (i.e., higher level, WIM Spectra 4 and 5, cause less cracking) were found to have an opposite effect in first- and third-stage cracking performance model development. These data should be fixed in the PaveM database for better future performance model development and Pavement ME calibrations.

CHAPTER 6. Longitudinal Cracking

6.1. Introduction

In jointed plain concrete pavements, longitudinal cracks form parallel to the direction of traffic, whereas transverse cracks appear in the travel direction. The mechanistic-empirical approach employed by MEPDG considers transverse cracking along with faulting and IRI as main distresses to design the JPCP, but not longitudinal cracking. Historically, longitudinal cracking has not been considered in pavement design due to lack of knowledge on mechanical processes involved in drying shrinkage, which are the critical factor for the occurrence of longitudinal cracking and also, because it does not happen in humid climates. Humid climates sufficient to cause longitudinal cracking generally occur west of the 100th meridian in the United States, the approximate boundary between the arid west and the humid midwest and east identified by Powell in the 1870s (Stegner, 1992). Much of the development of concrete pavement design methods such as MEPDG were originally developed at the University of Illinois, in the midwest.

Many studies in states with dry climates in the US have shown that longitudinal cracking in JPCP is as common as transverse cracking and it should be addressed in the design process. Based on pavement condition surveys in California, Harvey et al. (2000) stated that longitudinal cracking is as frequent as transverse cracking in California. They have observed that longitudinal cracking occurs mostly on the wheel path and in slabs with high faulting and can run the entire slab length and happens in consecutive slabs.

Chen and Won (2007) conducted field investigations on identifying the underlying causes of longitudinal cracking in concrete pavement in Texas. They found that late and shallow saw cutting of longitudinal saw cut joints, inadequate base support under the concrete slab, and having high CTE aggregates in the concrete mixtures were the main reasons for longitudinal cracking in Texas, however, they did not consider drying shrinkage impacts in their study.

Rao and Roesler's research has significantly contributed to understanding the Equivalent Built-In Temperature Difference (EBITD) and its impact on concrete pavements, particularly in California. EBITD accounts for the combined effects of nonlinear temperature, moisture, and shrinkage gradients reduced over time by creep. Their study involved constructing instrumented concrete slabs in Palmdale, California, and monitoring them over 24-hour cycles without load and under a slow-moving 40 kN rolling

wheel load. The analysis revealed high EBITD values ranging from –20ºC to –35ºC for low-restraint sections and 0ºC to –20ºC for higher-restraint sections, attributed to fast-setting high-early-strength concrete, superplasticizers, high-shrinkage cement, and daytime paving under desert conditions with low humidity and high wind speeds (Rao & Roesler, 2005). Their work also emphasized the significance of drying shrinkage, which primarily affects the top portion of the slab, leading to differential shrinkage strains and subsequent curling. Factors influencing drying shrinkage include aggregate type, cement content, water content, and curing conditions. Higher water and cement content were associated with increased shrinkage, while maximizing aggregate volume reduced shrinkage potential. These findings underscore the necessity of incorporating EBITD and drying shrinkage into pavement design models, particularly in extreme environments like California, to enhance the accuracy and reliability of performance predictions. Integrating these factors into mechanistic-empirical (ME) design methods can lead to more effective pavement management and maintenance strategies (Rao & Roesler, 2005).

Using finite-element analysis (RadiCAL), Hiller and Roesler (2002) compared the critical tensile stress near the transverse joint (critical for longitudinal cracking) to those at the mid-slab edge (critical for transverse cracking) for California-type JPCP and concluded that residual negative gradients due to built-in temperature curling and differential drying shrinkage together with traffic loading can cause either longitudinal, transverse, or corner fatigue cracks depending on the slab geometry and shoulder type.

Another study by Ruiz et al. (2008) measured the significant curled-up shape of concrete slabs through profile analysis and concluded that the main mechanism of longitudinal cracking was the action of heavy traffic loads on curled slabs. Xiao and Wu (2018) performed field investigation and numerical simulations for concrete pavement in Louisiana and concluded that in addition to construction problems, slab widened to 15 ft. would increase the likelihood of longitudinal cracking. They have also developed an empirical model that predicts the length of longitudinal cracking by considering traffic, age of service, slab geometry (length, width, shoulder type, and slab thickness), subgrade resilient modulus, and base stiffness as predictors, however, their empirical model does not utilize damage as an input variable and therefore is not compatible with MEPDG damage prediction results.

Lederle (2014) initiated a study to incorporate a longitudinal cracking prediction model in the MEPDG, one that was not included in the original MEPDG, based on mechanistic-empirical pavement design. A model compatible with the MEPDG framework for predicting and analyzing incremental damages from longitudinal cracking was developed, and stresses exerted from axle loading and environmental loading at critical locations related to longitudinal cracking were computed. In this approach, as usual, the concrete

pavement is designed for transverse cracking, IRI, and faulting and once all these design criteria were met, it will be checked for longitudinal cracking potentials. The longitudinal damage model determines the level of longitudinal damage at various locations along the transverse joint. The highest level of damage at any node along the transverse joint is considered as the level of longitudinal damage. The damage ratio will be computed as the ratio of longitudinal damage to transverse damage. If the damage ratio is less than 1, then transverse fatigue damage will control, though this does not guarantee that the design is acceptable, and that longitudinal cracking will not occur. A damage ratio greater than 1 indicates that longitudinal cracking will be the dominate failure mode but does not automatically disqualify the pavement design.

To minimize the amount of longitudinal cracking which will occur, the longitudinal cracking fatigue damage must be below the acceptable threshold that has not been set in the study. While the damage ratio is a useful tool in the design process, it should not be treated as the only criteria for determining if longitudinal cracking is a problem in a specific pavement design. A damage ratio less than 1 indicates that transverse cracking will be the predominate failure type but does not indicate that longitudinal cracking will not occur. Indeed, if both transverse and longitudinal fatigue cracking damage are high, both distresses could be seen. Likewise, a damage ratio greater than 1 does not guarantee that longitudinal cracking will be a problem. If both transverse and longitudinal fatigue cracking damage are very low, it is entirely possible that the damage ratio could be greater than one while neither fatigue damage is high enough to result in significant cracking. Therefore, the damage ratio should merely be used as a quick comparison tool to determine the predominate failure mode, but fatigue damage levels should also be examined.

All these studies have demonstrated the prevalence of longitudinal cracking in dry climates, indicating its significance as a design consideration for JPCP. To address this issue in California, an extensive factorial analysis of various design variables was conducted. Utilizing the ISLAB2000 finite element software, simulations were performed for each unique combination of design variables to understand the resultant stresses within the concrete slab and develop effective design strategies.

This study employed a factorial approach to evaluate the impacts of critical design variables on longitudinal cracking in JPCP, considering factors such as material properties, pavement thickness, joint spacing, and environmental conditions. By systematically varying these parameters, their collective influence on pavement performance was captured.

Each design variable was assigned representative values reflecting real-world scenarios encountered in California's concrete highway transportation infrastructure, ensuring the analysis accounted for inherent variability and uncertainty. By incorporating a diverse range of values, the study's robustness was enhanced, facilitating its applicability across different conditions. Additionally, finite element modeling was utilized to simulate stress distribution within the concrete slab under varying conditions, offering insights into the mechanisms governing longitudinal cracking.

In the subsequent sections, the variables considered in this study and the results of finite element analysis will be presented. Drawing from these insights, design recommendations are proposed, tailored to JPCP in California.

6.2. Design Variables Factorial Consideration in ISLAB2000 Runs

To explore the occurrence of longitudinal cracking and determine its precedence over transverse cracking in the design process, an analysis was conducted using a factorial approach with various design variables, load configuration, and environment conditions. By utilizing ISLAB2000 finite element software, the tensile stresses experienced within JPCP across different load configurations and design scenarios were evaluated.

The variables considered in the ISLAB2000 simulations are as follows:

- Shoulder type: Two shoulder types were examined - WRF and tied-concrete. For tied concrete, a slab width of 12 ft was utilized with a 10 ft shoulder, while for WRF, a slab width of 14 ft was adopted. The non-widened untied shoulder type has not been considered due to its poor transverse cracking performance, as demonstrated by the performance models developed in Chapter 5.
- Load transfer efficiency (doweled/undoweled): Two levels of load transfer efficiency were investigated - 50% for undoweled pavement and 85% for doweled pavement.
- Base type: HMA and LCB
- PCC slab thickness: 8” and 12”
- PCC slab length: 12 ft and 14 ft
- PCC slab thermal gradient: Four different temperature differences (between top and bottom of concrete slab) values (-50, -25, 0, and +20°F) were considered to account for diverse climate conditions across California.
- Axle type: single axle with 20 kip and a tandem axle with 35 kip with a steering axle of 14 kip and a wheelbase of 14 or 16ft (depending on the pavement geometry).

- Load location: Four different load locations were examined for different axle types, each potentially causing critical tensile stress for either transverse (in X direction) or longitudinal cracking (in Y direction).

Based on the above factorial, a total of 512 ISLAB2000 runs were conducted. Figure 6.1 illustrates the axle locations considered in the ISLAB2000 simulations. It displays the four distinct load positions on the 3x3 grid of concrete slabs. The top two figures (labeled A and B) illustrate the positioning of single and tandem axles at the midpoint of the central slab, potentially, a crucial location responsible for transverse cracking for both bottom up and top-down. In contrast, the lower two figures (labeled C and D) demonstrate load placement directly over the transverse joint, potentially, significant spots responsible for longitudinal cracking. All loads are exclusively applied to the central slab, from which the stresses for analysis were extracted. However, in the case of tandem axles, due to the axle configuration and the distance between the tandem axle and the steering single axle, one axle extends beyond the boundaries of the central slab (positioned on the adjacent slab), with the steering axle positioned on the opposite side of the central slab, as shown in figure D. Note that the pavement geometry and load placements are exclusively displayed for the tied-concrete cases with a slab length of 14 ft. Adjustments were made accordingly for pavements with WRF and/or slabs with a length of 12 ft.

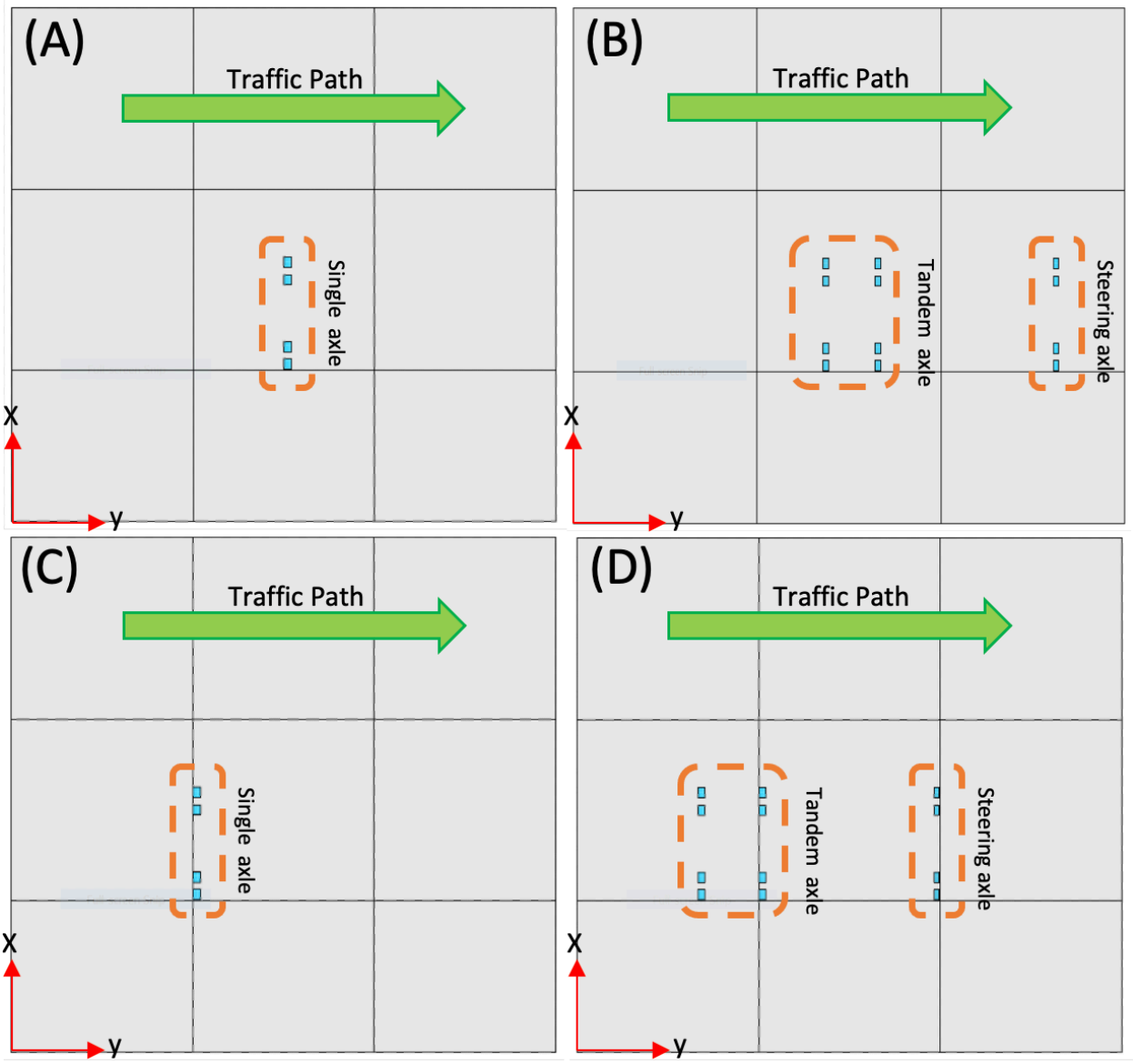

Figure 6.1: Different Axle load placements on a 3x3 grid of concrete slabs with tied shoulder in ISLAB2000

Note: Figure above shows the pavement geometry and load locations for 14 ft. slab with tied-concrete shoulder. The Y-direction aligns with the traffic path and the X-direction is perpendicular to it.

The following material properties and sublayer thicknesses were considered for all simulations:

- Concrete slab
  - CTE: $4.7 \times 10^{-6}\ °F^{-1}$
  - Modulus of elasticity: $4.5 \times 10^{6}\ psi$
  - Poisson ratio: 0.15
  - Density: 147 pcf

- Base
    - HMA
        - Thickness: 6”
        - CTE: 1.13×10^{-5} °F^{-1}
        - Modulus of elasticity: $0.8 \times 10^{5}\ psi$
        - Poisson ratio: 0.35
        - Density: 145 pcf
    - LCB
        - Thickness: 6”
        - CTE: 4.7×10^{-6} °F^{-1}
        - Modulus of elasticity: $2.2 \times 10^{6}\ psi$
        - Poisson ratio: 0.15
        - Density: 147 pcf

6.3. Example Run of ISLAB2000

In this section one example run of ISLAB2000 along with assumptions made during the simulations are described. ISLAB2000 uses linearly elastic constitutive models for the materials. This means that the materials are assumed to be isotropic (having identical properties in all directions) and linearly elastic, characterized by the elastic modulus and Poisson's ratio. These parameters suggest that the materials do not exhibit plasticity or time-dependent behavior such as creep or viscoelasticity under normal loading conditions within the scope of the program.

In the following, a detailed step-by-step description of a ISLAB2000 run for an 8-inch doweled jointed plain concrete pavement with 12 ft. concrete slab, LCB base, tied concrete shoulder, under static load of 18 kip single axle located at midslab and -25°F thermal gradient is explained.

6.3.1. Define the Pavement Geometry and Generate the Mesh

A 2x3 grid of 12-foot concrete slabs with 10-foot wide tied-concrete shoulders is modeled. The concrete shoulders are connected to the pavement using dowels, which are detailed in Section 6.3.4. Figure 6.2 shows the geometry defined in the simulation:

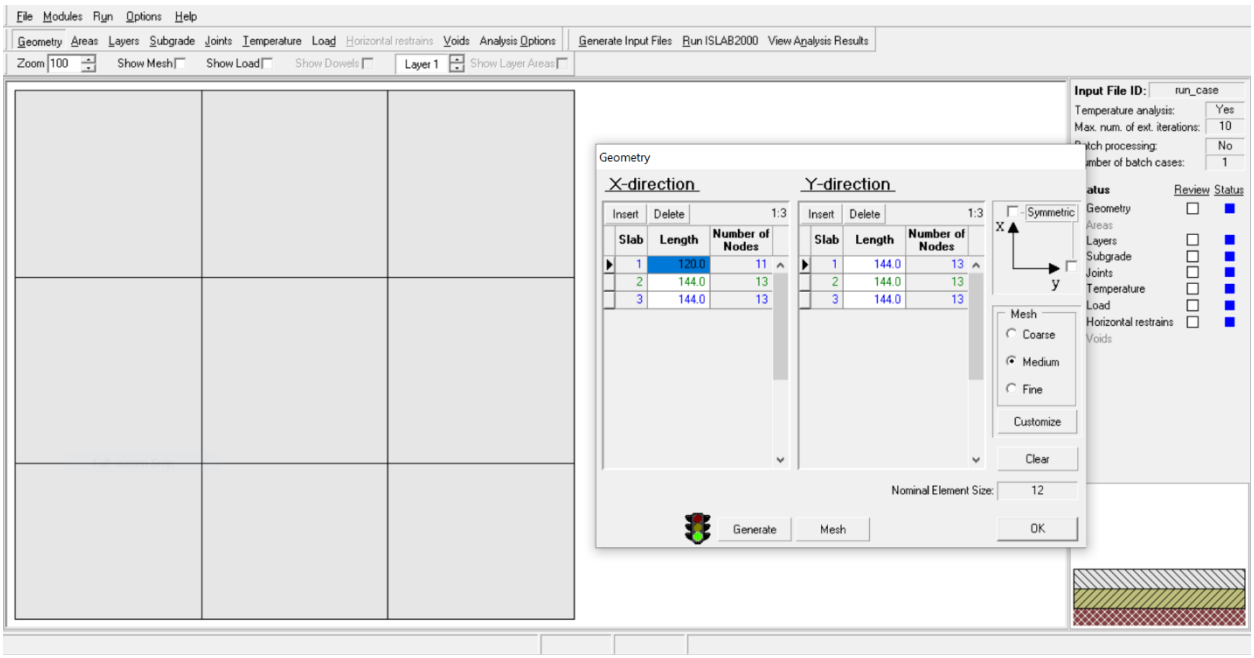

Figure 6.2: JPCP with tied-concrete shoulder geometry in ISLAB2000

Figure 6.3 shows the mesh on the pavement surface. There were three different mesh sizes, i.e. fine (6x6 in^2), medium (12x12 in^2), and coarse (24x24 in^2), and since the results were not meaningfully impacted by the choice of mesh size, the medium mesh size was chosen.

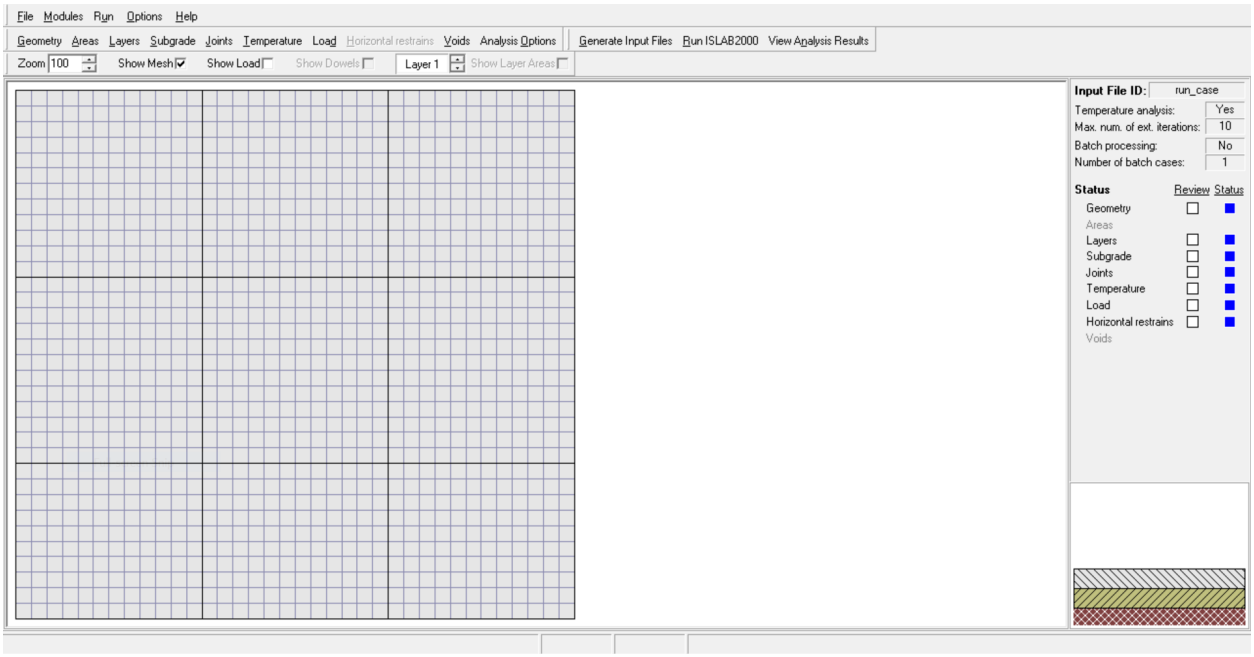

Figure 6.3: Illustration of mesh on JPCP surface in ISLAB2000

6.3.2. Define the PCC and Base Layer Properties

As mentioned earlier, ISLAB2000 uses linearly elastic constitutive models for the materials. Figure 6.4 shows the material properties used for concrete slab and base layer in ISLAB2000. Based on field observations from previous studies, as discussed in Chapter 5, the interaction between the base and the concrete slab was modeled as unbonded. This allows the concrete slab to lift off when subjected to tensile stresses in all directions.

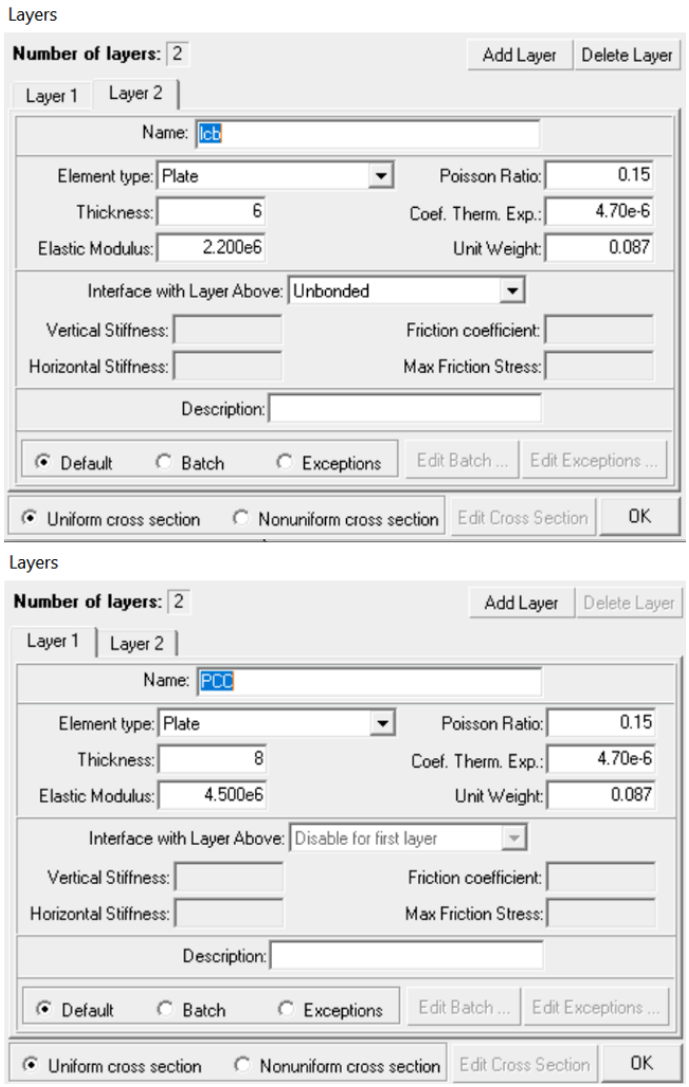

Figure 6.4: Material properties for concrete slab and base layers defined in ISLAB2000

6.3.3. Define the Subgrade Properties

ISLAB2000 employs a spring model to simulate the subgrade, representing the support provided by the underlying soil. This model uses discrete springs to mimic the elastic behavior of the subgrade, where each spring's stiffness is defined by the modulus of subgrade reaction, denoted as k-value. The springs' stiffness translates to vertical support, responding to applied loads and distributing stresses across the

pavement structure. This method allows for a simplified yet effective way to capture the interaction between the pavement and the subgrade, essential for accurate analysis and design of concrete pavements. Figure 6.5 shows how the subgrade has been modeled in ISLAB2000.

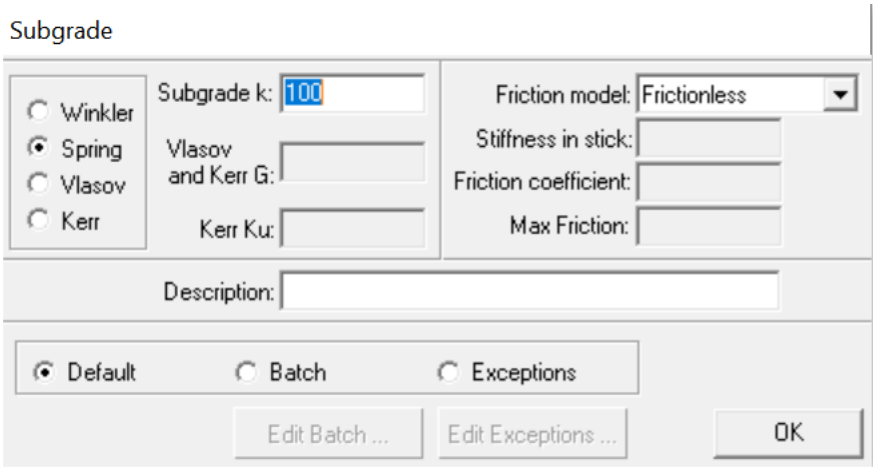

Figure 6.5: Subgrade defined as spring in ISLAB2000

6.3.4. Define the Joints and Load Transfer Efficiency for Dowels

Dowels are steel bars placed at joints in concrete pavements to transfer loads across the joints, ensuring load distribution and reducing differential deflection between adjacent slabs. They help maintain pavement continuity and prevent faulting and cracking. LTE quantifies the effectiveness of load transfer across a joint. An LTE of 85% means 85% of the load applied to one slab is transferred to the adjacent slab, reducing the load on the individual slab. An LTE of 0% means no load transfer, resulting in higher stress and potential damage to the slab.

Dowels are modeled using the Guo model in the ISLAB2000 program. This model assumes the dowel to be a beam element while adjusting the stiffness of the dowel to account for the dowel-concrete interaction at the joint. Figure 6.6 shows the variables defined for dowels and LTE in ISLAB2000.

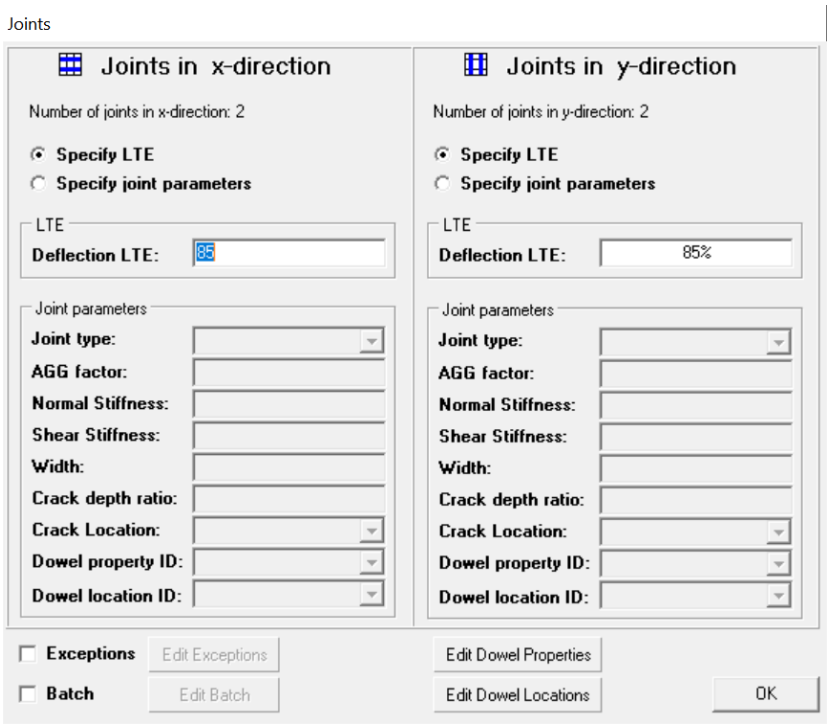

Figure 6.6: Dowel and load transfer efficiency definition in ISLAB2000

6.3.5. Define the Temperature Gradient

In ISLAB2000, thermal gradients in concrete pavements are modeled by defining temperature differences between the top and bottom surfaces of the slab. The software simulates the linear/non-linear temperature profile that occurs due to environmental factors, such as daily temperature fluctuations and solar radiation. Users can input specific temperature values at different depths, allowing ISLAB2000 to calculate the resulting thermal stresses and deformations within the slab. Figure 6.7 shows the values chosen for thermal gradients for both concrete slab and base layers.

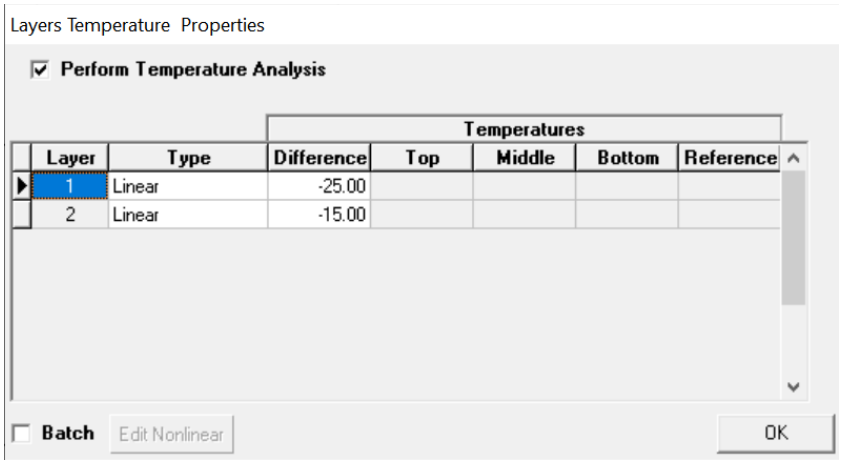

Figure 6.7: Thermal gradient definition in ISLAB2000

6.3.6. Define the Static Traffic Load

Figure 6.8 shows single axle variable definitions in the ISLAB2000. Figure 6.9 shows the placement of single axle on JPCP slab. It has been placed on midslab as it is the critical location for transverse cracking in this example.

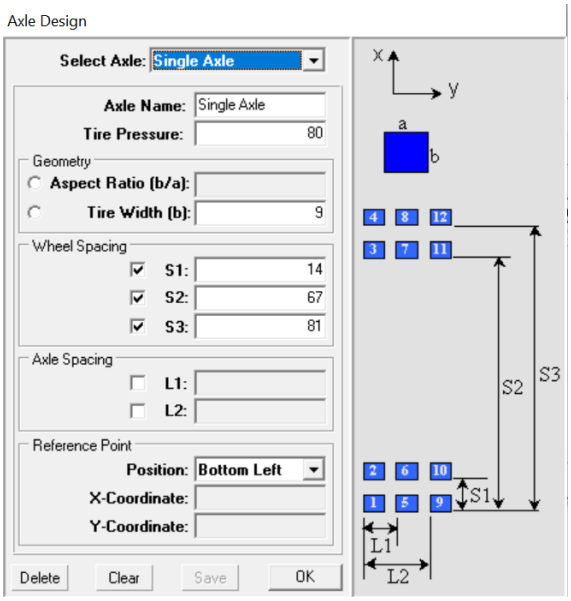

Figure 6.8: Single axle definition in ISLAB2000

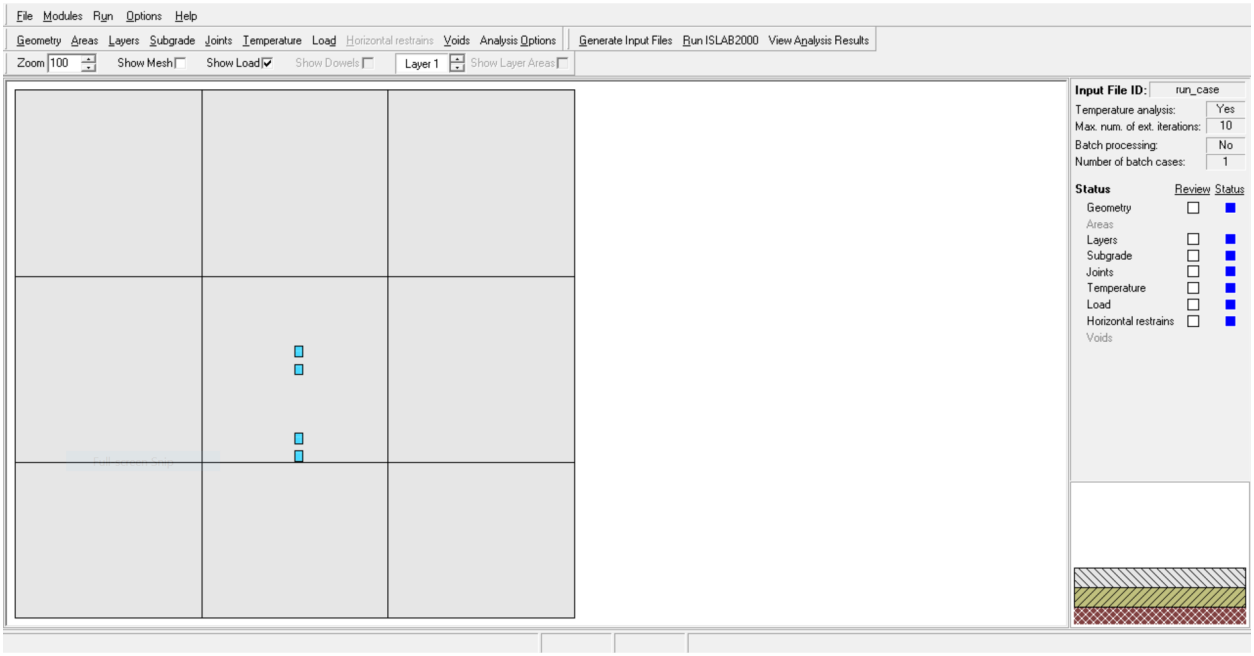

Figure 6.9: Single axle placement on JPCP with tied-concrete shoulder

6.3.7. Run the Simulation and Results

Figures 6.10 and 6.11 show the principal stresses at the bottom and top of the concrete slabs under the traffic load and thermal gradient. It could be seen that the high thermal gradient causes the bottom principal stresses that are the main cause of transverse cracking to reduce and instead the top principal stresses became much larger which will result in change of cracking pattern. More discussion on this will be provided in the following sections.

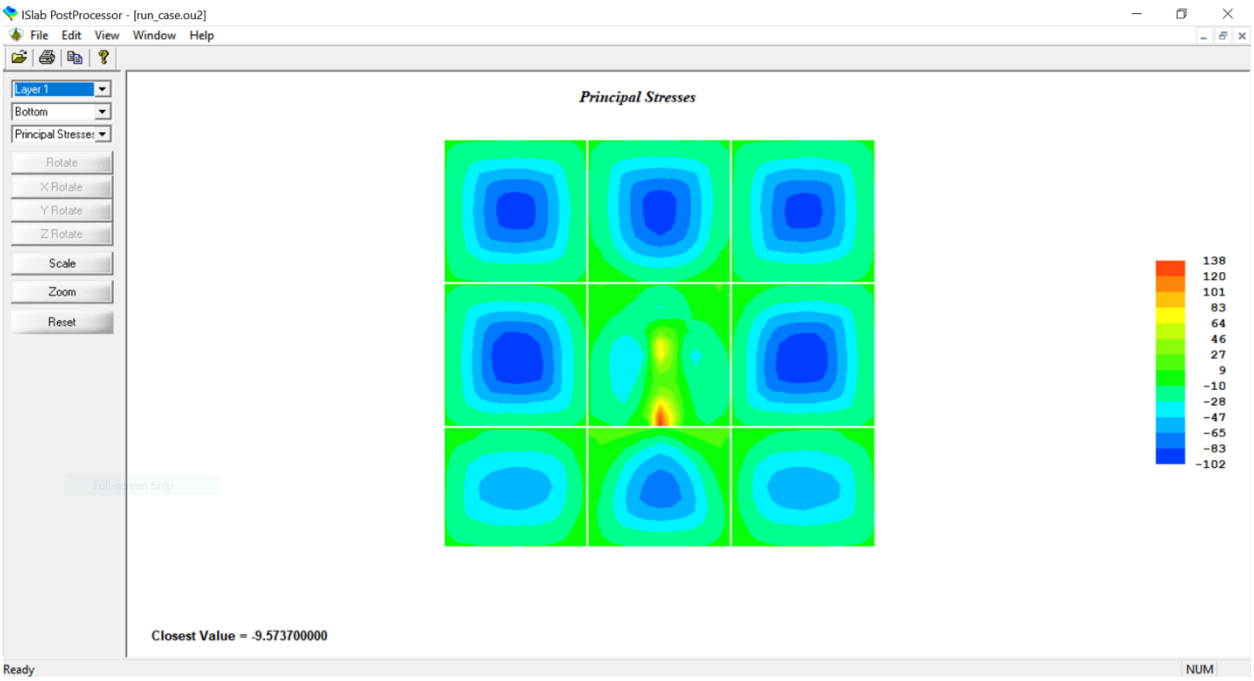

Figure 6.10: Principal stresses at the bottom of concrete slabs in ISLAB2000

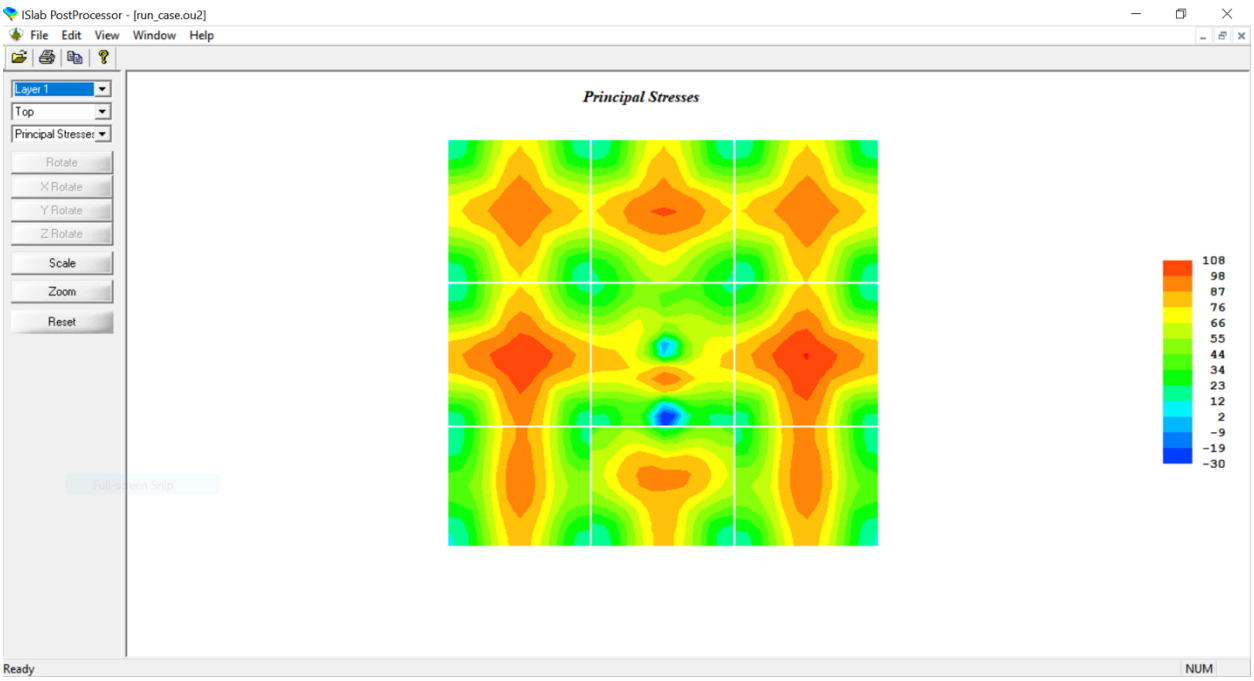

Figure 6.11: Principal stresses at the top of concrete slabs in ISLAB2000

6.4. Analysis of ISLAB2000 Runs and Design Recommendation

After executing each scenario in ISLAB2000, the software generates text files containing stress information in both the X-direction (perpendicular to the traffic path) and the Y-direction (along the traffic path) on the surface and bottom of the concrete slabs at various locations (nodes) along each plane. These results were collected and organized into a tabular dataset for further analysis, as detailed in this section.

Figure 6.12 displays the outcomes of all ISLAB2000 runs for pavements with HMA bases and 8-inch concrete slabs. For clarity, pavements with LCB bases and 12-inch concrete slabs were omitted from this visualization, although they exhibit the same trends depicted in this figure.

The X-axis of the graph represents variables related to load transfer and slab length. For instance, "doweled_12ft" indicates that the bar corresponds to doweled concrete pavement with 12 ft slabs. Meanwhile, the Y-axis represents the highest stress recorded under a specific set of variables. This stress is extracted from the direction perpendicular to the traffic path for longitudinal cracking and from the direction along the traffic path for transverse cracking. The color of the bars indicates the type of damage—transverse or longitudinal—and illustrates which stress is associated with each type of damage.

Each panel in the graph represents a consistent set of variables. Above the panels, the expected variables are indicated. For example, "Bottom, -50grad" signifies that the panels in that category relate to bottom stresses for pavements under a -50°F temperature difference. Similarly, on the right side of the panels, the corresponding variables are displayed. For instance, "tied_concrete, single_axle" indicates that the stresses shown in the panels within that category pertain to pavements with tied-concrete shoulders under single-axle loading. The x, y coordinates displayed on top of each bar indicate the location from which the stress was extracted.

The key insights from this graph are highlighted in specific areas, corresponding to negative thermal gradients for concrete pavements with WRF shoulders. The dashed purple lines are included to facilitate comparison between stresses leading to transverse and longitudinal cracking. The graphs reveal that stresses causing longitudinal cracking are considerably higher than those causing transverse cracking for pavements with WRF shoulders under extreme negative thermal gradients. This result is not observed for pavements with tied-concrete shoulders under extreme negative thermal gradients, nor for any pavement structure under neutral or positive thermal gradients.

This finding underscores that pavements under extreme negative thermal gradients, particularly those with WRF shoulder types, are more prone to longitudinal cracking compared to transverse cracking. This consideration should be incorporated into the pavement design for JPCP in climate regions of California experiencing similar climatic conditions.

With this observation in mind—that thermal gradient and shoulder type significantly influence the mode of JPCP failure—all variables in this study will be explored in more details to assess their impact on the mode of failure for JPCP. For all the cases described below, only the single axle type was considered, as changing the axle type to tandem did not change the overall trend seen in the analysis.

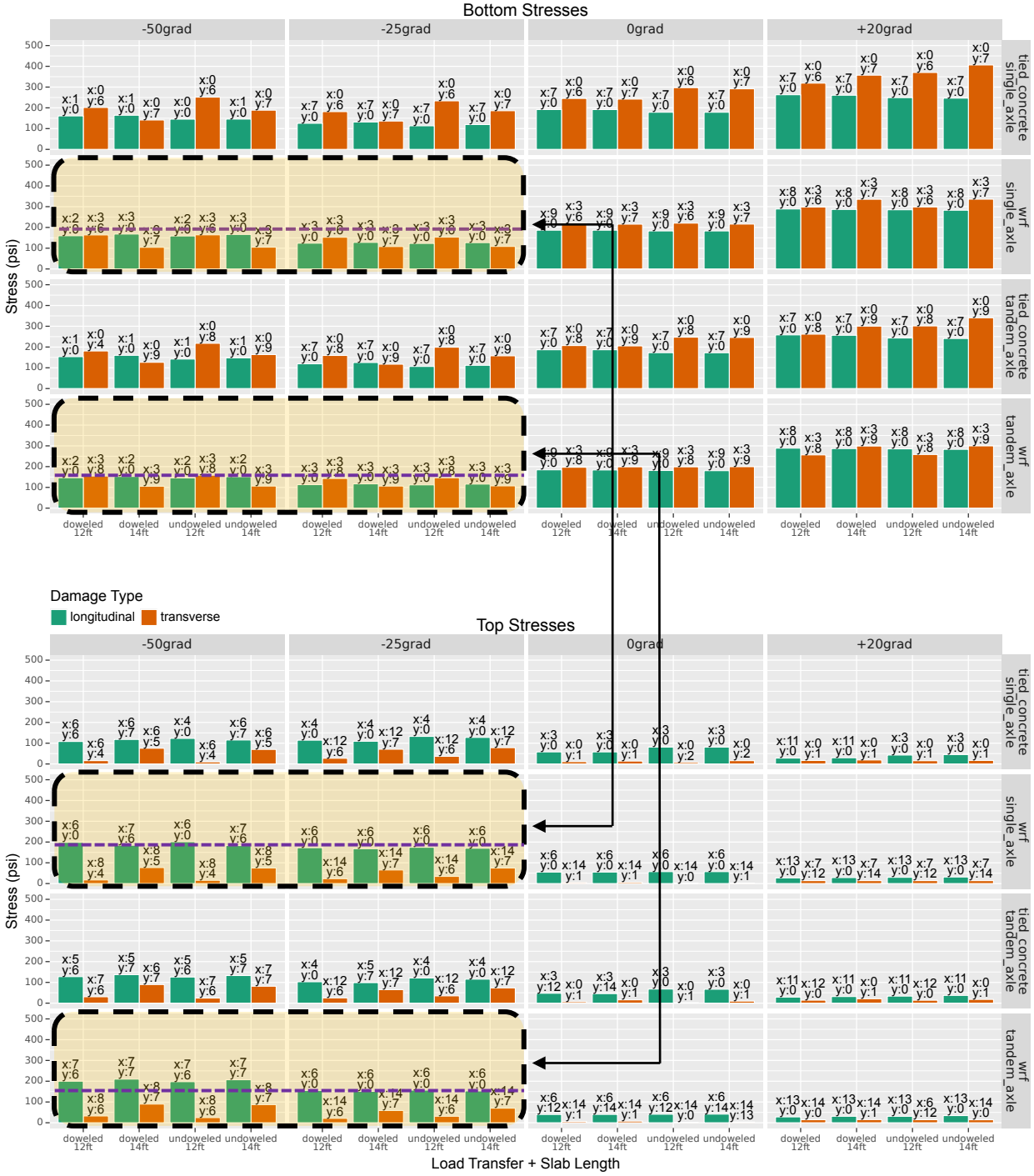

Figure 6.12: Comprehensive results of all ISLAB2000 runs

6.4.1. Shoulder Type and Thermal Gradient

Figure 6.13 demonstrates the impact of shoulder type and thermal gradient on the failure mode observed in JPCP. The data reveal that, across all ranges of temperature differences, pavements with tied concrete shoulders exhibit higher tensile stresses, leading to more transverse cracking compared to longitudinal cracking. However, they experience less transverse stress than pavements with non-widened untied shoulders, as observed in both field data and the performance model in previous chapters.. Conversely, JPCP with WRF shoulder type shows a different behavior, effectively reducing the tensile stresses causing transverse cracking compared to tied concrete pavements.

In instances of extreme negative thermal gradients, JPCP with WRF shoulders experience higher tensile stresses, resulting in longitudinal cracking. This underscores the importance of cautious consideration when constructing JPCP with WRF shoulders in California regions prone to such extreme thermal gradients. Alternatively, if such construction is deemed necessary, longitudinal cracking should be regarded as a critical design criterion, and the utilization of finite element programs may be prudent to optimize pavement design.

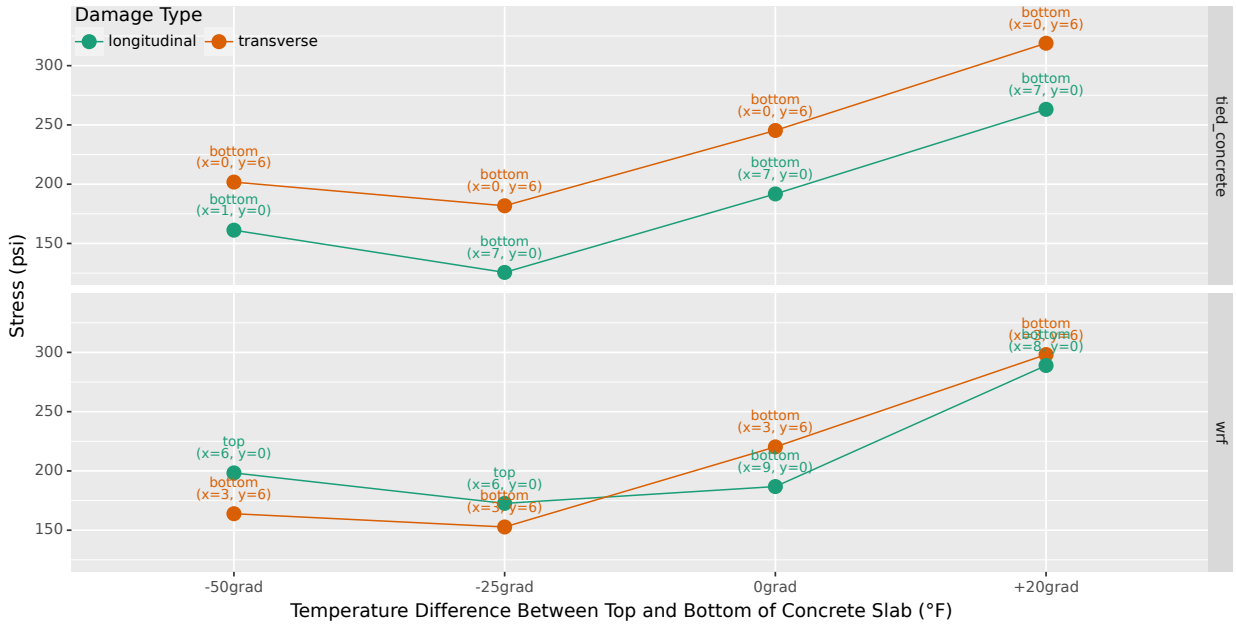

Figure 6.13: Effects of shoulder type and temperature difference

6.4.2. Load Transfer Efficiency

Figure 6.14 illustrates the influence of load transfer efficiency on stresses leading to transverse and longitudinal cracking. The top two panels, representing tied concrete pavement, demonstrate that doweled

concrete may reduce the tensile stresses causing transverse cracking while exerting minimal impact on stresses causing longitudinal cracking. In contrast, for pavements with WRF, the influence of load transfer efficiency appears to be minimal for both transverse and longitudinal cracking.

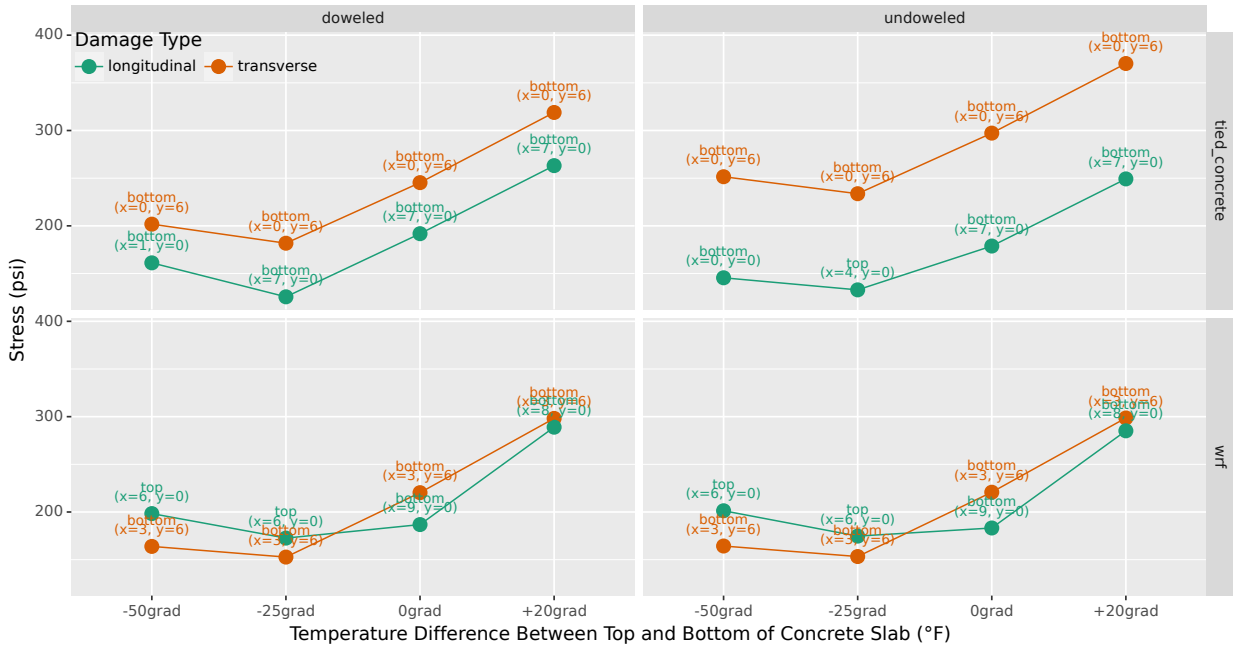

Figure 6.14: Effects of load transfer efficiency on mode of failure

6.4.3. Concrete Slab Length

Figure 6.15 illustrates the effect of slab length on JPCP performance concerning both transverse and longitudinal cracking. It is evident that longer slabs (slabs with length of 14 ft), result in higher tensile stresses leading to transverse cracking under neutral and positive thermal gradients. However, this trend does not hold true for more negative thermal gradients.

By looking at all the panels, it is also evident that the length of the slab has a negligible effect on the magnitude of stresses causing longitudinal cracking.

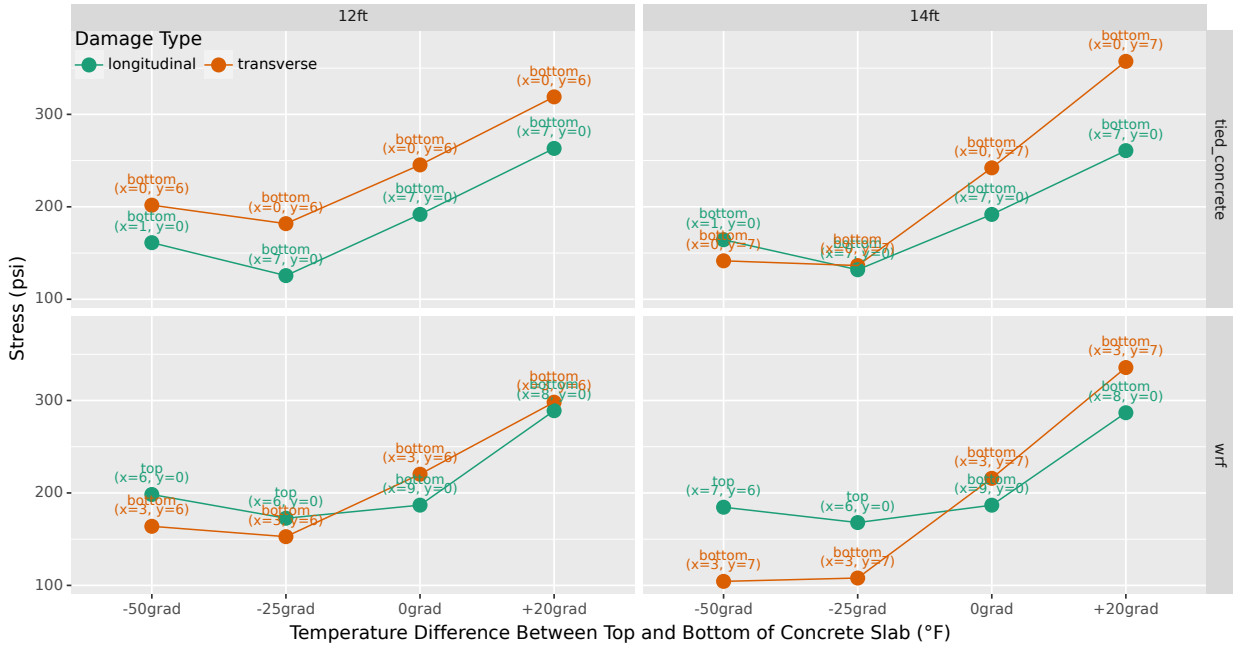

Figure 6.15: Effects of concrete slab length on mode of failure

6.4.4. Concrete Slab Thickness

Figure 6.16 depicts the impact of concrete slab thickness on both transverse and longitudinal cracking. As anticipated, thicker slabs result in decreased stresses, affecting both types of cracking. Another noteworthy observation is that increasing slab thickness may shift the mode of failure from longitudinal cracking to transverse cracking for pavements with WRF shoulder type under negative thermal gradients. Therefore, in scenarios where WRF is selected as the shoulder type in regions experiencing negative thermal gradients, it is advisable to increase pavement thickness to mitigate the risk of longitudinal

cracking, especially if the pavement was initially designed only for transverse cracking.

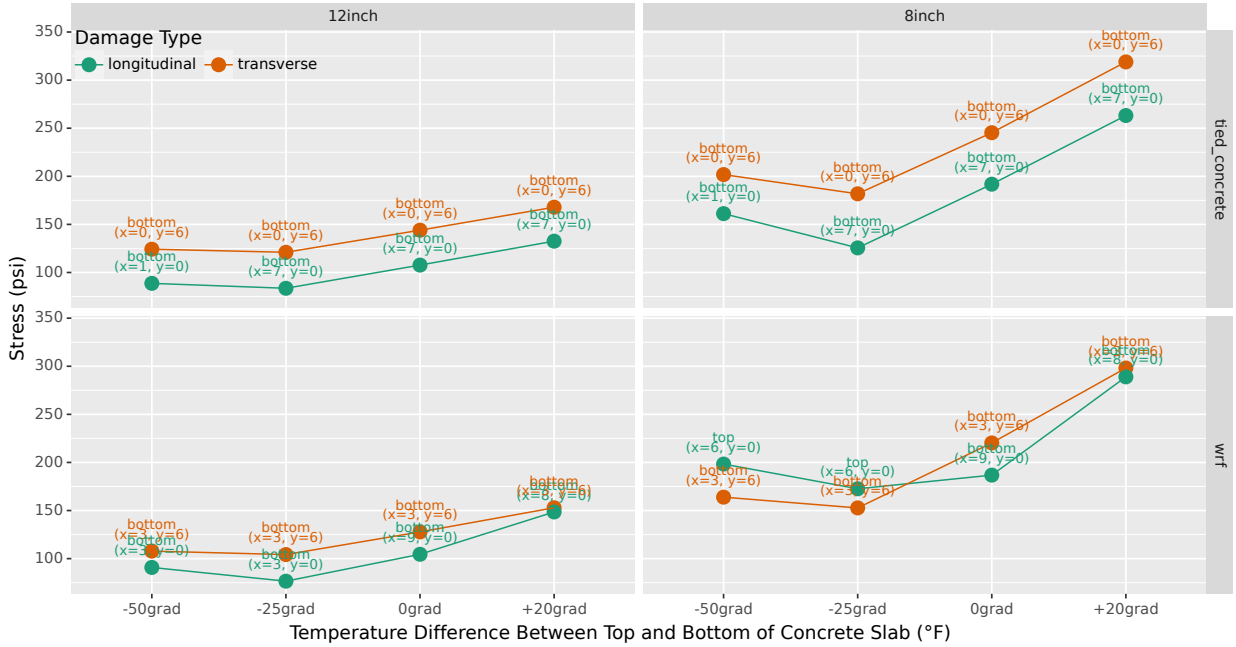

Figure 6.16: Effects of concrete slab thickness on mode of failure

6.4.5. Base Type

Figure 6.17 illustrates the influence of base type on the stresses in JPCP. Overall, there is no discernible pattern in this graph, suggesting that the base type does not significantly affect the mode of failure for JPCP.

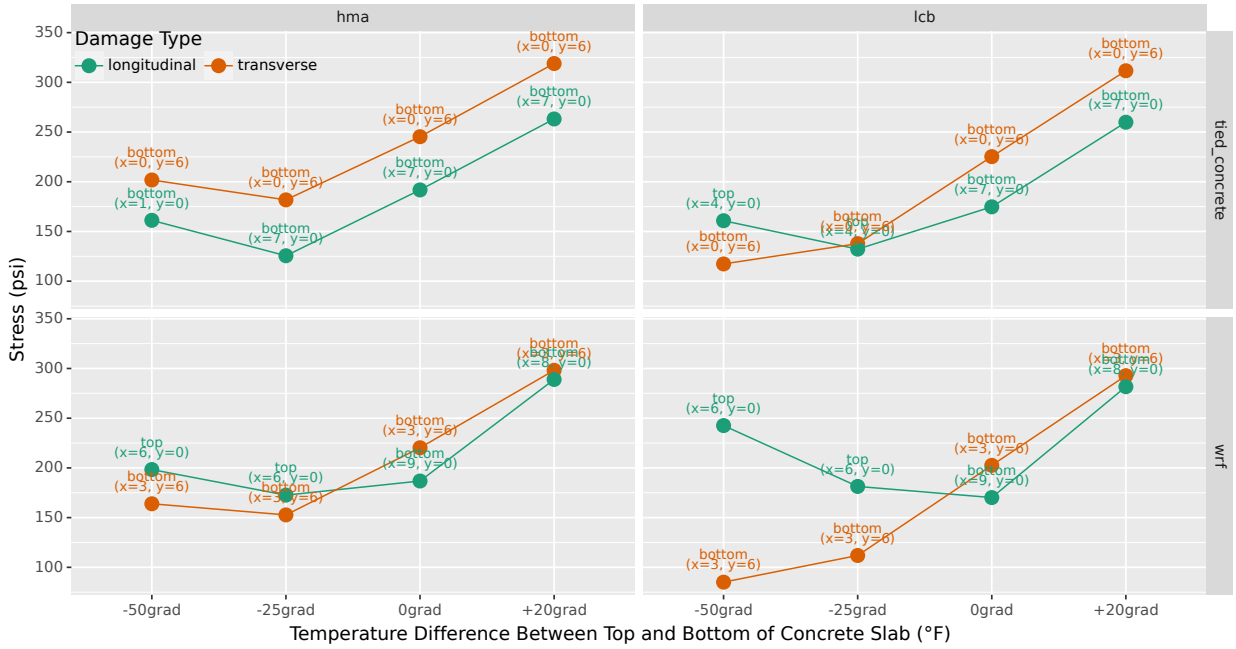

Figure 6.17: Effects of base type on mode of failure

6.5. Summary and Conclusion

Longitudinal cracks in JCPC, which form parallel to the direction of traffic, have historically been overlooked in pavement design. This disregard stemmed from a lack of understanding of the mechanical processes involved in drying shrinkage, particularly in humid climates where such cracking is rare. However, studies conducted in dry climate regions of the United States, including California, have highlighted the significance of longitudinal cracking as a prevalent distress in JPCP.

Various investigations have shed light on the underlying causes of longitudinal cracking, attributing it to factors such as late and shallow saw cutting of longitudinal joints, inadequate base support, and the presence of high CTE aggregates in concrete mixtures. Finite element analysis and field studies have further elucidated the role of factors like temperature curling, differential drying shrinkage, and traffic loading in inducing longitudinal cracks.

To address the issue of longitudinal cracking in California, an extensive factorial analysis was conducted, evaluating critical design variables' impact on pavement performance. Using ISLAB2000 finite element software, simulations were performed across different load configurations and environmental conditions.

The factorial analysis encompassed various design variables, including shoulder type, load transfer efficiency, base type, slab thickness, slab length, thermal gradient, axle type, and load location. A total of 512 ISLAB2000 runs were executed.

The results revealed significant insights into the influence of shoulder type and thermal gradient on the mode of failure in JPCP. Pavements with tied concrete shoulders exhibited higher tensile stresses leading to transverse cracking across all thermal gradients. However, JPCP with widened, reinforced, and fastened (WRF) shoulder type demonstrated a different behavior, effectively reducing stresses causing transverse cracking compared to tied concrete pavements. Under extreme negative thermal gradients, JPCP with WRF shoulders experienced higher tensile stresses, resulting in longitudinal cracking. In this study only 2 ft. WRF shoulder was considered.

Furthermore, the study explored the impact of load transfer efficiency, slab length, and concrete slab thickness on pavement performance. The load transfer efficiency had minimal effect on stresses causing transverse and longitudinal cracking. Longer slabs were found to induce higher stresses leading to transverse cracking under neutral and positive thermal gradients, while thicker slabs reduced stress levels

for both types of cracking. Notably, increasing slab thickness could shift the mode of failure from longitudinal cracking to transverse cracking for pavements with WRF shoulder type under negative thermal gradients.

In conclusion, to mitigate longitudinal cracking in climate regions experiencing extreme negative thermal gradients, which is primarily dry climates, the use of tied-concrete shoulders is recommended. Additionally, the study found that base type and slab length do not significantly affect the mode of failure and longitudinal cracking. Design criteria to prevent longitudinal cracking should prioritize using tied concrete instead of WRF and potentially incorporating thicker slabs.

CHAPTER 7. Summary of Contributions and Recommendations

The research presented in this thesis has provided significant insights into the performance and design of jointed concrete pavements (JPCP) in California. The contributions span several critical areas, including the development of performance prediction models, sensitivity analysis for calibration, Pavement ME model calibration for transverse cracking, and the investigation of longitudinal cracking mechanisms. These findings collectively enhance our understanding of JPCP behavior and offer practical recommendations for future research and design improvements.

In Chapter 3, a performance prediction model was proposed for the replaced slabs within slab replacement treatments done in California. Due to the categorical nature of slab condition variables, which can be either undamaged, first-stage cracked, or third-stage cracked, a cumulative link mixed regression model was proposed. Slab age, thickness, dowel condition, and WIM spectrum were determined as significant explanatory variables to be included in the model. While other variables such as slab length, base type, cement type, and climate region might also have significant effects, they were not assessed in this study due to a lack of sufficient data.

To better capture the effects of slab length and other design factors, a focused data collection effort is recommended, possibly involving the collection of GPS locations for replaced slabs so they can be tracked using APCS data. Given the distinct color of newly replaced slabs compared to original ones, developing computer vision algorithms to automatically identify and tag these slabs within the APCS data could be beneficial. Additional research areas could include exploring the use of reinforcement within the slabs (such as wire mesh or fibers) and improving construction practices for handling in-situ base material once the old slab has been removed.

In Chapter 4, a sensitivity analysis was performed as a first step in calibrating Pavement ME. This analysis identified the importance of different input variables and their effects on the outputs generated by Pavement ME's performance models for transverse cracking, faulting, and IRI. The study considered inputs grouped as pavement structural design variables, pavement material variables, traffic variables, and climate variables. The variables found to have the greatest influence on JPCP design were:

- **Transverse cracking:** PCC slab thickness, built-in curl-warp temperature, PCC coefficient of thermal expansion (CTE), PCC shortwave absorptivity, PCC compressive strength, and shoulder type.

- **Mean transverse joint faulting:** Load transfer (use of dowels), built-in curl-warp temperature, shoulder type, climate, AADTT, PCC coefficient of thermal expansion, PCC thickness, and subgrade type.
- **Smoothness index:** Load transfer (use of dowels), shoulder type, PCC coefficient of thermal expansion, PCC shortwave absorptivity, built-in curl-warp temperature, AADTT, PCC thermal conductivity, and PCC thickness.

In Chapter 5, the Pavement ME (V2.5.5) transverse cracking model for JPCP was calibrated using a large performance database collected from California's highway network as part of the annual condition survey. The APCS 2010–2011 provided per-slab information on first-stage, transverse, and longitudinal cracking data. A machine learning model was developed to predict the transverse cracking percentage of pavements with first-stage cracking. The computed transverse cracking data, combined with third-stage cracking data, were used to calibrate the Pavement ME transverse cracking model.

The conventional approach for calibrating Pavement ME performance models has several limitations:

- It requires expensive and time-consuming sampling and testing of materials properties for each section, resulting in a small number of sections being available for calibration.
- It ignores the fact that a design-bid-build (low-bid) designer does not know the performance-related properties of the materials the contractor will bring to the job; this results in a blurred understanding of the sources of variability and their consideration in the design reliability approach.

This new calibration approach proposed in this study considered variabilities in JPCP performance—such as between-project, within-project, and between-contractor variability—to produce more reliable results. The proposed calibration approach aimed to improve calibration and the reliability approach used in ME design by doing the following:

- Use all the good quality distress performance data and as-built data in the Caltrans PMS databases collected since 1978 and quality checked over the last 10 years; this provides orders of magnitude more performance data for calibration, with the data organized by project.
- Use median properties to match median performance and use the variability of observed median performance to determine between-project variability, after using Pavement ME to account for the effects of climate, pavement cross section, and traffic.

- Back-calculate within-project variability by matching the shape of observed performance time history.

These variabilities were incorporated into the Pavement ME transverse cracking model predictions for the forthcoming Caltrans JPCP design catalog. The calibration reduced the model's average error for the percent of slabs cracked from 13.3 to 0.039. An updated design catalog was developed, calibrated using Pavement ME transverse cracking model predictions with 50 percent and 95 percent reliabilities.

Key findings from the performance data include:

- JPCP with thicker and shorter slabs perform much better than those with thinner and longer slabs.
- The presence or absence of dowels in a JPCP does not impact its transverse cracking performance.
- Among JPCP base types, lean concrete base (LCB) has the poorest cracking performance, while CTB and HMA have the best.
- JPC pavements with untied flexible shoulders and no shoulders show more transverse cracking than those with tied concrete shoulders. Widened concrete shoulders do not perform well and exhibit similar performance to flexible shoulders.
- The Inland Valley, High Mountain, and South Mountain climate regions show the worst performance, while the South Coast, Central Coast, High Desert, and Desert regions show the best performance.
- The weigh-in-motion (WIM) spectra effect does not follow the expected trend; some spectra cause more cracking than others.
- The model predicts more cracking under higher Average Annual Daily Truck Traffic (AADTT) per lane.

For future work:

- Better data for PCC CTE and PCC compressive strength (as a surrogate for flexural strength) is needed, as these were not available for calibration but significantly impact the model's predictions.
- Fixing discrepancies in WIM spectra data in the PaveM database will improve future performance model development and Pavement ME calibrations.

In Chapter 6, an extensive factorial analysis was conducted to address longitudinal cracking in California, evaluating critical design variables' impact on pavement performance using ISLAB2000 finite element software. The analysis included shoulder type, load transfer efficiency, base type, slab thickness, slab length, thermal gradient, axle type, and load location.

The results showed significant insights into the influence of shoulder type and thermal gradient on the mode of failure in JPCP. Pavements with tied concrete shoulders exhibited higher tensile stresses, leading to transverse cracking, while those with WRF shoulders reduced stresses causing transverse cracking but were more prone to longitudinal cracking under extreme negative thermal gradients.

Furthermore, the study found that load transfer efficiency had minimal effect on stresses causing cracking, while longer slabs induced higher stresses leading to transverse cracking under certain thermal gradients. Thicker slabs reduced stress levels for both types of cracking and could shift the mode of failure from longitudinal to transverse cracking under negative thermal gradients for pavements with WRF shoulders.

To mitigate longitudinal cracking in dry climates with extreme negative thermal gradients, the use of tied-concrete shoulders is recommended. The study found that base type and slab length do not significantly affect longitudinal cracking. Design criteria should prioritize using tied concrete shoulders and potentially incorporating thicker slabs to prevent longitudinal cracking.

For future work, now that we know longitudinal cracking is prevalent in California and we have pinpointed the affecting variables, **a** longitudinal cracking model (transfer function) should be developed and incorporated into the Pavement ME models to account for the longitudinal cracking performance of JPCP in the ME design process.

REFERENCES

- American Association of State Highways Transportation Officials. 2010. Guide for the Local Calibration of the Mechanistic-Empirical Pavement Design Guide. (Accessed June 24, 2020)
- Christensen, R. H. B., 2015. Regression Models for Ordinal Data, R package version 2015.6-28. http://www.cran.r-project.org/package=ordinal/.
- Fu, P., Lea, J. D., Lee, J. N., and Harvey, J. T. 2013. Comprehensive evaluation of automated pavement condition survey service providers' technical competence. International Journal of Pavement Engineering, 14(1), 36–49. https://doi.org/10.1080/10298436.2011.643794
- Harvey, J. T., J. Roesler, J. Farver, and Liang, L. 2000. Preliminary Evaluation of Proposed LLPRS Rigid Pavement Structures and Design Inputs. University of California, Davis. Report No. FHWA/CA/OR-2000/02. www.ucprc.ucdavis.edu/PDF/Prelim%20Eval%20of%20Prop%20LLPRS.pdf. (Accessed March 1, 2019).
- Heath, A., Roesler, J., and Harvey, J. 2003. Modeling Longitudinal, Corner and Transverse Cracking in Jointed Concrete Pavements. International Journal of Pavement Engineering, Vol. 4 (1): 51–58.
- Hiller, J., and Roesler, J. 2002. Transverse Joint Analysis for Mechanistic-Empirical Design of Rigid Pavements. Transportation Research Record: Journal of the Transportation Research Board.
- Kannekanti, V. and Harvey, J. T. 2007. Field Calibration of MEPDG JPCP Distress Prediction Models. University of California Pavement Research Center, Davis and Berkeley. Research Report: UCPRC-RR-2007-02.
- Kannekanti, V., and Harvey, J. T. 2006. Sample Rigid Pavement Design Tables Based on Version 0.8 of the Mechanistic-Empirical Pavement Design Guide. University of California Pavement Research Center, Davis and Berkeley. Technical Memorandum: UCPRC-TM-2006-04. (Accessed March 1, 2019), www.ucprc.ucdavis.edu/PDF/MPEDG%20Stg%205%20Final%20UCPRC-TM-2006-04%20with%20FHWA.pdf.
- Kannekanti, V. and Harvey, J. T. 2006. Sensitivity Analysis of 2002 Design Guide Rigid Pavement Distress Prediction Models. University of California Pavement Research Center, Berkeley and Davis. Design Guide: UCPRC-DG-2006-01. www.ucprc.ucdavis.edu/PDF/UCPRC-DG-2006-01.pdf. (Accessed March 1, 2019).
- Kaplan, E. L., and Meier, P. 1958. Nonparametric Estimation from Incomplete Observations. Journal of the American Statistical Association, vol. 53, no. 282, pp. 457-481.
- Kassambara A., Kosinski, M., and Biecek, P. 2017. Drawing Survival Curves using 'ggplot2', http://www.sthda.com/english/rpkgs/survminer/, Version 0.4.0.

- Khazanovich L., Darter M. I., and Yu H. T. 2004. Mechanistic–Empirical Model to Predict Transverse Joint Faulting. In Transportation Research Record: Journal of the Transportation Research Board, No. 1896, Transportation Research Board of the National Academies, Washington, D.C., pp. 34–45.
- Kim, C., Lea, J. D., Kannekanti, V., and Harvey, J. T. 2019. Updating Weigh-in-Motion (WIM) Spectra in PaveM. University of California, Davis. Report No. UCPRC-TM-2018-01 (draft under review).
- Kohler, E. and Kannekanti V. 2008. Influence of Coefficient of Thermal Expansion on the Cracking of Jointed Concrete Pavements. 6th RILEM International Conference on Cracking in Pavements. Chicago.
- Lea, J. D. and Harvey, J. T. 2002. Data Mining of the Caltrans Pavement Management System (PMS) Database. University of California Pavement Research Center, Berkeley.
- Lea, J. D. and Harvey, J. T. 2015. A Spatial Analysis of Pavement Variablity. International Journal of Pavement Engineering, Vol. 16, No. 3, pp. 256-267.
- Lederle, R. E. 2014. Development of a Longitudinal Cracking Fatigue Damage Model for Jointed Plain Concrete Pavements Using the Principles of Similarity. PhD dissertation., University of Minnesota.
- Li, H., Harvey, J. T., Asselanis, J., Zhou, J., Guada, I., Kannekanti, V., and Wu, R. 2016. Preliminary Results from Visual Inspection and Laboratory Testing for ASR in Existing Concrete Cores from Bridge and Pavement in California. University of California, Davis. Report No. UCPRC-RR-2015-07. www.ucprc.ucdavis.edu/PDF/UCPRC-RR-2015-07.pdf. (Accessed March 1, 2019)
- Lu, Q., Jones, D., and Harvey, J. T. 2008. Estimation of Truck Traffic Inputs Based on Weigh-in-Motion Data in California. Technical Memo UCPRC-TM-2008-08, Davis.
- Macleod, D. R., and Monismith, C.L. 1979. Performance of Portland Cement Concrete Pavement. Department of Civil Engineering, Institute of Transportation Studies, University of California, Berkeley.
- Madanat, S., Nakat, Z., Farshidi, F., Sathaye, F., and Harvey, J. T. 2008. Development of Empirical-Mechanistic Pavement Mechanistic Pavement Performance Models Using Performance Models Using Data from the Washington Data from the Washington State PMS Database. Research Report UCPRC-RR-2005-05, Davis.
- Mateos, A., Saboori, A., Lea, J. D., and Harvey, J. T. 2022. Development of Caltrans Jointed Plain Concrete Pavement Design Catalog Tables Using Pavement ME. UC Davis: University of California Pavement Research Center. http://dx.doi.org/10.7922/G2Z31WZQ

- Mateos, A., Harvey, J. T., Paniagua, F., Paniagua, J., and Wu, R. 2018. Development of Improved Guidelines and Designs for Thin Whitetopping: Construction and Initial Environmental Response of Full-Scale BCOA Sections. UC Davis: University of California Pavement Research Center. Retrieved from https://escholarship.org/uc/item/14t4f662
- Miller, T. D. 2014. Field Performance Evaluation of Slabs Replaced with Rapid Strength Concrete.
- Mu, F., Mack, J. W., and Rodden, R. A. 2018. Review of national and state-level calibrations of AASHTOWare Pavement ME design for new jointed plain concrete pavement. International Journal of Pavement Engineering, 19(9), 825–831. https://doi.org/10.1080/10298436.2016.1210804
- National Cooperative Highway Research Program (NCHRP), Guide for Mechanistic-Empirical Pavement Design of New and Rehabilitated Pavement Structures (CITY TK: PUBLISHER TK, [cj: body copy lists the date of publication as 2002, not 2003] 2003).
- Ongel, A. and Harvey, J.T.. 2004. Analysis of 30 Years of Pavement Temperatures Using the Enhanced Integrated Climate Model (EICM). University of California, Davis. (Accessed March 1, 2019)
- Premkumar, L. and Vavrik, W. R. 2016. Enhancing Pavement Performance Prediction Models for the Illinois Tollway System. International Journal of Pavement Research and Technology, pp. 14-19, 5.
- R Core Team. 2013. R: A language and environment for statistical computing. in R Foundation for Statistical Computing, Vienn.
- Rezaei, A. and Harvey, J. T. 2013. Investigation of Tire/Pavement Noise for Concrete Pavement Surfaces: Summary of Four Years of Measurements. University of California Pavement Research Center, Davis and Berkeley. Research Report: UCPRC-RR-2013-12. www.ucprc.ucdavis.edu/PDF/UCPRC-RR-2013-12.pdf. (Accessed June 23, 2020)
- Saboori, A., Harvey, J. T., Lea, J. D., Lea, J., Wu, R., and Mateos, A. 2020. Pavement ME Sensitivity Analysis (Version 2.5.3). University of California Pavement Research Center, Davis and Berkeley. Research Report: UCPRC-RR-2019-02. (in progress)
- Saboori, A., Lea, J. D., Kannekanti, V. Saboori, A., and Harvey, J. T. 2018. Development of a Cracking Performance Prediction Model for Replaced Concrete Slabs in California. No. 18-04758. Transportation Research Board 97th Annual Meeting. Washington, DC.
- Sachs, S., Vandenbossche, J. M., and Snyder, M. B. 2015. Calibration of National Rigid Pavement Performance Models for the Pavement Mechanistic–Empirical Design Guide. Transportation Research Record, 2524(1), 59-67. https://doi.org/10.3141/2524-06
- State of California, Department of Transportation. 2004. Slab Replacement Guidelines.

- Stegner, W. 1992. Beyond the Hundredth Meridian: John Wesley Powell and the second opening of the West. New York: Penguin Books.
- Therneau, T.. 2015. A Package for Survival Analysis in S., https://CRAN.R-project.org/package=survival, Version 2.38.
- Tseng, E. 2012. The Construction of Pavement Performance Models for Flexible Pavement Wheelpath Cracking and IRI for the California Department of Transportation New Pavement Management System. Master's thesis, University of California, Davis.
- Wu, R., Harvey, J. T., Lea, J. 2022. A New Approach to Calibration and Use of Mechanistic-Empirical Design Methods. In: Di Benedetto, H., Baaj, H., Chailleux, E., Tebaldi, G., Sauzéat, C., Mangiafico, S. (eds) Proceedings of the RILEM International Symposium on Bituminous Materials. ISBM 2020. RILEM Bookseries, vol 27. Springer, Cham. https://doi.org/10.1007/978-3-030-46455-4_13
- Wu, R., Harvey, J. T., Lea, J. D., Mateos, A., Yang, S., and Hernandez, N. 2021. Updates to CalME and Calibration of Cracking Models. University of Californina Pavement Research Center, Davis, and Berekely. Research Repor: UCRPC-RR-2021-01
- Wu, R., Harvey, J. T., Lea, J., Jones, D., Louw, S., Mateos, A., Hernanzed, N., Shrestha, R., and Holland, J. 2022. Calibration of a Mechanistic-Empirical Cracking Model Using Network-Level Field Data. Transportation Research Record, vol. 2676, no. 12, pp. 127-139
- Zaabar, I. and Chatti, K. 2010. Calibration of HDM-4 Models for Estimating the Effect of Pavement Roughness on Fuel Consumption for U.S. Conditions. Transportation Research Record, 2155(1), 105-116. https://doi.org/10.3141/2155-12

APPENDIX: Project-Specific Detailed Materials Data

Project-specific data are variables specific to a pavement project that may vary due to different design criteria, environmental and traffic loading conditions, and/or the inherent randomness involved in pavement construction projects. These project-specific data are unavailable in the Caltrans PMS database and, therefore, they are missing for almost all JPCP projects undertaken in California. However, over the past few years, the University of California Pavement Research Center (UCPRC) has obtained essential project-specific data from parts of different research projects. These data include PCC compressive strength, PCC modulus of elasticity, PCC CTE, PCC shortwave absorptivity, and PCC density. These data were obtained by sampling from the various projects. Five data sources were used to set up this material input database.

- *Ground penetrating radar (GPR) data.* The objective of an earlier UCPRC GPR study was to create a lane-based pavement structure inventory database consisting of layer thickness and material types for the entire state highway network. The data collected as part of this project were used to establish fixed management sections for network-level and project-level PMS operations. As part of this project, some stateside Blind Verification Sections (BVS) were established to provide additional quality assurance. In this current report, the PCC CTE was the project-specific variable obtained from this GPR study.
- *Caltrans CTE database* (CaltransDB). After the 2006 sensitivity analysis that showed a very high sensitivity of transverse cracking in the MEPDG models to coefficient of thermal expansion (CTE), Caltrans required contractors to test and report CTE for several years. The Caltrans CTE database has the CTE test results taken from the JPC pavements while under construction during that period The map in Figure A.1 shows the distribution of specimens from the GPR study and the Caltrans CTE database. Many specimens in the Caltrans database had no latitude or longitude information, and therefore, there are a few data points from the Caltrans CTE database shown in the map below.

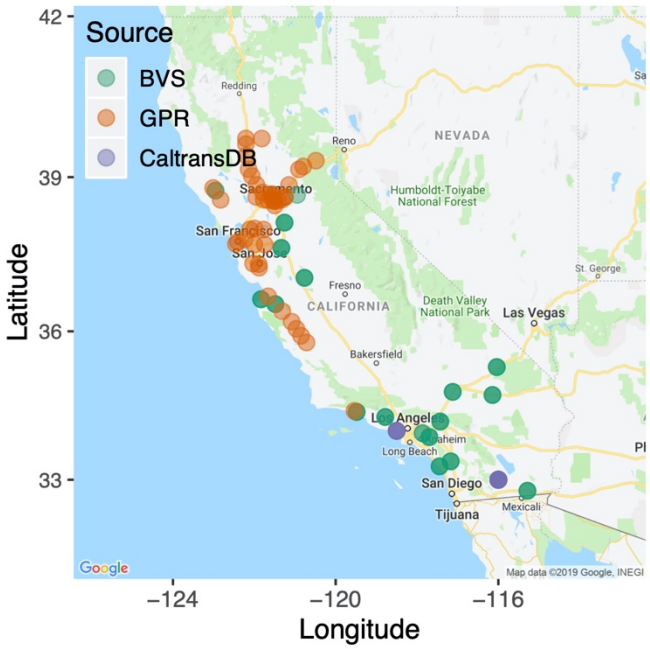

Figure A.1: Distribution map of cores taken across the state (GPR and CaltransDB)

- *Previous MEPDG calibration data.* These are data obtained from cores taken from different pavement sections across California as part of a 2007 MEPDG calibration project conducted by the UCPRC (Kannekanti and Harvey, 2007). These pavement sections include 52 concrete sections and 43 Crack, Seat, and Overlay (CSOL) sections. Figure A.2 shows the distribution of the pavement sections across the different climate regions and Caltrans districts in California. The project-specific data obtained as part of this study were PCC compressive strength, PCC modulus of elasticity, PCC CTE, PCC density, and PCC shortwave absorptivity (Kannekanti and Harvey, 2007).

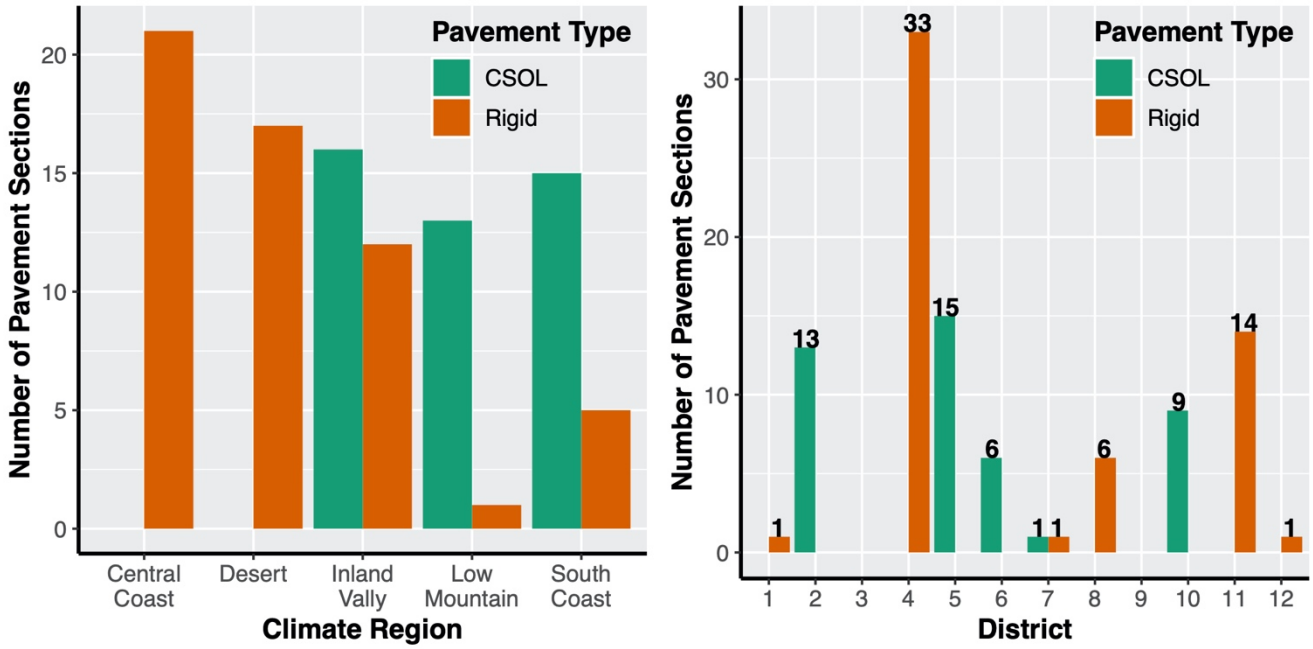

Figure A.2: Previous MEPDG calibration pavement sections distribution

- *Alkali-silica reaction (ASR) data.* The objective of the 2016 UCPRC ASR project (Li et al., 2019) was to look for the presence of alkali-silica reaction in California's pavements and bridges by evaluating core samples taken from pavement sections across the state. A total of 265 specimen cores were taken as part of this study, and PCC compressive strength and PCC density were measured for the samples.

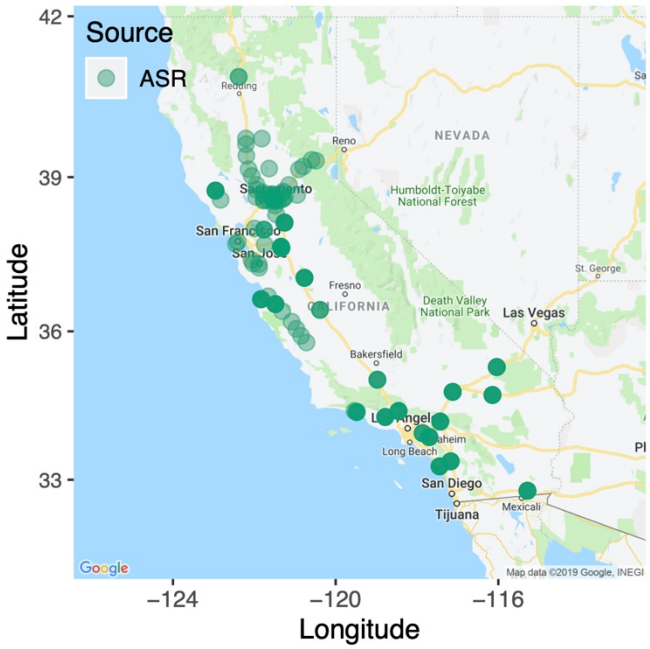

Figure A.3: Distribution map of cores taken across the state (ASR)

- *Stantec data.* These data were obtained by drilling core specimens to study the influence CTE on cracking of JPCP (Kohler and Kannekanti, 2008).

The following sections will show the distribution of each variable with their median and standard deviation. This information will be used in calibration of Pavement ME for pavement sections where project-specific inputs are unavailable. A more detailed discussion on this will be provided in the Pavement ME calibration report.

PCC Compressive Strength

Figure A.4 shows the distribution of the average within-project PCC compressive strength among samples taken from each project in the GPR and earlier MEPDG calibration studies. The compressive strengths were measured on cores taken at least several years and often many years after construction. The values shown have been converted from the long-term strengths to equivalent 28-day strengths using the MEPDG procedure to divide the long-term strength by a factor of 1.44. Equivalent 28-day values were used in Pavement ME. The compressive strengths adjusted to 28-day equivalents were also used for estimation of modulus of rupture and modulus of elasticity.

Compressive strength has an average of 4,539 psi with a standard deviation of 890 psi. Figure A.5 shows that the cumulative distribution of compressive strength has a 50th percentile (median) of 4,458 psi2. The values shown are long-term strengths taken from cores from all the structures, in most cases many years after construction.

Figure A.6 shows the variability in compressive strength within and between the projects. The line at the mid-height of each box indicates the average value of the compressive strength, and the box's two ends indicate one standard deviation above and below the mean for each specific project. The projects with only one core sample are shown as a single line in the figure. The numbers on top of the plot indicate the number of samples taken from each project.

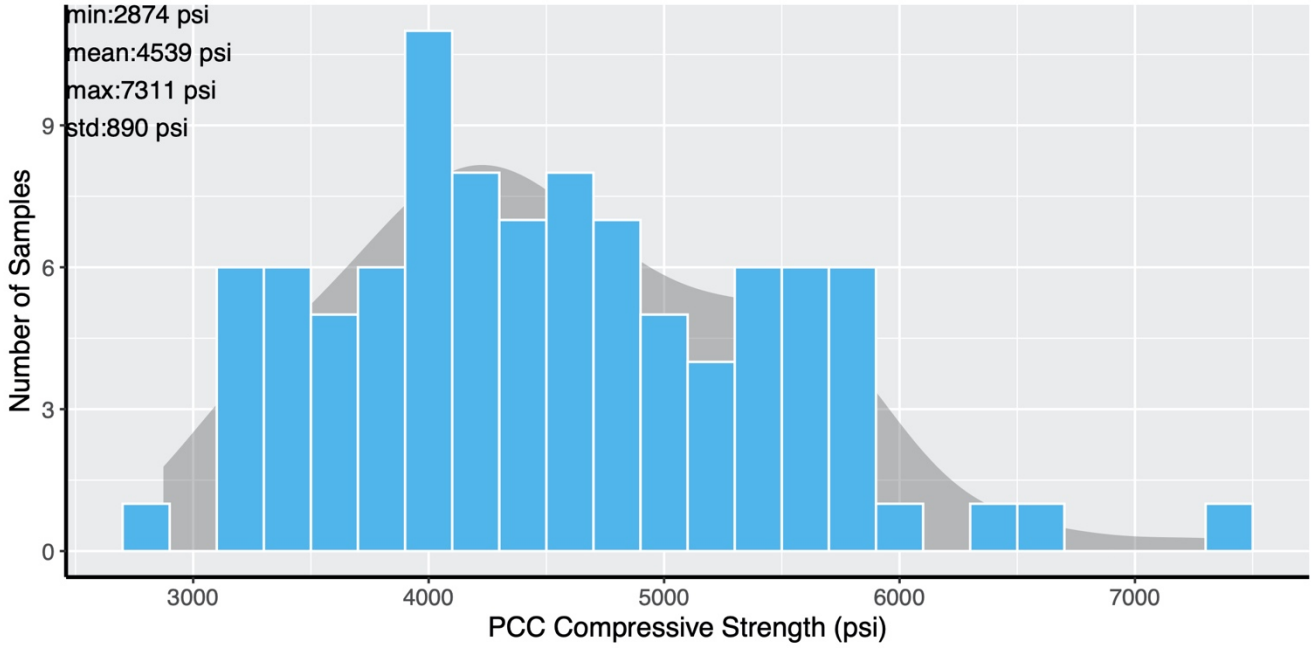

Figure A.4 : PCC compressive strength distribution across all projects

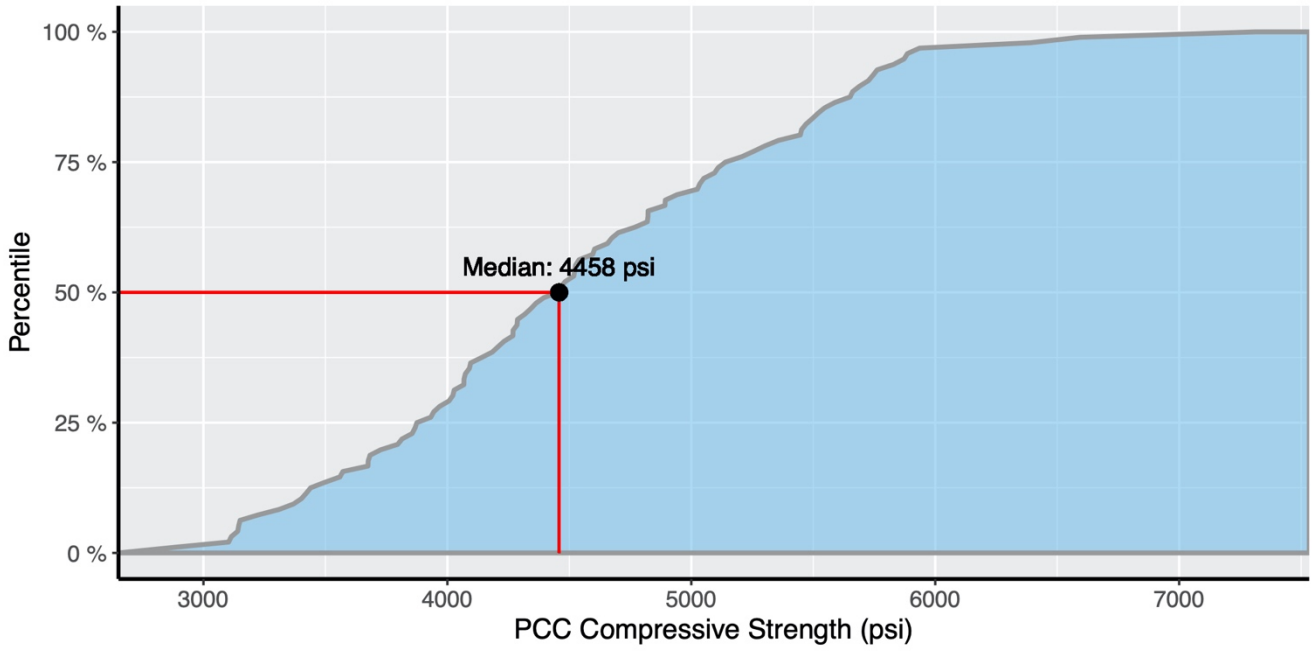

Figure A.5 : PCC compressive strength cumulative distribution

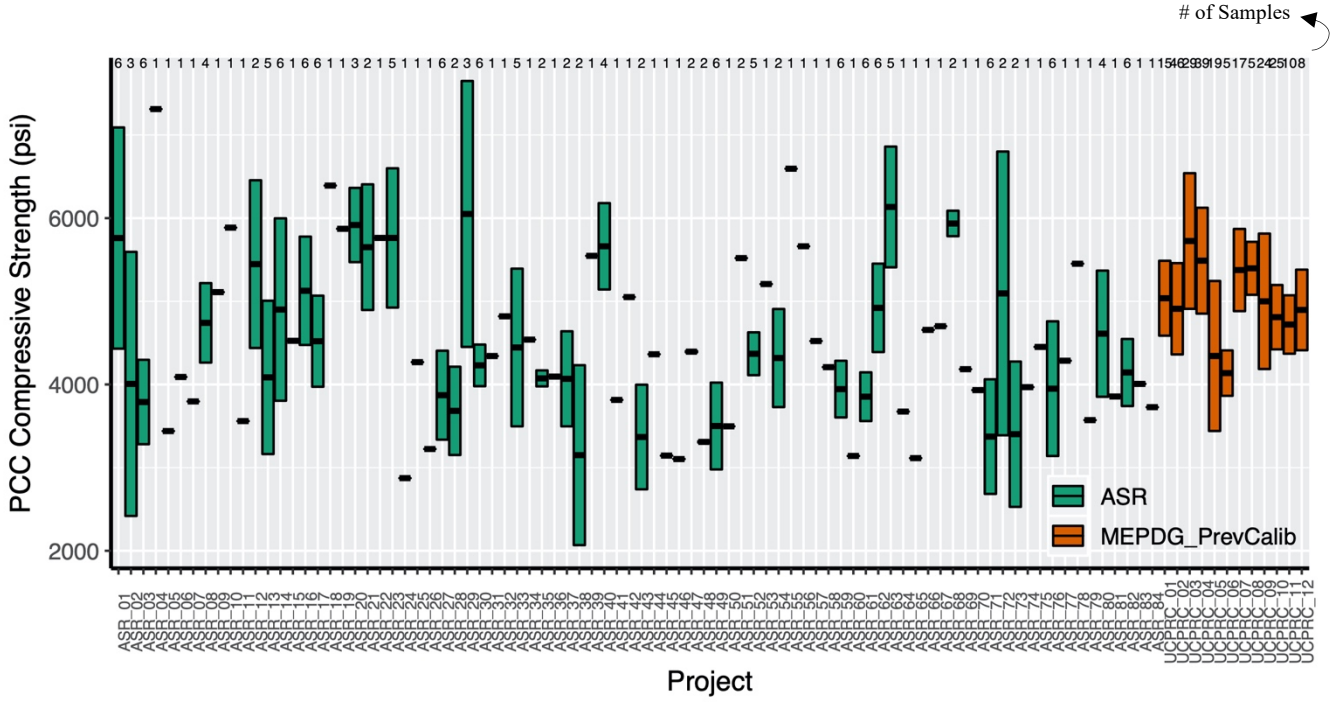

Figure A.6 : PCC compressive strength variability within projects

Coefficients of variation of measured within-project compressive strengths were:

- Average: 13.79 percent
- Median: 12.63 percent
- Standard deviation: 8.56 percent
- Maximum: 39.48 percent
- Minimum: 0.026 percent

PCC Estimated Modulus of Elasticity (28-day stiffness)

Modulus of elasticity was estimated from the PCC density and equivalent 28-day PCC compressive strengths by using the equation in the MEPDG: $E_e = 33\rho^{1.5} f_c'^{0.5}$, where E_e is the estimated modulus of elasticity, ρ is the density and *f*'c is the compressive strength. This equation is used in Pavement ME to calculate the modulus of elasticity based on the compressive strength and density input given by the user. Based on Figure A.7 and Figure A.8, the estimated modulus of elasticity has an average of 3,947 ksi with a standard deviation of 427 ksi. The 50th percentile (median) of the estimated modulus of elasticity is 3,934 ksi. Figure A.9 shows the variability in estimated PCC modulus of elasticity within and between the projects.

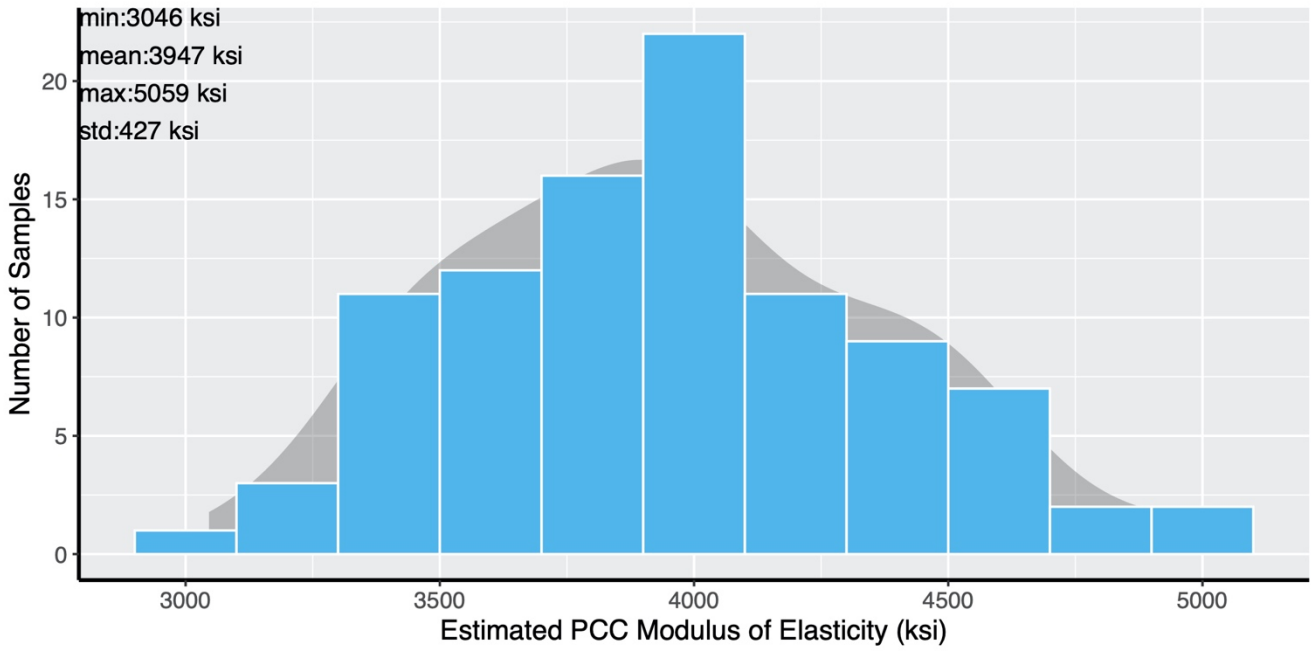

Figure A.7 : PCC estimated 28-day modulus of elasticity distribution across all projects

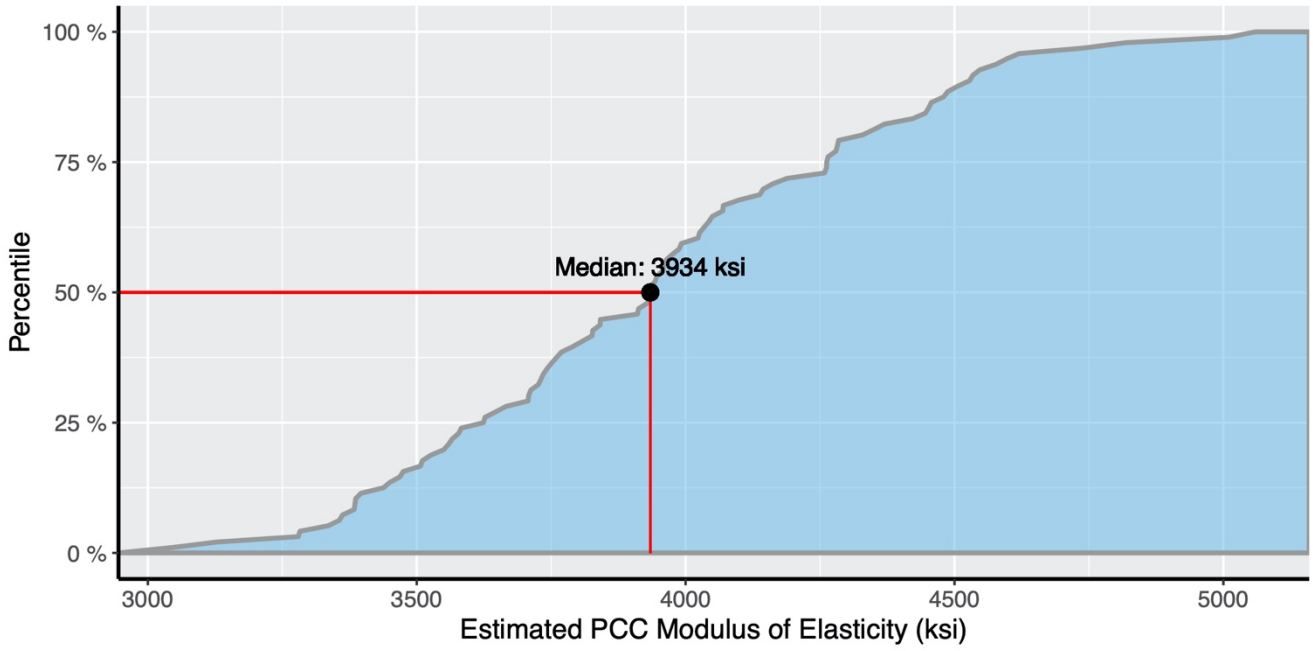

Figure A.8 : PCC estimated modulus of elasticity cumulative distribution

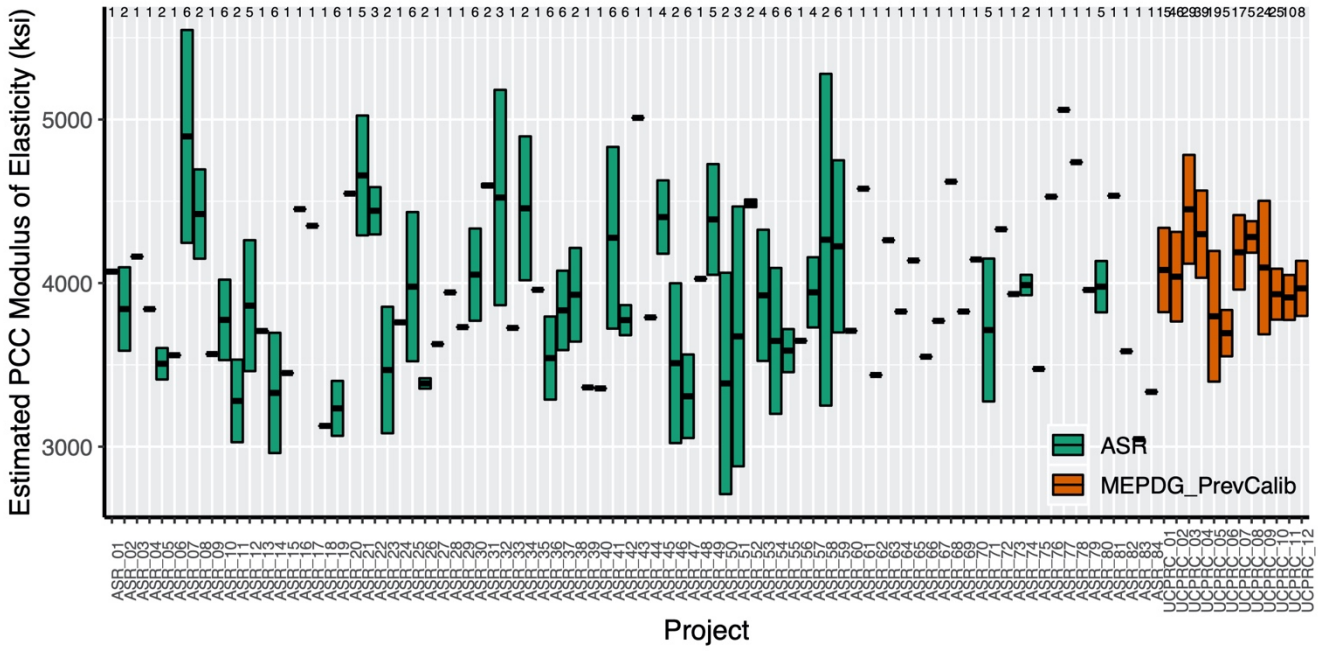

Figure A.9 : PCC estimated modulus of elasticity project-level variability

Coefficients of variation of estimated within-project modulus of elasticity values were:

- Average: 7.95 percent
- Median: 6.99 percent

- Standard deviation: 5.13 percent
- Maximum: 23.72 percent
- Minimum: 0.23 percent

Modulus of elasticity data were directly measured on cores on some sections as part of an earlier 2007 MEPDG calibration (Kannekanti and Harvey, 2007). Data were obtained from 224 samples across all projects. Since most of the projects had been in service for some decades at the time of the study, a factor of 1.2 was used to reduce the measurements to the 28-day stiffness. The measured modulus of elasticity from those sections had an average of 3,776 psi with a standard deviation of 347 psi. The 50th percentile (median) of the measured modulus of elasticity was estimated to be 3,786 psi. These measured values are reasonably close to those estimated from compressive strengths. The estimated values were used for the previous calibration of Pavement ME and were used for the upcoming calibration because the MEPDG models were calibrated using estimated values, and because the methodology for measuring the modulus of elasticity was performed using a non-standard research method.

PCC Estimated Modulus of Rupture

Modulus of rupture (MR) was not measured in either the previous MEPDG calibration or ASR studies, and was estimated using the 28-day compressive strengths using the equation $MR = 9.5\ {f_c'}^{0.5}$. The estimated MR has an average of 636 psi and a standard deviation of 62 psi with a median of 633 psi. Figure A.10 shows the distribution of the average within-project estimated PCC modulus of rupture. Figure A.11shows that the cumulative distribution of estimated PCC modulus of rupture has a 50th percentile (median) of 633 psi. Figure A.12 shows the variability in estimated PCC modulus of rupture within and between the projects.

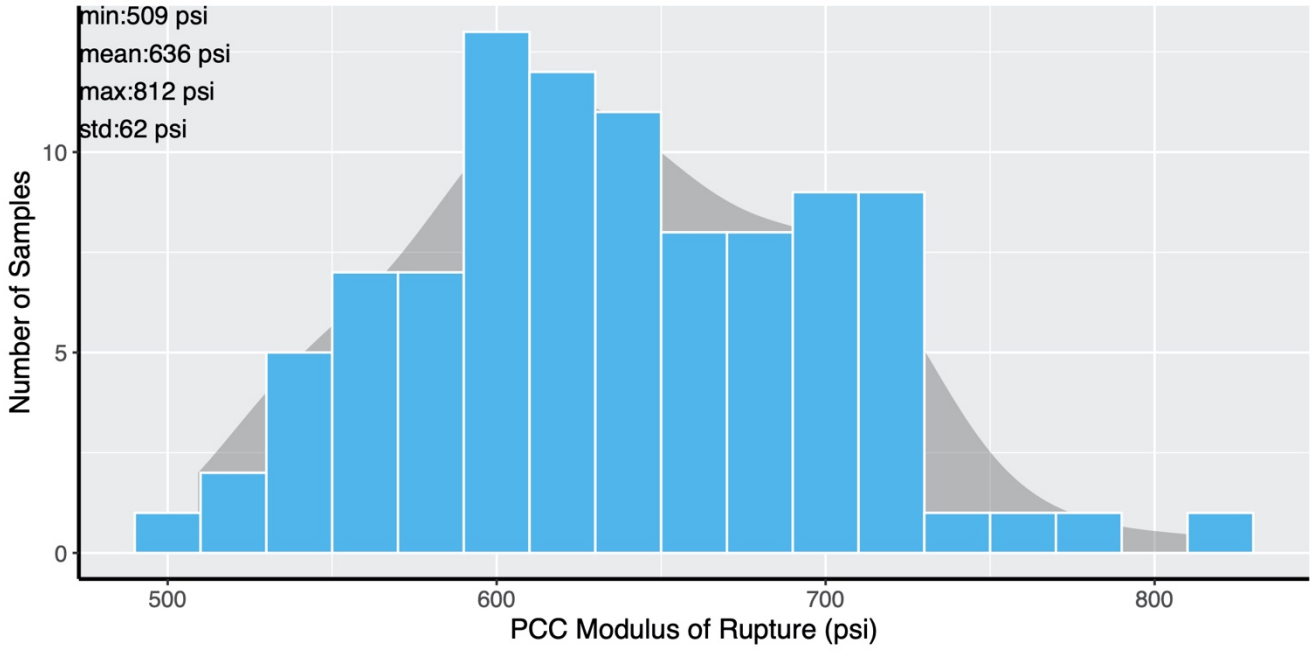

Figure A.10 : PCC estimated modulus of rupture distribution across all projects

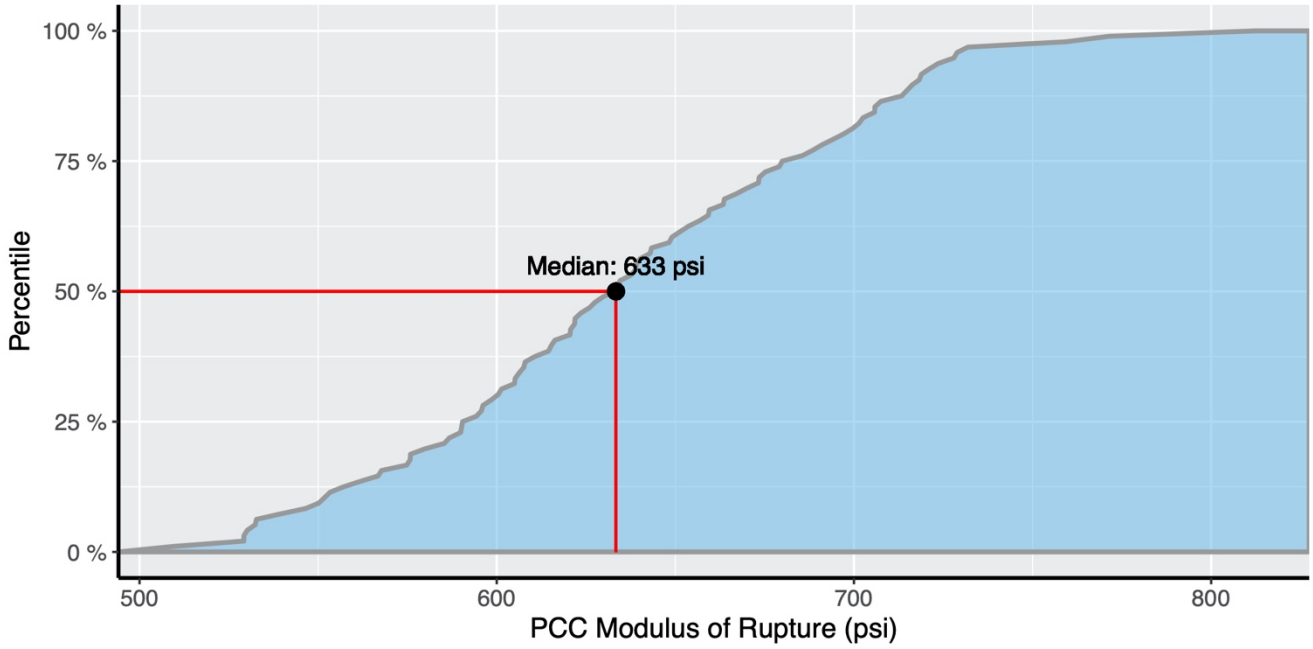

Figure A.11 : PCC estimated modulus of rupture cumulative distribution

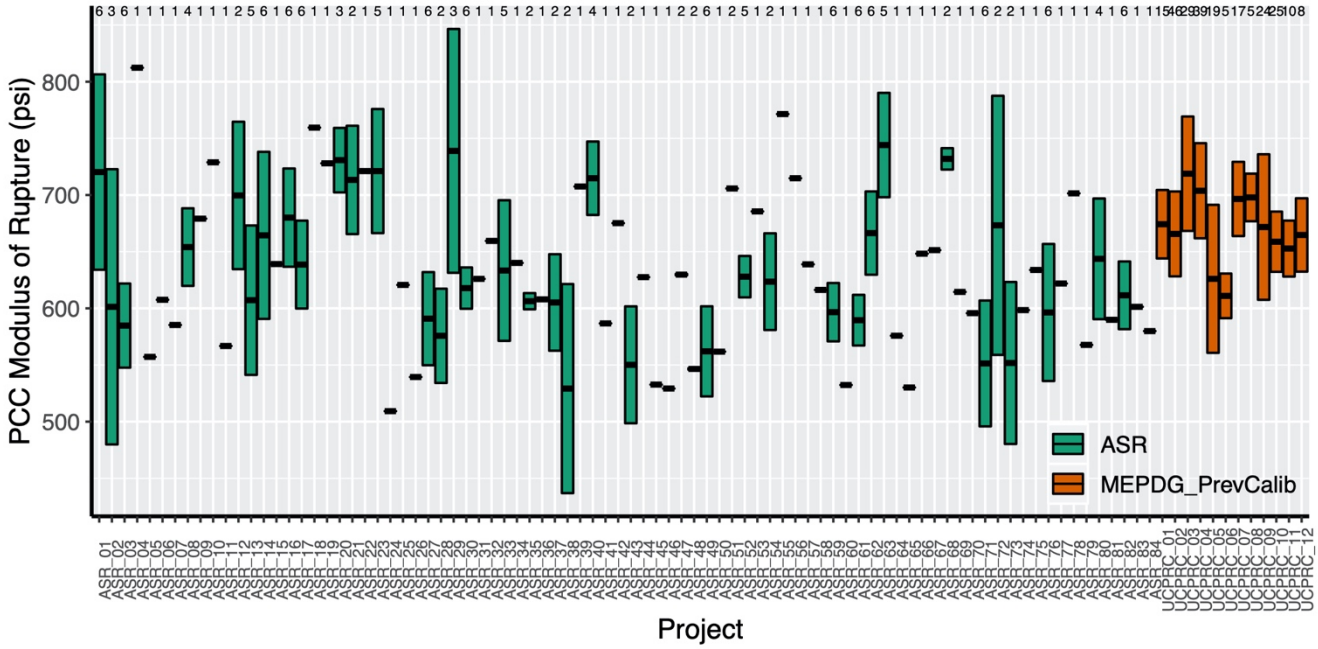

Figure A.12 : PCC Estimated modulus of rupture project-level variability

Coefficients of variation of estimated within-project modulus of rupture values were:

- Average: 6.99 percent
- Median: 6.38 percent
- Standard deviation: 4.39 percent
- Maximum: 20.43 percent
- Minimum: 0.13 percent

PCC Density

PCC density was measured as part of the ASR and previous MEPDG calibration studies (Kannekanti and Harvey, 2007). Density has an average of 147 pcf and a standard deviation of 3 pcf with a median of 147 pcf. Figure A.13 shows the distribution of the average within-project PCC density. Figure A.14 shows that the cumulative distribution of PCC density has a 50th percentile (median) of 147 pcf. Figure A.15 shows the variability in PCC density within and between the projects.

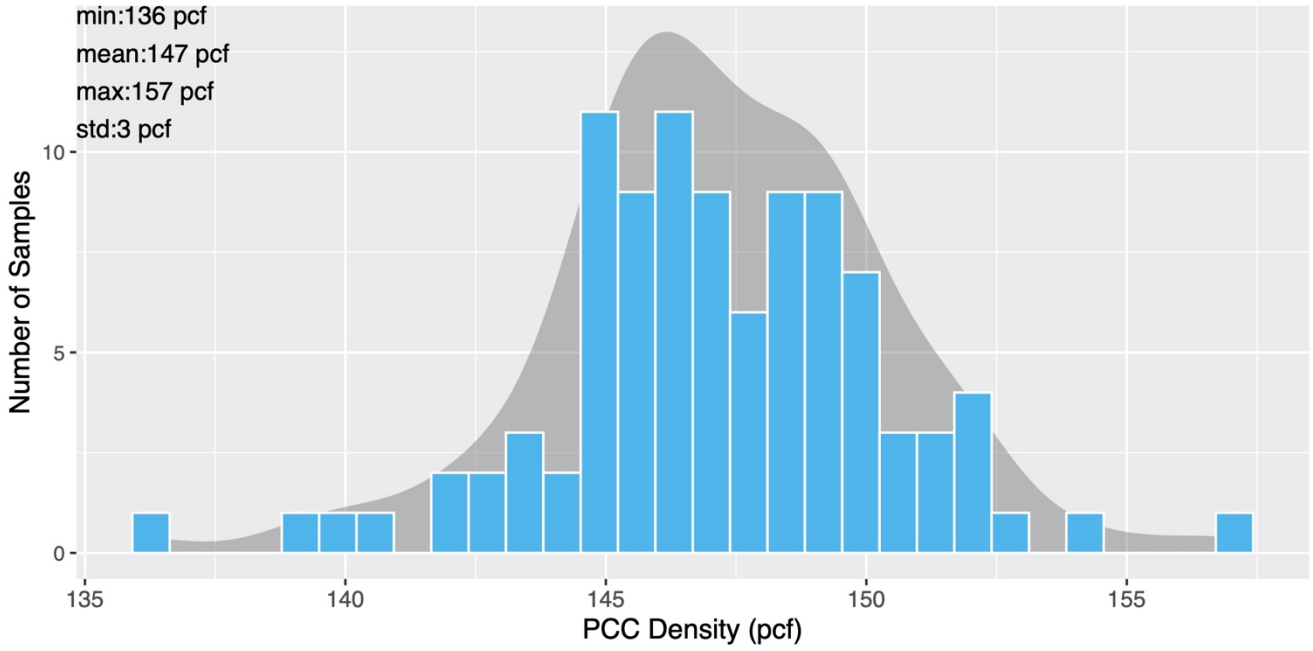

Figure A.13 : PCC density distribution across all projects

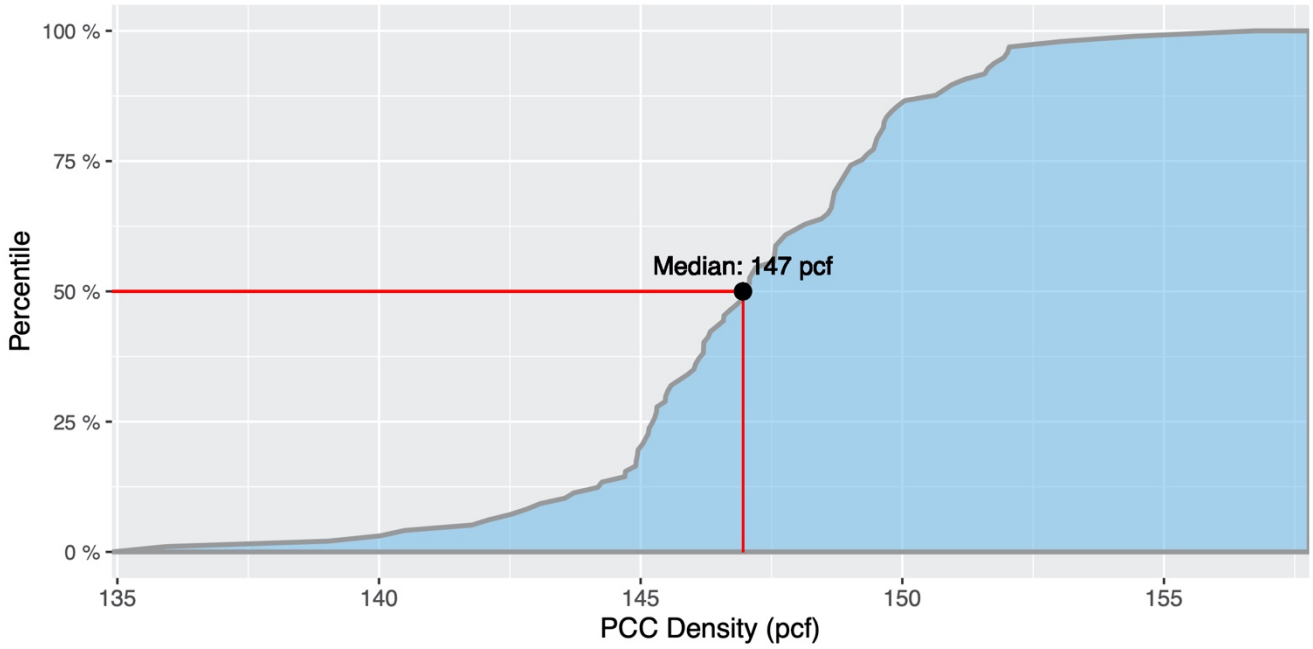

Figure A.14 : PCC density cumulative distribution

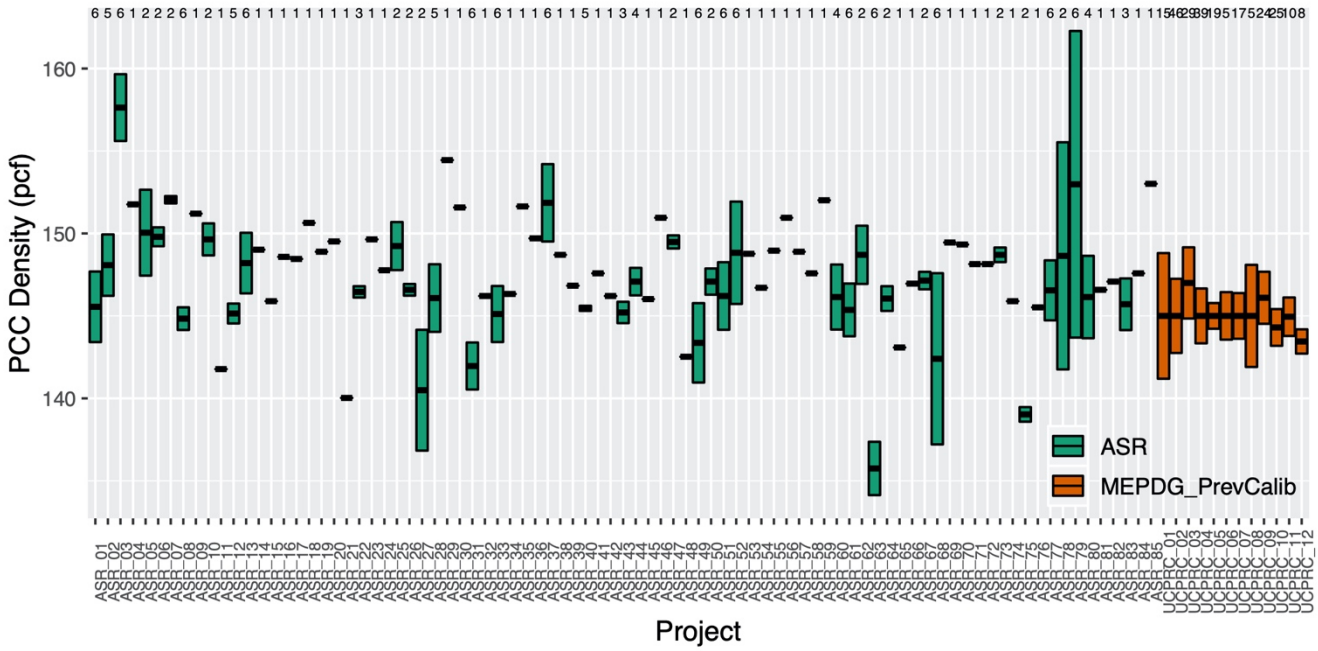

Figure A.15 : PCC density project-level variability

PCC Coefficient of Thermal Expansion

PCC CTE data were obtained from 2007 MEPDG calibration study (Kannekanti and Harvey, 2007), the GPR study, the Stantec project, and the Caltrans CTE database. The measured CTE values have an average of 4.91 microstrain/°F^{-1} with a standard deviation of 0.8 microstrain/°F^{-1} and a median of 4.8 microstrain/°F^{-1}. The measurements done by the UCPRC were not subject to the error in the reference metal identified by the FHWA after the measurements were made because it was verified that the metal with the erroneous reference value was not used in the UCPRC equipment. Figure A.16 shows the distribution of the average within-project PCC CTE. Figure A.17 shows that the cumulative distribution of PCC CTE has a 50th percentile (median) of 4.8 microstrain/°F^{-1}. Figure A.18 shows the variability in PCC CTE within and between the projects.

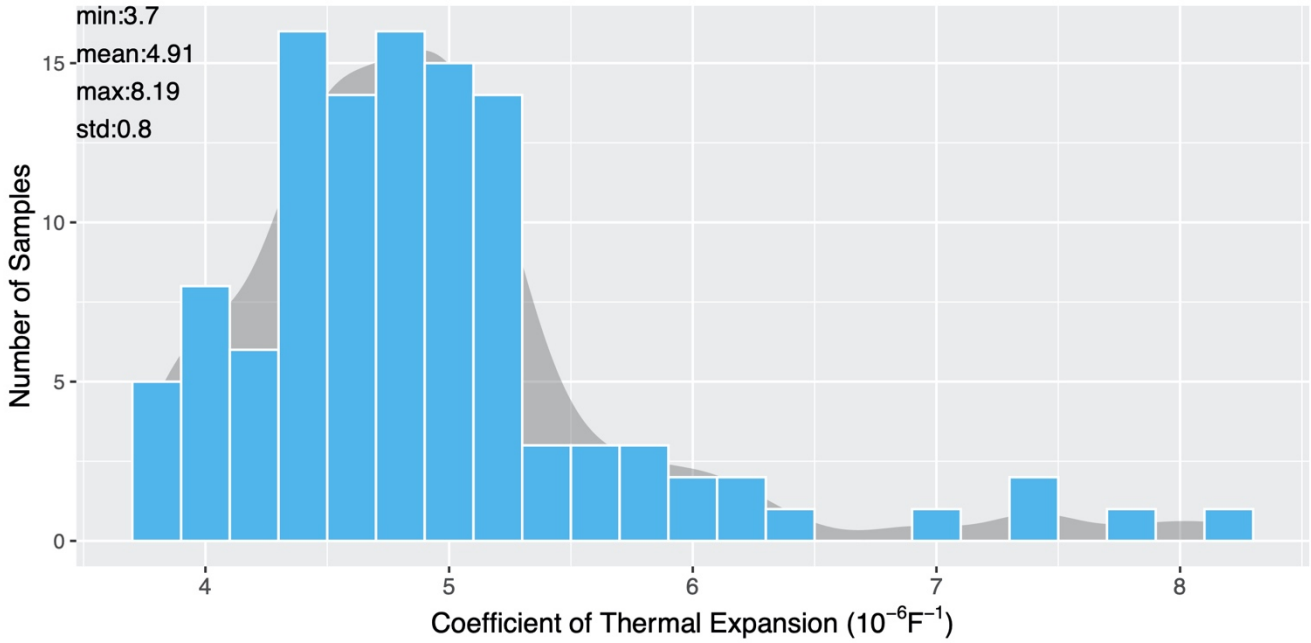

Figure A.16 : PCC coefficient of thermal expansion distribution across all projects

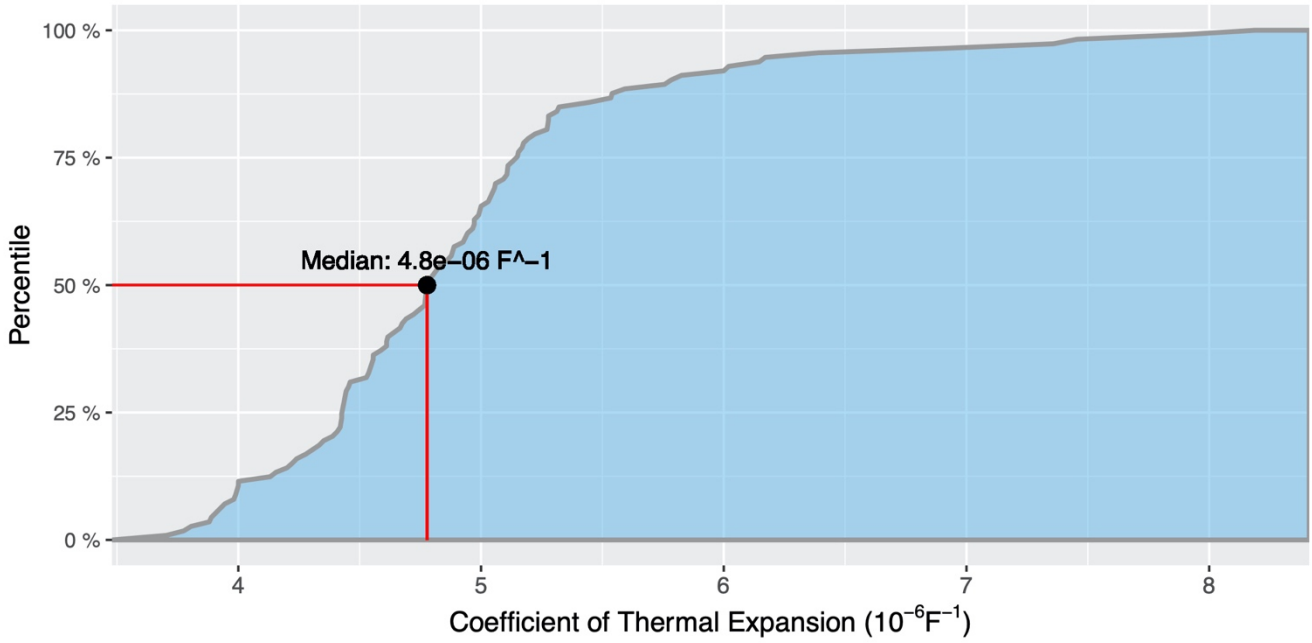

Figure A.17 : PCC coefficient of thermal expansion cumulative distribution

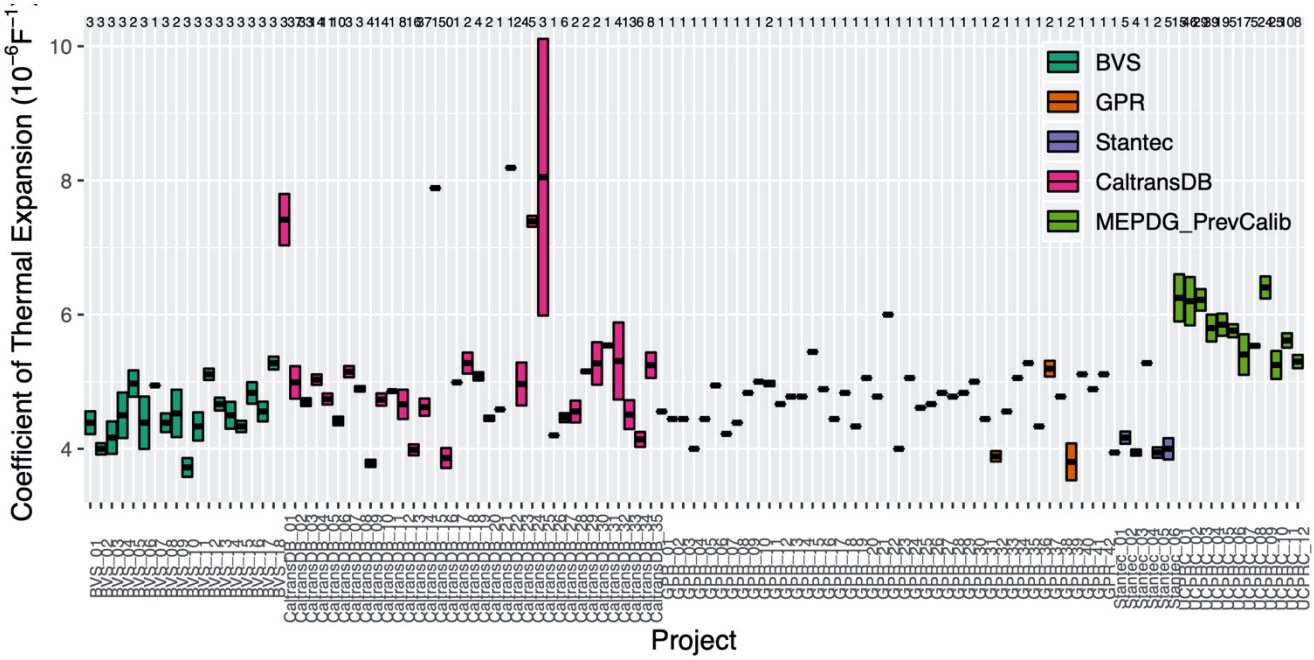

Figure A.18 : PCC coefficient of thermal expansion project-level variability

PCC Shortwave Absorptivity

Shortwave absorptivity data were collected as part of 2007 MEPDG calibration study (Kannekanti and Harvey, 2007) obtained from only three projects. The average value for shortwave absorptivity is 0.91 with a standard deviation of 0.02 and a median of 0.91. Figure A.19 shows the distribution of the average within-project PCC shortwave absorptivity. Figure A.20 shows that the cumulative distribution of PCC shortwave absorptivity has a 50th percentile (median) of 0.91. Figure A.21 shows the variability in PCC shortwave absorptivity within and between the projects. There were not many different unique

measurements for albedo and, therefore, the cumulative distribution graph became a step-graph, shown in Figure A.20, as if it is drawn from discrete values.

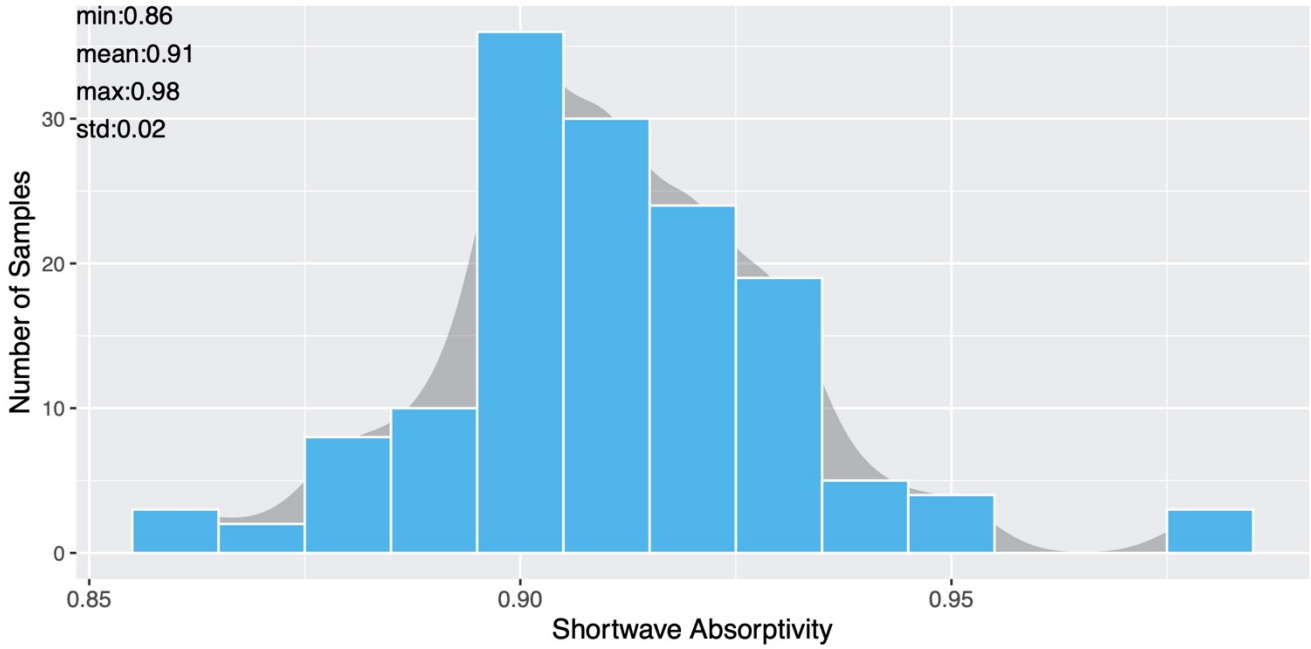

Figure A.19 : PCC shortwave absorptivity distribution across all projects

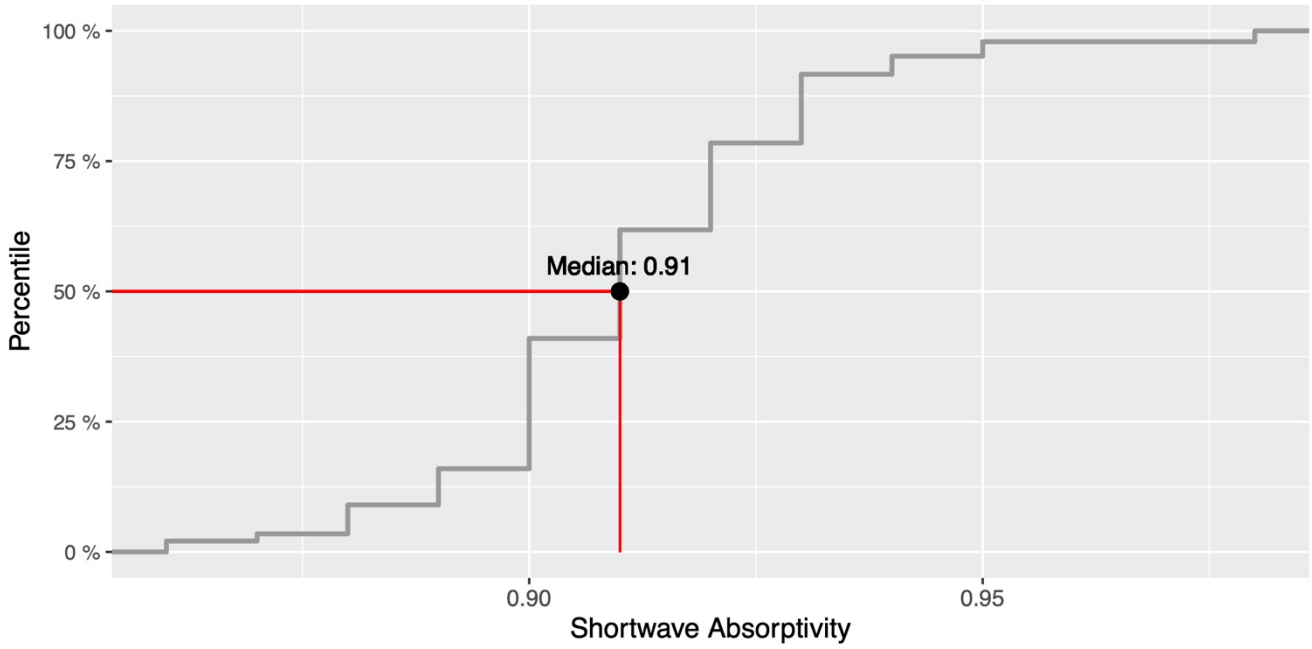

Figure A.20 : PCC shortwave absorptivity cumulative distribution

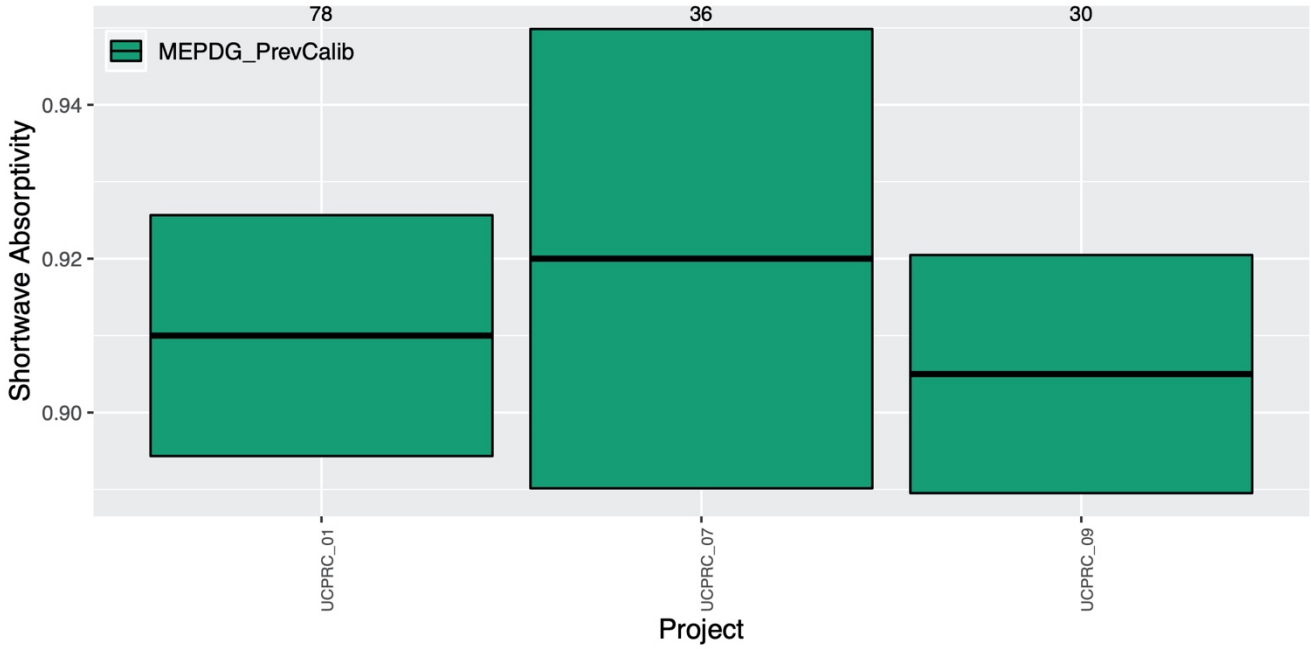

Figure A.21 : PCC shortwave absorptivity project-level variability

WIM Spectra

The following are the five weigh-in-motion (WIM) groups in California:

- Spectra 1 is the lightest *axle load distribution,* so-called because it has the highest load percentage (50 percent) of *single-counted axles,* that is, the sum of the number of single axles derived by adding up the number of single axles and each axle in a tandem axle between 20 and 30 kN.
- Spectra 2 is the second-lightest axle load distribution, with the largest percentage (about 65 percent) of single-counted axles concentrated between 20 and 40 kN.
- Spectra 3 is the medium axle load distribution, with its largest single-counted axle load proportion (70 percent) widely distributed between 20 and 50 kN, but with a light axle load proportion (20 kN) still slightly higher than the proportion of the heavy axle loads (60 kN).
- Spectra 4 is the second heaviest axle load distribution, with its single-counted axle loads fairly well distributed from 15 kN to 70 kN (between 10 and 20 percent); its proportion of single-counted axle loads at 20 kN is about the same as the proportion of single-counted axle loads at 50 kN.
- Spectra 5 is the heaviest axle load distribution, with its single-counted axle loads distributed more toward heavy axle loads (over 50 kN) than to light axle loads (under 40 kN).

Figure A.22 shows California's five WIM spectra. The Single Equivalent Axle Load Frequency y-axis variable is the result of splitting tandem axles in two and tridem axles in three (e.g., one tandem becomes

two singles with half the load each). The use of single equivalent axle loads is just a simplified way to determine the similarity between different WIM spectra. It does not impact the actual spectra being used in Pavement ME. Each WIM spectra (1 to 5) includes a detailed definition of truck types and axle weight distributions, similarly to the truck traffic class (TTC) classification in Pavement ME.

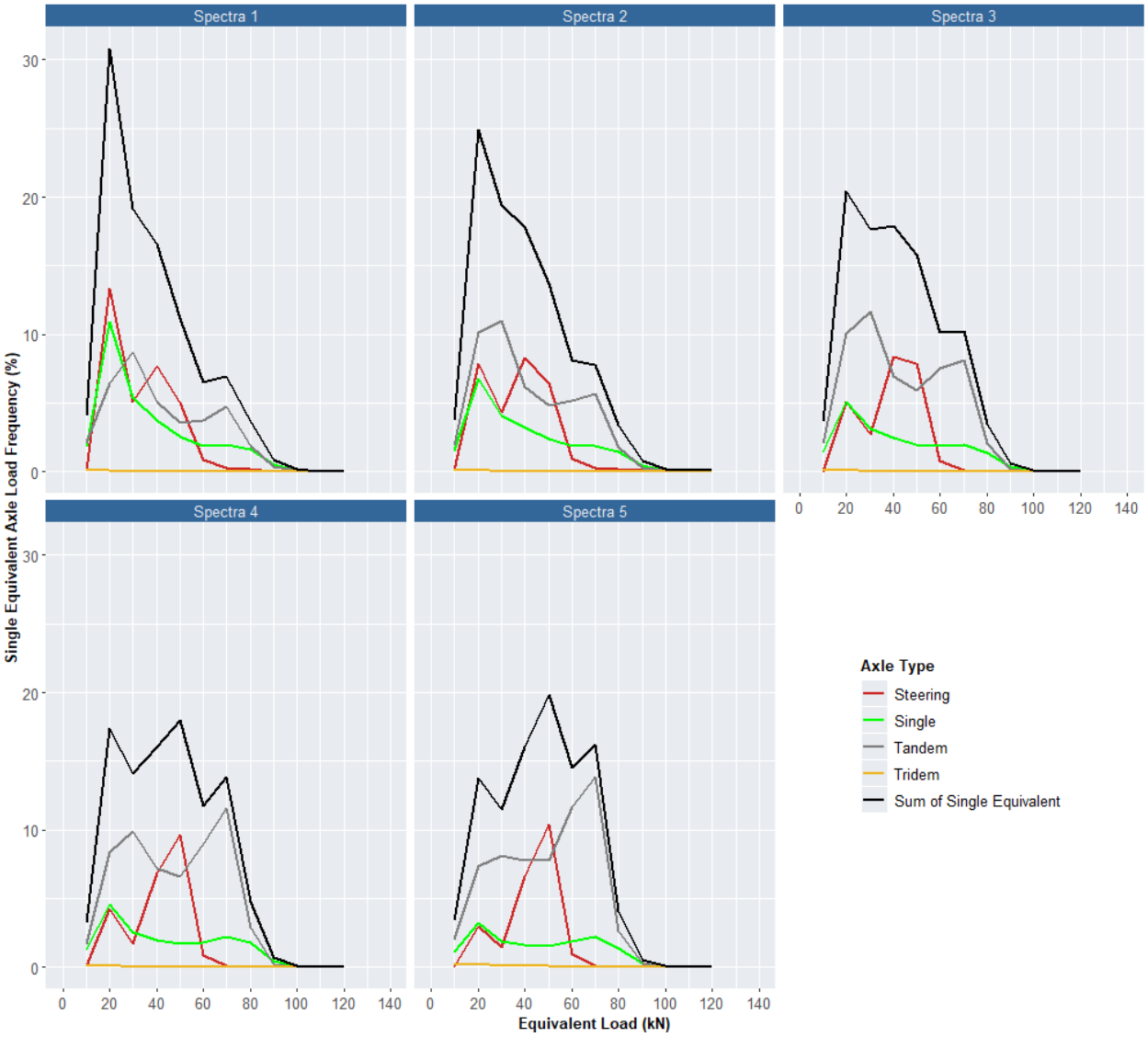

Figure A.22 : Five WIM spectra in California